



# Evaluation of soil compaction: effects, prevention, alleviation and detection

**Lidong Ren**

A dissertation submitted to Ghent University in fulfillment of the requirements for the  
degree of **Doctor of Bioscience Engineering: Natural Resources**

Academic year 2019-2020

**Dare to Think!**

**UGent**

**Dissertation supervisors:****Prof. dr. ir. Wim Cornelis**

Faculty of Bioscience Engineering, Ghent University

**Dr. Greet Ruyschaert**

Plant Science Unit Flanders Research Institute for Agriculture, Fisheries and Food (ILVO)

**Dr. Tommy D'Hose**

Plant Science Unit Flanders Research Institute for Agriculture, Fisheries and Food (ILVO)

**Board of examiners:****Prof. dr. ir. Pascal****Boeckx**

(Chairman)

Faculty of Bioscience  
Engineering,  
Ghent University**Prof. dr. ir. Kathy****Steppe**

(Secretary)

Faculty of Bioscience  
Engineering,  
Ghent University**Prof. dr. ir. Ann****Verdoodt**Faculty of Bioscience  
Engineering,  
Ghent University**Dr. ir. Jan Vermang**Department of  
Environment and  
Natural Energy,  
Flemish Government,  
Belgium**Prof. dr. Lars Juhl****Munkholm**Department of  
Agroecology  
Aarhus University  
Denmark**Dean: Prof. Dr. ir. Marc Van Meirvenne****Rector: Prof. Dr. ir. Rik Van de Walle**

**Dutch translation of the title:**

**EVALUATIE VAN BODEMVERDICHTING: EFFECTEN, PREVENTIE,  
VERLICHTING EN DETECTIE**

**Please refer to this work as follows:**

Lidong Ren, 2020. Evaluation of soil compaction: effects, prevention, alleviation and detection. PhD Thesis, Ghent University, Ghent, Belgium.

**ISBN-number: 978-94-6357-295-8**

The author and the promoters give the authorization to consult and to copy parts of this work for personal use only. Every other use is subject to the copyright laws.

Permission to reproduce any material contained in this work should be obtained from the author.

Cover illustration:

Front: Soil compaction schematic overview from Jan De Pue (2019).

## **Acknowledgements**

After completing the strict literary writing, it is the time to unrestrainedly express my gratitude for all the people and things during my PhD life.

First of all, I would express my grateful to my promotor Prof. Wim Cornelis. It is him who accepted me as a PhD student and opened the window of my research and life abroad. After joining his research group, he not only encouraged and supported me continuously but also gave me the great freedom to explore myself. Thanks for his useful and detailed comments during revising my drafts. His knowledge and life attitude will continuously affect my life.

Thank my two co-promoters from ILVO, Dr. Tommy D'Hose and Dr. Greet Ruysschaert. Thanks for allowing me to dig holes and trenches in their fields and providing all the necessary assistance. Those assistances are not only including discussion of the field experiment design but also working together in the fields. Those field working scenes are still clearly appearing in my mind and will always be there. My field experiments cannot finish without their help. Besides, I am also grateful for their critical comments and hardworking inputs for my manuscripts and thesis.

I would acknowledge to all the jury members for their time to evaluate this thesis and gave valuable comments to improve the quality of my thesis.

I would also like to acknowledge all the people meet in ILVO, specially for Thijs, Tom, Peter and Irene. Their friendly and professional assistance is grateful.

Thanks to all the people I met in Foulum during my visiting in Denmark. Special thanks to Lars, Mansonia, Sheela and Per. Their superb expertise inspired me a lot.

Thank my dear colleagues. I am lucky to meet all of you in this very international department. The first year was a bit hard to adapt to the new working environment.

Thanks to all the friendly and warmhearted colleagues for help: my first year officemate Nguyen, Geoffrey and Linh, they always gladly help me; Steffaan, Meisam Rezaei, Nele, Peter, Peter Finke, Mathieu, Patrick Dosche, Stany, Hui, Mesfine, Jeroen, Ellen. Also, later coming colleagues, Hellen, Junwei, Haichao, Orly, Temir, Ummehani, Eunice, Chihab, Desale, Daan, Sastrika, Angela, Jian, Christy and those unnamed ones. It is you who made my working life unforgettable. Thanks to our lab technician, Maarten Volckaet, for his friendly and patient help in the laboratory and field. Thanks for the company of my current officemates Linlin, Adriaan and Bashar. Special appreciation to Mr Jan De Pue, who is my colleague, officemate, tutor and friend.

Thanks to my unforgettable friends that met in Ghent. They made my life colorful in Ghent. Xiaoxi (yuan), Junfeng, Yuting, Meng qian, Meixia, Lijuan, Lipeng, Shiyuan, Guoliang, Ziyu, Xingyu, Mingshen, Linshan, Xiaogang, Dongdong Zhang, Dongdong Liu, Ouyang Lin, Shusheng, Wenlei, Xiaolin, Jinquan, Jun Li, Ruiqi, Jing(景) Li, Jing (静) Li and Pengyu.

Thanks the CSC scholarship for funding my life here. Thanks CWO and FWO funding that allowed me to participate the academic exchanging opportunities.

Lastly, I would deeply to express my gratitude to my dear family. Thanks for your understanding and support during all the past 24 years' education time. Special thanks to my dear girlfriend, WENLI. Thanks for your accompany and supporting!

Ghent

14-02-2020

## Table of content

<b>Acronyms and Symbols.....</b>	<b>V</b>
<b>Summary.....</b>	<b>IX</b>
<b>Samenvatting.....</b>	<b>XIII</b>
<b>Chapter 1. General introduction .....</b>	<b>1</b>
<b>1.1 Background.....</b>	<b>2</b>
<b>1.2 Effects of soil compaction .....</b>	<b>5</b>
1.2.1 Effects on soil physical and hydrological properties.....	5
1.2.2 Effects on environment and crop production .....	6
<b>1.3 Prevention of soil compaction.....</b>	<b>8</b>
1.3.1 Factors affecting soil stress .....	8
1.3.2 Soil precompression stress .....	10
1.3.3 Soil compaction risk modeling.....	10
1.3.4 Strategies to prevent soil compaction.....	13
<b>1.4 Alleviation of soil compaction .....</b>	<b>14</b>
1.4.1 Alleviation with tillage .....	14
1.4.2 Alleviation with bio tilling.....	16
<b>1.5 Detecting soil compaction distribution.....</b>	<b>17</b>
<b>1.6 Study area.....</b>	<b>19</b>
<b>1.7 Objectives .....</b>	<b>21</b>
<b>1.8 Outline of this thesis .....</b>	<b>22</b>
<b>Part I: Effects of soil compaction.....</b>	<b>25</b>
<b>Chapter 2: Quantifying the effects of top and sub soil compaction under a silt loam soil in West Europe.....</b>	<b>26</b>
<b>2.1. Introduction.....</b>	<b>27</b>
<b>2.2. Materials and methods .....</b>	<b>28</b>
2.2.1 Study site .....	28
2.2.2 Experimental design .....	30
2.2.3 Measurements.....	34
2.2.4 Data analysis.....	39
<b>2.3. Results .....</b>	<b>40</b>
2.3.1 Winter cover crop season 2016.....	40
2.3.2 Summer maize season 2017 .....	46
2.3.3 Effects of deep tillage in 2018 .....	55
<b>2.4. Discussion .....</b>	<b>57</b>
2.4.1 Effects of topsoil compaction .....	57
2.4.2 Effects of subsoil compaction.....	58
2.4.3 Alleviation of subsoil compaction by deep tillage .....	61
<b>2.5. Conclusions.....</b>	<b>61</b>

<b>Part II : Prevention of soil compaction .....</b>	<b>63</b>
<b>Chapter 3: Strategies to minimize soil compaction during seedbed preparation for winter rye.....</b>	<b>64</b>
<b>3.1. Introduction .....</b>	<b>65</b>
<b>3.2. Materials and methods .....</b>	<b>67</b>
3.2.1 Study site .....	67
3.2.2 Experimental design .....	68
3.2.3 Measurements and prediction .....	73
<b>3.3. Results .....</b>	<b>78</b>
3.3.1 Contact area, mean ground pressure and compaction risk.....	78
3.3.2 Soil physical property indicators.....	80
3.3.3 Effects on winter rye growth .....	86
<b>3.4. Discussion .....</b>	<b>88</b>
<b>3.5. Conclusions .....</b>	<b>91</b>
<b>Chapter 4: Effects of soil wetness and tyre pressure on soil physical quality and maize growth by a slurry spreader system .....</b>	<b>93</b>
<b>4.1. Introduction .....</b>	<b>95</b>
<b>4.2. Materials and methods .....</b>	<b>97</b>
4.2.1 Study site .....	97
4.2.2 Experimental design .....	97
4.2.3 Measurements and prediction .....	100
4.2.4 Maize season management, sampling and analysis .....	107
4.2.5 Data analysis.....	108
<b>4.3. Results .....</b>	<b>109</b>
4.3.1 Contact area, rut depth and mean ground pressure among treatments .....	109
4.3.2 Soil physical quality evaluation.....	110
4.3.3 X-ray micro-computed tomography analysis.....	116
4.3.4 Evaluation of soil compaction risk by Terranimo® .....	119
4.3.5 Maize biomass in relation to soil physical quality and total-N uptake .....	120
<b>4.4. Discussion .....</b>	<b>123</b>
4.4.1 Effects of soil moisture and tyre pressure on soil physical quality .....	123
4.4.2 Comparison of X-ray computed tomography analysis with conventional lab methods .....	125
4.4.3 Effects of traffic on maize growing season .....	127
<b>4.5. Conclusions .....</b>	<b>128</b>
<b>Part III : Alleviation of soil compaction.....</b>	<b>129</b>
<b>Chapter 5: Short-term effects of cover crops and tillage methods on soil physical properties and maize growth in a sandy loam soil .....</b>	<b>130</b>
<b>5.1. Introduction .....</b>	<b>131</b>
<b>5.2. Materials and methods .....</b>	<b>134</b>
5.2.1 Study site .....	134

5.2.2 Experimental design .....	136
5.2.3 Winter season management, sampling and analysis.....	138
5.2.4 Summer season management, sampling and analysis .....	139
5.2.5 Statistical analysis.....	143
<b>5.3. Results .....</b>	<b>143</b>
5.3.1 Winter cover crops season: root number density .....	143
5.3.2 Summer maize season .....	144
<b>5.4. Discussion .....</b>	<b>154</b>
<b>5.5. Conclusions .....</b>	<b>157</b>
<b><i>Chapter 6: Impact of potential bio-subsoilers on pore network of a severely compacted subsoil .....</i></b>	<b><i>159</i></b>
<b>6.1. Introduction .....</b>	<b>161</b>
<b>6.2. Materials and methods .....</b>	<b>164</b>
6.2.1 Soil samples .....	164
6.2.2 Experimental treatments.....	165
6.2.3 Image acquisition and processing.....	167
6.2.4 Statistical analyses.....	172
<b>6.3. Results .....</b>	<b>173</b>
6.3.1 Pore characteristics .....	173
6.3.2 Pore size distribution .....	177
6.3.3 Pore shape classification .....	179
<b>6.4. Discussion .....</b>	<b>182</b>
6.4.1 Effect of potential bio-subsoilers on pore network.....	182
6.4.2 Role of plant/root type in compaction mitigation.....	186
<b>6.5. Conclusion .....</b>	<b>189</b>
<b><i>Part IV: Detection of soil compaction spatial variability .....</i></b>	<b><i>191</i></b>
<b><i>Chapter 7: Detecting spatial variability of soil compaction using soil apparent electrical conductivity and maize canopy height .....</i></b>	<b><i>192</i></b>
<b>7.1. Introduction.....</b>	<b>193</b>
<b>7.2. Materials and methods .....</b>	<b>195</b>
7.2.1 Study site .....	195
7.2.2 ECa measurements and analysis .....	196
7.2.3 Soil sampling strategy.....	196
7.2.4 Maize canopy height measurements .....	199
7.2.5 Maize above-ground biomass .....	201
7.2.6 Statistical .....	201
<b>7.3. Results .....</b>	<b>202</b>
7.3.1 Soil properties and maize canopy height variability.....	202
7.3.2 Relationships between soil properties and ECa .....	206
7.3.3 Relationship between maize canopy height and soil properties.....	208
7.3.4 Relationship between maize canopy height and ECa .....	209

<b>7.4. Discussion .....</b>	<b>211</b>
7.4.1 Detecting soil compaction with ECa .....	211
7.4.2 Soil compaction with maize canopy height .....	212
7.4.3 ECa with maize canopy height.....	212
<b>7.5. Conclusions.....</b>	<b>213</b>
<b><i>Chapter 8 : General conclusions and future perspectives.....</i></b>	<b><i>215</i></b>
8.1 Effects of soil compaction .....	217
8.2 Strategies to prevent soil compaction .....	219
8.3 Alleviation of soil compaction .....	221
8.4 Detecting soil compaction .....	223
8.5 Concluding and future perspectives .....	225
<b><i>References:.....</i></b>	<b><i>226</i></b>
<b><i>Appendices:.....</i></b>	<b><i>243</i></b>
<b><i>Curriculum Vitae.....</i></b>	<b><i>261</i></b>

## Acronyms and Symbols

$\alpha$ (cm <sup>-1</sup> )	positively related to the reciprocal of air-entry pressure
AC	air capacity
ab	abnormal
AGB_d	dry above-ground biomass
AGB_f	fresh above-ground biomass
$b_0$	number of connected components
$b_1$	number of holes
$b_2$	number of tunnels
BD	bulk density
CHM	canopy height model
D	dry soil condition
DEM	digital elevation model
di	diameter of each macropore within the ROI
DT	deep tillage
DT_SC	deep tillage with topsoil compaction
DTM	digital terrain model
e	exceptional
ECa	soil apparent electrical conductivity
ECs	Soil salinity
EMI	electromagnetic induction
H	high subsoil compaction in the headland zone
$h$	matric suction
H_SC	high subsoil compaction with topsoil compaction in the headland zone

IT	intensive tillage indicated the mouldboard ploughing
K(h)	hydraulic conductivity curve
Ka	air permeability
Ks	saturated water conductivity
M	moist soil condition
MCH	maize 90% canopy height
n	pore-size distribution index
NDT	no deep tillage
NDT_SC	no deep tillage with topsoil compaction
OC	organic carbon content
Pact	actual vertical stress
PAWC	plant-available water capacity
Pc	soil precompression stress
PR	penetration resistance
$\theta(\eta)$	soil-water content ( $\text{cm}^3 \text{ cm}^{-3}$ ) at matric suction head $h$ (cm)
$\theta_p$	residual soil water content
$\theta_\sigma$	saturated soil water content
r	spearman's rank correlation coefficient
R2	coefficient of determination
RFC	relative field capacity
ROI	a region of interest (for x-ray CT)
RTK-GPS	Real-time kinematic GPS
S	standard tyre
S index	soil structure indicator according to Reynolds et al. (2009) and (Dexter, 2004)
SC	topsoil compaction (referring soil within plough depth)

SCI	soil compaction index
SD	standard deviation
SOC	soil organic carbon content
ST	strip tillage
SubVESS	visual evaluation of subsoil structure
SWRC	Soil water retention curves
TDR	time-domain reflectometry
$v$	Concentration factor
$v_a$	very abnormal
VESS	evaluation of soil structure
$V_i$	volume of each macropore within the ROI
W	wide tyre
WM	white mustard
WR	winter rye
X-ray CT	X-ray Computed Tomography
$\theta_m$	soil gravimetric water content



## Summary

From the working animals to steam engines, especially during the modernization of agriculture over the past decades, the weight of agricultural machines has dramatically increased, which greatly augmented the soil compaction risks. As a result, soil compaction has been recognised as one of the main threats to sustainable agriculture.

A systematic evaluation of soil compaction is still lacking. This is probably because evaluation methods were lacking or the cost of regenerating at a field scale are high. Besides, unlike soil erosion or salinization, soil compaction does not have a clear visible exposure and evident marks on the surface. Correspondingly, many adverse effects caused by soil compaction are often blamed on other causes and less is known about soil compaction. In this dissertation, four aspects of soil compaction were addressed: effects, prevention, alleviation and detection, named as “EPAD” system (an abbreviation of the first letter). The study was conducted on loam (silt loam to sandy loam) soils in the Flemish region of Belgium under temperate maritime climate and on sandy loam soil at Aarslev site of Denmark under a temperate climate.

In the “Effects” section, the effects of soil compaction were evaluated, from both freshly induced topsoil compaction by field traffic operations prior to sowing and already long-term existing subsoil compaction with two different levels, i.e., highly compacted in a headland zone and less compacted at an in-field zone.

In the “Prevention” section, strategies to minimize or prevent soil compaction by changing the operational characteristics of a seeding combination and a slurry spreader (i.e., tyre pressure, tyre type and soil moisture condition) were evaluated at loose and relatively compacted soil, respectively.

In the “Alleviation” section, it was mainly focused on testing subsoil compaction alleviation strategies by using deep tillage and different cover crops as bio drillers. Besides, the strip tillage which is rather new in the study area was also compared with the traditional mouldboard plough in alleviating topsoil compaction.

In the “Detection” section, Electromagnetic Induction and drone images were used to detect spatial variability of soil compaction within a field, which is urgently needed in precision agriculture.

The main outcomes of this dissertation are:

- ❖ **Effects:** Topsoil compaction induced by seedbed preparation did not affect maize (*Zea mays* L.) growth when traffic is limited. However, multiple machinery passes with overlapping tracks should be avoided as it can greatly decrease maize growth. In the winter season, all kinds of traffic did affect cover crop growth. For subsoil compaction, both visual evaluation and lab or field-based measurements indicate that soil physical and hydraulic properties, as well as root number density, were different between the headland (heavy compaction) and in-field zones (moderate compaction). As a result, water transport and root-water uptake were restricted in the headland zone. This resulted in a limited supply of water to the subsoil and higher water content in the topsoil in the wet winter season, which might have reduced winter rye growth because of poor drainage. On the contrary, subsoil compaction restricted access to water and nutrients in the subsoil causing a decrease in above-ground biomass of maize in the dry summer of 2017. Soil mineral N leaching risk was higher in the headland zone, most probably because of reduced nutrient uptake following restricted root growth. Crop growth was restricted in the headland zone during both winter and summer seasons.

❖ **Prevention:** When sowing a cover crop, the measured soil tyre contact area and mean ground pressure from a sowing machine were consistent with the Terranimo® modelling results, where dry soil moisture, wide tyre type and low tyre pressure had lower soil compaction risks. However, no differences in selected soil quality indicators were found among treatments with different soil moisture conditions at wheeling, tyre type and tyre pressure and only once trafficked. Differences only existed between trafficked and control treatments. Similarly, shoot biomass and root biomass density of winter rye were significantly ( $P < 0.05$ ) reduced in the trafficked parts compared to the controls under both moist and dry conditions at wheeling.

In the spring, by using a slurry spreader, soil physical properties were affected by soil moisture and tyre pressure. Penetration resistance was significantly higher ( $P < 0.05$ ) in the top 20 cm layer when trafficked under moist conditions than under dry conditions. A clear trend of increased bulk density and macro-porosity ( $0.05 < P < 0.10$ ) was observed between moist and dry conditions at 10 cm depth, while tyre pressure showed fewer effects. There was no significant difference in soil properties at greater depths. Terranimo® could well predict the contact area and mean ground pressure. It indicated considerable compaction risk from the tractor's rear wheels, though the overall compaction risk seemed overestimated as changes in soil compaction-related soil properties were minor.

❖ **Alleviation:** For topsoil compaction, strip tillage had the same alleviation function compared with mouldboard ploughing in this study year. However, it is still debatable about the effects of strip tillage on crop yield among different study areas.

For subsoil compaction, deep tillage significantly increased summer maize growth (i.e., maize canopy height) and the benefits can be detectable after three growing seasons (~1.5 years later). Biodrilling with tap-rooted cover crops has a great potential to alleviate subsoil compaction. Winter cover crops likewhite mustard increased the consecutive summer maize root number density at 30-40 cm depth compared with winter rye. Chicory and lucerne performed better than spring barley as reference, and radish and tall fescue by creating a larger, more connected and complex pore network as was demonstrated with X-ray CT-scans. Longer-term crop growth is needed to derive a marked loosening effect in the compacted layer.

- ❖ **Detection:** Detecting soil compaction in a field-scale was not possible by EMI in this site-specific study because of the variability of other soil properties (i.e. clay content). Interestingly, crop growth characteristics derived from drones were a good indicator of spatial variability of soil compaction. However, this study was restricted to one season and one field only. Further research is encouraged to test the possibility of using EMI to map soil compaction across different soil types and climate conditions.

## Samenvatting

Met de modernisering van de landbouw in de afgelopen decennia is het gewicht van landbouwmachines drastisch toegenomen, waardoor de risico's op bodemverdichting sterk zijn verhoogd. Als gevolg daarvan wordt bodemverdichting als een van de belangrijkste bedreigingen voor een duurzame landbouw gezien.

Een systematische evaluatie van bodemverdichting ontbreekt echter. Dit komt waarschijnlijk omdat de evaluatiemethoden ontoereikend zijn of omdat de kosten van herstel op veldniveau hoog zijn. Bovendien is bodemverdichting, in tegenstelling tot bodemerosie of verzilting, niet duidelijk zichtbaar en ontbreken vaak duidelijke sporen aan het oppervlak. Daarom worden negatieve effecten van bodemverdichting vaak toegeschreven aan andere oorzaken en wordt met bodemverdichting minder rekening gehouden. In dit proefschrift werden vier aspecten van bodemverdichting behandeld: effecten, preventie, opheffen en detectie, of kortweg "EPAD" genoemd (effects, prevention, alleviation, detection). Het onderzoek werd uitgevoerd op leem- en zandleembodems in de Vlaamse regio van België onder een gematigd zeeklimaat en op zandleembodems in Syddanmark in Denemarken onder een gematigd zeeklimaat.

In het deel "Effecten" werden de effecten van bodemverdichting geëvalueerd, zowel van nieuw geïnduceerde bovengrondverdichting door berijden vóór het zaaien als van reeds lang bestaande ondergrondverdichting en dit bij twee verschillende niveaus, met name sterk verdicht ter hoogte van de kopakker en minder verdicht op het middendeel. Het meten aan de kopakker laat toe in te schatten wat gevolgen van in de toekomst mogelijk toenemende verdichting kunnen zijn.

In het onderdeel "Preventie" werden strategieën om bodemverdichting te minimaliseren of te voorkomen door de operationele kenmerken van een

zaaicombinatie en een mengmestverspreider (d.w.z. bandenspanning, bandtype en bodemvoch) te wijzigen, respectievelijk bij losse en relatief verdichte grond geëvalueerd.

In het onderdeel "Opheffen" werd aandacht besteed aan het testen van strategieën om bodemverdichting (deels) op te heffen met diepbewerking en verschillende groenbedekkers. Daarnaast werd de in het studiegebied vrij nieuwe strokengrondbewerking vergeleken met de traditioneel ploegen voor het opheffen van de bovengrondse verdichting.

In de sectie "Detectie" werden Elektromagnetische Inductie en drone-beelden gebruikt om de ruimtelijke variabiliteit van de bodemverdichting binnen een veld te detecteren, wat een meerwaarde is voor de precisielandbouw.

De belangrijkste bevindingen van dit proefschrift zijn:

**Effecten:** Bodemverdichting geïnduceerd door zaaibedbereiding had geen invloed op de groei van maïs (*Zea mays* L.) wanneer het berijden beperkt was. Meerdere machinegangen met overlappende sporen moeten echter worden vermeden, omdat dit de groei van maïs sterk kan verminderen. In het winterseizoen had het berijden wel invloed op de groei van de gewassen, zoals bijvoorbeeld winterrogge (*Secale cereale* L.). Voor bodemverdichting geven zowel visuele evaluatie als laboratorium- of veldmetingen aan dat de fysische en hydraulische eigenschappen van de bodem, evenals de wortelaantaldichtheid, verschillend waren tussen de kopakker (zware verdichting) en de middendelen (matige verdichting). Als gevolg hiervan was watertransport en wateropname door wortels ter hoogte van de kopakker beperkt. Dit resulteerde in een beperkte watertoevoer naar de ondergrond en een hoger vochtgehalte in de bovengrond in het natte winterseizoen, waardoor de groei van winterrogge mogelijk werd beperkt door een slechte drainage. Integendeel, de

verdichting van de ondergrond beperkte de toegang tot water en voedingsstoffen in de ondergrond, waardoor de bovengrondse biomassa van maïs in de droge zomer van 2017 afnam. Het risico op uitspoeling van stikstof was hoger ter hoogte van de kopakker, hoogstwaarschijnlijk vanwege een verminderde opname van voedingsstoffen als gevolg van een beperkte wortelgroei. De groei van de gewassen op de kopakker werd zowel in het winter- als het zomerseizoen beperkt.

**Preventie:** Bij het zaaien van een groenbedekker waren het gemeten contactoppervlak van de band en de gemiddelde bodemdruk van de zaaimachine consistent met de resultaten bekomen met het Terranimo®-model, waarbij een laag bodemvochtgehalte, het type (brede) band en een lage bandenspanning minder risico's op bodemverdichting met zich meebrachten. Er werden echter geen verschillen in de geselecteerde bodemkwaliteitsindicatoren gevonden tussen behandelingen met verschillende bodemvochtcondities bij het rijden, het bandtype en de bandenspanning en slechts eenmalig verkeer. Er werden enkel verschillen gevonden tussen de bereden percelen en de onbereden controle. Op dezelfde manier nam de scheutbiomassa en de wortelbiomassadichtheid van winterrogge significant ( $P < 0,05$ ) af in de bereden percelen in vergelijking met de controles onder zowel vochtige als droge omstandigheden (tijdens het berijden).

In het voorjaar werden de fysische eigenschappen van de bodem na berijden met een mestverspreider beïnvloed door de bodemvochtigheid en de bandenspanning. De penetratieweerstand van de bodem was aanzienlijk hoger ( $P < 0,05$ ) in de bovenste 20 cm-laag wanneer er onder vochtige omstandigheden werd bereden dan onder droge omstandigheden. Er werd een duidelijke trend van verhoogde bulkdichtheid en macro-porositeit ( $0,05 < P < 0,10$ ) waargenomen tussen vochtige en droge condities op 10 cm diepte, terwijl de bandendruk minder effect

vertoonde. Er was geen significant verschil in bodemeigenschappen op grotere diepte. Terranimo® kon het contactoppervlak en de gemiddelde bodemdruk goed voorspellen. Dit duidde op een aanzienlijk verdichtingsrisico van de achterwielen van de tractor, hoewel het totale verdichtingsrisico overschat leek omdat de veranderingen in de bodemeigenschappen gering waren.

**Opheffen:** Voor bovengrondse verdichting had strokenbewerkingen dezelfde opheffunctie als het ploegen. Het werkelijke effect van strokenbewerkingen op de gewasopbrengst blijft echter onduidelijk. Bij bodemverdichting heeft diepe grondbewerking de groei van zomermaïs (d.w.z. de maïshoogte) significant verhoogd en zijn de voordelen na drie groeiseizoenen (~1,5 jaar later) aantoonbaar. Groenbedekkers met penwortels hebben een groot potentieel om de verdichting van de ondergrond te verlichten. Gele mosterd (*Sinapis alba* L.) resulteerde in een verhoging van de worteldichtheid van de daarna geteelde zomermaïs op 30-40 cm diepte ten opzichte van winterrogge. Chicorei (*Cichorium intybus* L.) en luzerne (*Medicago sativa* L.) presteerden beter dan de referentie zomergerst (*Hordeum vulgare* L.), en radijs (*Raphanus sativus* L.) en hoog zwenkgras (*Festuca arundinacea* L.) door het creëren van een groter, meer verbonden en complexer poriënnetwerk, zoals werd gedemonstreerd met X-stralen CT-scans. Een langer durende gewasgroei (langer dan de 1,5 jaar durende looptijd van de proef) is echter nodig om een duidelijker losmakend effect in de verdichte laag te kunnen waarnemen.

**Detectie:** Het detecteren van een verdichte laag met EMI was in deze site-specifieke studie niet mogelijk vanwege de variabiliteit van andere bodemeigenschappen (met name kleigehalte). Interessant is dat gewasgroeikarakteristieken gemeten met drones een goede indicator waren voor de ruimtelijke variabiliteit van

bodemverdichting. Deze studie was echter beperkt tot één seizoen en één veld. Verder onderzoek naar de mogelijkheid om EMI te gebruiken voor het in kaart brengen van bodemverdichting over verschillende bodemtypes en klimaatomstandigheden is aangewezen.



## **Chapter 1. General introduction**

### 1.1 Background

Soil compaction is the compression of unsaturated soil and refers to “the process by which the soil grains are rearranged to decrease void space and bring them into closer contact with one another, thereby increasing the bulk density” (Soil Science Society of America 1997). It can be evaluated by comparing soil strength (soil precompression stress, i.e., stress when soil changes from elastic to plastic deformation) with soil stress induced by wheels of machinery trafficking the soil. If the induced stress is close to or exceeds soil precompression stress, soil shows a risk to compaction (Keller *et al.* 2007; Schjønning *et al.* 2015). With the modernisation of agriculture, the weight of agricultural machines dramatically increased in the past decades. For instance, Keller *et al.* (2019) evaluated the wheel loads of combined harvesters using a Danish dataset (Schjønning *et al.* 2015) and of tractors based on a John Deere dataset (Deere & Company, Moine, IL, USA) over the last sixty years. They found that combined harvesters’ wheel loads have increased from ~1.5 Mg to 9 Mg, and that of tractors from ~1 Mg to more than 4 Mg. As a result, the simulated soil mechanical stress was also greatly increased even considered the increase of tyre volume (e.g., the increasing tyre width).

With long-time and ever-increasing mechanization in agriculture, soil compaction is recognised as one of the main threats to sustainable agriculture in Europe by the European Commission (Alameda *et al.* 2012). Estimates from Oldeman (1991) indicate that around one third of the arable land in Europe has been compacted to some degree and globally, around 68 Mha are affected by soil compaction, with 33, 18, 10, 2 and 1 Mha in Europe, Africa, Asian, Australia and North America, respectively. Data about the current state of soil compaction do not seem to be available. Unlike

soil erosion and salinization which show strong evidence on the soil surface, soil compaction is a hidden form of degradation without clear visible exposure and evident marks on the surface. This may lead to specific problems that are often blamed on other causes (Hamza and Anderson 2005).

Soil compaction has been studied for decades. In civil or construction engineering, soil compaction measurements and studies have existed for a long time while it did not attract attention in agriculture until the middle of the twentieth century, before which the focus was primarily on soil fertilization. This is probably because evaluation methods were lacking or the high cost of regenerating at field scale (Horn *et al.* 2007). According to the number of SCI publications on the topic of 'soil compaction' in the soil science category of Web of Science from 1955-2018, soil compaction research rapidly increased in the past three decades, with the first soil compaction publication in 1966 (Fig.1-1) though publications with other language has been seen before (for instance Söhne (1953) in German). A similar trend was also reported by Cornelis (2014), who used '\*soil compaction' as a searching keyword through all subjects. This research trend is also consistently corresponded with the agricultural machinery usage intensity as referred above.

With growing research interest and increasing numbers of articles, research questions evolved and expanded. At first, when soil compaction occurred with the appearance of agriculture machinery, researches were more focused on the effect of soil compaction on crop growth or production and factors that affect soil compaction (Soane *et al.* 1980a, 1980b; Soane *et al.* 1982) (also according to the title of SCI publications from 1960 to 1980). Later, research questions moved to subsoil compaction, which is not only related with crop production but also with environment

and sustainable development (Horn *et al.* 2000). Recently, with the steadily increasing mechanisation in agriculture, soil compaction levels are continuously changing accordingly. In addition to that, climate change leads to more extreme weather, e.g., exceedingly dry and hot weather, or wetter periods with increased rainfall intensities. As water retention and up- and downward water movement become more important, the evaluation of soil compaction becomes increasingly important. Improved or newly built technologies provide new opportunities, e.g., use of X-ray computed tomography (X-ray CT) and geophysics in soil science and precision agriculture systems. Those new technologies in agriculture have widely been used recently (Lamandé *et al.* 2013b; Colombi and Walter 2017; Romero-Ruiz *et al.* 2018; Keller *et al.* 2019; Ren *et al.* 2019b).

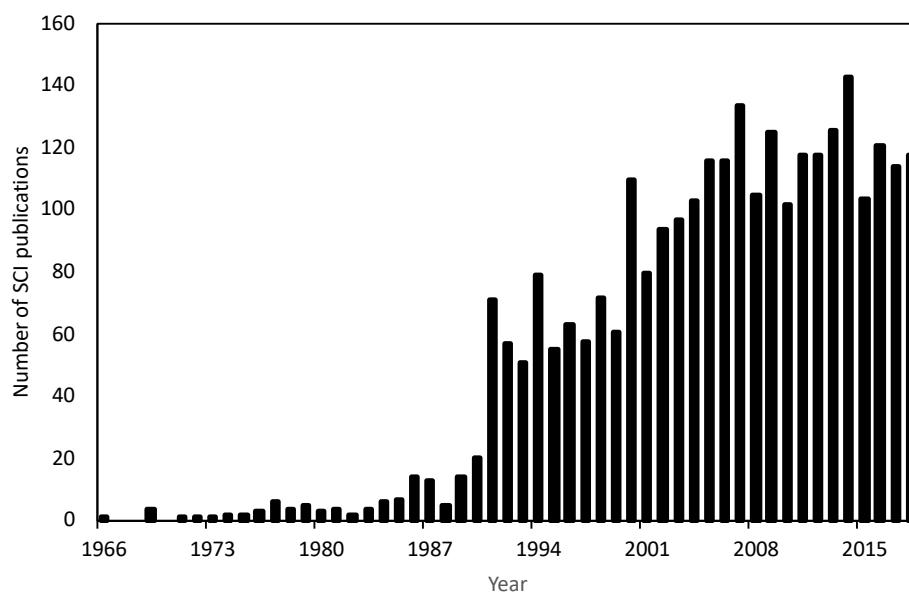


Fig.1-1. Number of SCI publications including the topic of 'soil compaction' in the soil science category of Web of Science per year (1955-2018).

## 1.2 Effects of soil compaction

Soil compaction can have both positive and negative effects. In civil engineering, compacted soil is welcomed as compacted soil has high strength. In agriculture, compaction can also have positive effects by holding water and nutrition in the top layer. For instance, it can increase the contact between seeds or roots and soil, which can be beneficial to plant growth (Håkansson 2005; Arvidsson and Hakansson 2014). Some studies show that soil compaction can even increase the unsaturated hydraulic conductivity as the small water filled pores' connectivity increased (Alaoui *et al.* 2011). However, most soil compaction has adverse effects and greatly threatens sustainable agriculture. Here, I will discuss the adverse effects of soil compaction on soil quality, crop growth and environment.

### 1.2.1 Effects on soil physical and hydrological properties

Soil compaction decreases soil air capacity and infiltration capacity, and increases bulk density and soil strength by altering the pore system (Soane *et al.* 1980a; Day and Bassuk 1994; Unger and Kaspar 1994; Hamza and Anderson 2005; Alaoui *et al.* 2011; Keller *et al.* 2013; Nawaz *et al.* 2013; Schjønning *et al.* 2013; Kuncoro *et al.* 2014; Schjønning *et al.* 2015). Those general conclusions have been reported widely. However, there are few field studies that quantify the effects of soil compaction on a range of soil physical quality indicators. Also, short-time experiments or experiments with less (but realistic) number of passes in contrast with multiple passes as in many studies are scarce. This is because differences in soil physical quality are more difficult to detect and the compaction effects are often not clear in such experiments (Arvidsson and Håkansson 1996; Berisso *et al.* 2012; Schjønning *et al.* 2013; Schjønning *et al.* 2016; Schjønning *et al.* 2017). Fortunately, emerging

methods such as X-ray CT, allow to detect soil pore structure directly and avoid the assumptions and restrictions of indirect methods (Katuwal *et al.* 2015a; Zhou *et al.* 2017).

### **1.2.2 Effects on environment and crop production**

The effects of soil compaction (both top and subsoil) on crop growth and the environment are not always straightforward. Previous studies show that compaction induces water runoff and soil erosion hence increases the risks for floods, mud streams and droughts; restricts water and gas movement; enhances leaching of nutrients and agrochemicals hence reduces water quality; increases emissions of greenhouse gases, particularly of N<sub>2</sub>O and CH<sub>4</sub> (van Asselen *et al.* 2009; Beylich *et al.* 2010; Bingham *et al.* 2010; Alaoui *et al.* 2011; Tracy *et al.* 2011; Cambi *et al.* 2015; Chamen *et al.* 2015). All above findings are soil and environment dependent, and further evaluation in different sites is needed.

Soil compaction can greatly affect root system architecture by enlarges soil mechanical impedance. The effects are mainly reflected in the following aspects: 1) soil compaction can greatly restrict root elongation and increase root diameter because thick roots normally have stronger penetration ability; 2) Root angle is the degree from soil horizontal surface and it increases at a certain degree of soil compaction because more roots need to penetrate this compacted layer. However, with the increasing of soil compaction level, root angle can be decreased because more horizontal roots developed (Correa *et al.* 2019); 3) Root tortuosity is the waviness of the growth pattern according to Popova *et al.* (2016). It increased with the increasing of soil compaction levels in the same soil type and increased with the decreasing of clay content among different soil types (Tracy *et al.* 2012; Popova *et al.* 2016); 4) Root

hairs which are root epidermal cells of unicellular and unbranched extensions, can also be decreased under compacted soil (Correa *et al.* 2019); 5) Root compensatory growth may appear in compacted soil, where root density was larger and less in the loose and compacted layer, respectively, compared with homogeneous loose soil (Correa *et al.* 2019). Overall, compacted soil can restrict root growth. However, it is poorly understood how the root system architecture responds to soil compaction for different crops and their benefits to improve soil structure is still not clear. An extended introduction on root growth can be found in chapter 5&6.

Soil compaction can greatly restrict crop yield or biomass. However, it also depends on soil type, crop type, climatic conditions and compaction levels. Research is lacking to quantify the effect of each factor separately (Correa *et al.* 2019). In general, crop yield is more sensitive for topsoil compaction (above tillage depth) compared with subsoil compaction; however, subsoil effects can last for decades (Håkansson and Reeder 1994). For instance, Håkansson and Reeder (1994) summarized multiple field studies and found yield losses from lower subsoil (deeper than 40 cm) to exist for more than 15 years, while top soil compaction affected yield for shorter time but with as much as 15% yield decrease (Fig.1-3). Note that the depth of top and sub soil layers is also related with ploughing depth, soil type and crop types. Therefore, quantifying the effects of different types of soil compaction on crop growth is still needed in different regions (Håkansson 2005).

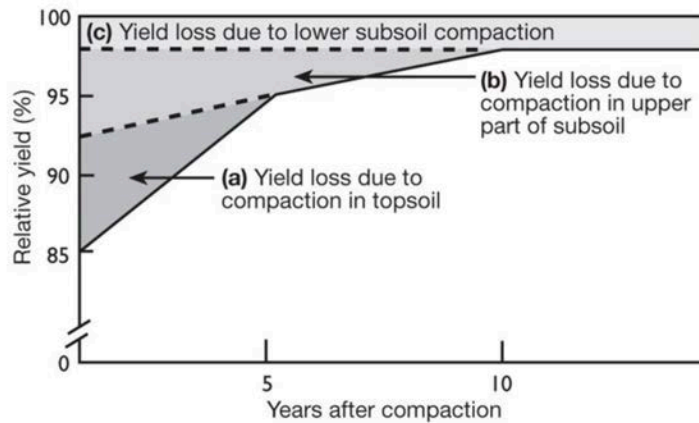


Fig.1-3. Relative crop yield on compacted soil under moldboard ploughing at different depth: (a) 0 - 25 cm (plough layer); (b) 25 - 40 cm; (c) > 40 cm; from Duiker (2005b) based on Håkansson and Reeder (1994).

## 1.3 Prevention of soil compaction

### 1.3.1 Factors affecting soil stress

Soil stress is the stress that relates to wheel load, tyre dimensions, tyre inflation pressure and soil properties (Keller *et al.* 2016). Wheel load is the top priority factor that should be considered in soil compaction (Fig.1-2a). It controls both top and subsoil compaction levels, especially for subsoil compaction. For instance, under the same soil conditions, wheel load is the main factor controlling vertical distribution of stress. Higher wheel load results in a higher concentration factor, which is used to describe the stress propagation shape and it becomes more narrow (or towards the central) with increasing of concentration factor, according to the elasticity theory (Fig.1-2b) (Söhne 1953; Lamandé and Schjønning 2011c). Correspondingly, stress penetrates much deeper under high wheel load (Lamandé *et al.* 2007). Wheel load is not only related to machinery weight but also to tractor types and machine combinations. For

instance, a tractor with a trailer can greatly increase the tractor's rear wheel load by adding transferred load from the trailer (Schjønning *et al.* 2006).

Tyre inflation pressure is the most easy and fast changeable factor. It directly affects the contact area and ground pressure which in turn affects soil stress and its distribution. Within a certain range, soil stress increases with tyre pressure with the latter explaining most variation in soil stress in both top and subsoil under different wheel loads (Schjønning *et al.* 2012). Soil properties affect contact area and stress propagation. For instance, under wet soil conditions, tyre-soil contact area increases and vertical soil stress propagates deeper because of an increasing concentration factor (Fig.1-2b) (Söhne 1953; Lamandé and Schjønning 2011c).

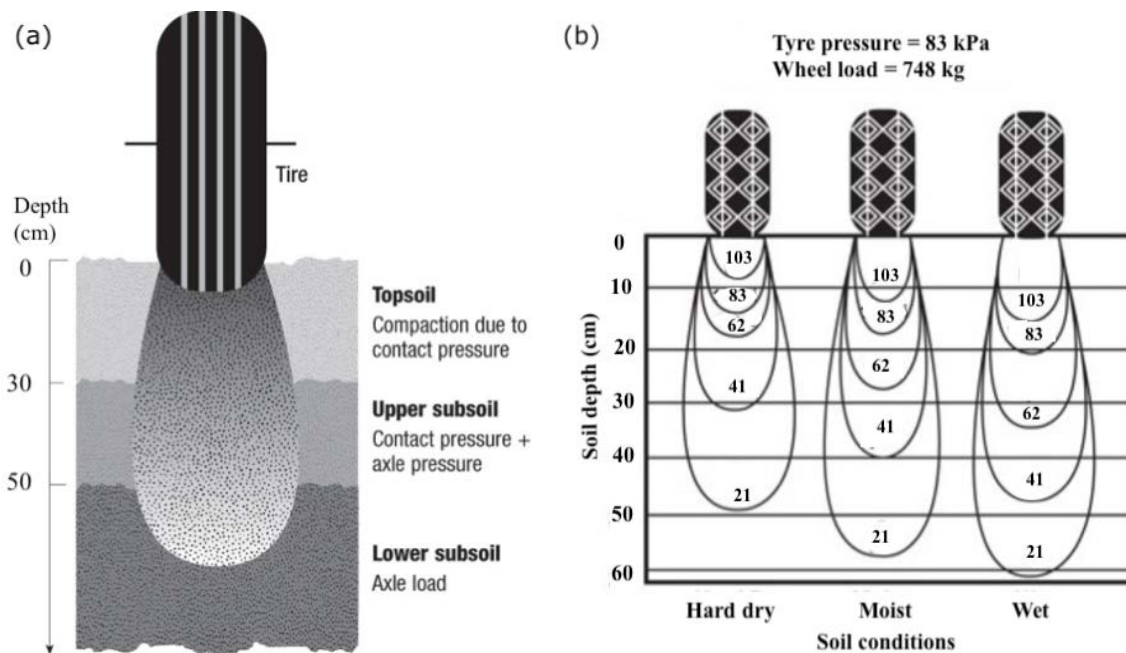


Fig.1-2. Factors affecting soil compaction: (a) wheel loads at different depths (Duiker 2005a); (b) effect of soil wetness on stress propagation based on Söhne (1953) equation (Dyck 2017).

### 1.3.2 Soil precompression stress

Soil precompression stress ( $P_c$ ) is defined as the stress when soil changes from elastic to plastic deformation. It is also defined as soil resistance to compressive stresses.  $P_c$  can be measured in a lab by using an uniaxial compression apparatus (oedometer) (De Pue *et al.* 2019a) or pedotransfer functions (Lebert and Horn 1991).  $P_c$  mainly depends on soil texture, bulk density, organic matter content and soil wetness (Lebert and Horn 1991; Hamza and Anderson 2005). Among them, wetness is regarded as the most important and most dynamic factor influencing soil compaction processes (Soane and Van Ouwerkerk 1994).

### 1.3.3 Soil compaction risk modeling

Modeling soil compaction risk is essential to predict the soil's vulnerability to compaction and understand the soil compaction process. In total, four main steps are involved in modeling soil compaction risk.

Firstly, the model's top boundary (i.e., tyre-soil contact area and soil boundary stress distribution) needs to be determined. The tyre-soil contact area has long been assumed as of circular shape and stress distribution was regarded as homogeneous within the contact area (Kirby 1999; Arvidsson *et al.* 2002; Poodt *et al.* 2003; Van den Akker 2004). However, those assumptions are not consistent with more recent findings showing that the distribution of the stress at the tyre-soil contact perpendicular to the driving direction exhibits two or more peaks (Keller 2005; Schjønning *et al.* 2008). Correspondingly, Berisso *et al.* (2013b) found that air permeability ( $K_a$ ) and continuity of soil pores were much smaller at the edge of the wheel ruts compared with mid-rut values. The reason for the widespread idea of the circular stress distribution is that there are too many parameters that make more precise predictions difficult (Söhne

1953; Smith *et al.* 2000). To overcome this problem, Keller (2005) proposed a simple method to predict contact area and stress distribution (both normal and shear stress) by using easily accessible machinery parameters, i.e., wheel load, tyre inflation pressure, recommended tyre inflation pressure at a given load, tyre width and tyre diameter. Later, this model was summarized and called FRIDA by Schjønning *et al.* (2008). Contact area ( $\Omega$ ) and normal stress distribution ( $\sigma(\mathbf{x}, \mathbf{y})$ ) in the FRIDA model are calculated as:

$$\Omega = \left\{ (x, y) \mid |x/a|^n + |y/b|^n \leq 1 \right\} \quad (1-1)$$

where  $\Omega$  is the soil-tyre contact area of a super ellipse ( $\text{m}^2$ );  $a$  and  $b$  are half the width of the minor and major axes (m), and  $n$  is a positive real number related to the shape;  $x$  is the distance along the driving direction and  $y$  is the distance perpendicular to the driving direction (m).

$$\sigma(x, y) = F_{\text{wheel}} C(\alpha, \beta, a, b, n) f(x, y) g(x, y)$$

$$\text{for } (x, y) \in \Omega \text{ and } 0 \text{ otherwise:} \quad (1-2)$$

$$f(x, y) = \left\{ 1 - \left| \frac{x}{l_x(y)} \right|^\alpha \right\} \quad (1-3)$$

$$g(x, y) = \left\{ \left( 1 - \left| \frac{y}{w_y(x)} \right| \right) \exp \left( -\beta \left( 1 - \left| \frac{y}{w_y(x)} \right| \right) \right) / gm \right\} \quad (1-4)$$

where  $F_{\text{wheel}}$  is the wheel load in kN;  $\alpha, \beta$  are form parameter for stress distribution in the driving direction and perpendicular to the driving direction, dimensionless;  $C(\alpha, \beta, a, b, n)$  is a function of the parameters  $\alpha, \beta, a, b$  and  $n$  which define an integration

constant ensuring that the total load is  $F_{\text{wheel}}$ , when integrating stress  $\sigma(x, y)$  over the contact area  $\Omega$ .  $g_m$  is the maximum value of  $g$  in the range  $(0 < y < w_y(x))$  expressed in terms of  $\beta$ : with for  $\beta \leq 1$ ,  $g_m = \exp(-\beta)$  and for  $\beta > 1$ ,  $g_m = \exp(-1)/\beta$ ; Furthermore,  $w_y(x)$  is the half width at  $x$  in the  $y$ -direction and  $l_x(y)$  is the half length of footprint at  $y$  in the  $x$ -direction.

The second step comprises calculating the stress propagation. Once the top boundary condition is fixed, vertical stress can be calculated. Depending on the way of predicting soil stress propagation, soil compaction models can be divided into two types, analytical and numerical ones. Analytical models are based on the Boussinesq equation (Boussinesq 1885), first introduced to evaluate stresses caused by external loads. Later, Fröhlich (1934) modified it and regarded the whole contact area as one point. Söhne (1953) improved it and considered the contact area as consisting of multiple points. For numerical models, finite element models (FEM) and discrete element models (DEM) are the most common used ones (Abu-Hamdeh and Reeder 2003). However, as numerical models normally require a large number of parameters and analytical models already provide in many cases satisfactory results, analytical models have been most widely adopted for soil compaction studies in an agricultural context. Examples are SOCOMO (Van den Akker 2004), SoilFlex (Keller *et al.* 2007) and Terranimo® (Lassen *et al.* 2013; Stettler *et al.* 2014). The Söhne (1953) equation that is used in Terranimo® can be written as:

$$\sigma_{zz} = \sum_{i=1}^{i=n} (\sigma_{zz})_i = \sum_{i=1}^{i=n} \frac{vP_i}{2\pi z^2} \cos^{\nu+2} \psi \quad (1-5)$$

where  $\sigma_{zz}$  is the vertical stress distribution in the contact area at depth  $z$ ;  $i$  is an element divided into  $n$  elements from the contact area;  $\psi$  is the angle in degrees between the

normal load vector and the position vector from the point load to the desired point;  $v$  is concentration factor according to Söhne (1953);  $z$  is depth;  $P_i$  is the point load for the  $i^{\text{th}}$  load cell (stress sensor) in the contact area.

The third step is the determination of soil strength. As stated in section 1.2.2, measuring soil strength is time consuming and till now most models choose pedotransfer functions for its prediction. Different pedotransfer functions have been proposed (Keller *et al.* 2007), but their accuracy still needs to improve (Schjønning *et al.* 2015).

Finally, when soil stress and its distribution are predicted (step 1-2), it can be compared with assessed soil strength (step 3) to evaluate soil compaction risk. Till now, no universal approach to link both soil stress and soil strength has been proposed. For instance, Keller *et al.* (2012) found that soil plastic deformation has accrued before stress reaches  $P_c$ , while in Terranimo<sup>®</sup>, compaction risk is divided into several degrees according to Rücknagel *et al.* (2015). Overall, there are still many improvements needed in modeling soil compaction. A more detailed discussion can be found in Keller and Lamande (2010).

### 1.3.4 Strategies to prevent soil compaction

All factors that affect soil strength and stress, as introduced above, can be considered for soil compaction prevention (i.e. reducing wheel load and increasing tyre-soil contact area). Besides, as the first traffic pass causes the major part of compaction (Bakker and Davis 1995; Nawaz *et al.* 2013), controlling traffic technology is another widely used solution (Nawaz *et al.* 2013; Bluett *et al.* 2019). For instance, controlled traffic farming can reduce the trafficked area to 10% or even less of a farming land (Bluett *et al.* 2019). As a result, controlled traffic farming was able to

reduce environmental impact and farm inputs compared with random traffic farming. For instance, nitrous oxide and methane emissions and water runoff were reduced by 21–45%, 372–2100% and 27–42%, respectively and associated fertilizers, pesticides, seeds and fuel use was reduced by 1–26%, 1–26%, 11–36%, and 23%, respectively (Gasso *et al.* 2013). Crop yield or biomass was significantly increased compared with random traffic farming (Antille *et al.* 2016). However, as pointed out by Schjønning (2018) in the RECARE project, it is a challenge to make all field operations to follow the same traffic lanes.

### **1.4 Alleviation of soil compaction**

Soil compaction alleviation can be separated into two categories, natural and artificial methods. Natural methods include dry/wet and freeze/thaw cycles and other biological cycles. Artificial methods mainly refer to tillage methods. In general, natural methods are slow and artificial methods are efficient, but always have adverse effects.

#### **1.4.1 Alleviation with tillage**

Tillage is a relatively efficient method to alleviate topsoil compaction and is widely used for seedbed preparation. Mouldboard ploughing is the most common one and can thoroughly loosen the topsoil over the full width of operation. However, many adverse effects have been reported about the technique of mouldboard ploughing. For instance, Wang *et al.* (2015) found that mouldboard ploughing decreased soil aggregate stability, which could greatly increase soil erosion risk. Consequently, some conservation tillage methods have been introduced. No-tillage is one of the main types but it could decrease crop yield because of soil compaction (Vetsch *et al.* 2007). Strip-

tillage has been regarded as a promising substitute method as it combines the benefits of both no-till and intensive tillage systems. For instance, Vetsch *et al.* (2007) found that strip-tillage resulted in less energy consumption, lower erosion risk and higher maize yield than no-till and chisel ploughing. Temesgen *et al.* (2012) compared strip-tillage with intensive tillage in a semi-arid area and found that strip-tillage decreased runoff and erosion, which greatly improved plant water availability resulting in higher maize yield. On the contrary, Vyn and Raimbault (1992) found that average maize yield was slightly lower in strip tillage than mouldboard plough-based intensive tillage in both silt loam and clay loam soil, while it was significantly lower in sandy loam soil within a 3 years' experiment. Licht and Al-Kaisi (2005) found that maize yield was not significantly different among strip tillage, no-till and chisel ploughing. In Belgium, Flemish farmers are forced to reduce soil erosion on their most erosion sensitive fields by the European Common Agricultural Policy (CAP). Since 2005, erosion control methods are compulsory on the most erosion sensitive fields as delineated by the erosion sensitivity map of Flanders (approximately 10.000 ha). In 2014, with the start of the new CAP, legislation in Flanders was further restricted: erosion control methods became compulsory on 50.000 ha, and the possible actions to be used were further elaborated. Strip tillage is regarded as a useful option to control soil erosion but it is still a new method in this region (Ryken *et al.* 2018), and its ability to alleviate topsoil compaction is still not clear.

To alleviate subsoil compaction, numerous deep tillage methods have been introduced, including deep ploughing, subsoiling and deep mixing (complete mixing of soil profiles) (Fig.1-4) (Schneider *et al.* 2017). Subsoiling is also referred to as deep ripping or deep chiseling, in which soil is only partially tilled. Deep ploughing is similar to mouldboard ploughing but with deeper tillage depth, which is resulting in complete

or semi-complete inversion of the tillage profile. Deep mixing is similar to deep ploughing but additionally mixes the topsoil and subsoil. In general, subsoiling is a potential method to alleviate compacted subsoil, not only because it is energy saving compared with the other two methods, but also because the loosening effects can last longer (Chaudhary *et al.* 1985; Gajri *et al.* 1994). However, some studies showed that subsoiling can also lead to easy re-compaction and settlement of soils. For instance, Reeder *et al.* (1993) studied the effects of five different subsoiling methods (different in coulters size or distance between shafts, all operating till 33 cm depth) on soil physical properties and crop yields in a silty clay loam soil. Results showed that two passes of a tractor already re-compacted the soil before the first crop was planted. A similar result was also found by Botta *et al.* (2006) and Schäfer-Landefeld *et al.* (2004). Both deep ploughing and mixing can greatly loosen soil but the alleviation effects cannot last long and they can be even harmful for the deep soil and crop growth in the following years (Munkholm *et al.* 2005; Olesen and Munkholm 2007; Schneider *et al.* 2017). Overall, deep tillage can be a choice to alleviate sub soil compaction, but the effects vary among different factors, like soil type, compaction levels and tillage depth.

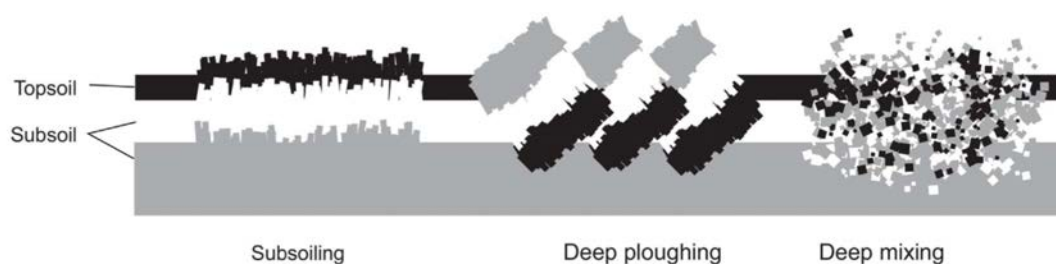


Fig.1-4 Schematic drawing of different deep tillage methods (Schneider *et al.* 2017)

#### 1.4.2 Alleviation with bio tilling

Crop roots could alleviate soil compaction and can be regarded as an environment-friendly method with low energy consumption. Rasse and Smucker

(1998) found that maize after alfalfa rotation had more roots in the compacted subsoil than maize after maize. Cover crops could positively affect maize root penetration into deeper compacted layers on no-till fields (Chen and Weil 2011) and cover crops with tap roots are more capable to penetrate compacted soil than fibrous-root crops (Chen and Weil 2010), but studies show that their benefit varies with cover crop species and compaction levels (Chen and Weil 2011; Goutal *et al.* 2012; Arvidsson and Hakansson 2014). The benefit for a specific major crop may be different depending on the cover crop species, environmental conditions and time, and is thus affected by compaction level, soil properties, ground water level, climate and planting/sowing time. However, data on cover crop root growth and their ability to alleviate soil compaction benefiting subsequent summer crops is still lacking in Europe. Besides, rotating crops within one or across seasons can also contribute to alleviate soil compaction. Linh (2016) pointed out that rotations of rice with upland crops significantly increased rice root growth compared with rice monocultures, which resulted from soil structure improvement and nutrition increase in the sub layer. Given the aforementioned function of roots in improving soil properties, it is essential to increase our knowledge on the interaction between soil compaction and plant root development.

### **1.5 Detecting soil compaction distribution**

Detecting soil compaction and its within-field variability is urgently needed for farming management (e.g., precision agriculture) and field research studies, where relatively homogenous fields need to be selected to reduce the soil variability. However, this is still a challenging task as traditional sampling methods are laborious and costly, especially for subsoils, which greatly restricts the soil survey map

resolution. In contrast, geophysical methods, like electromagnetic induction (EMI), are regarded as a promising option to detect soil properties because it can provide noninvasively, a high-resolution map at relatively low cost. According to Archie's law (Archie 1942), soil apparent electrical conductivity (ECa) is closely related to soil clay content, moisture content and salinity. As soil becomes compacted and soil bulk density increases, a unit volume of soil contains more clay and water and the contact between soil particles increased. This suggests that soil compaction could be measured indirectly from ECa. Many researchers have reported that bulk density increases with an increasing ECa or decreases with its converse, electrical resistivity (Brevik and Fenton 2004; Keller *et al.* 2017; Romero-Ruiz *et al.* 2018). At a soil profile scale, electrical resistivity (inverse of ECa) has shown the ability to detect traffic tracks (Besson *et al.* 2004; 2013). In a field scale, Hoefer *et al.* (2010) found a strong relationship between ECa and mechanical strength,  $K_o$  (a stress-at-rest coefficient, see Horn *et al.* (2007)), especially in areas with high penetration resistance. On a coarse sand field, Al-Gaadi (2012) found that ECa was positively correlated with man-made compaction levels and this correlation decreased with increasing soil moisture content (below field capacity). In a puddled paddy rice field, Islam *et al.* (2014) found ECa increased with increasing soil compaction levels. However, those site-specific results could only be true in case the soil properties (soil clay content, moisture content and salinity) are homogeneous or at least show little variation. Besson *et al.* (2004) found no clear correlation between soil compaction and ECa in a newly ploughed profile.

## 1.6 Study area

Two main study areas were used. The first one is located near Ghent, Belgium. Here, three fields were selected named as VRV field ( $50^{\circ}56'59.8''\text{N}$   $3^{\circ}47'05.2''\text{E}$ ), Crookstraat field ( $50^{\circ}59'06.2''\text{N}$   $3^{\circ}45'25.7''\text{E}$ ) and Gansberghelaan field ( $50^{\circ}58'54.3''\text{N}$   $3^{\circ}46'38.8''\text{E}$ ) (Fig. 1-5). All the fields are relatively flat and no runoff occurs. Soil texture is sandy loam and climate is temperate maritime with mild winters and warm summers (Kottek et al., 2006). The average annual temperature is  $10.5^{\circ}\text{C}$  and the average annual precipitation is 852.4 mm (average values of 1981- 2016). No irrigation system is applied in this area. Specific crop rotations in each field will be discussed in each chapter.

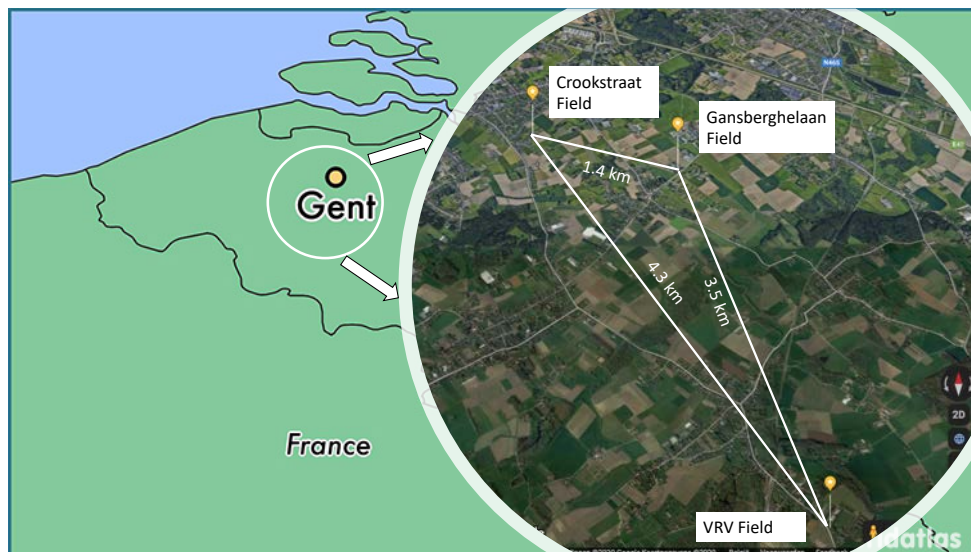


Fig.1-5 Study locations near Ghent, Belgium based on Google maps.

Similar with the situation of Europe (section 1.1), soil compaction has become a great threat to sustainable agriculture development in Belgium. According to the RAI-SOILCOMP project, which was organized to raise the awareness of soil compaction on the economic and environmental effects and further to prevent soil degradation by

researchers from Netherland, Sweden and Flanders (Belgium), 59% of the area was under high compaction risk. Moreover, 34% of the Belgian farmers had problems with soil compaction. Among them, 50% of the farmers believed alleviation methods are too expensive and 15% of the farmers believe alleviation methods are ineffective while 30% said they even did not know exactly what alleviation measure to take.

Conventional mouldboard ploughing is still the main tillage method in Belgium, with having around 90% of the arable land while conservation tillage was only having 10% after the first introduction in 1970s based on a survey in 2005 (D'Haene 2008). Moreover, there is almost no no-tillage method in Belgium. This is because crop production is mostly decreased under conservation tillage. However, with increased interest in preventing soil erosion and improving energy efficiency, both farmers and policy makers realised the importance of conservation tillage methods in recent years (Vermang 2012).

The second study area is located in Denmark (Fig. 1-6). This study site is used in chapter 6 based where a soil column experiment is conducted. The sampling field is at Aarslev (55°18'18"N, 10°26'52"E). Soil texture is sandy loam (USDA). Previous to the sampling, a compaction experiment with farm machinery was executed over four consecutive years (2010-2013). A detailed description of this compaction experiment can be found in Schjønning et al. (2016). After sampling, those soil columns were transported to the Foulum site (56°29'06.5"N, 9°34'56.7"E), in Denmark, for the further soil column experiment. More detail will be provided in chapter 6.

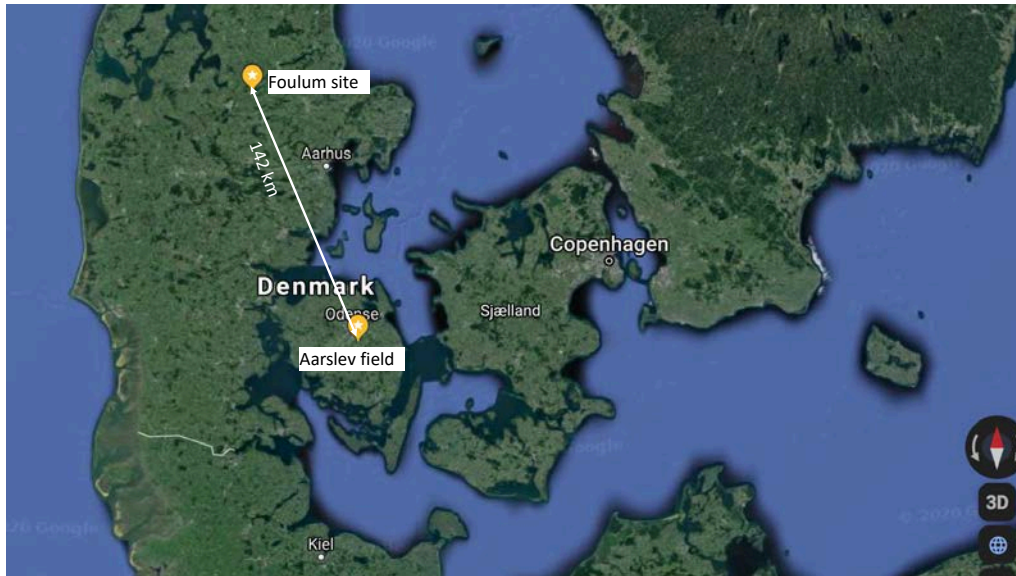


Fig.1-6 Sampling location (Aarslev field) and experimental site (Foulum site) in Denmark by Google maps.

## 1.7 Objectives

The overall objective of this dissertation is to better understand the land degradation processes of soil compaction in this study areas and to provide practical agricultural management suggestions for the local farmers and stadtholders. It evaluated the effects of soil compaction, practical prevention strategies, alleviation methods and the possibility of detecting soil compaction spatial variability by using geophysical method and drone images.

We hypothesized that 1) soil compaction not only restricts crop growth but also results in adverse effects on the environment (i.e., restricted water movement and increased nutrient leaching); 2) By choosing the right soil moisture condition and adjusting agricultural machinery parameters, soil compaction risk can be avoided or decreased; 3) cover crops have a high potential to alleviate subsoil compaction and

strip tillage will not negatively affect maize growth compared with traditional plough tillage method; 4) ECa and maize canopy height could be suitable indicators for soil compaction at field level.

Specific research questions that will be addressed in this dissertation are listed below:

- 1) How do different kinds of soil compaction (both top and sub) affect soil properties and crop growth? Three conditions were selected: (a) a temporary induced surface compaction treatment; (b & c) long term existing sub soil compacted plots with or without subsoiling;
- 2) To what extent could soil compaction be prevented by choosing different soil moisture conditions and agriculture machineries. Two conditions were evaluated: (a) during seedbed preparation; (b) during slurry application;
- 3) How effective are (deep) tillage and bio-till cover crops in alleviation soil compaction? Both strip and deep tillage methods were tested on their potential to alleviate soil compaction; the ability to alleviate sub-compaction by different crops was also evaluated;
- 4) Could soil compaction variation be detected by using geophysical methods and drone images within a field? Fast and easy methods, Electromagnetic Induction, Electrical Resistivity Tomography and drone images are compared with conventional field and lab methods.

## **1.8 Outline of this thesis**

The outline of this thesis is based on the research questions stated above. A brief framework figure, based on the “EPAD” system (effects, prevention, alleviation

and detection), is shown in Fig. 1-7. Firstly, an overall review of the research background is presented in chapter 1. In chapter 2, the effects of soil compaction were evaluated, from both newly induced top and already existing sub-compaction. In chapter 3 and 4, strategies to minimize or prevent soil compaction by changing the operational characteristics of a sowing machine and a slurry spreader (i.e., tyre pressure, tyre type and soil moisture condition) were evaluated at loose and relatively compacted soil, respectively. Meanwhile, the effects of soil compaction from those treatments on soil physical quality and crop growth were also presented. In chapter 5 and 6, they are mainly focused on alleviating subsoil compaction by using different cover crops. Besides, strip tillage, which has only recently been introduced in the study area, was also evaluated in terms of alleviation of soil compaction for crop growth. In chapter 7, Electromagnetic Induction and drone images were used to detect soil compaction variability within a field. In the last chapter, general conclusions and recommendations for future research are presented.

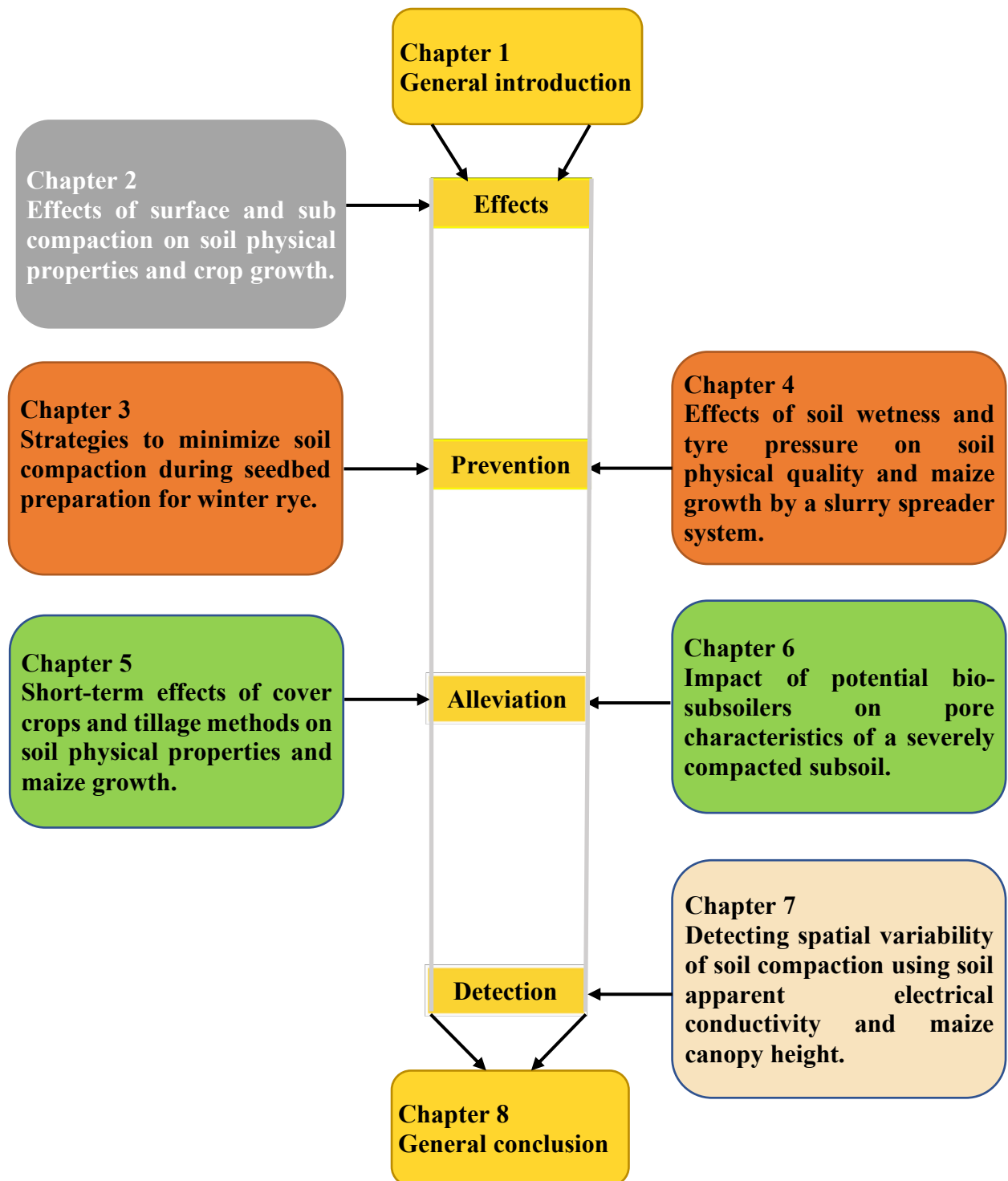


Fig.1-7. Thesis schematic of the “EPAD” system.

## **Part I: Effects of soil compaction**

## **Chapter 2: Quantifying the effects of top and sub soil compaction under a silt loam soil in West Europe**

## 2.1. Introduction

With the modernisation of agriculture, the weight of agricultural machines dramatically increased in the past decades (Schjønning *et al.* 2015). A case study from Denmark shows that wheel loads of harvesters and tractors have increased from ~1.5 Mg to 9 Mg and from ~1 Mg to more than 4 Mg, respectively, in the past sixty years (Keller *et al.* 2019). Such drastic increase in wheel load induces a high risk of soil compaction, which has been recognised by the European Commission as one of the main threats to sustainable agriculture all over Europe (Alameda *et al.* 2012).

Many studies have evaluated the effects of soil compaction on soil structure, plant growth and environment (Unger and Kaspar 1994; Horn *et al.* 1995; Huber *et al.* 2008; Schjønning *et al.* 2015; Keller *et al.* 2019). In general, most reports indicate that soil compaction decreases soil structural quality and restricts plant growth. However, because of the variation in compaction depth and levels, conclusions are not consistent. Besides, an appropriate system evaluation among soil properties, water and nutrition movement, and crop growth at different sites (or climate conditions) is still lacking. For instance, Schjønning *et al.* (2015) reported that the water balance and thus the promotion of drought under compacted soil is not clear. Similarly, the effect of soil compaction on nutrient leaching is dubious as soil compaction can reduce nitrogen leaching by decreasing permeability, but could also result in increased leaching of nutrients resulting from restricted root elongation, which reduces nitrogen uptake by plants (Håkansson 2005; Gasso *et al.* 2013) or an increase in preferential flow (Torbert and Reeves 1995).

The objectives of this study were to investigate: 1) the effects of topsoil compaction on water movement, nutrition leaching and maize growth induced by tractor with a

rotary harrow just before the seedbed preparation that followed a 30 cm depth mouldboard ploughing; 2) the effects of different subsoil (30-90 cm) compaction levels induced by a long time accumulation of farm work on water and nitrogen movement and crop growth; 3) the alleviation effects of deep tillage on soil properties and crop growth in a very dry and hot growing season. This kind of extreme weather condition is predicted to occur more frequently in the future because of climate change and strategies to resilient this kind of extreme weather is essential for food security (Stott 2016). Unlike most studies on soil compaction, this study did not create (unrealistic) compaction levels by wheel trafficking with different loads or several passes but selected a farmer's field that was highly compacted by previous farming operations.

## **2.2. Materials and methods**

### **2.2.1 Study site**

In this study, the VRV field was used. Prior to our experiment, potatoes (*Solanum tuberosum* L.) followed by winter rye (*Secale cereale* L.) as cover crop, were grown in 2015 and maize (*Zea mays* L.) was grown in the summer of 2016. Climate in the study area is temperate maritime with mild winters and warm summers (Kottek *et al.* 2006). Besides, there was a relative dry winter and spring from September 2016 to May 2017 and an exceptional hot and dry summer in 2018 (Table 2-1). The water table is at approx. 5 m depth (Database Subsurface Flanders, [www.dov.vlaanderen.be](http://www.dov.vlaanderen.be)).

Table 2-1. Meteorological conditions during the study period (data according to Uccle station and analysis from the Royal Meteorological Institute of Belgium, RMI).

Seasons	Temperature (°C)	Precipitation (mm)
Autumn 2016 (SEP-NOV)	11.1 (10.9) n	162.2 (219.9) n
Winter 2016 (DEC-FEB)	3.9 (3.6) n	<b>127.3 (220.5) va</b>
Spring 2017 (MAR-MAY)	11.3 (10.1) a	<b>108 (187.8) va</b>
Summer 2017 (JUN-AUG)	18.6 (17.5) a	179.9 (224.6) n
Autumn 2017 (SEP-NOV)	11.3 (10.9) n	226.5 (219.9) n
Winter 2017 (DEC-FEB)	3.8 (3.6) n	232.6 (220.5) n
Spring 2018 (MAR-MAY)	<b>11.5 (10.1) va</b>	150.7 (187.8) n
Summer 2018 (JUN-AUG)	<b>19.8 (17.5) e</b>	<b>134.7 (224.6) a</b>
Autumn 2018 (SEP-NOV)	11.8 (10.9) n	168.5 (219.9) n

Note: Normal values (in parentheses) and degree of abnormality defined over the period 1981-2010 with n: normal (< 6 years); a: abnormal (6-10 years); va: very abnormal (10 years) years); e: exceptional (> 30 years).

The soil texture and organic carbon content which was measured at three randomly selected locations and at three depths, is given in Table 2-2. They were measured with the sieve-pipette method (Gee and Bauder 1986) and Walkley and Black (1934) method, respectively, on soil samples collected at three randomly selected locations in the field. At each location, three subsamples were taken and mixed. The soil is classified as Luvisol (Dondeyne *et al.* 2014) and has a silt loam to loam texture (USDA).

Table 2-2. Soil texture and organic carbon content of the experimental field.

Depth (cm)	Sand (>0.05 mm) (g kg <sup>-1</sup> )	Silt (0.05-0.002 mm) (g kg <sup>-1</sup> )	Clay (<0.002 mm) (g kg <sup>-1</sup> )	SOC (g kg <sup>-1</sup> )	Texture (USDA)
0-30	325.2 ± 56.0	593.6 ± 50.1	74.8 ± 16.7	16.2 ± 1.8	Silt loam
30-60	277.9 ± 112.1	580.9 ± 127.9	115.4 ± 24.1	3.8 ± 0.4	Silt loam
60-90	371.0 ± 19.1	484.8 ± 36.0	142.2 ± 18.5	2.1 ± 0.6	Loam

SOC: soil organic carbon content.

### 2.2.2 Experimental design

In the autumn of 2016, two zones within the field were selected according to penetration resistance measurements: a headland zone (starting 15 m from the field boundary) where subsoil was highly compacted and an in-field zone (in the middle of the field), where subsoil was less compacted but a clear plough pan existed (Fig. 2-1). In the headland zone, six plots were laid out, each measuring 6×12 m (Fig. 2-2). In the in-field zone, 12 plots were installed within three blocks and each plot was 6×20 m large. On 07/10/2016, deep tillage was induced on half of the plots in the in-field zone by a tractor-mounted subsoiler perpendicular to the driving direction of the common tillage operations on the field (Fig.2-3a). Tillage depth was 0.5 m and distance between the shanks was 0.9 m (Fig.2-3b). Winter rye was sown three days later on 10/10/2016. In the winter rye winter season of 2016-2017, there were thus two treatments in the in-field zone, i.e. deep tillage (DT) and no deep tillage (NDT) as a control. In the headland zone, no specific treatment was introduced. This resulted in three levels of subsoil compaction. All measurements were made in three replicated plots for each

treatment except for penetration resistance and soil moisture, which were measured in all plots resulting in six replicated plots in each treatment.

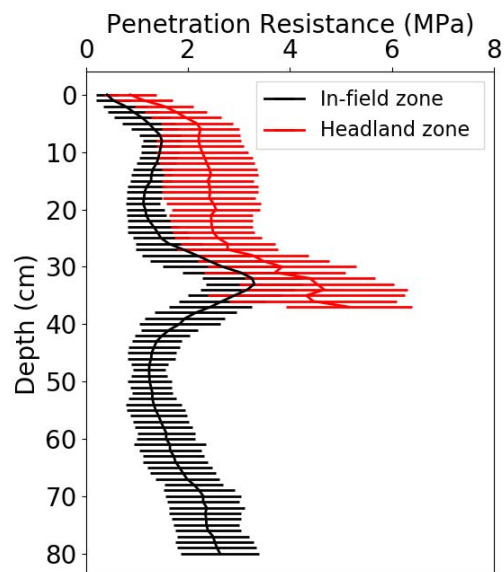
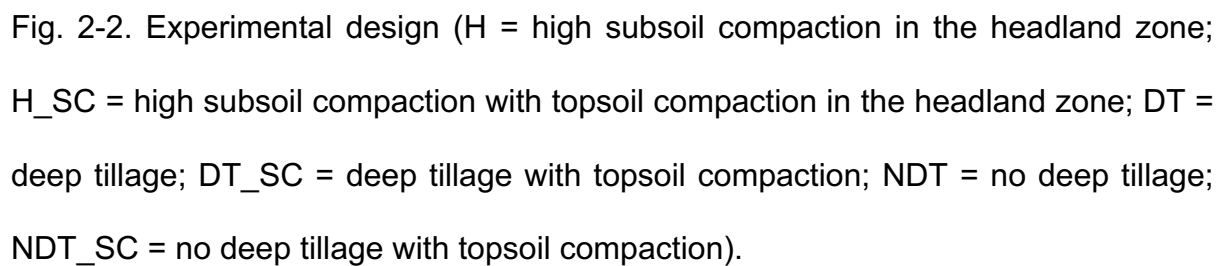


Fig. 2-1. Penetration resistance measured on 29/04/2016. The error bars are standard errors ( $n=90$  and  $110$  for in-field and headland zone, respectively). Note that PR could not be measured below 40 cm in the headland zone because the resistance to the cone was so high resulting from a very high degree of compaction.



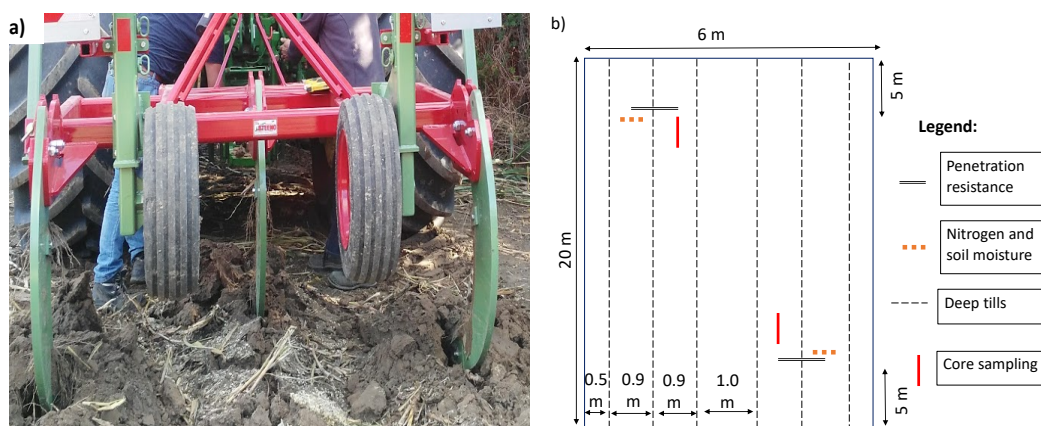


Fig. 2-3. Deep tillage until a depth of 0.5 m: a) subsoiler with shanks 0.9 m apart and b) penetration resistance, deep till, nitrogen, soil moisture, maize root and core samples sampling locations in one deep tillage plot. Panel b is not on scale.

After cutting the winter rye (26/04/2017), slurry was distributed by a slurry spreader (27/04/2017), followed by in-furrow ploughing (till 30 cm depth) with a conventional mouldboard plough in the next day. To simulate compaction which might occur during seedbed preparation, topsoil compaction (SC) was induced immediately after the ploughing (perpendicular to the ploughing direction, 28/04/2017) as an additional experimental factor by track-by-track wheeling with a John Deere 6150R in combination with a rotary cultivator (not operating) (Fig. 2-4) in both the in-field and headland zone. In the in-field zone, there were four treatments, i.e., DT, DT\_SC, NDT and NDT\_SC. In the headland zone, two treatments were evaluated, i.e., H and H\_SC. The full experimental design is shown in Fig. 2-2. Conventional seedbed preparation with a rotary harrow (8 cm depth) took place on the 2<sup>nd</sup> of May after which the maize was sown on the 4<sup>th</sup> of May in rows (with 75 cm interrow spacing,  $10^5$  seeds ha<sup>-1</sup>, and 6 cm sowing depth) in the same direction as ploughing and slurry application.



Fig. 2-4. Topsoil compaction induced by a rotary cultivator after mouldboard ploughing.

## 2.2.3 Measurements

### 2.2.3.1 Winter cover crop season 2016-2017

On 25/11/2016, penetration resistance (PR) was measured using a hand-held penetrometer (Eijkelkamp Soil & Water) to 70 cm depth. The cone had a 1 cm<sup>2</sup> base area, a 11.28 mm nominal diameter and a 60° top angle. Measurements were done along two transects per plot (10 measuring points with 15cm interval at each transect), perpendicular to deep-tillage operation (Fig. 2-3b). One disturbed soil moisture sample was also collected near each transect at the same time using a 3-cm diameter bipartite gouge auger (Eijkelkamp Soil & Water). Soil moisture samples were collected to 60 cm depth at 10 cm intervals. Dry soil mass was measured after oven-drying at 105 °C for 24 h.

On 25/04/2017, before cutting the winter rye, soil moisture samples were collected to 90 cm depth at 30 cm depth intervals. Sampling positions were located at a distance of 15 cm of the locations which were selected at 25/11/2017. Winter rye growth was assessed by weighting shoots and roots. A 1 × 1 m<sup>2</sup> above-ground

biomass harvesting zone was randomly selected per plot, resulting in three replications per treatment. The winter rye height was measured with a ruler in five replications per plot in the above-ground biomass harvesting zone. Plants were then cut with scissors and their dry weight (75°C, 48 hours) was determined. Root samples, including roots and the surrounding undisturbed soil, were collected in the winter rye row with an 8-cm diameter root auger, in 15-cm increments, till 50-cm depth within the above-ground biomass harvesting zone (also three replications). The soil structural quality of the root auger samples was first assessed with the visual evaluation of soil structure (VESS) method. The original VESS method (Ball *et al.* 2007; Guimarães *et al.* 2011) developed for topsoil blocks taken with a spade and the visual evaluation of subsoil structure (SubVESS) (Ball *et al.* 2015) developed for subsoil were combined to score soil structural quality (Sq and Ssq, respectively). For VESS and SubVESS, soil quality scores ranged from 1 to 5, with 1 representing the best soil quality and 5 the worst for both of them. After that, dry root biomass density was determined by washing the samples on a 50- $\mu$ m mesh sieve and drying the remaining roots at 75°C for 48 hours.

On 25/04/2017, undisturbed soil samples were taken at 20, 35 and 50 cm depth (the middle of the core) in 100 cm<sup>3</sup> standard sharpened steel cores (5.1 cm height and 5 cm diameter) using a dedicated auger (Eijkelkamp Soil & Water). This was done at both plot sides (Fig. 2-3b). Air permeability ( $K_a$ ) was measured on all six cores per treatment and depth, at 100 hPa matric suction using the steady-state method of Grover (1955). More details can be found in chapter 5. After that, three soil cores per treatment and depth were used to measure the water retention curve according to the procedure outlined in Cornelis *et al.* (2005). Matric suctions of 10, 30, 50, 70, 100, 340,

1,020 and 15,300 cm were selected. Soil-water retention curves were plotted by fitting the Van Genuchten (1980) model to the observed data:

$$\theta(h) = \begin{cases} \theta_r + \frac{\theta_s - \theta_r}{\left[1 + |\alpha h|^n\right]^m} & h < 0 \\ \theta_s & h \geq 0 \end{cases} \quad (2-1)$$

where  $\theta_r$  and  $\theta_s$  are residual and saturated soil-water content ( $\text{cm}^3 \text{ cm}^{-3}$ ), respectively. The parameter  $\alpha$  ( $\text{cm}^{-1}$ ) is positively related to the reciprocal of air-entry pressure,  $n$  is a pore-size distribution index being positively related to the slope of the soil-water retention curve and  $m=1-1/n$ .  $\theta(h)$  is soil-water content ( $\text{cm}^3 \text{ cm}^{-3}$ ) at matric suction  $h$  (cm).

### 2.2.3.2 Summer maize season 2017

After maize sowing (04/05/2017), soil-water content was measured by time-domain reflectometry (TDR) using two-rod CS655 sensors, 12 cm in length, 0.32 cm in diameter, and 3.2 cm interspacing between rods (Campbell Scientific). The sensors were horizontally installed at 15 and 50 cm depth. Soil moisture content was recorded hourly from 15/06/2017 to 18/09/2017. The calibration curve presented in Nelissen *et al.* (2015), who worked on a nearby field with the same soil type, was used. Sensors were installed in four plots of block A (one replicate per treatment) in the in-field zone and on four plots (two replicates per treatment) in the headland zone (see Fig. 2-2). In each plot, TDR sensors were installed in one location at two depths.

On 01/08/2017, root distribution was observed using the trench profile method (Van Noordwijk *et al.* 2001). First, a 60-cm deep trench profile (parallel with the maize row) was dug in between two maize rows (75 cm) of each plot (see Fig.2-3). The observed profile wall was carefully prepared with a sharp knife removing soil that covered the surface to display roots. Then, a wooden frame with  $2.5 \times 2.5$  cm cells was used to record root number by counting the number of roots in each cell. Because of the large amount of workload, this was done in only two replications (two plots in each treatment) in each treatment. This was also true for the core samples described below.

Undisturbed core soil samples (total volume of  $250 \text{ cm}^3$ , 5 cm in height and 8 cm in diameter) were taken vertically in a stepwise manner at 10, 35 and 50 cm depth using a dedicated hammering tool (METER Group) from the middle of each root trench on 01/08/2017. Unlike in the winter season of 2017, this time it was more attention to the hydraulic conductivity curve ( $K(h)$ ) which affects both saturated and unsaturated water movement, as De Pue *et al.* (2019b) reported that  $K(h)$  can be greatly overestimated when deriving it from saturated hydraulic conductivity and the water retention curve as often done. Soil water retention curves (SWRC) and  $K(h)$  were measured simultaneously with the evaporation method (HYPROP®, METER Group). The saturated water conductivity ( $K_s$ ) was measured by the falling head method with KSAT® equipment (METER Group). The bimodal, Peters-Durner-Iden (PDI) model (Peters 2013; Iden and Durner 2014; Peters 2014) was used to fit SWRC and  $K(h)$  curves to the observations, which greatly increased the fitting accuracy. For the hydraulic conductivity curves, both the measured  $K_s$  and  $K(h)$  were used.

Penetration resistance was measured (18/09/2017) as described in section 2.3.1, but at 7.5 cm intervals between measurements. As the subsoil was very dry

( $\sim 0.15 \text{ kg kg}^{-1}$ ), the cone could not penetrate deeper than 30 cm and only the top 30 cm layer data are presented.

In addition, disturbed soil samples were collected in DT, NDT, and all six plots of H (representing H and H\_SC of the summer season 2017) at both heads of each plot between maize lines for total mineral nitrogen analysis ( $\text{NO}_3\text{-N} + \text{NH}_4\text{-N}$ ) according to ISO TS14256-1: 2003 procedure. At each location (see plot sampling design in Fig.2-3b), three subsoil samples were mixed, resulting in 6 composite samples (replications) for each treatment. The soil samples were taken at 30 cm increments to 90 cm depth on 09/02/2017 ( $\sim 3$  months before sowing) and on 11/10/2017 ( $\sim 1$  month after harvest).

Maize was harvested as silage on 19/09/2017. Above-ground biomass was recorded and weighed to determine their fresh above-ground biomass. After that, four plants per plot were randomly selected to determine dry above-ground biomass at  $70^\circ \text{C}$  for 48 hours. For maize biomass, the intensity of traffic tracks during seedbed preparation was also considered and separated into two conditions: 1) less traffic, where with reduced or no traffic tracks, i.e., with only one pass or with no traffic; 2) more traffic, i.e., with two passes with a rotary harrow and one pass with a sowing machine and slurry spreader. Note that all the other measurements indicated above (except maize above-ground biomass) were done in the less traffic zone.

### **2.2.3.3 Effects of deep tillage in 2018**

To test the medium-term effects of deep tillage on soil properties PR was measured again in the in-field zone on plots with and without deep tillage on

09/04/2018, i.e. before the clipping of winter rye. The measurement procedure was the same as described in section 2.3.1.

To test the effects of deep tillage on crop growth in the exceptionally hot and dry summer of 2018, maize canopy height was determined from a drone image (i.e. 90% highest maize plants) on 14/09/2018. The detail analysis of maize canopy height based on the drone images can be found in Chapter 7. Maize canopy height was extracted from each plot by using QGIS to compare the differences among treatments.

Maize above-ground biomass was also harvested in three plots of DT and NDT. In each plot, two maize rows (each 4 m long and covering 3 m<sup>2</sup> area) were harvested in the less traffic zone. After that, maize dry above-ground biomass was determined the similarly as in 2017.

#### **2.2.4 Data analysis**

For the winter season of 2016-2017 and the maize canopy height in 2018, one-way analysis of variance (ANOVA) was used with three subsoil compaction levels (H, DT and NDT) and two subsoil compaction levels (DT and NDT) as the only factor, respectively. Differences between the treatments were assessed using the LSD (least significant difference) multiple comparison test at 0.05 probability level. Non-parametric analyses (Mann-Whitney or Kruskal–Wallis test) were used if data failed to meet parametric assumptions.

In the summer of 2017, soil core-based properties and root distribution were determined in two replicates per treatment and only mean values are reported. For the other properties, a two-way ANOVA was used with topsoil and subsoil compaction as two factors. For maize dry biomass, as traffic effects were only considered in the in-field zone, the statistical analysis was conducted in two steps. Firstly, a two-way

ANOVA was conducted with factors of topsoil and subsoil compaction levels in the area with limited traffic. Secondly, the factor 'traffic' was induced and only data in the in-field zone were used in a three-way ANOVA. The LSD test at 0.05 probability level was used to compare the means among treatments. ANOVA analyses were conducted by SPSS Statistics 25.

### **2.3. Results**

#### **2.3.1 Winter cover crop season 2016**

The visual evaluation of soil structure (VESS) did not show significant differences among treatments in the top 30 cm (Table 2-3). However, in the 30-50 cm layer, SubVESS indicated higher values for mottling, porosity and aggregates in the headland (i.e., the H treatment) than in the in-field area (i.e., in treatments DT and NDT). This resulted in significantly higher final Ssq score in the headland area compared with in-field zone. No differences were found between DT and NDT.

During the winter season (24-11-2016), soil moisture content was higher compared with that in spring (25-4-2017), especially in the top layer (0-30cm) (Fig. 2-5). On 24-11-2016, soil moisture content was higher in H than in DT at 10-20 cm, while it was significantly lower at 40-60 cm in H compared with DT. On 25-4-2017, differences were only found between H, and DT and NDT at 30-60 cm, like on 24-11-2016.

Table 2-3. Visual evaluation of soil structure (VESS &amp; SubVESS, n=3) in the winter cover crop season 2016.

Treatments	VESS (0-30 cm)			SubVESS (30 -50 cm)					
	0-10	10-20	20-30	mottling	strength	porosity	roots	aggregate	Ssq scores
H	1.00±0.00a	1.83±0.29a	2.67±0.29a	<b>3.83±0.29a</b>	3.33±1.53a	<b>4.33±0.58a</b>	4.67±0.58a	<b>4.33±0.58a</b>	<b>4.33±0.29a</b>
DT	1.00±0.00a	1.83±0.29a	2.50±0.50a	1.67±0.58b	2.33±0.58a	2.00±0.00b	3.50±1.32a	2.67±0.58b	2.50±0.50b
NDT	1.17±0.29a	2.00±0.00a	2.17±0.29a	2.33±0.58b	2.33±0.58a	3.00±1.00b	3.00±0.00a	3.00±0.00b	2.83±0.58b

Mean values with standard deviation and different letters are significantly different across each column ( $P \leq 0.05$ ,  $n = 3$ ). H=high subsoil compaction; DT= deep tillage; NDT= no deep tillage. Note, soil quality decreased with the increasing of scoring, ranging from 1 to 5 (Ball *et al.* 2007; Guimarães *et al.* 2011; Ball *et al.* 2015).

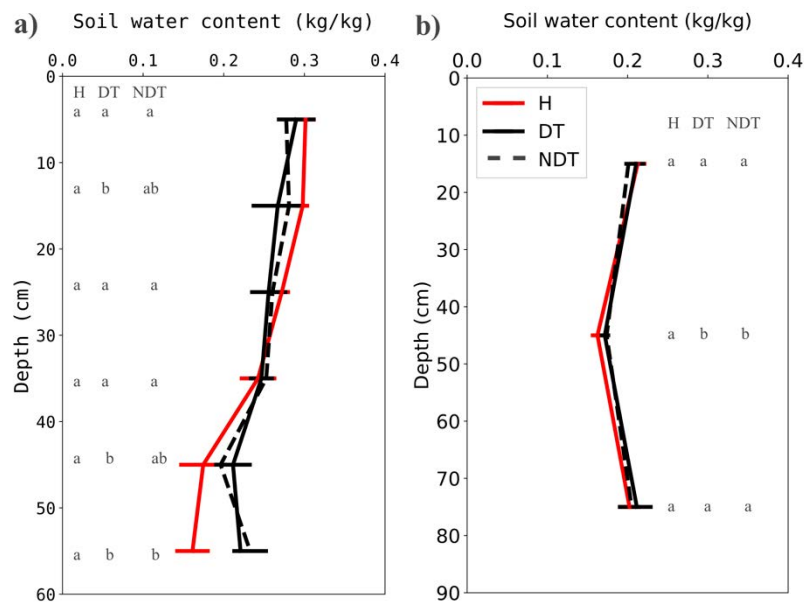


Fig. 2-5. Gravimetric water content on 24-11-2016 (a) and 25-4-2017 (b). The error bars are standard errors ( $n=6$  for DT and NDT;  $n=12$  for H). Letters at the same depth designate significant differences at the 5% probability level (H=high subsoil compaction; DT= deep tillage; NDT= no deep tillage).

Penetration resistance was clearly much higher below ~30 cm depth under all treatments, with highest values in the H treatment. In DT, the tines of the deep tillage are clearly visible showing lower values for penetration resistance (see ellipse in Fig. 2-6).

Bulk density increased with depth with mean value of 1.40, 1.66 and 1.70 g cm<sup>-3</sup> in the 20, 35 and 50 cm layer for all treatments, respectively (Fig. 2-7a). At 50 cm depth, bulk density was significantly ( $P = 0.02$ ) higher in H than in the other treatments. No differences were found for pore size distribution at 20 cm depth. At 35 cm depth, macroporosity was significantly smaller in H as compared with the other treatments. At 50 cm depth, both macroporosity and microporosity were significantly smaller in H than that in the other treatments. Deep tillage decreased microporosity at 35 cm depth.

The full water retention curves and pore size distribution can be found in the Appendix S.1&2.

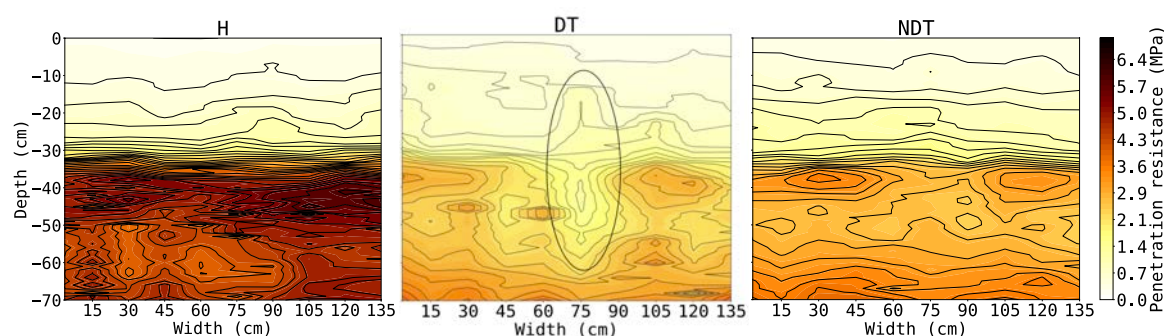


Fig. 2-6. Penetration resistance measured on 25-11-2016 (H=high subsoil compaction; DT= deep tillage; NDT= no deep tillage).

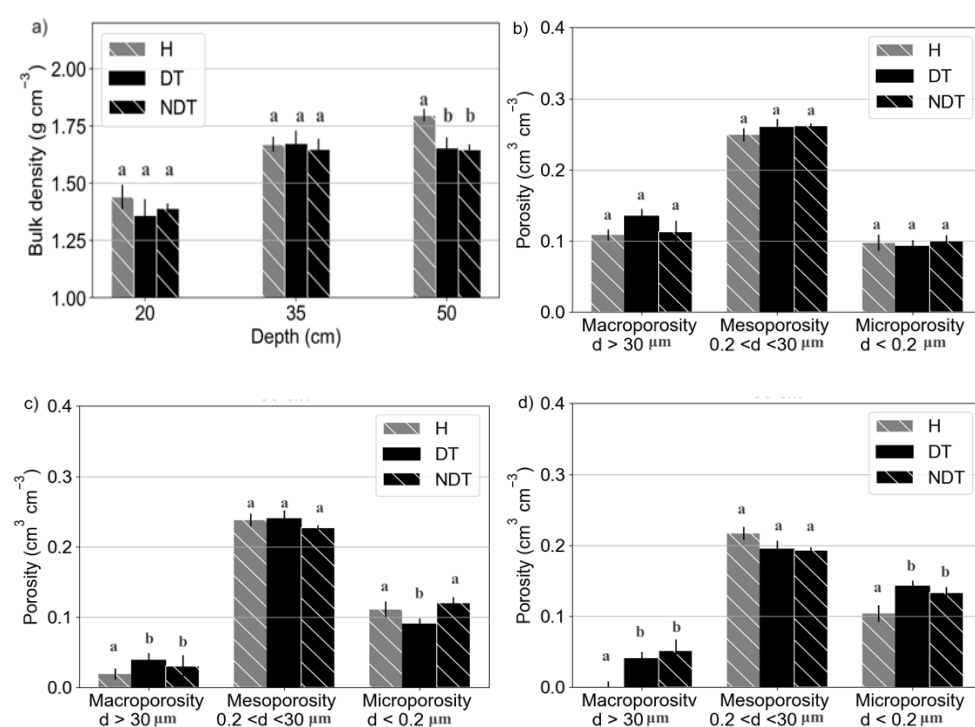


Fig. 2-7. Bulk density per depth (a) and pore size distribution at 20 cm (b), 35 cm (c) and 50 cm (d) depth, according to the treatments (H= high subsoil compaction area; DT=deep tillage; NDT=no deep tillage). The error bars are standard deviation (SD; n = 3). Different letters in each group indicate significant differences ( $P \leq 0.05$ ).

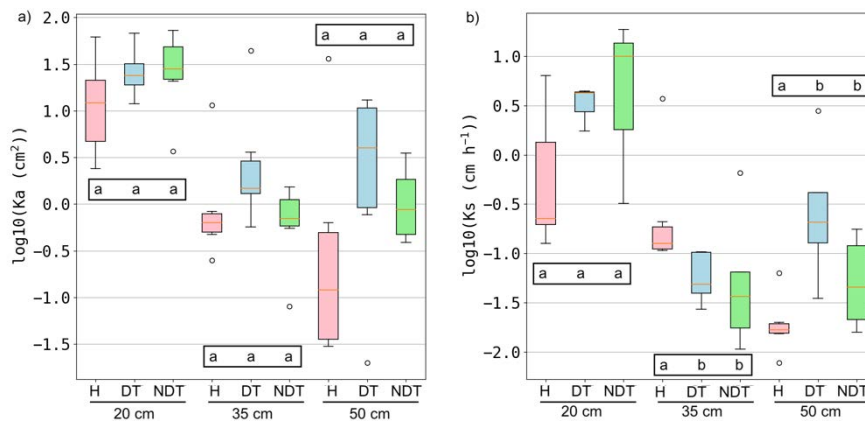


Fig. 2-8. Air permeability  $K_a$  (a) and saturated water conductivity  $K_s$  (b) measured at each depth with 6 replications (H=highly subsoil compaction; DT= deep tillage; NDT= no deep tillage). Difference letters in each group indicate significant differences ( $P \leq 0.05$ ).

The H treatment had the lowest average  $K_a$  at all depths, while  $K_a$  was not significantly different within each depth (Fig. 2-8a).  $K_a$  decreased with depth in H, while it was similar or not decreasing between 35 and 50 cm depth within DT and NDT. A similar trend was found for  $K_s$  (Fig. 2-8b) except at 35 cm depth, where H was higher than DT and NDT and at 50 cm where H was lower than DT and NDT.

Table 2-4. Winter rye dry root biomass, dry above-ground biomass (AGB) and height.

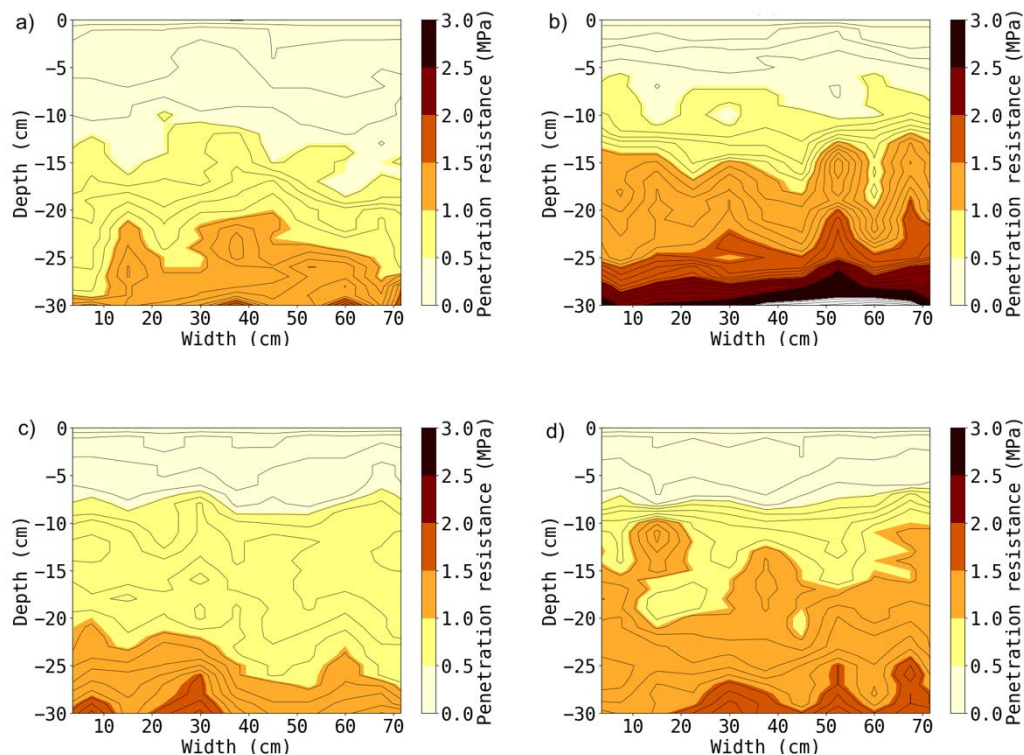
Treatment	Dry root biomass (kg m <sup>-3</sup> )						AGB_d (kg m <sup>-2</sup> )	Height (m)
	0-10 cm	10-20 cm	20-30 cm	30-40 cm	40-50 cm	0-50 cm		
H	0.80±0.18a	<b>0.43±0.08a</b>	0.39±0.14a	0.10±0.10a	<b>0.00±0.00a</b>	0.34±0.31a	0.49±0.05a	<b>0.53±0.04a</b>
DT	0.82±0.19a	0.27±0.05b	0.23±0.09a	0.13±0.02a	0.01±0.01b	0.29±0.30a	0.52±0.06a	0.63±0.04b
NDT	0.94±0.20a	0.26±0.05b	0.19±0.06a	0.20±0.04a	0.03±0.02b	0.32±0.34a	0.50±0.04a	0.64±0.04b

Mean values with standard deviation; different letters are significantly different across each column ( $P \leq 0.05$ ,  $n = 3$ ). H=high subsoil compaction; DT= deep tillage; NDT= no deep tillage, AGB\_d = dry above-ground biomass.

Similar with soil properties, some differences in crop properties between highly (H) compacted headland areas and less-compacted in-field areas (DT and NDT) were found (Table 2-4). At 10-20 cm, dry root biomass was significantly ( $P=0.02$ ) higher in H than in the DT or NDT and it was marginally ( $p=0.07$ ) higher at 20-30 cm, while at 30-40 cm it had a lower trend ( $P=0.2$ ) and at 40-50 cm, no roots were found in H. In DT and NDT, roots could still penetrate below 40 cm. For the total dry root biomass, no significant differences have been found. Dry above-ground biomass was not significantly different across the treatments, whereas winter rye height was significantly lower ( $\geq 0.1$  m) in H ( $P=0.04$ ).

### 2.3.2 Summer maize season 2017

The compaction induced by track-by-track wheeling with a rotary cultivator in 2017 resulted in clear differences in PR among all treatments (Fig. 2-9). In general, PR in the top 30 cm was significantly higher with topsoil compaction (SC) than without, especially at 10-20 cm. Yet, PR was lower than 2 MPa at most depths for all treatments, which is regarded as the threshold value restricting root growth (Lipiec *et al.* 2003). At 18-09-2017 when PR was recorded, soil water content decreased with depth and differences between headland zone and in-field zone were only found at 50-60 cm. Apparently, it was measured error for H\_SC approved by the measurements in June, July and August (see Appendix S.3).



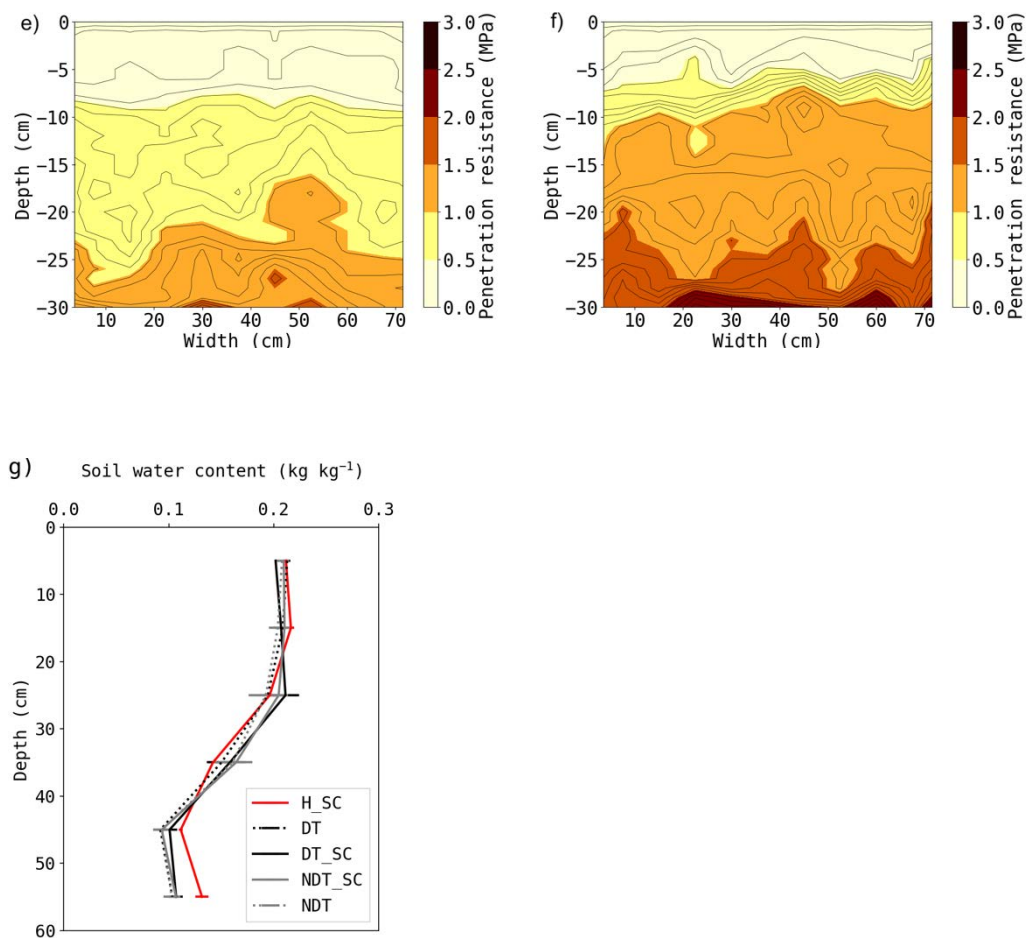


Fig. 2-9. Penetration resistance ( $n=10$ ) without (a,c,e) and with (b,d,f) topsoil compaction in H (a,b), DT (c,d) and NDT (e,f) treatment and soil water content (g) with 95% confidence interval ( $n=3$ ) measured on 18-09-2017 (H = high subsoil compaction; DT = deep tillage; NDT = no deep tillage; SC = topsoil compaction). PR could not be measured below 30 cm as soil was too hard and soil water content was not determined for the H treatment .

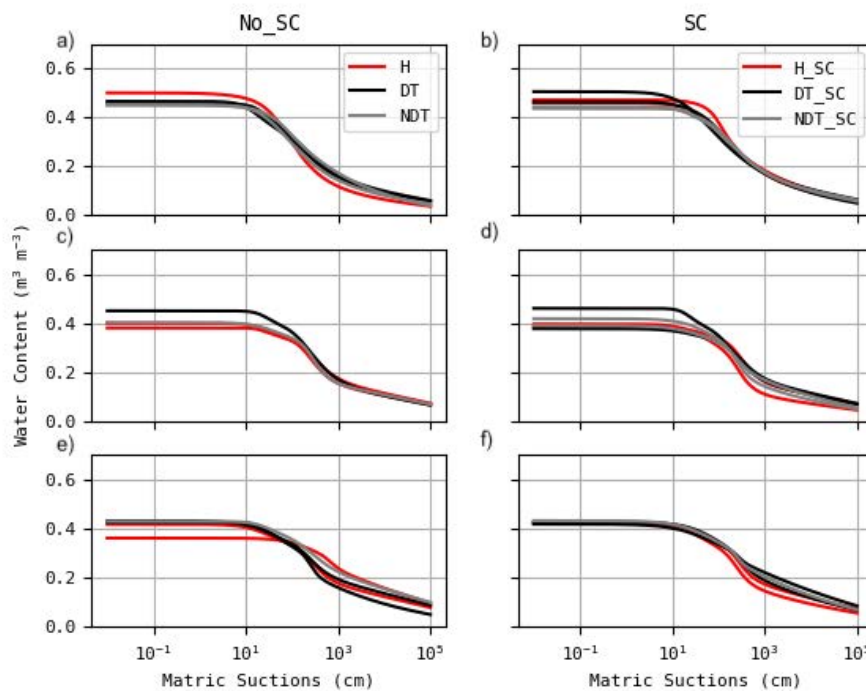


Fig. 2-10. Soil water retention curves (fitted with PDI bimodal model) without (a,c,e) and with (b,d,f) topsoil compaction at 15 cm (a,b), 35 cm (c,d) and 50 cm (e,f) depth with two replications for each treatment (H, DT and NDT).

When interpreting the SWRCs (Fig. 2-10), less macropores (matric suction smaller than 100 cm) seem to be present at 50 cm depth in the headland zone (both H and H\_SC). No other clear trend in the SWRCs could be perceived (Fig. 2-10). Measured SWRC for all samples can be found in appendix S4.

Near saturated hydraulic conductivity (0-10 cm matric suction) was slightly higher without topsoil compaction than with compaction at 15 cm depth (Fig. 2-11), and lower in the headland zone than in the in-field zone at 35 cm depth. At 50 cm depth, no differences were detectable.

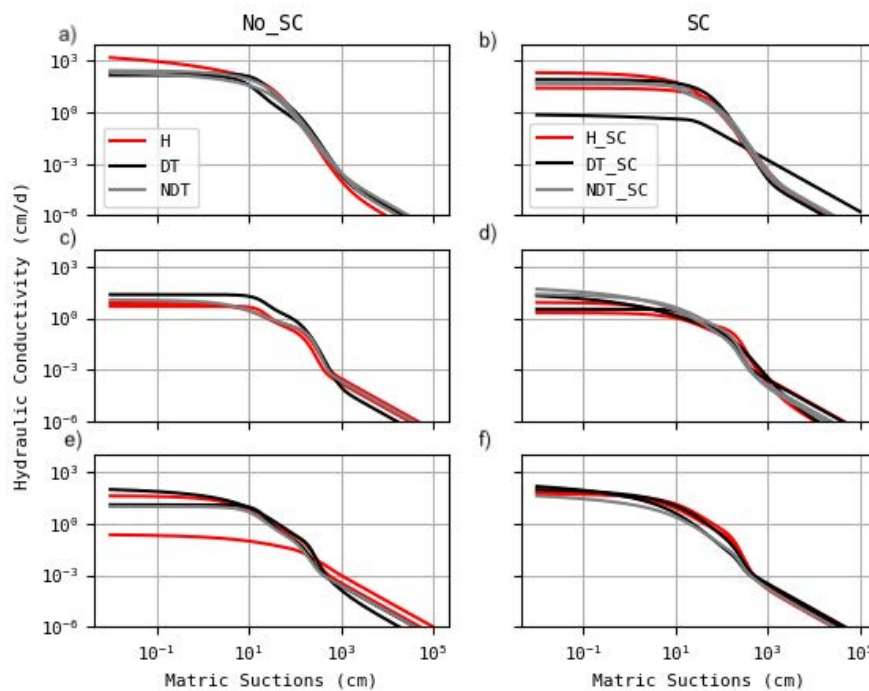


Fig. 2-11. Hydraulic conductivity curves (fitted with PDI model using both  $K_s$  and  $K(h)$  data) without (a,c,e) and with (b,d,f) topsoil compaction at 15 cm (a,b), 35 cm (c,d) and 50 cm (e,f) depth with two replications for each treatment (H, DT and NDT).

At the higher matrix suctions ( $10 - 10^3$  cm),  $K(h)$  was slightly higher in the headland zone than in the in-field zone, but only at 50 cm depth. No clear trend was found at the other depths. Measured SWRC curves for all samples can be found in appendix S5.

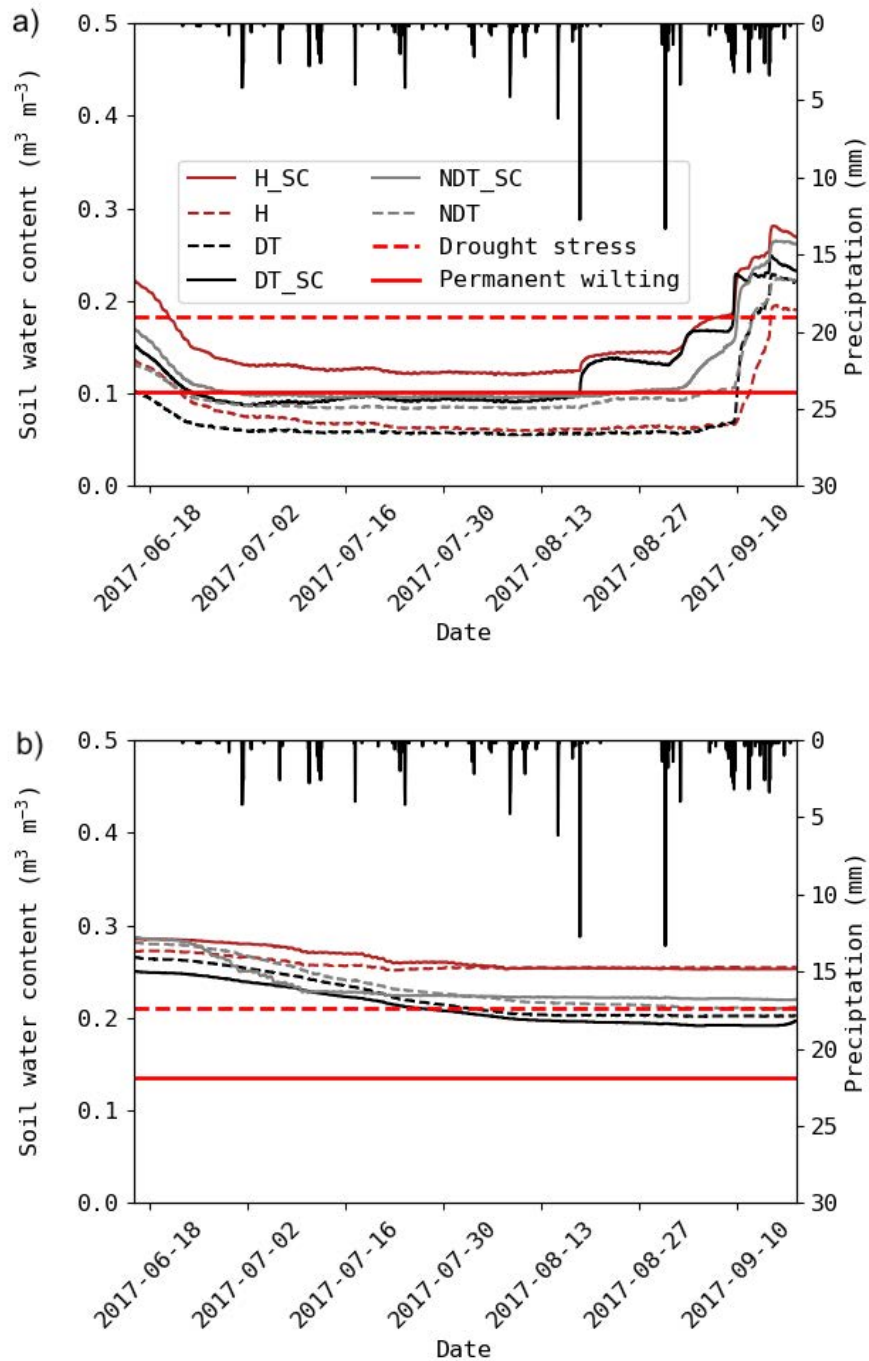


Fig. 2-12. Change in soil water content (measured by TDR) at 15 (a) and 50 cm (b) depth and precipitation (based on ILVO weather station) during the maize growing season of 2017. Drought stress and permanent wilting matric suctions are 600 cm (for high evaporative demand) and 8,000 cm, respectively according to Wesseling *et al.* (1991) for maize grown in the Netherlands.

For all treatments, at 15 cm depth, water content decreased in the beginning of June and became stable at around  $0.1 \text{ m}^3 \text{ m}^{-3}$  (Fig. 2-12) for several weeks, during which small rain events did not affect water content at that depth. By the end of August, it increased again resulting from two major rain events with more than 13 mm rain followed by several rainy days. Interestingly, the first major rains only increased soil moisture in the plots with topsoil compaction and the soil moisture increase in the plots without topsoil compaction began later. At 50 cm depth, water content was steadily decreasing till the second week of August and did not respond to any rain event.

In the topsoil compaction treatments (SC), soil water content was slightly higher at 15 cm depth, while no clear differences were found at 50 cm depth within the whole measuring period. With respect to the subsoil compaction treatments, water content was larger in the headland zone (H) than in the in-field zone (DT, NDT) at 50 cm depth from the beginning of July.

To compare recorded soil-water content with threshold values for drought stress and permanent wilting, matric suctions 600 cm (for high evaporative demand) and 8000 cm, respectively, were taken according to Wesseling *et al.* (1991) for maize grown in the Netherlands. Using average SWRCs at 15 and 50 cm depth in the summer season, for drought stress, a matric suction of 600 cm corresponds with a soil-water content of  $0.18$  and  $0.21 \text{ m}^3 \text{ m}^{-3}$ , respectively. For permanent wilting point, soil-water contents of  $0.10$  and  $0.14 \text{ m}^3 \text{ m}^{-3}$ , respectively, can be taken. From the end of July until August, soil moisture was around permanent wilting point at the top layer. At 50 cm depth soil moisture was around drought stress from mid-July onwards.

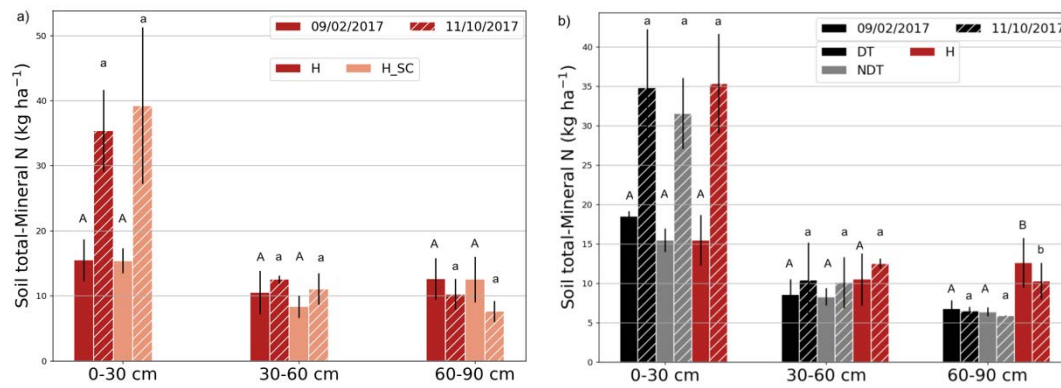


Fig. 2-13. Soil total mineral nitrogen (NO<sub>3</sub>-N+NH<sub>4</sub>-N) content at two sampling times for topsoil compaction levels (a) and subsoil compaction levels (b). The error bars are standard deviations (SD; n = 6). Different letters (uppercase and lowercase letters for sampling time on 09/02/2017 and 11/10/2017, respectively) in each group indicate significant differences ( $P \leq 0.05$ ).

Soil total mineral nitrogen measured one month after harvest (11/10/2017) was higher than that measured three months before sowing (09/02/2017) at 0-30 depth, while it was almost constant at 30-60 and 60-90 cm (Fig. 2-13). For topsoil compaction treatments, there was no difference among all three layers (Fig. 2-13a). For subsoil compaction treatments, there was no difference among treatments at 0-30 and 30-60 cm layer, but it was higher in the headland zone (H) than in the in-field zone (DT and NDT) at 60-90 cm layer at both sampling dates. This indicates that nitrogen leaching can be significantly higher in the headland zone where the subsoil is highly compacted.

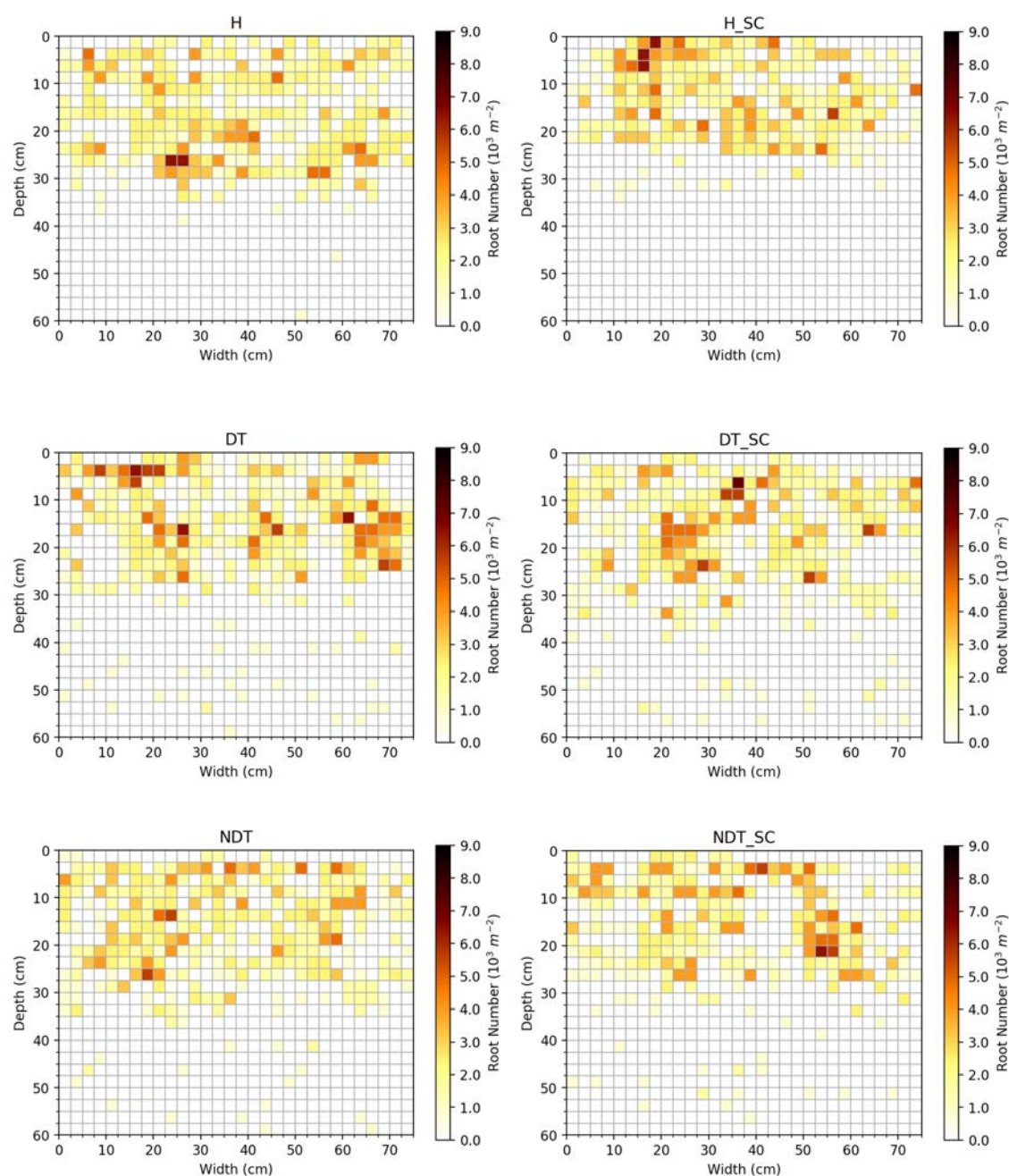


Fig. 2-14. Average (n=2) maize root number density distribution in each treatment (H = high subsoil compaction; DT = deep tillage; NDT = no deep tillage, SC = topsoil compaction) measured on 01/08/2017.

In all treatments, maize roots mainly accumulated in the upper 30 cm, i.e., above the plough pan (Fig. 2-14). However, in the in-field zone (DT, DT\_SC, NDT and NDT\_SC), few roots penetrated through the plough pan, which was not the case in the headland zone.

Table 2-5. Maize above-ground dry biomass harvested as silage on 19/09/2017. (H=high subsoil compaction; DT= deep tillage; NDT= no deep tillage). Standard deviation is in parentheses (Only significant results in the three-way ANOVA are shown).

Zone	Factors	Dry above-ground biomass (10 <sup>3</sup> kg ha <sup>-1</sup> )	P
In-field and headland zone (Two-way ANOVA)	<b>Topsoil compaction levels</b>		
	Topsoil compaction	21.51 (0.51)	0.847
	No topsoil compaction	21.37 (0.51)	
	<b>Subsoil compaction levels</b>		
	Highly compacted (H)	20.31 (0.62)	0.12
	Deep tillage (DT)	22.11 (0.62)	
	No deep tillage (NDT)	21.91 (0.62)	
	H : DT	-	0.06
	H : NDT	-	0.08
	DT : NDT	-	0.83
	H : (DT + NDT)	-	0.06
	<b>Top : Sub (interactions)</b>	-	0.54
In-field zone (Three-way ANOVA)	<b>Traffic leves</b>		
	Less	22.01 (0.39)	< 0.01
	More	19.34 (0.39)	
		<b>Top : Sub : Traffic (interactions)</b>	-

Under the limited traffic conditions, there were no differences between the with and without topsoil compaction treatments (Table 2-5). As for subsoil compaction levels, H had the lowest dry above-ground biomass, showing 8% lower compared with DT ( $P = 0.06$ ), while NDT only decreased by 0.9% compared with DT ( $P = 0.83$ ). There was no interaction effect between topsoil and subsoil compaction. In the in-field zone (DT and NDT), more traffic significantly decreased maize dry biomass compared to the area with less traffic. There was no interaction effect between topsoil and subsoil compaction and traffic.

### **2.3.3 Effects of deep tillage in 2018**

The effect of deep tillage was still detectable in April 2018, 1.5 years after it was applied (in October 2016) (Fig. 2-15a&b), in a ~20 cm width zone where the tine had passed. Soil water content at the day of PR measurements was not different between the two tillage treatments (Fig. 2-15b).

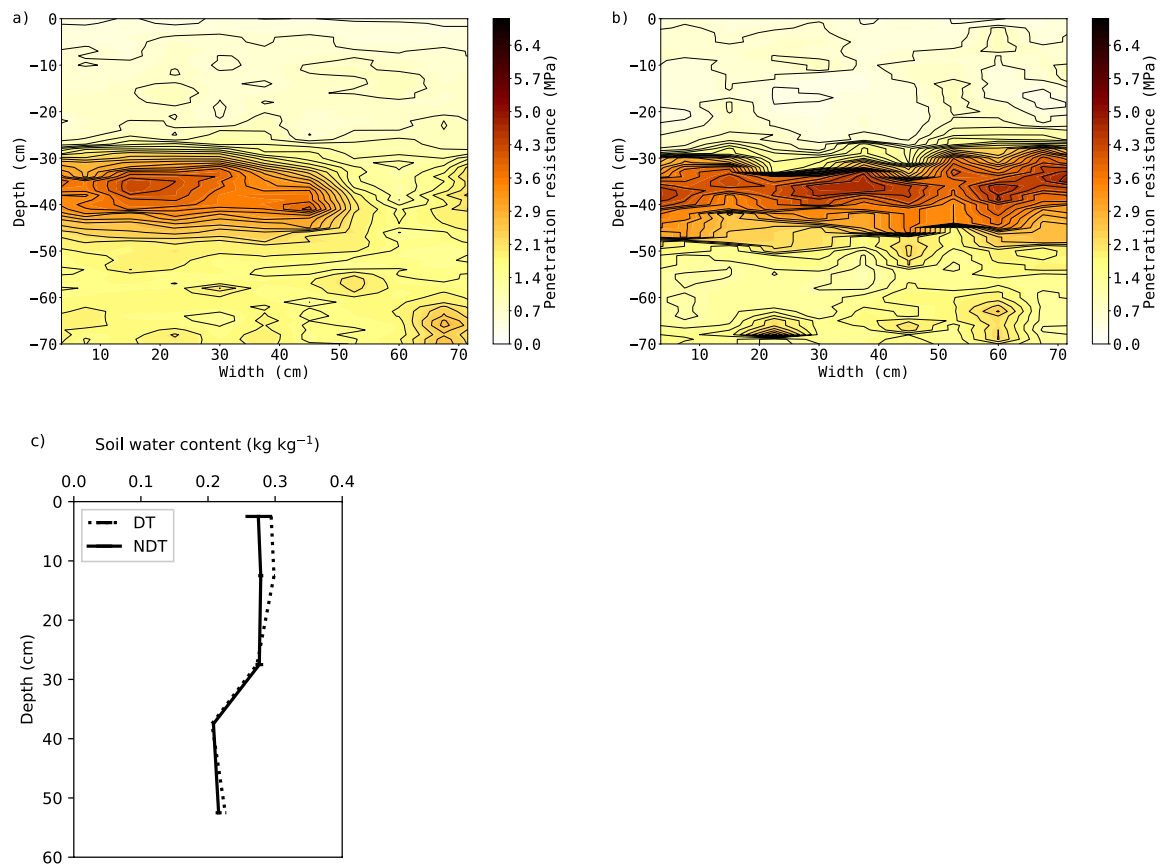


Fig. 2-15. Penetration resistance in DT (a) and NDT (b) and soil-water content (c) measured on 09/04/2018 (DT = deep tillage; NDT = no deep tillage).

Table 2-6. Maize canopy height and dry above-ground biomass under deep tillage and without deep tillage condition in 2018 (standard deviation in the parenthesis; n=6). Different letters indicate differences at  $P \leq 0.05$  level).

Treatments	90% maize	Dry above-ground biomass
	canopy height (m)	( $10^3 \text{ kg ha}^{-1}$ )
DT	2.73 (0.03) b	21.93 (1.92) a
NDT	2.66 (0.01) a	20.81 (1.03) a

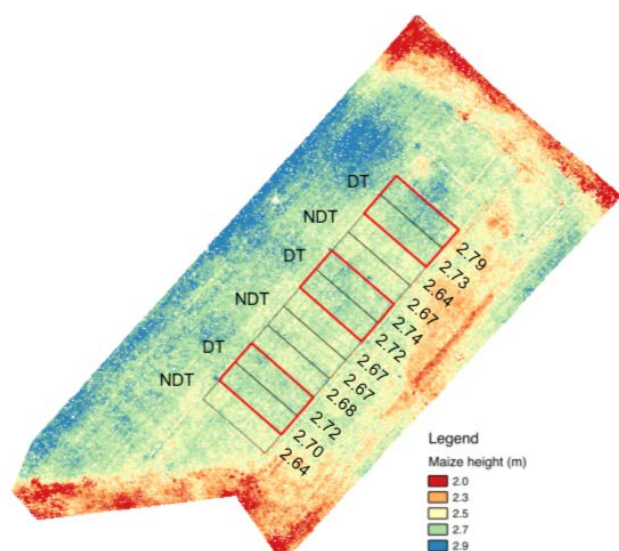


Fig. 2-16. Maize canopy height under different subsoil compaction levels (H = high subsoil compaction; DT = deep tillage; NDT = no deep tillage). Values shown in the figure are average 90% maize canopy heights per plot.

Maize canopy height was significantly higher in DT than in NDT (Fig. 2-15 and Table 2-6). However, no significant difference ( $P = 0.52$ ) was found for dry above-ground biomass between DT and NDT but the average value increased 5% in DT compared with NDT.

## 2.4. Discussion

### 2.4.1 Effects of topsoil compaction

Crop growth can be more sensitive to topsoil compaction than to subsoil compaction. For instance, Håkansson and Reeder (1994) also observed that a decreased crop biomass was largely caused by topsoil compaction (Håkansson and Reeder 1994). This was supported when considering the traffic tacks in the summer maize season of 2017, where maize dry above ground biomass decreased by 12% in

more trafficked areas compared with areas with limited traffic. However, this does not necessarily mean that topsoil compaction always restricts crop growth. Arvidsson and Håkansson (2014) and Colombi *et al.* (2018) reported that a certain degree of soil compaction is needed for optimal plant growth, especially following a freshly ploughed soil. This can be explained by the increase of contact area between soil and plant roots (Håkansson 2005; Alaoui *et al.* 2011; Arvidsson and Håkansson 2014). Soil that is too loose, will restrict water and nutrient uptake. In our study, using a tractor with a rotary harrow to compact the topsoil after a mouldboard ploughing did not affect maize growth. Besides, soil water content was slightly larger in all the topsoil compacted treatments than no topsoil compaction which could be the results of decrease of water uptake by maize or increase of unsaturated soil water conductivity by decreasing the large cracks among clods under topsoil compaction treatments.

For N leaching, no effect of topsoil compaction was found at different depths (till 90 cm) in the headland zone. A possible reason is that topsoil compaction did not restrict maize root growth (Fig. 2-14) which is one of the main N leaching factors under relatively dry conditions (Zhang *et al.* 2013). Similarly, Kussow (2000) found no differences in N leaching under different topsoil compaction levels in a silt loam soil under relatively dry field conditions.

### **2.4.2 Effects of subsoil compaction**

In general, subsoil in both the in-field and headland zone was seriously compacted with PR exceeding 3 MPa, even at a high soil moisture content at the subsoil with  $\sim 0.30$  kg/kg (Fig. 2-5a and Fig. 2-6), and with BD being larger than  $1.6 \text{ Mg m}^{-3}$  (Fig. 2-7). According to the literature, the threshold PR value for root growth is

2-3 MPa (Materechera *et al.* 1991; Da Silva *et al.* 1994; Lipiec and Hatano 2003; Bengough *et al.* 2011) and for BD, Reynolds *et al.* (2009) suggested that for medium to fine-textured soil there is a potential yield loss by excessive mechanical resistance to root elongation when BD is above  $1.4 \text{ Mg m}^{-3}$ , while Huber *et al.* (2008) suggested a threshold BD value of  $1.6 \text{ Mg m}^{-3}$  for soils with a clay content below  $167 \text{ g kg}^{-1}$  like in our study. Correspondingly, roots distribution was greatly restricted in both in-field and headland zone in our study.

Soil penetration resistance was larger in H for the subsoil compared with the NDT (Fig. 2-6). But for the BD, it was only larger at 50 cm depth in H. This could in part be explained by the different soil moisture content between in-field and headland zone at 30-60 cm layer when measuring the PR on 25/04/2017. Soil saturated water conductivity was larger at 35 cm depth in H, which should be because of the bio macropores. However, at 50 cm, Ks was significantly smaller in the headland zone than in the in-field zone because roots and worms cannot penetrate the highly compacted sublayer in the headland zone. This can be proven by the soil macropores at 50 cm depth (Appendix S.6).

As a result of differences in soil physical and hydraulic properties in the subsoil among treatments, water transport and nutrient uptake was different between the headland and the in-field zones, which also affects plant growth. Subsoil water permeability was lower in the headland, resulting in a longer time to replenish to the subsoil and making topsoil wetter (Fig. 2-5). Moreover, a highly compacted subsoil restricted root growth, resulting in limited or no water and nutrient uptake in the dry summer season, where the soil water content at 50 cm depth decreased relatively less in the headland zone compared with that in the in-field zone (Fig. 2-12b). Similar results were reported in a topsoil compaction study in Switzerland where maize

extracted more water from the topsoil and the decrease in subsoil water content was delayed because of the restricted root elongation (Colombi *et al.* 2018). This was also supported by visual inspection of the maize leaves, showing that more leaves died in the headland zone as compared to the in-field zone, indicating more drought stress (Appendix S.7).

The higher N content measured at 60-90 cm depth illustrates a higher risk for N leaching in highly subsoil compacted condition (Fig. 2-13). The exact reason for the higher risk for N leaching is still not clear; whether it is caused by increased preferential flow or restricted root uptake. However, according to the soil water conductivity curves (Fig. 2-11;  $n = 2$ ), water transmittivity most probably did not play a role, as hydraulic conductivities did not vary much between the treatments, especially when soil was not saturated. Besides, De Pue *et al.* (2019b) pointed out water movement occurs primarily in the soil matrix rather than by preferential flow in this study area. Therefore, restricted plant root uptake might be the main reason. Similarly, other researchers also referred that restriction of root elongation might lead to higher nutrient leaching in compacted soil (Håkansson 2005; Gasso *et al.* 2013). To gain further insight, research on bare soil or with isotope labeling is recommended.

Maize dry above-ground biomass in 2017 was lower ( $P = 0.06$ ) in the headland zone than in the in-field zone (DT and NDT) (Table 2-5). This is consistent with the water content, nitrogen content and root distribution in the sub layer where maize cannot get access to water and nutrients in the dry summer in the headland zone while still some roots can penetrate the plough pan layer in the in-field.

### **2.4.3 Alleviation of subsoil compaction by deep tillage**

Though it was not possible to detect differences in soil properties based on the core samples collected in between two tines of the deep tillage, PR was clearly different in the areas where a tine had passed compared to the areas in between the tines (Fig. 2-6). Moreover, the effect of deep tillage was still clearly detectable after 1.5 years in this field (Table 2-6). There was no differences in soil water content in DT and NDT because there was no saturated water movement in the dry summer season. The tilled area, which is expected to have a higher  $K_s$  but not a higher  $K(h)$  could thus not contribute to promote water supply to the roots following the light rain events. However, maize canopy height was significantly higher in DT than in NDT in the dry summer of 2018 indicating that deep tillage can allow maize to access the deep water and nutrients (Fig. 2-15 and Table 2-6). Overall, the deep tillage applied in this study looks suitable to alleviate subsoil compaction. More research would be needed to detect the longest beneficial time of this application.

## **2.5. Conclusions**

The effect of both topsoil and subsoil (below 30 cm depth) compaction on soil physical and hydraulic properties, N content and crop growth parameters was evaluated. Topsoil compaction from multiple traffic passes during field preparation for maize growing could cause a significant decrease in maize dry above-ground biomass compared to areas with limited passes, but no differences in maize biomass were found under simulated topsoil compaction i.e., a single pass of a tractor with rotary harrow.

Three different levels of subsoil compaction were compared, i.e., a highly compacted headland zone, a less compacted in-field zone and an in-field zone where deep tillage had alleviated the subsoil compaction. Both visual evaluation and lab or field based measurements indicate that soil physical and hydraulic properties, as well as root number density, were different between the headland and in-field zones. As a result, water transport and root-water uptake were restricted in the headland zone. This made very limited water can supply to the subsoil and higher water content in the topsoil in the winter season, which reduced winter rye growth because of poor drainage. On the contrary, subsoil compaction restricted maize access to water and nutrition from the sub layer causing maize above-ground biomass to decrease in the dry summer.

The risk for soil mineral N leaching was higher in the headland zone, most probably because of reduced nutrient uptake following restricted root growth. Crop growth was restricted in the headland zone during both winter and summer seasons. The effect of deep tillage, i.e. soil loosening, remained for more than 1.5 years and it significantly increased maize canopy height in the extremely dry and hot summer of 2018.

In summary, attention should be paid to minimize the area with more traffic during seedbed preparation. Subsoil compaction decreases crop growth by restricting deep water and nutrient availability, resulting in less resilience to extreme weather conditions. Deep tillage was shown to be a promising way to alleviate this kind of subsoil compaction.

## **Part II : Prevention of soil compaction**

### **Chapter 3: Strategies to minimize soil compaction during seedbed preparation for winter rye**

This chapter is based on:

Lidong Ren, Amelia Baibay, Tommy D'Hose, Greet Ruyschaert, Jan De Pue, Wim M. Cornelis (2019). Strategies to minimize soil compaction during seedbed preparation for winter rye. *Geoderma* (under review).

### 3.1. Introduction

Soil compaction is a worldwide threat to sustainable agriculture resulting from its various adverse impacts on soil quality, crop growth and the environment (Unger and Kaspar 1994; Huber *et al.* 2008; Keller *et al.* 2013). In Europe, numerous compaction studies have been conducted in the Nordic countries where soil is much wetter during farming time than in the other regions (Arvidsson and Håkansson 1996; Berisso *et al.* 2012; Schjønning *et al.* 2013). With long-time and ever increasing mechanization in agriculture, soil compaction is recognised as one of the main threats to sustainable agriculture in Europe by the European Commission (Alameda *et al.* 2012).

Soil stress relates to tyre dimensions, tyre inflation pressure, wheel load and soil properties. Among these, tyre inflation pressure is the most easily and fast changeable factor. It directly affects the tyre and soil contact area, and ground pressure which in turn affects soil stress and its distribution. Within a certain range, soil stress increases with tyre pressure and tyre pressure explains most variation in soil stress in both top and subsoil under different wheel loads (Schjønning *et al.* 2012). Wetness is regarded as the most important and dynamic factor influencing soil compaction processes (Soane and Van Ouwerkerk 1994). Under wet conditions, tyre-soil contact area increases and vertical soil stress propagate goes deeper because of an increasing concentration factor according to the elasticity theory (Söhne 1953; Lamandé and Schjønning 2011c). Till now, few studies have evaluated the effects of tyre types, inflation pressures and soil moisture conditions together in a field scale.

For the few existing studies, most of them focused on the stress distribution instead of soil properties change, and field studies or experiments with different number of passes are even less. Besides, as differences in soil physical quality are

more difficult to detect, soil compaction effects are poorly understood (Arvidsson and Håkansson 1996; Berisso *et al.* 2012; Schjønning *et al.* 2013; Schjønning *et al.* 2016; Schjønning *et al.* 2017). Under freshly ploughed or loose soil condition, it is not clear how soil moisture and tyre pressure affect soil physical properties. Besides, crop growth is more sensitive to topsoil compaction and topsoil compaction caused by seedbed preparation cannot be eliminated before sowing. Hence, understanding the minimized soil compaction strategies are essential in agronomy.

The Terranimo® model (Lassen *et al.* 2013; Stettler *et al.* 2014) allows to evaluate the risk of soil compaction by comparing soil stress and soil precompression stress. It was already tested on many sites in Nordic countries (Keller 2005; Arvidsson and Keller 2007; Schjønning *et al.* 2008). However, whether the predicted risk are effectively reflected in a change in soil physical quality has hardly been tested, and it has been tested less in newly ploughed or loose soil.

In general, compaction is seen as having negative impacts on crop emergence, growth, yield and quality, due to hindered root development or lack of oxygen (Batey 2009; Chamen *et al.* 2015). Plants even appear to be more sensitive to detect soil compaction than traditional lab tests to measure soil properties (Arvidsson and Håkansson 1996; Roger-Estrade *et al.* 2004; Nawaz *et al.* 2013). Therefore, evaluation of plant growth is a usefull supplement to detecting soil compaction effects.

The objectives of this study were a) to evaluate the effects of tyre types, tyre pressures of sowing machines and soil moisture during seedbed preparation on physical soil properties and winter rye growth; b) to evaluate the effects of traffic passes on soil properties and sensitivity of different soil property indicators; c) to

evaluate the performance of Terranimo<sup>®</sup> model by comparing predicted soil compaction risk with real deterioration in soil compaction indicators.

### 3.2. Materials and methods

#### 3.2.1 Study site

The Gansberghelaan Field was used in this study. Prior to our experiment, potatoes (*Solanum tuberosum* L.) as the main crop, were grown. Climate in the study area is temperate maritime with mild winters and warm summers (Kottek *et al.* 2006). The mean annual temperature is 10.5 °C and the average annual precipitation is 852.4 mm (average values of 1981- 2016). No irrigation system is applied in this area..

Table 3-1. Soil texture and organic carbon content for every 30 cm depth interval.

Depth (cm)	Sand (>0.05 mm) (g kg <sup>-1</sup> )	Silt (0.05-0.002 mm) (g kg <sup>-1</sup> )	Clay (<0.002 mm) (g kg <sup>-1</sup> )	SOC (g kg <sup>-1</sup> )	Texture (USDA)
0-30	462.3 ± 7.3	471.3 ± 8.5	66.6 ± 2.8	8.9 ± 0.7	Sandy loam
30-60	437.9 ± 2.2	473.2 ± 10.3	86.7 ± 22.8	4.1 ± 0.4	Loam
60-90	395.2 ± 33.2	468.2 ± 18.7	132.5 ± 29.1	1.8 ± 0.3	Loam

SOC: soil organic carbon content. Geometric mean ± standard deviation of six samples.

The soil is classified as Haplic Luvisol (Dondeyne *et al.* 2014) and has a sandy loam to loam texture (USDA) (Table 3-1). Soil texture was determined with the sieve-pipette method (Gee and Bauder 1986) on six locations randomly taken within the field at every 30 cm depth and soil organic carbon was determined according to Walkley and Black (1934)

### 3.2.2 Experimental design

Soil compaction was induced during sowing a cover crop, winter rye (*Secale cereale* L.) with a sowing combination (Fig. 3-1), consisting of a tractor with a 900 kg front weight (for tractor balance) and a conventional rotary harrow-mounted seed drill. After the harvest of the potatoes and before the sowing of the winter rye, soil was loosened (15cm depth) by means of a cultivator, perpendicular to the sowing direction. The experiment took place in the autumn and winter of 2015. A 54 m × 50 m test area was selected which was relatively homogenous according to an Electromagnetic Induction (EMI) survey (more information can be found in Chapter 7 about this method ) and field texture test (by hand) as depicted in Fig. 3-2a. The area was divided into two sections: one where operations were conducted under moist conditions (W) and one under dry conditions (D). The dry experiment took place on October 23, 2015 and the moist one on November 11, 2015. Between this period, several rainy days resulted in total 14.10 mm rain. During each wheeling experiment, soil-water content was measured gravitationally from composite samples taken at three depth intervals (0- 10, 10-30 and 30-60 cm), with a Gouge in 2 x 4 (4 transects of 2 replications) and in 4 × 4 replicates for the dry and moist site, respectively. They were converted into volumetric water content by multiplying bulk density (see section 2.3.2) for each layer (Fig. 3-3). During the wheeling experiment, each section was further divided into four

treatments (SL, WL, SH and WH) with each of them a combination of standard (S) or wide (W) tyres with high (H) or low inflation pressure (L). Each treatment was trafficked back and forth, resulting in four wheeling tracks per plot with two wheeling tracks adjacent in the middle. An extra treatment was reserved in the moist condition by an SH tyre for an experiment with two passes instead of one, making a total of nine treatments (Fig. 3-2b). During the operation, two different tractors were used for the two types of tyres (standard or wide). The wheel loads of tractors were measured with a balance. All the parameters of different tractor-rotary harrow-mounted seed drill combinations are shown in Table 3-2. The sowing depth was 2-3 cm.



Fig. 3-1. Sowing system with John Deere 6170R tractor (a. standard tyres. b. wide tyres).

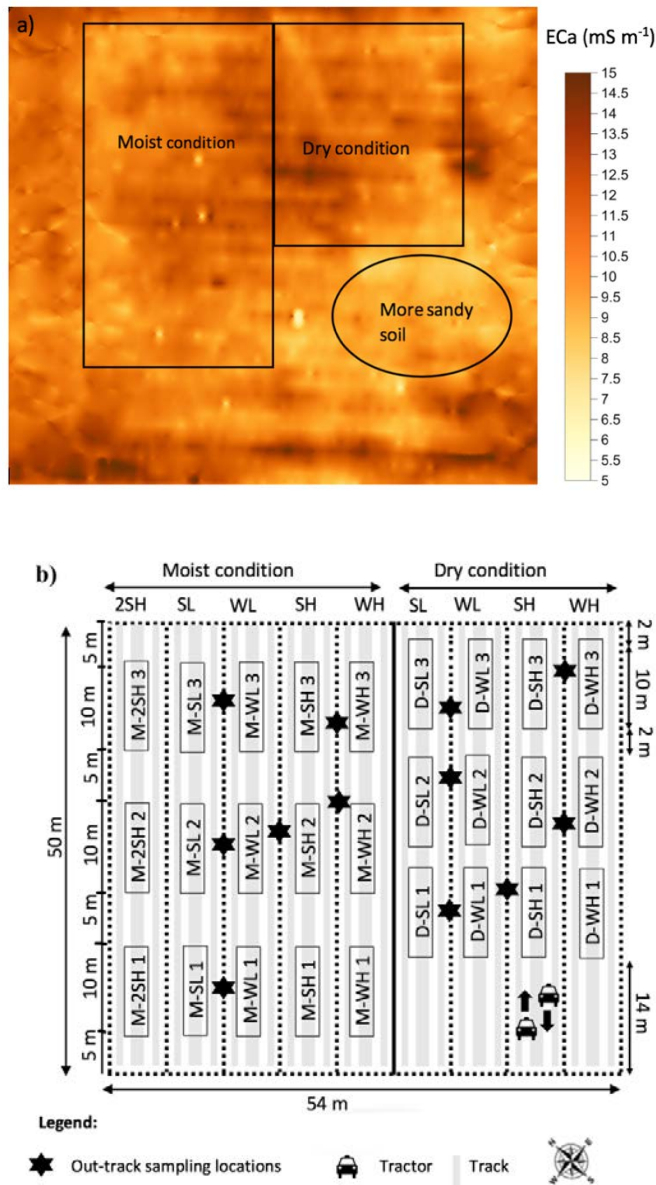


Fig. 3-2. Apparent electrical conductivity (ECa) map of the studied field in 0-25 cm layer (a) and experimental design (b) (D = Dry condition; M = Moist condition; S = Standard tyre; W = Wide tyre; H = High tyre pressure; L = low tyre pressure; M-2SH = Moist condition + two passes + standard tyre + high tyre pressure; '1', '2' and '3' represents three replicates in each treatment; out-track samples were used as control treatments).

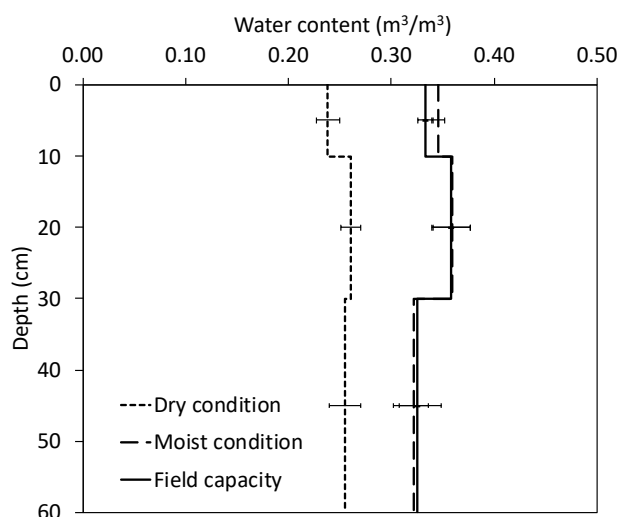


Fig. 3-3. Soil-water content during sowing under dry and moist condition (n=3) and at field capacity (n=6; matric potential of -330 hPa). Error bars stand for standard error.

Table 3-2. Characteristics of the different tractor-rotary harrow-mounted seed drill combinations.

	Standard tyres (S)		Wide tyres (W)	
	Low pressure (SL)	High pressure (SH)	Low pressure (WL)	High pressure (WH)
Tractor type	John Deere 6170R	John Deere 6170R	John Deere 6150	John Deere 6150
Front tyre type	Michelin Multibib 540/65 R30	Michelin Multibib 540/65 R30	Michelin MachXbib 710/55 R30	Michelin MachXbib 710/55 R30
Front tyre width (cm)	54	54	71	71
Front wheel load (kg)	1719	1719	1650	1650
Rear tyre type	Michelin Multibib 650/65 R42	Michelin Multibib 650/65 R42	Michelin MachXbib 900/50 R42	Michelin MachXbib 900/50 R42
Rear tyre width (cm)	65	65	90	90
Rear wheel load (kg)	2486	2486	2390	2390
Front and rear tyre pressure (kPa)	100	140	50	100

After sowing, three plots were delineated on each treatment for repeated sampling and measurements (Fig. 3-2). The plots were 10 m long and 6 m width (Fig. 3-4). They were spaced out differently in the moist and dry sections to avoid heterogeneous hot spots in the field as revealed by the EMI and field texture test. In the dry section, they were separated by 2 m, whereas in the moist section, this was 5 m.

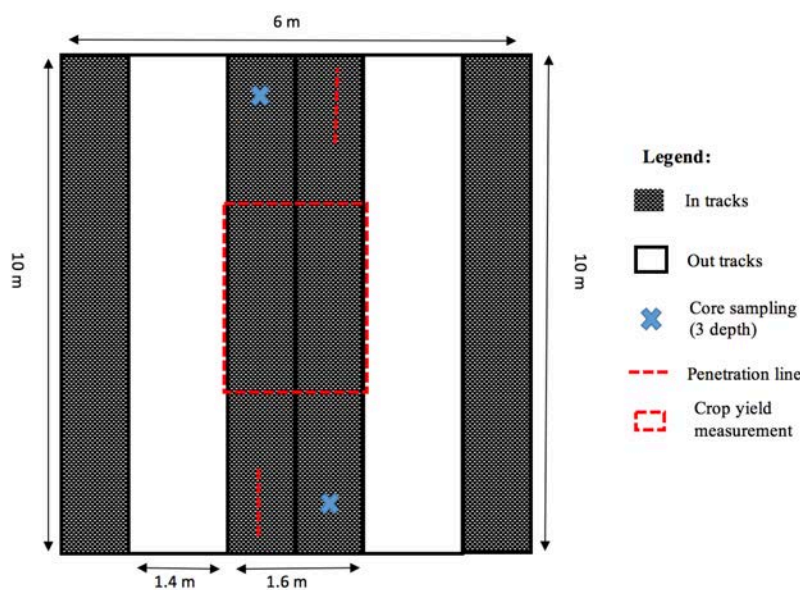


Fig. 3-4. Sampling strategy in one plot.

Within each plot, the sampling locations were in the two connected tracks and different sampling zones were allocated for each measurement (Fig. 3-4). An area of  $5 \times 1$  (or  $1.6$ )  $\text{m}^2$  was preserved in the center for crop harvesting. The two  $2.5 \times 1$  (or  $1.6$ )  $\text{m}^2$  plot heads were used for soil sampling and for penetration resistance measurements. Care was taken to take all measurements and sampling at the center of the wheel track. There was no control plot as such; instead, reference points were taken between the tracks (no-trafficked position) and averaged. In each section (moist

and dry), six reference points were selected, taken according to a random S shape. The points are considered as the control treatment.

### 3.2.3 Measurements and prediction

#### 3.2.3.1 Tyre contact area and rut depth

The contact area was measured once per treatment by spreading chalk powder around the rear left tyre of the tractor as illustrated in Fig. 3-5. The rut depth was manually measured along one transect perpendicular to the driving direction with five measurements per transect on the ridge of the tread and five in between. Mean ground pressure (MGP) was calculated using wheel load divided by contact area.

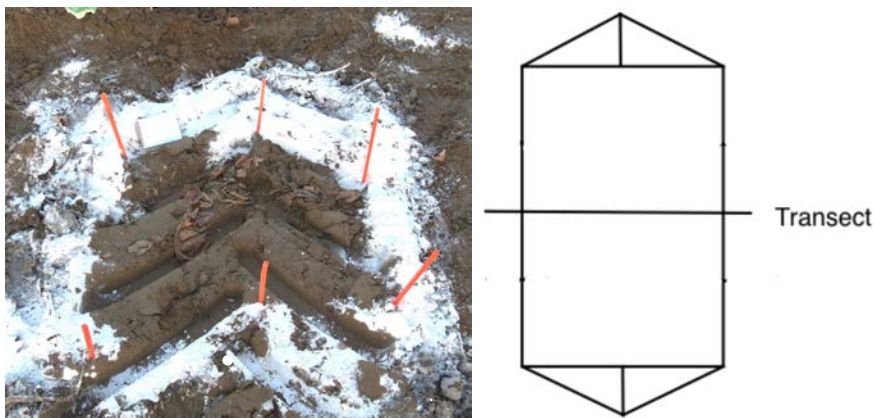


Fig. 3-5. Illustration of measuring contact area and rut depth along a transect.

#### 3.2.3.2 Soil physical properties

After sowing the winter rye in both dry and moist conditions, penetration resistance (PR) was measured using a hand-held penetrometer (Eijkelkamp Soil & Water) to 70 cm depth. The cone had a 1 cm<sup>2</sup> base area, a 11.28 mm nominal diameter

and a 60° top angle. Ten penetrations were taken per plot with five (at 7.5 cm interval) at each plot head (Fig. 3-4), for 30 replicates per treatment. For the control, ten penetrations were taken per location. One soil moisture sample was taken in 10-cm increments till 70 cm depth in each plot.

Undisturbed soil sample was collected in 100 cm<sup>3</sup> standard sharpened steel cores (5.1 cm height and 5 cm diameter) at the same time with PR. Core samples were collected at 15, 25, 35 and 55 cm depth at both sides of each plot, resulting in six replications per treatment. One core sample was also sampled for each control location (Fig. 3-2b). Saturated hydraulic conductivity ( $K_s$ ) was determined by the falling-head method according to Reynolds and Elrick (2002). After that, three soil cores per treatment were used to measure water retention curves according to the procedure outlined in Cornelis *et al.* (2005). Matric suction heads of 10, 30, 50, 70, 100, 340, 1,020 and 15,300 cm were selected. Soil-water retention curves were plotted by fitting the Van Genuchten (1980) model:

$$\theta(h) = \begin{cases} \theta_r + \frac{\theta_s - \theta_r}{\left[1 + |\alpha h|^n\right]^m} & h < 0 \\ \theta_s & h \geq 0 \end{cases} \quad (3-1)$$

where  $\theta_r$  and  $\theta_s$  are residual and saturated soil-water content (cm<sup>3</sup> cm<sup>-3</sup>), respectively.  $\alpha$  (cm<sup>-1</sup>) is positively related to the reciprocal of air-entry pressure, and  $n$  is a pore-size distribution index, being positively related to the slope of the soil-water retention curve and  $m=1-1/n$ .  $\theta(h)$  is soil-water content (cm<sup>3</sup> cm<sup>-3</sup>) at matric suction head  $h$  (cm).

Other soil physical quality parameters, like air capacity (AC, air pores volume between soil water suction at 100 and 0 cm), relative field capacity (RFC, the percentage of soil water field capacity and saturated water content), plant-available

water capacity (PAWC, soil water content between soil water suction at 100 and 15,000 cm) and S index were calculated according to Reynolds *et al.* (2009) and (Dexter 2004). Table 3-3 shows all the hydro-physical relevance and threshold values of all selected parameters.

Table 3-3. Meaning and threshold values of hydro-physical parameters for the selected soil type.

Parameter	Hydro-physical relevance	Threshold value	Reference
Bulk density (BD, Mg m <sup>-3</sup> )	aeration, strength, and ability to store and transmit water	< 0.9 “low”; 0.9–1.2 “good”; > 1.2 “high” unit	Reynolds et al., (2009)
Penetration resistance (PR, MPa)	impedance to roots compactness	< 2 “ok”; 2-3 “limiting”; >3 “very limiting”	Lipiec and Hatano (2003)
Saturated hydraulic Conductivity (Ks, cm d <sup>-1</sup> )	flow and transport rates	< 1 “very poor”; < 10 “poor”, < 100 “reasonable”	Lipiec and Hatano (2003)
Available water Content (AWC, cm <sup>3</sup> cm <sup>-3</sup> )	water storage and provision to plants	> 0.2 “ideal”; 0.15-0.2 “good”; 0.10-0.15 “limited”; < 0.10 “poor, droughty”	Reynolds et al., (2009)
Relative field capacity (RFC, i)	air-water balance microbial production of nitrate	0.6-0.7 “optimal”; < 0.6 “water deficit”; < 0.5 “high water deficit”; > 0.7 “air deficit”; > 0.8 “high air deficit”	Reynolds et al., (2009)
Air capacity (AC, cm <sup>3</sup> cm <sup>-3</sup> )	aeration	> 0.14 “ok”; < 0.14 “bad”; < 0.10 “very bad”;	Reynolds et al., (2009)
S index (S, -)	soil structure	< 0.02 “very poor”; 0.02 < S < 0.035 “poor”; 0.035 < S < 0.05 “good”, S > 0.05 “very good” (3)	Dexter (2004)

### 3.2.3.3 Predicting the risk of soil compaction

To predict the risk of soil compaction, the Terranimo® model ([www.terranimodk.dk](http://www.terranimodk.dk)) was used. Tractor type, wheel load, tyre parameters, soil texture and matric suction (wetness) were used as input data. In Terranimo®, the top boundary condition and the stress distribution at the tyre-soil contact interface, is computed with the FRIDA model (Schjønning *et al.* 2008). Soil stress propagation was calculated using FRIDA-fitted top boundary conditions as input to the Söhne (1953) model. Concentration factor ( $\nu$ ) was calculated by an exponential pedotransfer function based on the matric potential (pF). Soil precompression stress is calculated by a pedotransfer function that includes the soil matric suction head expressed as pF (log of matric suction head with head expressed in cm) and clay content (not published).

The risk of soil compaction is indicated by a soil compaction index (SCI) calculated with the following equation by Rücknagel *et al.* (2015):

$$SCI = \log (P_{act}/P_c) \quad (3-2)$$

where  $P_{act}$  is the calculated, actual vertical stress, and  $P_c$  is soil precompression stress. Three classes are distinguished:  $SCI \leq 0$  means no soil compaction risk;  $0 < SCI \leq 0.20$  indicates medium risk and  $SCI > 0.20$  is a serious alert. Negative values of SCI (stress lower than precompression stress; no risk of compaction) are set to zero.

Soil precompression stress was calculated per 10-cm interval from measured clay content (Table 3-1) and volumetric soil-water content with the latter being converted to matric suction head using the water-retention curves measured at four depths per treatment (see 2.3.2). Below 60 cm depth, hydraulic equilibrium was assumed with a water table taken at 1 m depth according to ground water table database in Flanders (Database Subsurface Flanders, [www.dov.vlaanderen.be](http://www.dov.vlaanderen.be)).

#### **3.2.3.4 Crop biomass and root density**

Before the mechanical destruction of the cover crop, winter rye growth was assessed through the weighting of shoots and roots on April 6, 2016. A 30 × 30 cm area was randomly selected per plot in the crop yield measurement zone (Fig. 3-4), conducting three replications per treatment. For the control, three locations (among those six locations) were selected for both dry and moist conditions to sample shoot biomass and root density. The winter rye was cut with scissors and both the fresh weight and the dry weight (75°C, 48 hours) were determined. Root samples were collected with an 8-cm diameter root auger, in 10-cm increments for all treatments except for M-SL and M-WH, which were not included because little difference was expected. Dry root biomass and root density were determined after washing in a 50-µm mesh sieve and drying at 75°C for 48 hours.

#### **3.2.3.5 Statistical analysis**

For soil properties, statistical analysis was made in three distinctions, named as 'trafficked treatments', 'track' and 'passes'. 'Trafficked treatments' category included all treatments except for the 'M-2SH' and 'control'. 'Track' included 'Trafficked treatments' (All treatments were pooled in one group) and control. 'Passes' were only compared between 'M-2SH' and 'M-SH'. For crop properties, comparison was made for moist and dry conditions separately as the sowing data was not the same. The statistical analysis was performed using SPSS Statistics 25 combined with in-house written Python scripts. The general linear model was selected for analysis of variance

(ANOVA) and the least significant difference (LSD) was used for multiple comparison ( $P < 0.05$ ). Saturated soil water conductivity ( $K_s$ ) was log transformed to make the variance homogeneous. The statistical procedures are described in Gomez and Gomez (1984).

### **3.3. Results**

#### **3.3.1 Contact area, mean ground pressure and compaction risk**

Wide tyres had larger contact area (moist: +83%, dry: +43%) and smaller mean ground pressure (moist: -46%, dry: -32%) compared with standard tyres (Table 3-4). Likewise, low tyre pressure had larger contact area (moist: +31%, dry: +29%) and smaller mean ground pressure (moist: -20%, dry: -18%) compared with high tyre pressure. Dry soil conditions had smaller contact area (-8%) and larger mean ground pressure (+9%) for wide tyres compared with moist conditions but showed an unexpected trend for standard tyres. It was proved to be an unexpected result for standard tyres further when compared with the Terranimo® modeling results. Overall, the Terranimo® predicted results matched the measured ones well (RMSE=0.07 m<sup>2</sup> and 14.30 kPa, respectively). For rut depth, it was larger with high tyre pressure and narrower tyre width in moist conditions but the opposite result was found in dry conditions.

Table 3-4. Measured and predicted contact area, ground pressure and rut depth in each treatment for the rear wheel (mean  $\pm$  standard deviation).

Moisture conditions	Treatments	Measurements			Predicted with Terranimo®	
		Contact area (m <sup>2</sup> )	Rut depth (cm)	MGP (kPa)	contact area (m <sup>2</sup> )	MGP (kPa)
Dry	SH	0.31	6.21 $\pm$ 0.77	80	0.38	65
	SL	0.37	9.27 $\pm$ 1.34	67	0.40	61
	WH	0.41	6.06 $\pm$ 1.18	58	0.48	49
	WL	0.56	5.29 $\pm$ 1.37	43	0.60	39
Moist	SH	0.27	8.94 $\pm$ 0.45	92	0.39	63
	SL	0.31	6.75 $\pm$ 0.11	80	0.41	60
	WH	0.44	9.00 $\pm$ 1.72	54	0.49	48
	WL	0.62	5.94 $\pm$ 1.34	39	0.61	39

S: standard tyre; W: wide tyre; D: dry condition; M: moist condition; L: low pressure; H: high pressure. MGP: Mean ground pressure (kPa).

To further explain the changes in soil physical indicators (section 3.2.), the Terranimo® model was used to predict compaction risk along soil profiles (Table 3-5). It shows that soil compaction risk only existed in the top layer (0-30 cm). Under dry conditions, the tractor with standard tyres showed higher compaction risk compared with the tractor with wide tyres, and the compaction risk depth was deeper under the tractor with standard tyres. Tyre pressure also influenced the compaction risk. It increased with increasing tyre pressure. Surprisingly, there was no compaction risk in 'WL' treatment. Moreover, the front axle even showed higher compaction risk than the rear axle, which could be due to the added balance weight (900 kg) in the front. Overall, under moist conditions, trends were similar to those under dry conditions but the compaction risk increased as soil precompression stress decreased when soil became wetter, which is also supported by elasticity theory.

Table 3-5. Soil compaction index (SCI) calculated as the log to the ratio of stress and precompression stress.

Moisture condition	Treatments	Axle	Soil depth (m)					
			0.1	0.2	0.3	0.4	0.5	0.6
Dry	SH	Front	0.26	0.16	0.03	0.00	0.00	0.00
		Rear	0.25	0.18	0.08	0.00	0.00	0.00
	SL	Front	0.22	0.13	0.01	0.00	0.00	0.00
		Rear	0.20	0.14	0.06	0.00	0.00	0.00
	WH	Front	0.16	0.07	0.00	0.00	0.00	0.00
		Rear	0.10	0.05	0.00	0.00	0.00	0.00
	WL	Front	0.00	0.00	0.00	0.00	0.00	0.00
		Rear	0.00	0.00	0.00	0.00	0.00	0.00
Moist	SH	Front	0.31	0.21	0.08	0.00	0.00	0.00
		Rear	0.30	0.23	0.14	0.00	0.00	0.00
	SL	Front	0.28	0.19	0.07	0.00	0.00	0.00
		Rear	0.26	0.20	0.11	0.00	0.00	0.00
	WH	Front	0.21	0.13	0.02	0.00	0.00	0.00
		Rear	0.15	0.11	0.04	0.00	0.00	0.00
	WL	Front	0.05	0.00	0.00	0.00	0.00	0.00
		Rear	0.00	0.00	0.00	0.00	0.00	0.00

SCI = 0: No compaction risk;  $0 < \text{SCI} \leq 0.2$ : Intermediate compaction risk (yellow color);

SCI > 0.2: High compaction risk (red color). S: standard tyre; W: wide tyre; D: dry condition; M: moist condition; L: low pressure; H high pressure.

### 3.3.2 Soil physical property indicators

According to a Spearman's correlation test (Table 3-6), soil quality indicators extracted from core samples (except Ks, based on 6 samples), i.e., BD, AWC, RFC, AC and S index, were significantly ( $P < 0.01$ ) correlated with the hydraulic parameters  $\theta_r$ ,  $\theta_s$ ,  $\alpha$ , and  $n$ . Hence, only the first five soil property indicators were selected for further analysis. Among those five soil property indicators, only BD was significantly

correlated with all the rest four indicators whereas RFC and AC, S index and AWC were only significantly correlated with each other, respectively.

Table 3-6. Spearman's correlation coefficients (for all treatments) among soil quality indicators.

	BD	AWC	RFC	AC	S	$\theta_r$	$\theta_s$	$\alpha$	n
BD	1.000	<b>-0.422**</b>	<b>0.623**</b>	<b>-0.694**</b>	<b>-0.301**</b>	<b>0.272**</b>	<b>-0.828**</b>	<b>-0.487**</b>	0.163
AWC		1.000	0.023	0.036	<b>0.643**</b>	-0.065	<b>0.382**</b>	<b>-0.175*</b>	<b>0.325**</b>
RFC			1.000	<b>-0.992**</b>	-0.065	<b>0.589**</b>	<b>-0.278**</b>	<b>-0.757**</b>	<b>0.305**</b>
AC				1.000	0.110	<b>-0.565**</b>	<b>0.366**</b>	<b>0.752**</b>	<b>-0.288**</b>
S					1.000	<b>0.291**</b>	<b>0.222**</b>	<b>-0.273**</b>	<b>0.826**</b>
$\theta_r$						1.000	0.005	<b>-0.450**</b>	<b>0.624**</b>
$\theta_s$							1.000	<b>0.360**</b>	-0.104
$\alpha$								1.000	<b>-0.535**</b>
n									1.000

BD = bulk density, PR = penetration resistance, AWC = available water Content, RFC = relative field capacity, AC = air capacity, S = S index,  $\theta_r$  = residual soil water content ( $\text{cm}^3 \text{ cm}^{-3}$ ),  $\theta_s$  = saturated soil water content ( $\text{cm}^3 \text{ cm}^{-3}$ ),  $\alpha$  ( $\text{cm}^{-1}$ ) is a parameter related to the reciprocal of air-entry pressure, and  $n$  is a pore-size distribution index.

Penetration resistance and soil water content distribution within 70 cm depth is shown in Fig. 3-6 and the P value of statistic analysis (average of each layer) from 10 cm (exculding 0-10 cm data as this layer was disturbed by the sowing) to 60 cm depth is given in Table 3-7. As the soil water content which was determined during the PR measurements, did not significantly differ between treatments. Therefore, all penetration resistance values can be compared. In generally, a clear plough pan was

present in all plots, indicating seriously deep layer compaction in this study area. Besides, the absolute PR value was not high which is because the water content was high, a bit larger than the field capacity ( $\sim 0.2$  kg/kg). Among treatments, PR was not affected by moisture conditions, tyre type and tyre pressure but PR of the trafficked treatments was significantly larger ( $P < 0.05$ ) compared with the control in the top 30 cm. A significant difference ( $P = 0.02$ ) was found between single pass and multiple passes at 20-30 cm depth. Below 30 cm depth, some differences did exist between treatments and the control which were more likely caused by various depth of plough pan as no compaction risk below 30 cm according to Terranimo®.

In accordance with the finding on PR at 15 cm depth, significant ( $P < 0.05$ ) compaction effects on BD, Ks, RFC and AC were only found between single trafficked treatments and the control (Table 3-7). However, interaction effects among moisture, tyre type and tyre pressure did also exist. For AWC, only the above interaction effects were found, with D-SH had the lowest value. There were no differences in S at all depths. At 25 cm depth, differences between single trafficked treatments and the control were only found in AWC. Besides, moisture conditions significantly ( $P < 0.05$ ) affected AWC, RFC and AC. RFC was also different ( $P < 0.05$ ) with tyre type and tyre pressure, and AC with tyre pressure. Interestingly, a decreasing trend ( $P = 0.09$ ) was found for AC when comparing two-passes at 20-30 cm depth, meaning that large pores ( $> 30 \mu\text{m}$ ) did decrease under two-passes. This was consistent with the penetration resistance values reported above. Similarly, an increasing trend ( $P = 0.10$ ) was observed between passes for RFC (Table 3-7 and Fig. 3-7), which is limiting below 0.6 or above 0.7. Below 30 cm depth, the minor differences found were not attributed to the treatments and will not be discussed here.

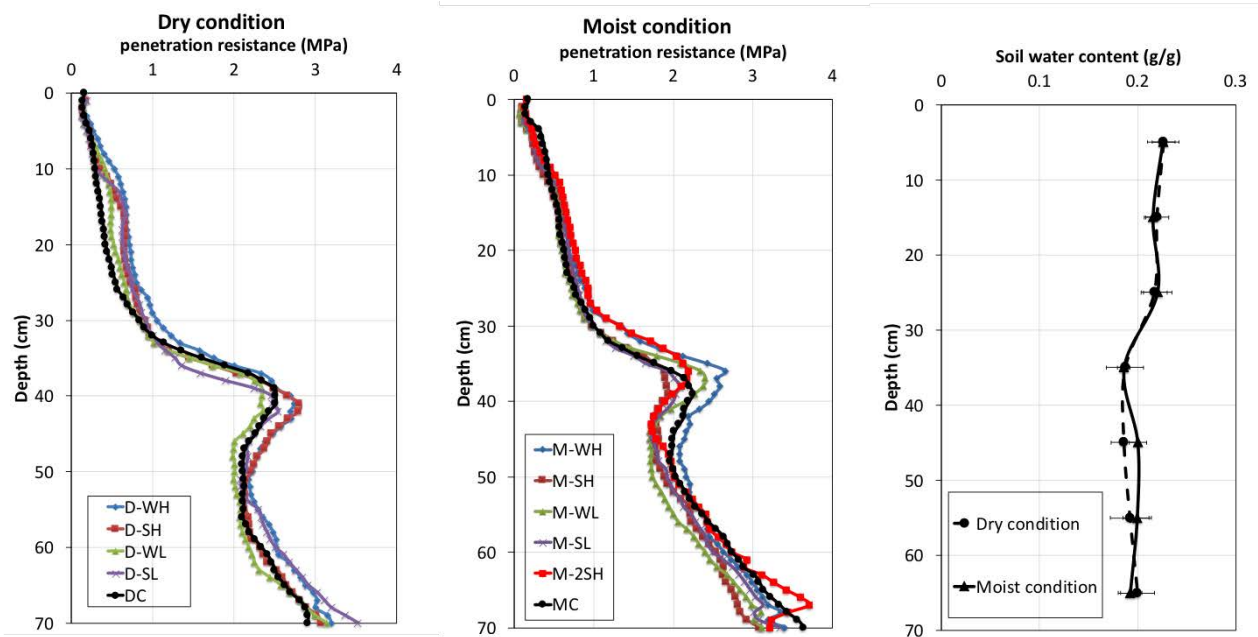


Fig. 3-6. Mean penetration resistance ( $n=30$ ) and soil-water content ( $n=15$ ) for all treatments after sowing. Error bars stand for standard error. Note that soil-water content and penetration resistance was measured on December 18, 2015 in plots that were trafficked on October 23, 2015 (dry) and November 11, 2015 (moist) (see Fig. 3-3) (D = Dry condition; M = Moist condition; S = Standard tyre; W = Wide tyre; H = High tyre pressure; L = low tyre pressure; M-2SH = Moist condition + two passes + standard tyre + high tyre pressure; MC = moist control; DC = dry control).

### Chapter 3

Table 3-7. Statistical analysis (P value) of the selected soil physical properties.

	15 cm							25 cm							35 cm							55 cm						
	PR	Ks	BD	AW C	RF C	AC	S	PR	Ks	BD	AW C	RF C	AC	S	PR	Ks	BD	AW C	RF C	AC	S	PR	Ks	BD	AW C	RF C	AC	S
Moisture (m) <sup>1</sup>	0.39	0.25	0.53	0.41	0.81	0.87	0.75	0.25	0.32	0.52	<u>0.04</u>	<u>0.01</u>	<u>0.02</u>	0.29	<u>0.00</u>	0.05	0.89	0.94	0.42	0.42	0.81	0.38	0.99	0.54	0.67	0.03	<u>0.04</u>	0.22
Tyre type (t) <sup>1</sup>	0.65	0.67	0.31	0.98	0.99	0.94	0.93	0.41	0.12	0.43	0.47	<u>0.05</u>	0.07	0.34	<u>0.00</u>	0.27	0.71	0.44	0.67	0.62	0.70	0.71	0.14	0.90	0.70	0.46	0.60	0.21
Tyre Pressure (p) <sup>1</sup>	0.53	0.28	0.42	0.47	0.89	0.96	0.27	0.07	0.54	0.57	0.12	<u>0.00</u>	<u>0.01</u>	0.38	<u>0.01</u>	0.37	0.43	0.28	0.57	0.73	0.05	0.39	0.84	<u>0.00</u>	0.52	0.38	0.27	0.24
m x t <sup>1</sup>	0.49	0.61	0.23	0.76	0.74	0.89	0.53	0.71	0.89	0.14	0.74	0.54	0.42	0.37	0.17	0.33	0.76	0.82	0.40	0.40	0.29	0.31	0.94	<u>0.02</u>	0.85	0.18	0.14	0.29
m x p <sup>1</sup>	0.49	0.21	0.85	0.55	0.58	0.63	0.35	0.93	0.76	0.66	0.20	0.12	0.19	0.36	0.70	0.59	0.16	0.66	0.31	0.50	0.31	0.12	0.32	0.31	0.10	0.98	0.91	0.76
t x p <sup>1</sup>	<u>0.04</u>	0.37	0.10	0.35	0.65	0.78	0.21	0.19	0.68	0.15	0.55	0.37	0.35	0.36	0.84	0.88	0.03	0.02	0.21	0.11	0.11	<u>0.01</u>	0.78	0.51	0.48	0.25	0.25	0.51
t x p x m <sup>1</sup>	0.48	0.42	0.29	<u>0.05</u>	<u>0.01</u>	<u>0.01</u>	0.14	0.20	0.04	<u>0.01</u>	0.65	<u>0.01</u>	<u>0.01</u>	0.38	<u>0.01</u>	0.49	0.27	0.08	0.47	0.69	0.38	0.25	0.32	0.97	0.30	0.76	0.74	0.19
Track <sup>2</sup>	<u>0.00</u>	<u>0.01</u>	<u>0.00</u>	0.68	<u>0.00</u>	<u>0.00</u>	0.47	<u>0.01</u>	0.29	0.08	<u>0.02</u>	0.80	0.65	0.76	0.47	<u>0.01</u>	0.70	0.40	0.46	0.45	0.50	0.76	<u>0.01</u>	<u>0.00</u>	<u>0.02</u>	<u>0.00</u>	<u>0.00</u>	0.09
Passes <sup>3</sup>	0.15	0.21	0.33	0.99	0.96	0.89	0.14	<u>0.02</u>	0.48	0.28	0.29	0.10	0.09	0.37	0.12	0.72	0.81	0.21	0.31	0.36	0.83	0.15	0.48	0.10	0.06	0.26	0.23	0.41

<sup>1</sup> P-values are displayed among 'Trafficked treatments'; <sup>2</sup> P-values are displayed between 'in track' and 'control'; <sup>3</sup> P-values are displayed between 'M-SH' and 'M-2SH. P < 0.05 labeled with underline and shading. PR was used in four layers: 10-20 cm, 20-30 cm, 30-40 cm and 40-60 cm. BD = bulk density, PR = penetration resistance, Ks = saturated hydraulic Conductivity, AWC = available water Content, RFC = relative field capacity, AC = air capacity, S = S index.

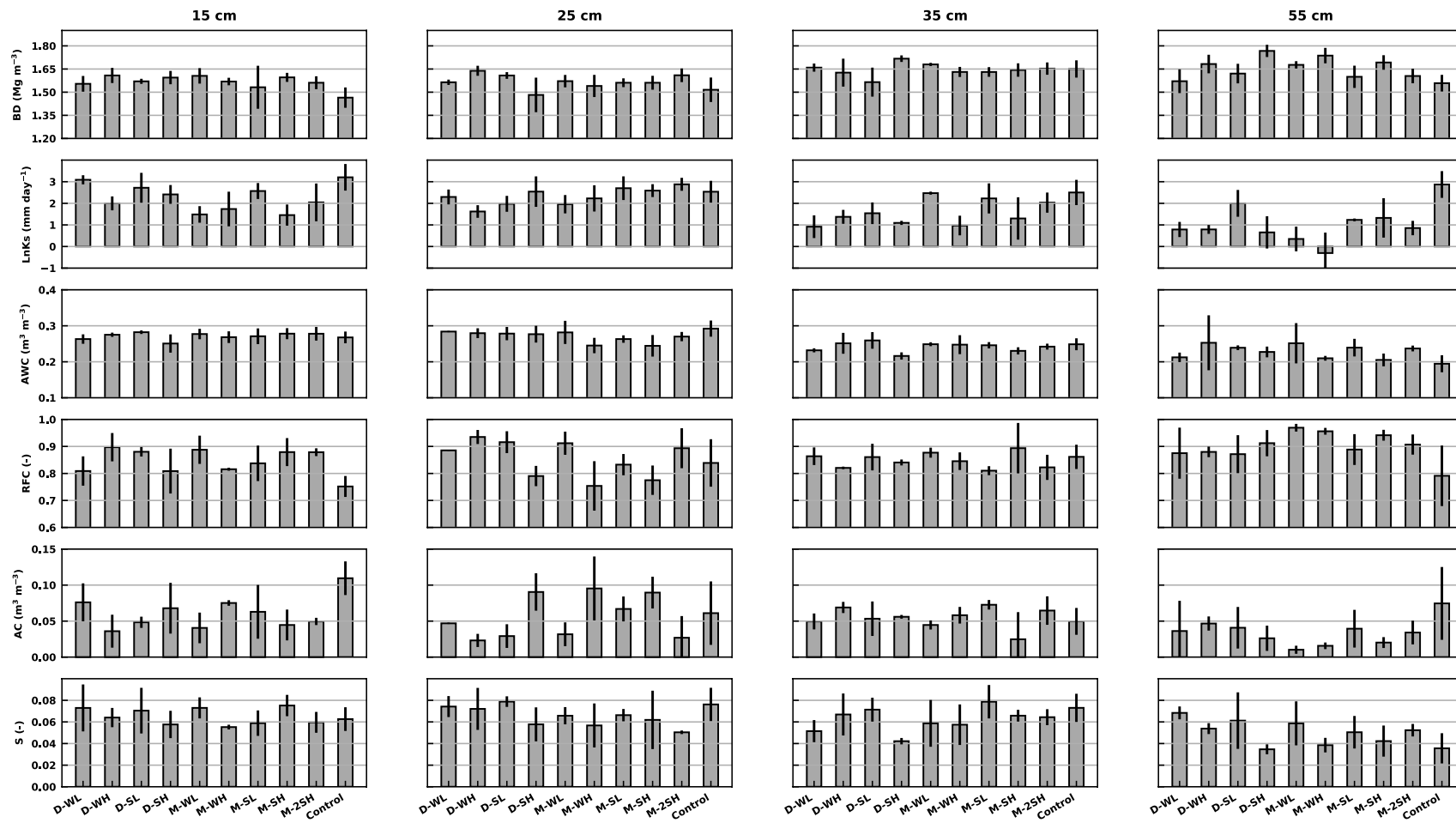


Fig. 3-7. Selected soil physical properties. The error bars are 95% confidence interval ( $n=3$ ,  $n=6$  for Ks) (BD = bulk density, PR = penetration resistance,  $\ln(K_s)$  =  $\log_{10}$  transformed saturated hydraulic conductivity, AWC = available water Content, RFC = relative field capacity, AC = air capacity, S = S index) (D = Dry condition; M = Moist condition; S = Standard tyre; W = Wide tyre; H = High tyre pressure; L = low tyre pressure; M-2SH = Moist condition + two passes + standard tyre + high tyre pressure; control = average of moist and dry conditions).

### 3.3.3 Effects on winter rye growth

Winter rye biomass was significantly ( $P < 0.05$ ) reduced in the trafficked parts compared with their controls under both moist and dry conditions (Fig. 3-8). Dry shoots biomass was ~40% lower for the dry trafficked treatments and ~80% lower for the moist trafficked treatments compared with the corresponding control treatment. The loss of productivity was particularly visible when the field was trafficked under moist conditions, showing almost no crop cover within the tracks (Fig. 3-9). There was no difference among trafficked treatments for both dry and moist conditions but the M-2SH biomass decreased by 23% compared with M-SH in moist condition.

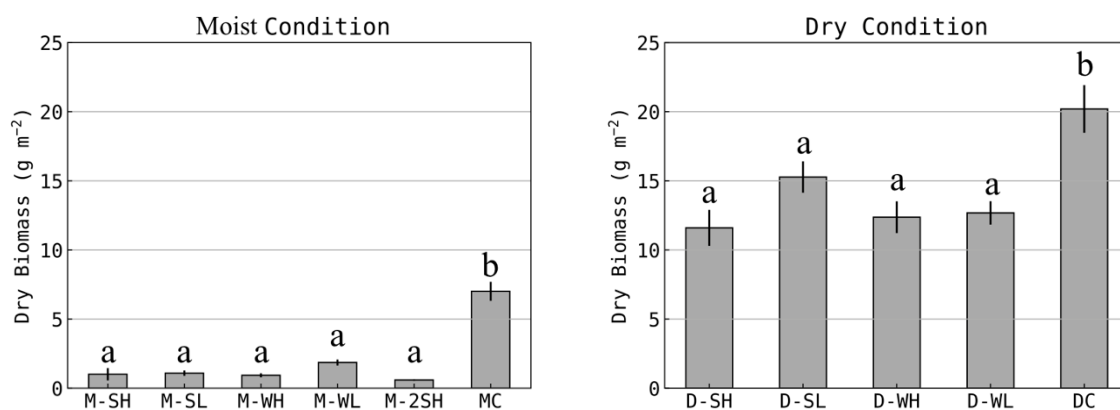


Fig. 3-8. Dry above ground biomass among treatments under each soil moisture condition. The error bars are standard deviation (SD;  $n=3$ ). Different letters indicate significant differences ( $P < 0.05$ ) (D = Dry condition; M = Moist condition; S = Standard tyre; W = Wide tyre; H = High tyre pressure; L = low tyre pressure; M-2SH = Moist condition + two passes + standard tyre + high tyre pressure; MC = moist control; DC = dry control).

The trends observed for the shoots were also reflected in root density (Fig. 3-9). Under dry conditions, there was no difference between all treatments at 0-10 and

10-20 cm depths. At 20-30 cm depth, it differed between control and trafficked treatments. Under moist condition, no roots could be detected below 10 cm depth at trafficked treatments and a difference was found between control and trafficked ones at 0-10 cm depth.

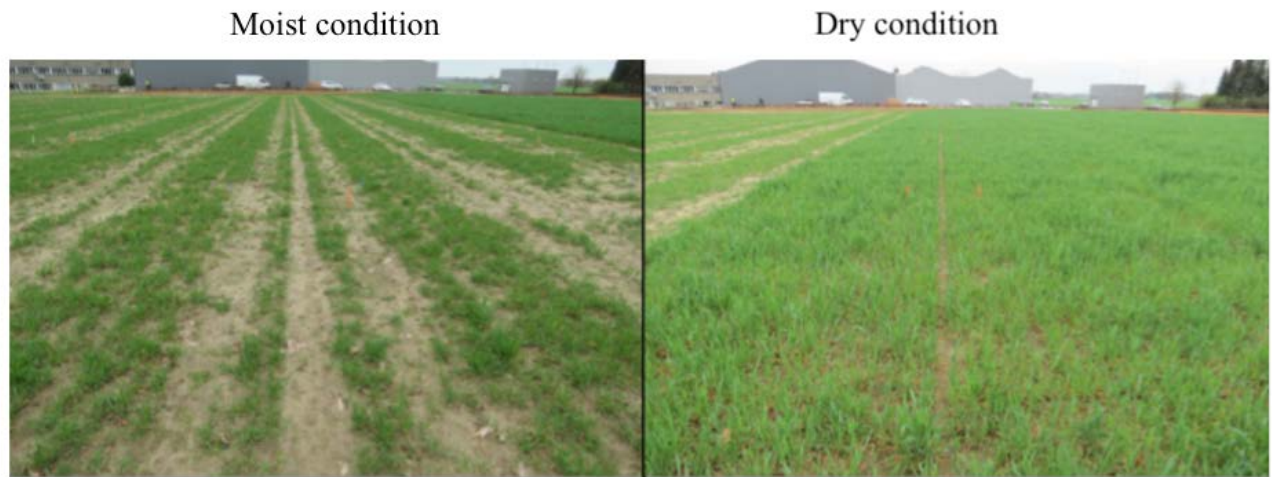


Fig. 3-9. Winter rye growth conditions before the mechanical destruction (6<sup>th</sup> April) in moist and dry treatments.

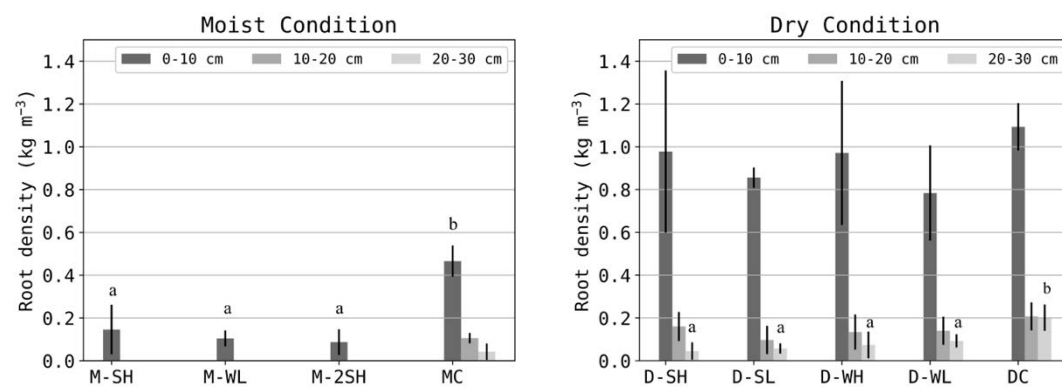


Fig. 3-10. Root mass density among treatments under each condition. The error bars are standard deviation (SD; n=3). Different letters indicate significant differences at each depth ( $P < 0.05$ ) (D = Dry condition; M = Moist condition; S = Standard tyre; W = Wide tyre; H = High tyre pressure; L = low tyre pressure; M-2SH = Moist condition + two passes + standard tyre + high tyre pressure; MC = moist control; DC = dry control).

### 3.4. Discussion

The positive effects of the tested strategies to minimize soil compaction were well confirmed by the measured and predicted tyre contact area and mean ground pressure. Firstly, tyre type (with different tyre width), greatly affected tyre-soil contact area. Table 3-4 shows contact area increased with increased tyre width. Correspondingly, mean ground pressure decreased with increasing tyre width. This was confirmed by other studies with a variety of tyre types and soil conditions (Keller 2005; Lamandé *et al.* 2007; Schjønning *et al.* 2008; Lamandé and Schjønning 2011b). Secondly, inflation pressure could greatly affect tyre-soil contact area and thus stress distribution at soil surface. Traditionally, inflation pressure is used to directly estimate the mean ground pressure with conversion factor of 1.2 but Schjønning and Lamandé (2010) have shown that this overestimates the mean ground pressure as the mean ground pressure not only depends on the inflation pressure but also the tyre loads, tyre parameters, recommended inflation pressure and soil precompression stress (Keller 2005; Schjønning *et al.* 2008; Lamandé and Schjønning 2011a). However, being consistent with Karafiath and Nowatzki (1978), Schjønning and Lamandé (2010) also found a positive linear relation between mean ground pressure and inflation pressure. This study also suggests that the traditional method overestimates the mean ground pressure, while Terranimo® slightly underestimated the measured mean ground pressure (Table 3-4). Thirdly, the tyre-soil contact area increased with wetter soil conditions, as was also reported by (Lamandé and Schjønning 2011b, 2011c). However, for the standard tyre types, finding a higher contact area was unexpected, which might be because only one replication was measured for each treatment or further indicates the poor understanding of the effects of soil precompression stress on tyre-soil contact area (Keller and Lamandé 2010). More research is needed to clarify this.

Overall, both at dry and moist soil conditions, low tyre pressure and wide tyres resulted in larger tyre-soil contact area and lower mean ground pressure. Therefore, from the tyre-soil surface perspective, those selected strategies were useful to minimize soil compaction risk.

By using tyre-soil contact stress distribution as upper boundary condition, soil stress distribution along the soil profile was estimated with the Söhne (1953) equation. It was compared with pedo-transfer based soil precompression stress to evaluate the compaction risk. Generally, the Terranimo® predicted soil compaction risk showed a similar trend with mean ground pressure and compaction risk was presented to 30 cm depth (Table 3-5). In contrast, soil physical quality indicators did not always show differences between trafficked treatments. Especially for S index, no difference was found, even not between in-track and out-track position. According to Naderi-Boldaji and Keller (2016), S index is highly correlated with soil compaction levels when using pedo-transfer function based results. This could be because of differences between trafficked treatments being too small to be detectable. Moreover, because of previous agricultural operations on the field which are wide-spread in the study area, the soil already showed some degree of compaction (compared with the threshold values in Table 3-3 with control treatments). Whereas the soil thus represents that of a typical crop land in study area, this made detecting differences more challenging. For instance, the Ks and AC were very small, and close to 'poor' condition (Table 3-3), even in the control treatment.

Moreover, the lack of agreement between predicted risk of soil compaction and observed changes could be due to shortcomings of Terranimo®. For example, Terranimo® predicts soil precompression stress based on soil texture and wetness in the subsoil. The tool is still lacking validate data for the topsoil. Including bulk density

or another parameter that represents the state of compaction might improve the prediction of soil precompression stress in Terranimo<sup>®</sup>. In addition to that, there is still lack of validated data under loosen or newly ploughed soil to improve the Terranimo<sup>®</sup> soil stress functions, whereas the accuracy of sensors (like load cells or Bolling probes, Keller *et al.*, 2016) to measure stress and the corrections needed to convert to real measured stress values (Keller and Lamande 2010; Schjønning 2019). Besides, the definition of compaction risk index is also controversial. For instance, Keller *et al.* (2012) found soil compaction risk can occur even when the actual stress is smaller than the precompression stress. But in general, soil precompression stress is still regarded as the threshold value (Stettler *et al.* 2014; Rücknagel *et al.* 2015).

Crop growth is sensitive to soil compaction. In this study, winter rye biomass was significantly higher in the control area than in the trafficked area and root growth was restricted when the field was trafficked under both moist and dry conditions as compared to the control (Fig. 3-8&3-10). Similarly, Kriebstein *et al.* (2014) reported a decrease in root biomass (by 60.5%) and root length (44.7%) for smooth brome (*Bromus inermis* L.) on a compacted sandy loam soil. This could be explained by the increased penetration resistance and bulk density under the trafficked area. It can not only restrict crop growth by increasing the root growth resistance but also by limiting soil aeration. As the winter season was relatively wet in this study area, drainage is essential to have a good aeration for crop growth. However, in the trafficked zone, soil water conductivity was smaller resulting in a decreased air capacity. This was mostly pronounced under moist conditions. This is in agreement with other studies. For instance, Radford *et al.* (2001) found a 23% reduction of wheat, sorghum and maize dry matter yield under high load traffic on a moist soil, while the effects were limited on dry soil.

Winter rye growth is more related with topsoil properties, as differences in topsoil physical properties (moisture, bulk density and conductivity) explained 80% of the dry above-ground biomass difference in our study. Similarly, Nevens and Reheul (2003) examined the effects of topsoil and subsoil compaction on silage maize' (*Zea mays* L.) growth and found that topsoil compaction significantly decreased dry biomass while no difference was found between subsoiled (partially tilled to 0.75 m) and control treatment.

### 3.5. Conclusions

The measured soil tyre contact area and mean ground pressure were consistent with the Terranimo® modeling results, with dry conditions, wide tyre and low tyre pressure having lower soil compaction risk. However, no difference was found among single trafficked treatments for selected soil quality indicators. Penetration resistance was significantly higher ( $P < 0.05$ ) in the top 20 cm layer under trafficked treatments compared with control (i.e. no trafficked part). At 15 cm depth, soil quality indicators such as BD, AC, RWC, Ks showed differences between the trafficked treatments and the control but AWC was not affected. Deeper down the profile, the effects became less detectable. Between single and two passes treatments under moist condition, soil physical property indicators' difference was found for PR ( $P = 0.02$ ) and AC ( $P = 0.09$ ) at 20-30 cm depth.

Shoot biomass and root density of winter rye were reduced in the trafficked parts compared to their controls under both moist and dry trafficking conditions, but there was no difference among trafficked treatments for both moisture conditions and passes. Overall, the above strategies are useful to minimize soil compaction from the

compaction risk (or stress) perspective but soil physical properties were less affected except between one pass and two passes treatment under moist condition.

## **Chapter 4: Effects of soil wetness and tyre pressure on soil physical quality and maize growth by a slurry spreader system**

This chapter is based on:

Lidong Ren, Tommy D'Hose, Greet Ruyschaert, Jan De Pue, Redouane Meftah, Veerle Cnudde, Wim M. Cornelis (2019). Effects of soil wetness and tyre pressure on soil physical quality and maize growth by a slurry spreader system. *Soil and Tillage Research*, 195, 104344.



#### 4.1. Introduction

Soil compaction is a worldwide threat to sustainable agriculture owing to its various adverse impacts on soil quality, crop growth and the environment (Unger and Kaspar 1994; Huber *et al.* 2008; Keller *et al.* 2013). In Europe, due to decades of increasing mechanization in agriculture, soil compaction is recognised as one of the main threats to sustainable agriculture by the European Commission (Alameda *et al.* 2012).

Soil compaction risk can be evaluated by comparing the soil's precompression stress – i.e., stress when soil changes from elastic deformation to plastic deformation - and the soil stress induced by wheels of machinery trafficking the soil. If the induced stress is close to or exceeds soil precompression stress, soil shows a risk to compaction (Schjønning *et al.* 2015). Soil precompression stress ( $P_c$ ) is currently the best way to quantify the impacts of traffic on agricultural fields (Schjønning *et al.* 2015), and mainly depends on soil texture, bulk density, organic content and soil wetness (Hamza and Anderson 2005). Among these, wetness is regarded as the most important and most dynamic factor influencing soil compaction processes (Soane and Van Ouwerkerk 1994).  $P_c$  increases with decreasing soil moisture irrespective of soil texture (Schjønning *et al.* 2015).

Soil stress is determined by tyre dimensions, tyre inflation pressure, wheel load and soil properties, including soil wetness. Tyre inflation pressure is the factor most easily and fast to change. It directly affects the tyre-soil contact area and ground pressure which in turn affects soil stress and its distribution. Within a certain range, soil stress increases with tyre pressure and tyre pressure could explain most variation in soil stress in both top and sub soil layers under different wheel loads (Schjønning *et al.* 2012). Under wet conditions, the tyre-soil contact area and the depth of soil

stress transmission increases because of an increasing concentration factor according to the elasticity theory (Lamandé and Schjønning 2011c).

With soil stress being highly determined by tyre pressure, manufacturers of tyres recommend, depending on axle load, tyre model and size, and speed, tyre pressures for field operations. These pressures are substantially lower than those recommended for road traffic. In practice, however, most farmers or contractors do not deploy a tyre pressure-control system and thus traffic their fields with inappropriate pressures.

The Terranimo® model (Lassen *et al.* 2013; Stettler *et al.* 2014) allows to evaluate the risk of soil compaction by balancing soil stress and soil precompression stress. It was already tested on many sites in Nordic countries with most studies focusing on measuring and simulating soil stress distribution and propagation (Keller 2005; Arvidsson and Keller 2007; Schjønning *et al.* 2008). However, whether the predicted risks are effectively reflected in a change of soil physical quality has been hardly tested. Moreover, studies that evaluate the effects of soil compaction on a range of soil physical quality indicators are few, especially field studies and short-time experiments or experiments with a less (but realistic) number of passes. In these cases, differences in soil physical quality are more difficult to detect and the compaction effects are often not clear (Arvidsson and Håkansson 1996; Berisso *et al.* 2012; Schjønning *et al.* 2013; Schjønning *et al.* 2016; Schjønning *et al.* 2017). Further improvements in X-ray CT scanning, however, allow now to detect soil pore structure directly and avoid the assumptions and restrictions of indirect methods (Katuwal *et al.* 2015a; Zhou *et al.* 2017). As a consequence, Lamandé *et al.* (2013b) found the X-ray CT method to be more sensitive to detect soil structural changes caused by compaction than classical methods of soil physical analysis. Besides, the effects of

heavy traffic on the next season's crop growth after mouldboard ploughing are still unclear.

The objectives of this study were to 1) evaluate the effects of recommended soil wetness (dry vs moist) and tyre inflation pressures ( 'field' vs 'road' pressures), and their interaction, on physical quality of soil trafficked by a tractor-slurry spreader combination; 2) verify the change in soil physical quality indicators with X-ray micro-CT derived parameters; 3) evaluate the Terranimo® model in its ability to provide a reasonable prediction of soil stress distribution parameters and eventually soil compaction risk; 4) evaluate the effects of traffic on soil quality and maize growth (*Zea mays* L.) during a subsequent growing season.

## **4.2. Materials and methods**

### **4.2.1 Study site**

The VRV field was used to conduct this experiment in spring 2016. More information about this field can be found in chapter 2.

### **4.2.2 Experimental design**

A combination of tractor and slurry spreader (slurry tank with injector and equipped with a tyre pressure control system) (Fig. 4-1) was used to induce soil compaction after clipping the winter rye (which was done on 18/04/2016). The recommended pressure in the slurry spreader tyres was 300 kPa for transport on the road and 100 kPa for carrying out activities on the field. Thus, in this study both slurry

spreader tyre pressures were tested with 100 kPa representing the low-pressure treatment (L) and 300 kPa the high-pressure treatment (H). The pressure in the front and rear tractor tyres remained unchanged and were set to 100 and 160 kPa, based on a recommendation for road traffic. A tyre pressure control system was attached to the tractor to remotely change the tire pressure of the slurry spreader.



Fig. 4-1. Tractor-slurry spreader combination used in this study.

To test the effects of soil wetness on soil compaction, natural rainfall was used to vary soil wetness conditions. In April, soils are typically moist in the study area because of a low evaporative demand during winter. This is also the time when farmers typically prepare their field for the next growing season. In the moist conditions treatment (M), the field was trafficked on 18/04/2016. To test the effect of postponing field operations till soils are drier, a dry condition treatment (D) started on 09/05/2016 after a period with only few rains (24 mm) within the two preceding weeks. Soil water content was measured gravimetrically on 12 samples which were taken per plot in depth increments of 10 cm till 60 cm depth. Samples were oven-dried at 105 °C for 48 hours. Gravimetric soil-water content was converted to volumetric soil-water content

using bulk density values measured in each layer (see 2.3.2). The variation of volumetric soil-water content with depth at both dates is shown in Fig. 4-2. The average soil-water content in the top 0-30 cm was  $0.293 \text{ m}^3 \text{ m}^{-3}$  (pF 2.51) and  $0.241 \text{ m}^3 \text{ m}^{-3}$  (pF 2.86) for moist and dry conditions, respectively.

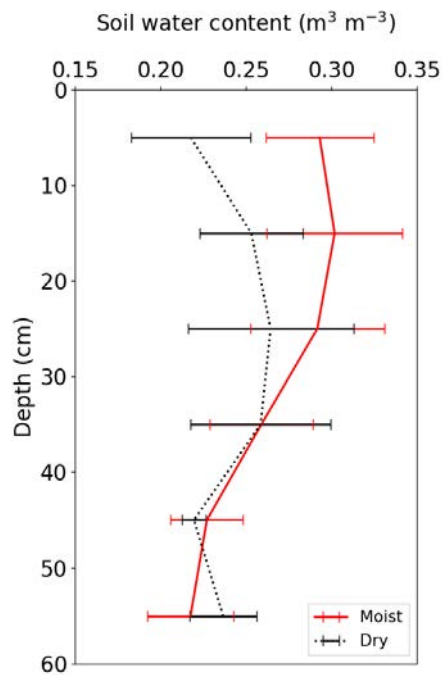


Fig. 4-2. Average soil-water content profile and standard deviation at moist (18/04/2016) and dry conditions (09/05/2016) ( $n = 12$ )

Combining the treatments outlined above, four treatments were established, representing moist conditions-high tyre pressure (MH), moist conditions-low tyre pressure (ML), dry conditions -high tyre pressure (DH) and dry conditions-low tyre pressure (DL). The four treatments were applied in three randomized blocks with each plot measuring  $6 \times 20 \text{ m}^2$ . The exact place of the trial in the field parcel was selected by measuring soil physical and chemical properties ensure a homogeneous field trial (appendix S1 and S2). The slurry spreader had two axes, a content of  $16 \text{ m}^3$  and the

working width was 5.6 m. The GPS-operated tractor was exactly driving along the center line of each plot, leaving an un-injected zone of 0.2 m at both plot sides.

After the traffic experiment with slurry spreader, a conventional mouldboard plough was used for in-furrow ploughing (till 30 cm depth), followed by seedbed preparation with a rotary harrow (8 cm depth). The next day, on 14/05/2016, maize was sown in the four treatments in rows (with 75 cm interrow spacing,  $10^5$  seeds  $\text{ha}^{-1}$ , and 6 cm sowing depth) perpendicular to the previous traffic lanes.

## 4.2.3 Measurements and prediction

### 4.2.3.1 System weight, tyre contact area and rut depth

The weight of the slurry spreader was determined before and after spreading of every three replicate plots. Per plot, 1000 kg slurry was applied, corresponding with  $170 \text{ kg N ha}^{-1}$ . The slurry spreader, with initial weight of 23,400 kg, thus weighted 22,400, 21,400 and 20,400 kg at the end of each plot or 21,400 kg on average. The tank was then filled and the procedure repeated on the other treatments. The total weight of the tractor was 7350 kg. The support load (i.e., load transfer from the trailer to the tractor) was according to the manufacturer 3,000 kg when filled with slurry. The load distribution of the tractor was 6/4 and the support load added to the tractor weight was calculated as (P. Schjønning, 2018, personal communication):

$$AL_{\text{front}} = -0.25 \text{ SL} \quad (4-1)$$

$$AL_{\text{rear}} = 1.33 \text{ SL} \quad (4-2)$$

where SL is the support load, and  $AL_{\text{front}}$  and  $AL_{\text{rear}}$  are the added load to the front and rear axle of the tractor, respectively. Thus, the wheel load of the tractor and slurry

spreader (Table 4-1) was calculated according to the weight of tractor-slurry spreader system, tractor weight, and support load.

Table 4-1: Characteristics of the tractor and slurry spreader.

	Tractor		Slurry spreader			
	Front tyre	Rear tyre	Low pressure		High pressure	
Machine type	John Deere 6175R (175 HP)		Dezwaef Tandem (2 axels)			
Tyre type	Michelin Multibib	Michelin Multibib	Alliance 380	flotation	radial	
	540/65 R30	650/65 R42	800 / 60 R32			
Wheel load (kg)	1200	4200	5350			
Tyre width (cm)	54	54	80			
Tyre pressure (kPa)	100	160	100	300		

The tyre contact area was measured in three replicates per treatment at the end of each plot by spreading chalk powder around the rear left tyre of the spreader as illustrated in Fig. 4-3. The rut depth was manually measured along three transects perpendicular to the driving direction with five measurements on each ridge of the tread and five in between.

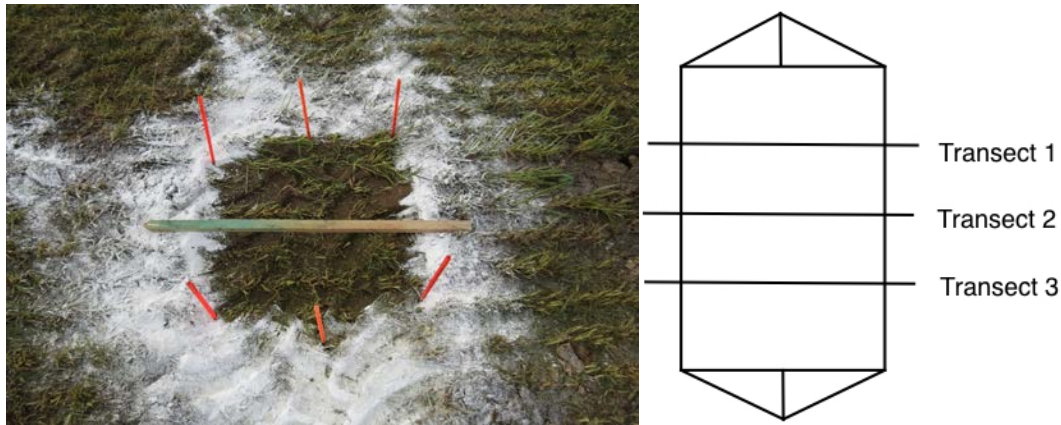


Fig. 4-3. Illustration of measuring contact area (left) and rut depth along three transects (right).

#### 4.2.3.2 Soil physical properties

Immediately after each slurry application, penetration resistance (PR) was measured using a hand-held penetrometer (Eijkelkamp Soil & Water) to 80 cm depth. The cone had a 1 cm<sup>2</sup> base area, a 11.28 mm nominal diameter and a 60° top angle. Penetration resistance was measured along two transects per plot, perpendicular to the driving direction and in and outside (only on one side of the track) the wheel tracks using a mold with 11 openings made at 7.5 cm intervals (Fig. 4-4). By moving the mold, a total of 15 penetration measurements was made per transect, 10 of which were at in-track (at 7.5 cm interval) and five were at out-track positions (at 15 cm interval). To compare PR under different wetness conditions, a simple linear regression correction model developed by Lapen et al. (2004) for a loam soil under none recently tilled conditions (Lapen *et al.* 2004):

$$PR_c = PR_d + 13.52 (\theta_d - \theta_w) \quad (4-3)$$

where  $PR_c$  is corrected PR (MPa);  $PR_d$  is dry condition PR (MPa); and  $\theta_d$  and  $\theta_w$  are soil water content ( $m^3 m^{-3}$ ) at dry and moist condition, respectively.

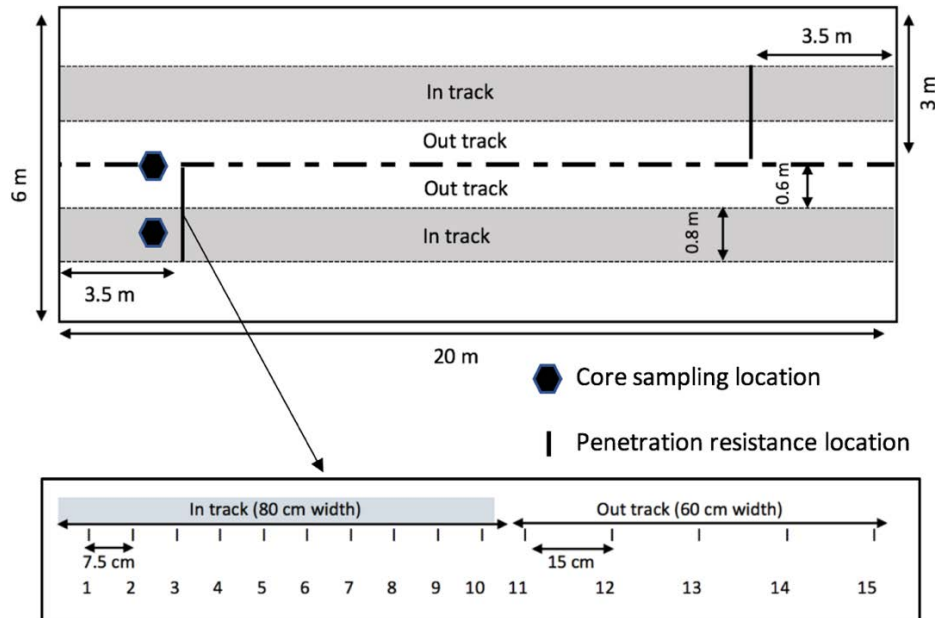


Fig. 4-4. Sampling design in one plot (above) and a detail illustration for penetration resistance measurement (below).

Three days after slurry injection, one undisturbed soil sample per plot was collected in 100 cm<sup>3</sup> standard sharpened steel cores (5.1 cm height and 5 cm diameter) at 10, 20, 35 and 55 cm depth at in-track and out-track positions, ~20 cm away from the PR measurement location (Fig. 4-4), resulting in six samples per depth and treatment. Soil sampling and establishment of water retention curves with a sandbox and pressure chambers combination were carried according to the procedure outlined in Cornelis *et al.* (2005). Matric suction heads of 10, 30, 50, 70, 100, 340, 1,020 and 15,300 cm were selected. Bulk density was determined within this procedure by oven-drying at 105 °C for 48 hours.

Air permeability ( $K_a$ ) was measured at 100 cm matric suction head using the steady-state method of Grover (1955). An air permeameter was devised allowing a float to displace air through a core sample. The float, a metal cylinder open at the bottom and suspended in an annular water reservoir, acts as an air chamber (Ball and Smith 2000) pushing air through the soil sample after loosening a counterweight. The flux readings were taken from timing the fall of the float over a given distance (Pulido Moncada *et al.* 2017). Measurements were repeated twice for each sample and  $K_a$  was calculated as:

$$K_a = \frac{q \eta_{air} l_{sample}}{\Delta P} \quad (4-4)$$

where  $K_a$  is the air permeability ( $\mu\text{m}^2$ ),  $q$  is the flux ( $\text{m}^3 \text{m}^{-2} \text{s}^{-1}$ ),  $\eta_{air}$  is the viscosity of air ( $\text{kg m}^{-1} \text{s}^{-1}$ ),  $l_{sample}$  is the length of the soil sample (m), and  $\Delta P$  is the pressure head differences across the sample (m).

For pore size distribution, the classification of Kay and Lal (1997) was chosen: micropores if  $d < 0.2 \mu\text{m}$ , mesopores if  $0.2 < d < 30 \mu\text{m}$  and macro-pores if  $d > 30 \mu\text{m}$ , with  $d$  the equivalent diameter. The first class consists of residual pores in which chemical interactions at molecular level occur and have, according to the capillary equation, a maximum matric suction head equal to that at permanent wilting point (15,300 cm). The second class represents storage pores which are extremely important to plant growth and with matric suction head boundaries corresponding to permanent wilting point and field capacity (100 cm). These boundaries resemble those of plant-available water capacity (Reynolds, 2009). The third class consists of transmission pores that are critically important for transmission of air and water, and determine the soil's air capacity (Reynolds, 2009).

#### 4.2.3.3 X-ray micro-computed tomography imaging analysis

To further observe changes in pore characteristics, X-ray micro-CT was used (Cnudde and Boone 2013). Two extreme treatments were selected, MH and DL, at 10 and 35 cm depth at in-track and out-track positions. In total, eight undisturbed 100 cm<sup>3</sup> core samples were selected from the undisturbed core samples (see section 2.3.2). After the soil samples were equilibrated to 100 cm matric suction head on the sand box, they were scanned at HECTOR (Masschaele et al., 2013), the high-energy scanner of the Ghent University Centre of X-ray Tomography (UGCT). The X-ray tube was operated with a voltage of 150 kV and power of 20 W. At the exit of the tube, an aluminum filter was placed in order to filter out the low energy photons. The stage was progressively rotated and the samples were scanned over a 0 – 360° range at 0.163° intervals. The exposure time was set at 1000 ms. The parameters settings led to a spatial resolution of 60 µm.

The tomographic images were reconstructed with the Octopus Reconstruction software (Vlassenbroeck *et al.* 2007) and then analyzed with Octopus Analysis (Brabant *et al.* 2011)). At first, it was necessary to determine the region of interest (ROI) to have a constant volume for each layer and all the following parameters were calculated from the ROI to make them comparable. For 10 cm depth samples, a cylindrical ROI with a 47-mm diameter and 45-mm height was selected, while a diameter of 47 mm and height of 18 mm were selected for the 35 cm depth samples because of two incomplete samples. For each ROI, contrast enhancement and filtering were applied and the pore space was segmented using a dual threshold method. Features smaller than two voxels were removed. The following parameters were extracted from the 3D analysis: mean maximum opening, i.e. the mean diameter of the largest inscribed sphere in each object; mean equivalent diameter, i.e. the mean

diameter of a sphere with the same number of voxels as the object; mean number of neighbors, i.e. the mean number of connected objects; pore number density, i.e. the total number of detectable pores in one volume; mean sphericity, i.e. the ratio of the mean maximum opening and the mean equivalent diameter; and Euler number, i.e. a measure for multi-connectivity and defined according to Fukuma (2007) as:

$$X = b_0 - b_1 + b_2 \quad (4-5)$$

where  $b_0$  is the number of connected components;  $b_1$  is the number of holes and  $b_2$  is the number of tunnels.

#### 4.2.3.4 Predicting the risk of soil compaction

To predict the risk of soil compaction in each treatment, the Terranimo® model V.2.0 ([www.terranimodk.dk](http://www.terranimodk.dk)) was used. Tractor and slurry spreader type, wheel load, tyre parameters, soil texture and matric suction (wetness) were used as input data.

In Terranimo®, surface stress distribution is computed with the FRIDA model (Schjønning *et al.* 2008). Higher tyre pressure (like four times higher than that recommended for the tyres in the Terranimo® dataset) might show higher uncertainty because of lack of experimental data. Therefore, in the high-pressure treatments, only 240 kPa was used instead of 300 kPa. Soil normal stress propagation was simulated with the Söhne (1953) model. The concentration factor ( $v$ ) was calculated by a build-in exponential pedotransfer function based on the matric suction head (expressed as pF, i.e., log of matric suction head with head expressed in cm; equation not published).

Soil precompression stress was calculated by a build-in pedotransfer function that mainly includes pF and clay content (equation not published). It was calculated at

every 10-cm interval from measured clay content (Table 2-1, every 30 cm layer's average value was used) and volumetric soil-water content (Fig. 4-2) with the latter being converted to matric suction head using the water-retention curves measured at four depths per treatment (see 2.3.2). Soil precompression stress was only calculated for the top 60 cm depth.

The risk of soil compaction was calculated with a soil compaction index (SCI) according to Rücknagel *et al.* (2015):

$$SCI = \log (P_{act}/P_c) \quad (4-6)$$

where  $P_{act}$  is the stress calculated according to the Söhne (1953) model, and  $P_c$  is soil precompression stress calculated by the pedotransfer function. Three classes were distinguished:  $SCI < 0$  means no soil compaction risk;  $0 < SCI < 0.20$  indicates medium risk and  $SCI > 0.20$  is a serious alert. Negative values of SCI (stress lower than precompression stress; no risk of compaction) were given as zeroes in the report generated by Terranimo®.

#### 4.2.4 Maize season management, sampling and analysis

In the maize growing season, soil penetration resistance was measured on 29/06/2016 (leaf stage) in all the plots and undisturbed ring samples were only taken in MH and ML, in which most pronounced differences were expected. All the sampling locations (around 0.3 m away from the before sowing sampling location) and the procedure were consistent with section 2.3.2. In addition, disturbed soil samples were collected in MH and ML at both heads of each plot at in- and out-track positions (near core sampling location) for total mineral nitrogen analysis ( $NO_3-N + NH_4-N$ ) according

to ISO TS14256-1: 2003 procedure. At each location, three replicate samples were mixed and in total 12 sampling locations were chosen for each treatment with six at in-track and six at out-track positions. The soil samples were taken at 30 cm increments to 90 cm depth on 30/06/2016 (1.5 months after sowing) and on 03/10/2016 (after harvest). Maize was harvested as silage on 28/09/2016 for all treatments. Above-ground biomass was harvested in ten middle rows of each plot with five plants at in- and out-track positions per row. In total, per plot, 50 maize plants were selected at in- and out-track positions and weighed to determine their fresh yield. After that, four plants were randomly selected to determinate dry above-ground biomass at 70 ° C for 48 hours.

### 4.2.5 Data analysis

Data were analyzed using SPSS Statistics 25 following the statistical procedures described in Gomez *et al.* (1984). A distinction was made between 'in-track' and 'out-track' and the soil physical quality indicator values were analyzed according to two methods. In the first method, only the 'in-track' data was used and the test was analyzed as a two-way ANOVA with factors soil-water content and tyre pressure. In the second method, the 'in-track' and 'out-track' data were used, and the test was analyzed as a Split-Plot Design with two factors ('treatment' and 'track (in and out)'). If a significant difference of the 'treatment' factor was observed, a post-hoc test was performed to show significant differences ( $P < 0.05$ ) among those four different treatments.

### 4.3. Results

#### 4.3.1 Contact area, rut depth and mean ground pressure among treatments

Table 4-2 shows that tyre pressure of the slurry spreader wheels had significant effects on contact area, rut depth and mean ground pressure under both dry and moist conditions. Under dry conditions, contact area, rut depth and mean ground pressure with low tyre pressure changed +67%, -15%, -40%, respectively, compared with high tyre pressure. Under moist condition, changes were +19%, -35% and -16%, respectively. Likewise, for a given tyre pressure, soil moisture conditions significantly affected those parameters, except for contact area under low pressure. The contact area and mean ground pressure predicted with Terranimo<sup>®</sup> matched the measured ones very well (RMSE of 0.08 m<sup>2</sup> and 21.73 kPa, respectively) and fell within its confidence interval (95%), except for treatment DH.

Table 4-2. Measured and predicted contact area, ground mean pressure and rut depth (mean  $\pm$  standard deviation).

Treatments	Measurements			Predicted using Terranimo <sup>®</sup>		
	Contact area (m <sup>2</sup> )	Rut depth (m)	MGP (kPa)	contact (m <sup>2</sup> )	area	MGP (kPa)
DL	0.50 $\pm$ 0.03a	0.02 $\pm$ 0.00a	90.00 $\pm$ 0.83bc	0.51		103
DH	0.30 $\pm$ 0.03b	0.03 $\pm$ 0.00b	150.25 $\pm$ 10.50a	0.42		125
ML	0.52 $\pm$ 0.04a	0.04 $\pm$ 0.01bc	87.36 $\pm$ 3.51b	0.56		95
MH	0.44 $\pm$ 0.03c	0.06 $\pm$ 0.01d	103.44 $\pm$ 12.57c	0.46		115

Values with different letters are significantly different ( $P \leq 0.05$ ) ( $n=3$ ). D: dry condition; M: moist condition; L: low pressure; H: high pressure. MGP: Mean ground pressure (kPa).

### 4.3.2 Soil physical quality evaluation

#### 4.3.2.1 Among treatments

In the vertical direction, a very clear plough pan was present at ~30-40 cm depth with PR reaching 5 MPa (Fig. 4-5 and Table 4-3) for all treatments. Below this layer, PR decreased dramatically in the 40-60 cm depth range and increased slightly from 60 to 80 cm depth. It should be noted that the values shown represent actual PR values, uncorrected for soil-water content. This means that under drier conditions, PR values are unconditionally higher than under wetter conditions, i.e. irrespective of the treatment effect.

Table 4-3 shows results of the two-way ANOVA ( $P$  values) considering moisture, tyre pressure and their interaction (labeled with 1). In the top 20 cm, PR (now corrected for soil-water content; Eq. 3) was significantly larger ( $P < 0.05$ ) when soil was trafficked under moist conditions than when dry. Below 30 cm depth, PR was higher in the dry treatment than in the moist and significantly different ( $P < 0.05$ ) in the 30-50 cm depth range. No difference between high and low tyre pressure was found except for an irregular value in the top 10 cm.

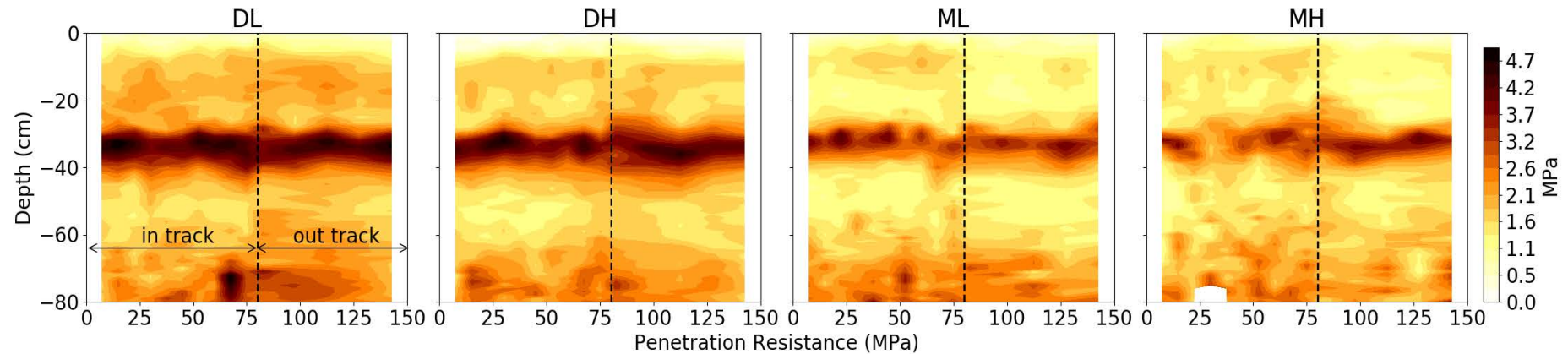


Fig. 4-5. Uncorrected soil PR ( $n=6$ ) perpendicular to the driving direction in each treatment just after slurry traffic (D: dry condition; M: moist condition; L: low pressure; H: high pressure). Uncorrected means that they were not corrected for soil-water content and thus present actual values.

Table 4-3. Corrected (for soil-water content; Eq. 3) penetration resistance (MPa) at different depths (mean  $\pm$  standard deviation).

Factor	0-10 cm	10-20 cm	20-30 cm	30-40 cm	40-50 cm	50-60 cm	60-70 cm	70-80 cm
Moisture conditions								
Moist	1.06 $\pm$ 0.30	1.30 $\pm$ 0.32	1.67 $\pm$ 0.38	2.46 $\pm$ 0.68	1.33 $\pm$ 0.42	1.45 $\pm$ 0.43	1.91 $\pm$ 0.66	2.35 $\pm$ 0.56
Dry	0.12 $\pm$ 0.26	1.13 $\pm$ 0.51	1.61 $\pm$ 0.58	3.64 $\pm$ 0.72	1.90 $\pm$ 0.46	1.51 $\pm$ 0.34	1.91 $\pm$ 0.53	2.47 $\pm$ 0.78
Tyre pressure								
Low	0.64 $\pm$ 0.53	1.26 $\pm$ 0.45	1.69 $\pm$ 0.52	3.16 $\pm$ 0.94	1.64 $\pm$ 0.57	1.50 $\pm$ 0.39	1.94 $\pm$ 0.60	2.48 $\pm$ 0.70
High	0.43 $\pm$ 0.55	1.14 $\pm$ 0.42	1.57 $\pm$ 0.48	3.04 $\pm$ 0.89	1.64 $\pm$ 0.46	1.46 $\pm$ 0.38	1.87 $\pm$ 0.59	2.34 $\pm$ 0.67
Moisture X pressure								
DL	0.22 $\pm$ 0.04a	1.27 $\pm$ 0.05a	1.78 $\pm$ 0.06b	3.81 $\pm$ 0.09	1.99 $\pm$ 0.06a	1.59 $\pm$ 0.05a	1.96 $\pm$ 0.08	2.55 $\pm$ 0.13
DH	0.02 $\pm$ 0.04b	0.98 $\pm$ 0.05b	1.44 $\pm$ 0.06a	3.47 $\pm$ 0.09	1.81 $\pm$ 0.06a	1.43 $\pm$ 0.05b	1.86 $\pm$ 0.09	2.41 $\pm$ 0.11
ML	1.06 $\pm$ 0.04c	1.25 $\pm$ 0.05a	1.61 $\pm$ 0.06b	2.50 $\pm$ 0.09	1.29 $\pm$ 0.06b	1.41 $\pm$ 0.05b	1.92 $\pm$ 0.08	2.43 $\pm$ 0.10
MH	1.06 $\pm$ 0.04c	1.38 $\pm$ 0.07a	1.76 $\pm$ 0.06b	2.39 $\pm$ 0.11	1.38 $\pm$ 0.07b	1.50 $\pm$ 0.06b	1.87 $\pm$ 0.11	2.21 $\pm$ 0.14
Treatments								
DL	0.24 $\pm$ 0.35b	1.31 $\pm$ 0.58b	1.75 $\pm$ 0.68	3.79 $\pm$ 0.69a	1.99 $\pm$ 0.48a	1.69 $\pm$ 0.45a	2.04 $\pm$ 0.53	2.60 $\pm$ 0.97a
DH	0.02 $\pm$ 0.04a	0.98 $\pm$ 0.41a	1.52 $\pm$ 0.60	3.49 $\pm$ 0.70b	1.90 $\pm$ 0.45a	1.50 $\pm$ 0.39b	1.85 $\pm$ 0.55	2.36 $\pm$ 0.64ab
ML	0.99 $\pm$ 0.29c	1.22 $\pm$ 0.30b	1.60 $\pm$ 0.44	2.55 $\pm$ 0.66c	1.32 $\pm$ 0.34b	1.38 $\pm$ 0.40c	1.93 $\pm$ 0.73	2.36 $\pm$ 0.64b
MH	1.01 $\pm$ 0.31c	1.30 $\pm$ 0.35b	1.72 $\pm$ 0.50	2.49 $\pm$ 0.84c	1.41 $\pm$ 0.45b	1.53 $\pm$ 0.41b	1.88 $\pm$ 0.66	2.16 $\pm$ 0.65b
Track								
In	0.55 $\pm$ 0.55	1.21 $\pm$ 0.44	1.64 $\pm$ 0.50	3.10 $\pm$ 0.91	1.64 $\pm$ 0.52	1.48 $\pm$ 0.38	1.95 $\pm$ 0.64	2.41 $\pm$ 0.71
Out	0.48 $\pm$ 0.45	1.18 $\pm$ 0.47	1.65 $\pm$ 0.69	3.19 $\pm$ 0.90	1.75 $\pm$ 0.51	1.60 $\pm$ 0.50	1.91 $\pm$ 0.58	2.31 $\pm$ 0.81
Statistical analysis								
Moisture <sup>1</sup>	<b>0.00</b>	<b>0.00</b>	0.31	<b>0.00</b>	<b>0.00</b>	0.33	0.90	0.18
Tyre pressure <sup>1</sup>	<b>0.01</b>	0.14	0.15	<b>0.02</b>	0.45	0.51	0.41	0.15
Moisture x Pressure <sup>1</sup>	<b>0.01</b>	<b>0.00</b>	<b>0.00</b>	0.22	<b>0.02</b>	<b>0.03</b>	0.80	0.75
Treatments <sup>2</sup>	<b>0.00</b>	<b>0.00</b>	0.18	<b>0.00</b>	<b>0.00</b>	<b>0.00</b>	<b>0.09</b>	<b>0.02</b>
Track <sup>2</sup>	<b>0.02</b>	0.37	0.99	0.24	<b>0.03</b>	<b>0.02</b>	0.57	0.25
Treatment x track <sup>2</sup>	<b>0.00</b>	0.15	0.22	0.54	0.19	<b>0.01</b>	0.19	0.92

<sup>1</sup> p-values are displayed using two-way ANOVA (only in-track data used);  $P < 0.10$  is indicated in bold;  $P < 0.05$  is indicated in bold and underlined. <sup>2</sup> p-value are displayed using

Split-Plot Design with two factors (treatment and track). D: dry condition; M: moist condition ; L: low pressure; H high pressure.

Table 4-4. Bulk density, porosity and soil moisture content at different pF value at 10 (left) and 20 (right) cm depth (mean  $\pm$  standard deviation).

Factor	Bulk density (Mg m <sup>-3</sup> )	Total porosity (m <sup>3</sup> m <sup>-3</sup> )	K <sub>a</sub> (μm <sup>2</sup> )	Pore size distribution (m <sup>3</sup> m <sup>-3</sup> )			Bulk density (Mg m <sup>-3</sup> )	Total porosity (m <sup>3</sup> m <sup>-3</sup> )	K <sub>a</sub> (μm <sup>2</sup> )	Pore size distribution (m <sup>3</sup> m <sup>-3</sup> )		
				d > 30 μm	30 μm > d > 0.2 μm	d < 0.2 μm				d > 30 μm	30 μm > d > 0.2 μm	d < 0.2 μm
Moisture conditions												
Moist	1.49 ± 0.06	0.44 ± 0.02	52.47 ± 30.79	0.10 ± 0.02	0.24 ± 0.02	0.10 ± 0.01	1.39 ± 0.11	0.47 ± 0.42	45.65 ± 25.09	0.11 ± 0.04	0.24 ± 0.03	0.13 ± 0.03
Dry	1.42 ± 0.07	0.47 ± 0.03	33.08 ± 28.13	0.13 ± 0.04	0.23 ± 0.02	0.11 ± 0.01	1.37 ± 0.10	0.48 ± 0.03	35.67 ± 10.71	0.13 ± 0.04	0.23 ± 0.03	0.11 ± 0.01
Tyre pressure												
low	1.43 ± 0.04	0.46 ± 0.02	40.43 ± 28.10	0.13 ± 0.03	0.22 ± 0.02	0.10 ± 0.01	1.40 ± 0.07	0.47 ± 0.04	48.48 ± 20.61	0.12 ± 0.03	0.23 ± 0.03	0.12 ± 0.02
High	1.48 ± 0.09	0.44 ± 0.03	48.61 ± 34.17	0.10 ± 0.04	0.24 ± 0.02	0.10 ± 0.01	1.37 ± 0.13	0.48 ± 0.05	28.94 ± 7.88	0.12 ± 0.05	0.24 ± 0.03	0.12 ± 0.03
Treatments												
DL	1.42 ± 0.04	0.46 ± 0.01	35.86 ± 22.18	0.14 ± 0.02a	0.22 ± 0.01	0.10 ± 0.01	1.41 ± 0.08	0.47 ± 0.03	47.21 ± 14.12	0.12 ± 0.03	0.24 ± 0.03	0.12 ± 0.02
DH	1.44 ± 0.07	0.46 ± 0.03	32.22 ± 34.98	0.10 ± 0.04b	0.25 ± 0.02	0.11 ± 0.01	1.37 ± 0.10	0.48 ± 0.04	30.68 ± 17.98	0.14 ± 0.04	0.24 ± 0.02	0.11 ± 0.02
ML	1.44 ± 0.07	0.46 ± 0.03	44.71 ± 23.64	0.12 ± 0.03ac	0.23 ± 0.01	0.11 ± 0.00	1.38 ± 0.08	0.48 ± 0.03	65.71 ± 41.36	0.12 ± 0.04	0.24 ± 0.02	0.11 ± 0.02
MH	1.49 ± 0.06	0.44 ± 0.02	42.10 ± 29.35	0.10 ± 0.01bc	0.24 ± 0.02	0.10 ± 0.10	1.39 ± 0.11	0.48 ± 0.04	32.28 ± 9.01	0.11 ± 0.04	0.23 ± 0.02	0.12 ± 0.01
Track												
in	1.45 ± 0.07	0.45 ± 0.03	44.31 ± 30.52	0.12 ± 0.04	0.23 ± 0.02	0.10 ± 0.01	1.38 ± 0.10	0.48 ± 0.04	40.66 ± 18.93	0.12 ± 0.04	0.24 ± 0.03	0.12 ± 0.02
out	1.44 ± 0.06	0.46 ± 0.02	33.86 ± 24.33	0.12 ± 0.03	0.24 ± 0.02	0.10 ± 0.00	1.39 ± 0.08	0.48 ± 0.03	50.30 ± 34.12	0.12 ± 0.03	0.24 ± 0.01	0.11 ± 0.01
Statistical analysis												
Moisture <sup>1</sup>	0.08	0.06	0.17	0.10	0.31	0.21	0.73	0.73	0.52	0.40	0.87	0.41
Tyre pressure <sup>1</sup>	0.22	0.18	0.63	0.08	0.11	0.59	0.71	0.71	0.12	0.89	0.82	0.90
Moisture x Pressure <sup>1</sup>	0.69	0.64	0.34	0.45	0.33	0.16	0.64	0.64	0.27	0.57	0.44	0.51
Treatments <sup>2</sup>	0.46	0.34	0.67	0.09	0.11	0.22	0.85	0.85	0.20	0.79	0.86	0.86
Track <sup>2</sup>	0.63	0.70	0.37	0.84	0.66	0.76	0.90	0.90	0.41	0.90	0.77	0.44
Treatment x track <sup>2</sup>	0.30	0.30	0.22	0.39	0.33	0.63	0.43	0.43	0.95	0.28	0.64	0.74

<sup>1</sup> p-values are displayed using two-way ANOVA;  $P < 0.10$  is indicated in bold;  $P < 0.05$  is indicated in bold and underlined. <sup>2</sup> p-value are displayed using Split-Plot Design with two factors (treatment

and track). D: dry condition; M: moist condition ; L: low pressure; H high pressure.

At 10 cm depth, when considering moisture and tyre pressure, no significant differences ( $P < 0.05$ ) in bulk density and total porosity were found between high and low tyre pressure, and between dry and moist conditions (Table 4-4). Yet, a clear trend was found ( $P < 0.10$ ) with bulk density and total porosity being respectively higher and lower when the slurry was applied under moist conditions as compared to dry conditions. Furthermore, there was a clear effect ( $P \leq 0.10$ ) of moisture conditions and tyre pressures on macroporosity ( $d > 30 \mu\text{m}$ ). When considering both treatment and position relative to the track, there were no significant differences among all the selected indicators except for macro-porosity, with DL showing larger values than DH and MH, while the differences between DL and ML were only marginal ( $P = 0.12$ ).

At 20 cm depth, there were no differences among all those factors and no interaction was observed (Table 4-4). At 35 cm and 55 cm depth, though some differences were found, they probably resulted from minor soil heterogeneity (Appendix S5).

#### **4.3.2.2 Between in-track and out-track positions**

To evaluate the difference between in- and out-track positions, a split-plot design analysis was conducted (Table 4-3 and 4, labeled with 2). Significant differences ( $P < 0.05$ ) for PR between in- and-out track positions were found in the 0-10 cm depth range. This is also visible in the uncorrected data, especially in the moist treatment (Fig. 4-5). Surprisingly, no differences were found between in- and out-track positions for the indicators extracted from core samples.

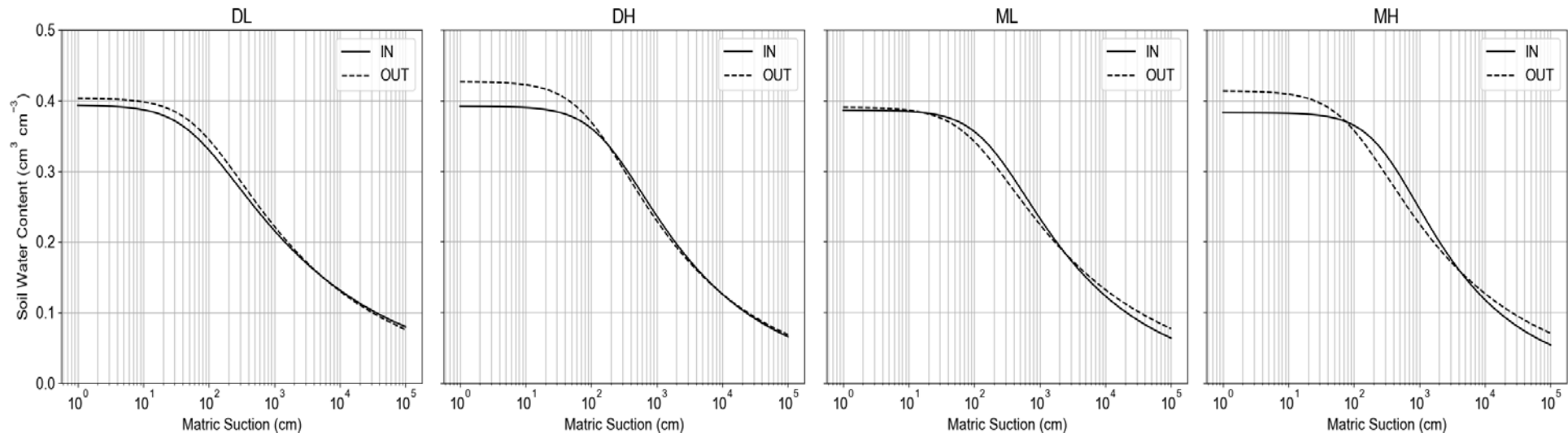


Fig. 4-6. Soil water retention curves ( $n=3$ ) from in and out the track positions in each treatment at 10 cm depth (D: dry condition; M: moist condition; L: low pressure; H high pressure)

Figure 4-6 shows the soil water retention curves at 10 cm depth . Tyre inflation pressure substantially affected the water retention curve between saturation and 100 cm of matric suction head, i.e., the range that represents the water retained in macropores. At low tyre pressures, in- and out-track curves did not differ much, whereas at high tyre pressures, much less water was retained at the in-track positions within this suction range. The effects were similar when comparing dry and moist conditions. Above 100-cm matric suction head (or when considering mesopores), there was no effect when soils were dry. Under moist conditions, however, more water was retained in the in-track treatment within that range of suction, indicating an increase in relative mesopore volume, particularly under high tyre pressures. Similar results were found at 20 cm depth, whereas below that depth, no differences were found between treatments (appendix S5). However, when comparing soil-water retention curves of the compacted plough pan (35 cm depth) with those from less compacted layers, the relative volume of macropores dramatically decreased and measured values were less variable among replications (appendix S4 and S5).

### **4.3.3 X-ray micro-computed tomography analysis**

#### **4.3.3.1 Among treatments**

At 10 cm depth, macro-porosity was larger under dry than moist conditions for all samples (Table 4-5). The Euler number was smaller in dry than in moist conditions, which indicated that more individual pores were generated and pore connectivity decreased when soil where moist at trafficking. This was also supported by the smaller mean neighbor number and the smaller  $K_a$  under moist conditions. Mean maximum opening and equivalent diameter were lower the moist treatment compared with the

dry one, which reveals that more compacted samples in the moist one showed fewer large pores. Interestingly, pore number density was larger under moist conditions than under dry conditions, while mean sphericity remained unaffected.

Table 4-5. Pore characteristic from X-ray micro-CT at 10 and 35 cm depth (n=1).

Micro-CT derived									Lab measurements	
		Macroporosity (d > 120 μm)	Euler number	Mean maximum opening (μm)	Mean equivalent diameter (μm)	Mean neighbor number	Mean Sphericity	Total pore number density	Macroporosity (d > 120 μm)	K <sub>a</sub> (μm <sup>2</sup> )
10 cm										
MH	In	0.014	31013	80.40	160.10	2.24	0.53	0.52	0.057	74.14
	Out	0.028	16056	314.74	392.78	2.27	0.54	0.29	0.063	33.06
DL	In	0.051	23327	160.14	292.86	2.28	0.59	0.42	0.133	11.43
	Out	0.068	13196	199.90	371.30	2.50	0.59	0.27	0.083	20.04
35 cm										
MH	In	0.017	16718	123.29	245.26	1.98	0.53	0.50	0.050	5.04
	Out	0.014	10223	130.48	248.45	2.11	0.55	0.34	0.024	2.79
DL	In	0.023	13974	150.80	281.18	2.01	0.57	0.53	0.028	2.70
	Out	0.012	10652	117.85	220.41	1.79	0.57	0.46	0.043	0.53

In = in-track position; Out = out-track position; D: dry condition; M: moist condition; L: low pressure; H: high pressure.

At 35 cm depth, a similar trend was observed but with less differences. However, the parameters measured in the lab with conventional methods of soil physical analysis did not show consistent trends.

#### 4.3.3.2 Between in-track and out-track positions

At 10 cm depth, macro-porosity was larger at out-track positions than in-track for all treatments (Table 4-5). The Euler number was smaller out-track than in-track, which indicates more individual pores and decreased pore connectivity in the

compacted treatments. This was again supported by the mean neighbor number showing fewer neighbors in the compacted treatments and a lower  $K_a$  under moist conditions. Mean maximum opening and equivalent diameter were lower at in-track positions compared with in out-track positions, which reveals that compacted samples showed fewer large pores. Interestingly, pore number density was larger at in-track than at out-track positions, while mean sphericity remained unaffected in all treatments and depths. The difference in pore architecture between in-track and out-track positions is clearly illustrated by the 2D slice in Fig. 4-7. At 35 cm depth, both X-ray micro-CT and lab measured parameters did not show reasonable trends when comparing the treatments.

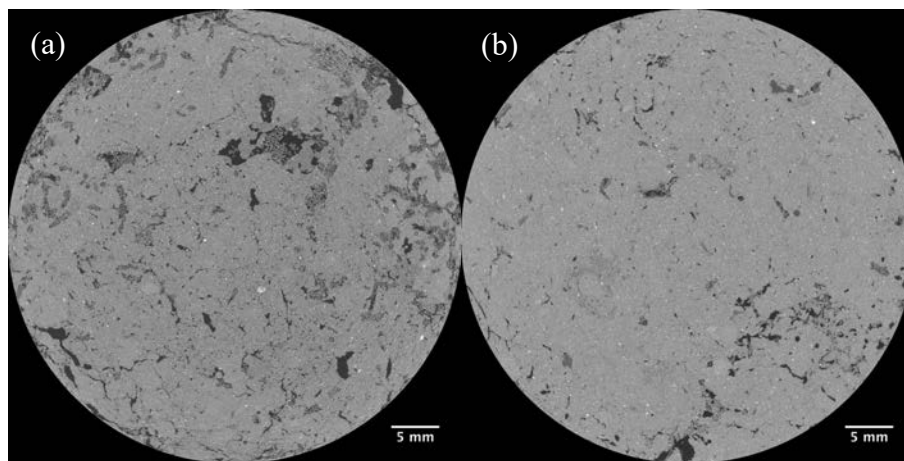


Fig. 4-7. 2D horizontal slice of soil core taken at out-track (a) and in-track (b) position of field trafficked under MH treatment at 10 cm depth.

Overall, lab measured macro-porosity ( $d > 120 \mu\text{m}$ ) related well with X-ray micro-CT macro-porosity ( $r=0.75$ ;  $P=0.037$ ), and  $K_a$  showed a highly significant trend with the Euler number ( $r=0.80$ ;  $P=0.016$ ).

#### 4.3.4 Evaluation of soil compaction risk by Terranimo®

To further explain the changes in soil physical quality indicators, the Terranimo® model was used to predict compaction risk. Table 4-6 shows the compaction risk in terms of SCI within the top 60 cm depth. Simulations indicated that soil compaction risk only existed above 40 cm depth and that it was primarily induced by the slurry spreader and the rear tractor axle. In the low tyre pressure treatment, soil compaction risk was even higher from the rear axle of the tractor than from the trailer. This is often ignored by farmers who don't believe tractors could also show as high compaction risk as trailers. When focusing on the slurry spreader, MH showed highest compaction risk within the top 0.4 m depth, while DL had the least compaction risk.

Table 4-6. Soil compaction index (SCI) calculated as the log to the ratio of stress and precompression stress.

Treatments	Machine	Axle	Soil depth (m)					
			0.1	0.2	0.3	0.4	0.5	0.6
DL	Tractor	Front	0.00	0.00	0.00	0.00	0.00	0.00
		Rear	0.31	0.23	0.13	0.00	0.00	0.00
	Slurry spreader	Front	0.25	0.20	0.12	0.00	0.00	0.00
		Rear	0.25	0.20	0.12	0.00	0.00	0.00
DH	Tractor	Front	0.00	0.00	0.00	0.00	0.00	0.00
		Rear	0.31	0.23	0.13	0.00	0.00	0.00
	Slurry spreader	Front	0.37	0.30	0.20	0.06	0.00	0.00
		Rear	0.37	0.30	0.20	0.06	0.00	0.00
ML	Tractor	Front	0.11	0.00	0.00	0.00	0.00	0.00
		Rear	0.41	0.34	0.25	0.00	0.00	0.00
	Slurry spreader	Front	0.35	0.30	0.24	0.00	0.00	0.00
		Rear	0.35	0.30	0.24	0.00	0.00	0.00
MH	Tractor	Front	0.11	0.00	0.00	0.00	0.00	0.00
		Rear	0.41	0.34	0.25	0.00	0.00	0.00
	Slurry spreader	Front	0.47	0.40	0.32	0.04	0.00	0.00
		Rear	0.47	0.40	0.32	0.04	0.00	0.00

Note: SCI=0: No compaction risk; 0<SCI<0.2: Intermediate compaction risk (yellow color); SCI>0.2: High compaction risk (red color). D: dry condition; M: moist condition ; L: low pressure; H high pressure.

### **4.3.5 Maize biomass in relation to soil physical quality and total-N uptake**

#### **4.3.5.1 Among treatments**

In the summer maize growing season, no differences were found for bulk density between 'tyre pressure', 'treatments' and 'track' (Table 4-7 and appendix S6 and S7). Interestingly, macroporosity was marginally larger ( $P = 0.12$ ) in ML compared to MH at 10 cm depth. The difference in macroporosity observed at 10 and 20 cm depth between low and high tyre pressure was not significant ( $P = 0.42$  and  $P = 0.31$ , respectively). Penetration resistance (moisture content at  $0.21 \text{ kg kg}^{-1}$  for 0-30 cm layer) was significantly larger ( $P = 0.04$ ) in ML and MH compared to DL and DH when considering both in-track and out-track positions together. A higher ( $P = 0.09$ ) 'N-out' (soil mineral N after harvest + N-uptake by maize) and maize N-uptake ( $P = 0.07$ ) were found in the low pressure as compared with the high pressure treatments (Table 4-8). No differences were found in maize above-ground dry biomass among treatments.

#### **4.3.5.2 Between in-track and out-track positions**

Overall, the selected soil physical properties were not different between in-track and out-track positions. However, above-ground dry maize biomass was significantly ( $P = 0.00$ ) larger at out-track positions compared with in-track positions (Table 4-8), though this difference only existed in DH treatment.

Table 4-7. Top layer soil physical properties in the maize growing season (mean  $\pm$  standard deviation).

Factor	Bulk density (g cm <sup>-3</sup> )		Macroporosity (m <sup>3</sup> m <sup>-3</sup> )		Average PR (MPa)
	10 cm	20 cm	10 cm	20 cm	0-30 cm
Moisture conditions					
Moist	x	x	x	x	0.67 $\pm$ 0.18
Dry	x	x	x	x	0.65 $\pm$ 0.19
Tyre pressure					
Low	1.39 $\pm$ 0.10	1.35 $\pm$ 0.04	0.13 $\pm$ 0.04	0.15 $\pm$ 0.01	0.65 $\pm$ 0.18
High	1.45 $\pm$ 0.12	1.33 $\pm$ 0.10	0.09 $\pm$ 0.05	0.11 $\pm$ 0.05	0.66 $\pm$ 0.19
Treatments					
DL	x	x	x	x	0.60 $\pm$ 0.17a
DH	x	x	x	x	0.65 $\pm$ 0.21a
ML	1.47 $\pm$ 0.08	1.35 $\pm$ 0.07	0.13 $\pm$ 0.03	0.14 $\pm$ 0.03	0.73 $\pm$ 0.21b
MH	1.40 $\pm$ 0.08	1.37 $\pm$ 0.09	0.09 $\pm$ 0.03	0.12 $\pm$ 0.04	0.65 $\pm$ 0.17ab
Track					
In	1.42 $\pm$ 0.10	1.34 $\pm$ 0.07	0.11 $\pm$ 0.04	0.13 $\pm$ 0.04	0.66 $\pm$ 0.18
Out	1.44 $\pm$ 0.08	1.38 $\pm$ 0.08	0.11 $\pm$ 0.04	0.14 $\pm$ 0.04	0.65 $\pm$ 0.21
Statistical analysis					
Moisture conditions <sup>1</sup>	x	x	x	x	0.40
Tyre pressure <sup>1</sup>	0.51	0.83	0.42	0.31	0.80
Moisture x Pressure <sup>1</sup>	x	x	x	x	<b>0.07</b>
Treatments <sup>2</sup>	0.18	0.68	0.12	0.40	<b><u>0.00</u></b>
Track <sup>2</sup>	0.70	0.48	0.90	0.80	0.91
Treatment x track <sup>2</sup>	0.86	0.47	0.87	0.46	<b><u>0.02</u></b>

<sup>1</sup> p-values are displayed using two-way ANOVA (only in-track data used);  $P < 0.10$  is indicated in bold;  $P < 0.05$  is indicated in bold and underlined. <sup>2</sup> p-value are displayed using Split-Plot Design with two factors (treatment and track). D: dry condition; M: moist condition; L: low pressure; H high pressure; PR: penetration resistance; x: without measurement.

## Chapter 4

Table 4-8. Maize above-ground biomass and total-N balance (mean  $\pm$  standard deviation).

Factor	Maize above-ground biomass		Soil total-Mineral N 0-90 cm (kg ha <sup>-1</sup> )				Soil N-balance 0-90 cm (kg ha <sup>-1</sup> )		
	dry 10 <sup>3</sup> (kg ha <sup>-1</sup> )	N-uptake (kg ha <sup>-1</sup> )	1.5-month sowing	after	5-days harvest	after	N-in	N-out	(N-in) – (N-out)
Moisture conditions									
Moist	20.38 $\pm$ 1.05	213.76 $\pm$ 30.43	x		x		x	x	x
Dry	19.86 $\pm$ 1.79	211.80 $\pm$ 25.68	x		x		x	x	x
Tyre pressure									
Low	19.44 $\pm$ 1.70	227.65 $\pm$ 27.36	107.95 $\pm$ 29.66		41.79 $\pm$ 11.02		171.04 $\pm$ 2.72	275.47 $\pm$ 30.05	-104.42 $\pm$ 29.86
High	20.80 $\pm$ 1.70	197.91 $\pm$ 17.58	91.90 $\pm$ 24.66		41.54 $\pm$ 3.07		169.19 $\pm$ 0.67	235.39 $\pm$ 6.26	-66.20 $\pm$ 7.02
Treatments									
DL	20.55 $\pm$ 0.67	213.23 $\pm$ 21.60	x		x		x	x	x
DH	20.72 $\pm$ 2.77	211.65 $\pm$ 35.15	x		x		x	x	x
ML	21.52 $\pm$ 0.72	240.00 $\pm$ 29.26	97.73 $\pm$ 25.58		42.20 $\pm$ 9.00		171.04 $\pm$ 2.43	282.39 $\pm$ 26.54	-111.34 $\pm$ 26.85
MH	20.59 $\pm$ 1.24	206.48 $\pm$ 16.32	95.35 $\pm$ 22.59		41.60 $\pm$ 3.18		169.19 $\pm$ 0.69	248.09 $\pm$ 15.43	-78.90 $\pm$ 15.73
Track									
In	20.12 $\pm$ 1.43	212.78 $\pm$ 26.87	99.93 $\pm$ 27.32		41.67 $\pm$ 7.71		170.12 $\pm$ 2.06	255.43 $\pm$ 29.30	-85.32 $\pm$ 28.54
Out	21.57 $\pm$ 1.34	222.90 $\pm$ 29.20	93.15 $\pm$ 19.90		42.33 $\pm$ 5.64		170.12 $\pm$ 2.06	275.04 $\pm$ 23.64	-104.93 $\pm$ 23.55
Moisture conditions <sup>1</sup>	0.49	0.90	x		x		x	x	x
Tyre pressure <sup>1</sup>	0.11	<b>0.07</b>	0.33		0.96		0.32	<b>0.09</b>	0.10
Moisture Pressure <sup>1</sup>	x 0.90	0.50	x		x		x	x	x
Treatments <sup>2</sup>	0.79	0.18	0.81		0.79		0.15	<b><u>0.02</u></b>	<b><u>0.03</u></b>
Track <sup>2</sup>	<b><u>0.00</u></b>	0.38	0.50		0.82		1.00	0.14	0.15
Treatment x track <sup>2</sup>	<b><u>0.00</u></b>	0.57	0.18		0.86		1.00	0.64	0.65

N-in = Soil mineral-N before sowing + cattle slurry (102 kg N ha<sup>-1</sup>) + mineral fertilizer (40 kg N ha<sup>-1</sup>); N-out = Soil mineral-N at 5-days after harvesting + maize N-uptake (kg N ha<sup>-1</sup>). <sup>1</sup> p-values are displayed using two-way ANOVA (only in-track data used);  $P < 0.10$  is indicated in bold;  $P < 0.05$  is indicated in bold and underlined. <sup>2</sup> p-value are displayed using Split-Plot Design with two factors (treatment and track). D: dry condition; M: moist condition; L: low pressure; H high pressure; x: without measurement.

## 4.4. Discussion

### 4.4.1 Effects of soil moisture and tyre pressure on soil physical quality

Soil compaction risk is widely accepted to depend on soil moisture content as the soil precompression stress decreases with increasing soil moisture content (Schjønning *et al.* 2015). Most field studies have been conducted under moist to wet conditions (near pF 2) and found clear differences in assessed soil properties between compacted and control treatments (Lamandé and Schjønning 2011c; Schjønning *et al.* 2017). Compared to those studies, the soil was relatively dry in this study, because it was conducted under realistic practical conditions, resulting in much smaller differences. Yet, differences were detectable, with PR showing a higher response than parameters derived from core samples. This should not necessarily indicate that penetration resistance shows greater sensitivity to soil compaction but could be rather due to the much larger number of samples taken per depth for PR (N=60) in comparison with the three replicated soil cores taken to derive the other soil physical quality indicators.

Tyre pressure could affect soil stress by changing tyre-soil contact area. For instance, under dry conditions, the contact area at low tyre pressure (100 kPa) increased with 67% compared with that at high tyre pressure (300 kPa). However, soil physical properties were not significantly ( $P = 0.05$ ) affected by tyre pressure, though there was a clear trend ( $0.05 < P < 0.1$ ) in lower pressures resulting in less compaction (except for PR), particularly under moist soil conditions. When considering the load transfer from the trailer to the tractor, the tractor's rear wheel load was greatly increased, resulting in a high

compaction risk. This could mask the difference induced by the slurry spreader among treatments as most damage could already have been made by the tractor passes.

According to the modeling results, soil stress already exceeded soil precompression stress in the top layer (0-30 cm); this would then result in marked differences in soil physical properties between in- and out-track positions. However, significant ( $P = 0.05$ ) differences were not found among all the selected lab-measured soil physical and hydraulic properties at the corresponding depths, although a trend was visible ( $0.05 < P < 0.10$ ) for PR. There are several plausible explanations for the lack of marked differences.

First, the distribution of the stress at the tyre-soil contact perpendicular to the driving direction was not uniform but showed two or more peaks (Keller 2005; Schjønning *et al.* 2008). For instance, Berisso *et al.* (2013b) found that  $K_a$  and continuity of soil pores were much smaller at the edge of the wheel ruts compared with mid-rut values because of higher shear stress at the edge. Our sampling position was in the middle of the tracks, which could reduce the observed treatment effects.

Secondly, conventional lab measurements show several drawbacks in detecting impacts of wheeling as compared to more responsive X-ray CT derived parameters (Lamandé *et al.* (2013b). This is further elaborated in a separate section (see 4.4.2). Thirdly, changes in soil properties typically could be seen as an accumulation process which need repeated and longtime wheeling. For example, Arvidsson (2001) and Schjønning *et al.* (2016) did not detect PR differences between compacted and control treatments until 2 to 4 years after trafficking. Fourthly, the equations currently applied in Terranimo® are based on most recent knowledge and availability of data. There is,

however, still room for improvement whenever new data or insights become available. The risk for soil compaction was estimated by balancing soil stress and soil precompression stress. The pedotransfer function currently used to predict precompression stress only considers clay content and soil wetness. This might result in an underestimation of soil precompression stress, particularly for soils that already show some degree of compaction, and thus an overestimation of risk to compaction. Also, Schjønning *et al.* (2016) noticed a mismatch between predicted risk to soil compaction and the very compaction observed in a field.

Lastly, soil heterogeneity, even at the local scale (Johannes *et al.* 2017) and resulting in relatively high standard deviations, might have obscured our results. Relatively small ring samples do not always consider the spatial variability of soil clods, which can be circumvented by profile methods (Arvidsson and Håkansson, 1996; Roger-Estrade *et al.*, 2004).

#### **4.4.2 Comparison of X-ray computed tomography analysis with conventional lab methods**

X-ray micro-CT can well measure soil physical properties and can provide complementary or even more information in a direct way compared with conventional lab methods. For instance, at 10 cm depth, soil macro-porosity ( $d > 120 \mu\text{m}$ ) as derived from X-ray micro-CT and from the lab method, showed a good correlation ( $r = 0.75$ ) (Table 4-5). However, under moist conditions,  $K_a$  measured in-track was larger than out-track which could not be explained by porosity alone. With X-ray micro-CT, a higher connectivity in the in-track samples was detected, which explains their higher  $K_a$ . After

all, there was a good relation ( $r = 0.80$ ) between the micro-CT-derived Euler number that represents connectivity and the lab-derived  $K_a$ . Similarly, Pöhlitz *et al.* (2018) found a close relationship between morphometric micro-CT parameters and mechanical parameters from stress-strain tests.

Conventional lab methods show limitations in both sampling and measurement compared with X-ray micro-CT method. For instance, soil and cylinder wall do not show a perfect contact because of the sampling artifacts, like the presence of roots, residues or other more rigid substances. Furthermore, it is always a challenge to measure soil volume precisely, which is used to determine soil porosity and other volume-averaged composite soil properties. In contrast, X-ray micro-CT results can exclude the sample boundaries and only select a specific ROI which makes the results more precise, as was demonstrated by, e.g., Lamandé *et al.* (2013a).

However, one drawback of X-ray micro-CT is its limited resolution for a certain sample volume typically taken to represent local soil physical properties (often at least  $10^{-4} \text{ m}^3$  with a  $\sim 0.05 \text{ m}$  diameter). Like in this study, information below  $120 \text{ }\mu\text{m}$  pore size was lost, which could even lead to incorrect interpretations. For instance, uncorrected soil air permeability and hydraulic conductivity which might be dominated by smaller pores in some occasions (Katuwal *et al.* 2015c). Moreover, further downsizing the volume could increase the risk of not selecting a volume representative for the soil property of interest (Zhou *et al.* 2017). Also note that X-ray CT results were only based on one replication, which might be less representative.

#### 4.4.3 Effects of traffic on maize growing season

Mouldboard ploughing is an adequate way to alleviate topsoil compaction, but its success depends on soil and crop type (Arvidsson and Håkansson 1996). Arvidsson and Håkansson (1996) found that with fine soil textures being more coherent, their soil surface was rougher and traffic effects can be persistent for several years even after ploughing. However, detecting differences in soil properties is more challenging than when considering crop biomass, especially with small ring samples, which do not well consider the spatial variability of soil clods (Arvidsson and Håkansson 1996; Roger-Estrade *et al.* 2004). Consistent with this, differences in soil quality indicators were hardly detectable with point-based methods for the silt loam soil in this study. Interestingly, similarly as in the study of Arvidsson and Håkansson (1996), where dry above-ground biomass of most crops (winter wheat, barley, peas and potatoes) showed an average decrease of 11.4% in trafficked treatments compared with control treatments despite the absence of marked differences in soil physical properties, dry above-ground maize biomass decreased by 6.7% at in-track positions compared with out-track positions in this study. If not directly affected by the above soil physical properties, the biomass decline can be explained by the soil and plant nutrition balance. For instance, Arvidsson and Håkansson (1996) found that crop nitrogen uptake was smaller in the compacted treatments (after ploughing) compared with the control, especially in the earlier growth stage. Unfortunately, they did not measure the soil nitrogen content. In our study, when considering the nitrogen balance, maize nitrogen uptake was not different between in- and out-track positions. However, at in the out-track positions, soil N-out was higher ( $P = 0.14$ ; Table 4-8). This suggests a higher mineralization rate at out-track positions because the N-in was not

difference. This could result from a larger air permeability in association with better soil structure at out-track positions before and during maize growing season.

### 4.5. Conclusions

Soil wetness and tyre pressure during slurry spreader conduction did affect soil physical properties. Penetration resistance was significantly larger ( $P < 0.05$ ) in the top 20 cm layer when trafficked under moist conditions than under dry conditions. A clear trend of increased bulk density and macro-porosity ( $0.05 < P < 0.10$ ) was observed between moist and dry conditions at 10 cm depth, while tyre pressure had less effects. X-ray micro-CT parameters were more responsive to slight changes in the degree of compaction than conventional lab methods. There was no significant difference for soil properties at greater depths. Terranimo<sup>®</sup> could well predict the contact area and mean ground pressure. It indicated considerable compaction risk from the tractor's rear wheels, though the overall compaction risk seemed overestimated as changes in soil compaction-related soil properties were minor.

In the summer maize growing season, soil quality indicator and nitrogen content differences were not detectable between in-track and out-track positions. However, for maize growth under this loamy soil study, topsoil ploughing was not sufficient to eradicate the negative compaction effects induced by slurry spreader traffic, which resulted in a ~7% lower dry above-ground maize biomass at in-track positions compared with out-track positions.

### **Part III : Alleviation of soil compaction**

## **Chapter 5: Short-term effects of cover crops and tillage methods on soil physical properties and maize growth in a sandy loam soil**

This chapter is based on:

Lidong Ren, Thijs Vanden Nest, Greet Ruyschaert, Tommy D'Hose, Wim M. Cornelis (2019). Short-term effects of cover crops and tillage methods on soil physical properties and maize growth in a sandy loam soil. *Soil and Tillage Research*, 192, 76-86.

## 5.1. Introduction

Soil compaction is recognised as one of the main threats to sustainable agriculture by the European Commission (Alameda *et al.* 2012) as it has various adverse impacts on soil quality, crop growth and the environment (Unger and Kaspar 1994; Huber *et al.* 2008; Keller *et al.* 2013). Crop roots could alleviate soil compaction by bio-drilling and can be regarded as a low-energy consuming environment-friendly solution. Chen and Weil (2011) found that on no-till fields cover crops positively affect maize root penetration into deeper compacted layers and that (cover) crops with tap roots like forage radish (*Raphanus sativus* var. *longipinnatus*) and rapeseed (*Brassica napus*) are more capable to penetrate compacted soil than fibrous-rooted crops like rye (*Secale cereale*) (Chen and Weil 2010). Overall, roots with greater diameter and/or sharper root tip opening angle may penetrate compacted soils better and faster than roots with smaller diameters or blunt opening angle (Materechera *et al.* 1991; Colombi *et al.* 2017b). However, the benefits of cover crops vary depending on crop species and compaction level (Chen and Weil 2011; Goutal *et al.* 2012; Arvidsson and Hakansson 2014). In Belgium, cover crops are used as a cost-effective means to control soil erosion and, as catch crops, reduce nitrogen leaching to water bodies. Two recommended species in the region are white mustard (*Sinapis alba*) and winter rye, which are tap and fibrous rooted, respectively. Studies on cover crops root growth, their ability to alleviate soil compaction and their beneficial effect on the yield of consecutive main crops are still lacking in Europe.

Seedbed-preparing tillage might be fast and efficient to control topsoil compaction. Mouldboard ploughing is a widely-used intensive tillage method that thoroughly loosens the topsoil over the full width and depth of operation (Laufer and Koch 2017). However,

many adverse effects associated with mouldboard ploughing have been reported (Wang *et al.* 2015). In response to this, various conservation tillage methods have been introduced. A promising method is strip tillage, which is a conservation tillage method that only tills the sowing row. It combines the benefits of both no-till and intensive tillage systems. For instance, Vetsch *et al.* (2007) found that strip tillage resulted in less energy consumption, lower erosion risk and larger maize yield than no-till and chisel ploughing in a clay loam soil in USA. However, there is still controversy about the effects of strip tillage on crop yield. Temesgen *et al.* (2012) compared strip tillage with intensive tillage in a semi-arid area and found it to decrease runoff and erosion, which greatly improved plant water availability resulting in larger maize yield. In contrast, Vyn and Raimbault (1992) found that average maize yield was slightly lower with strip tillage than with mouldboard plough-based intensive tillage in both silt loam and clay loam soil, while it was significantly lower in sandy loam soil. Licht and Al-Kaisi (2005) observed that maize yield was not significantly different among strip tillage, no-till and chisel ploughing. In Belgium, Flemish farmers are forced to reduce soil erosion on sensitive fields by the good agricultural practices of the European Common Agricultural Policy (CAP). Strip tillage is regarded as a useful option to control soil erosion but it is still new in the study region (Ryken *et al.* 2018), and its effects on soil properties and crop growth are still not clear. Since farmers in this part of the world often have negative experiences with conservation practices because of yield reductions (Van den Putte *et al.*, 2010), they are reluctant to introduce them.

Unlike aboveground biomass and yield, less is known about root distribution. Many field methods for root assessment have been developed, e.g., core method, core-break

method, trench method and the minirhizotron method (Van Noordwijk *et al.* 2001), but they all have their advantages and disadvantages. Minirhizotrons allow to observe root growth continuously in time series, but they are not suitable for compacted soil because roots grow preferentially along the tubes (Chen 2009). In the core method, regarded as the most classical one, roots are washed out for further analysis like to examine root biomass, root length and root surface area. Alternatively, cores can be broken by hand and the number of roots protruding from break faces can be recorded as in the core-break method (Van Noordwijk *et al.*, 2000). However, observing spatial root distribution is more difficult with the above methods. This problem can be overcome by the trench method, enabling to directly show root distribution in a two-dimensional profile, which is particularly useful to detect root spatial heterogeneity distribution under strip tillage.

The overall aim of the study was to better understand how maize growth conditions can be sustainably optimized on fields with root-penetrating limitations due to soil compaction in a temperate climate. The specific objectives were to test i) whether tap-rooted white mustard shows higher root penetration than fibrous-rooted winter rye on sandy loam with compacted subsoil and ii) to what extent cover crop species and seedbed-preparing strip tillage or mouldboard plough-based intensive tillage affect root distribution and above-ground biomass of the consecutive maize crop. This study focuses on short-term effects as farmers believe that strip tillage might reduce maize yields and thus are very reluctant to start practising it. It is hypothesized that cover crops with a tap root system improve maize root growth compared to cover crops with a fibrous root system under both tillage methods and that strip tillage following cover crops will not negatively affect maize growth. Unlike most studies on soil compaction, this study did not

create (unrealistic) compaction levels by wheel trafficking with different loads or passes, but selected a farmer's field that was highly compacted by previous farming operations. Because of relatively dry in winter and spring during the study period, this study presents a conservative test on the ability of cover crops and/or tillage on remediating soil compaction problems. Such conditions might be expected to occur more frequently in the future in this Western European study area because of climate change.

## **5.2. Materials and methods**

### **5.2.1 Study site**

The Crookstraat Field was used to conduct this experiment from August 2016 to September 2017. The study period was very dry, especially in winter and spring, and coincided with the Western-European drought of the first half of 2017 (Table 5-1). No irrigation system is applied in this area and the water table was ~1 m depth according to the water level in drainage ditches and soil profile observations. The soil is classified as Eutric Retisol (Dondeyne *et al.* 2014) and has a sandy loam texture (USDA). Table 5-2 shows some basic soil properties in the top 60 cm. Soil texture was determined with the sieve-pipette method (Gee and Bauder 1986) on three samples randomly taken within the field and soil organic carbon was determined according to Walkley and Black (1934).

Table 5-1. Meteorological condition during the study period (data according to Uccle station and analysis from the Royal Meteorological Institute of Belgium, RMI)

Seasons	Temperature (°C)	Precipitation (mm)	Relative humidity (%)
Autumn 2016 (SEP-NOV)	11.1 (10.9) n	162.2 (219.9) n	80 (82) va
Winter 2016 (DEC-FEB)	3.9 (3.6) n	127.3 (220.5) va	84 (84) n
Spring 2017 (MAR-MAY)	11.3 (10.1) a	108.0 (187.8) va	68 (74) e
Summer 2017 (JUN-AUG)	18.6 (17.5) a	179.9 (224.6) n	68 (73) e
Autumn 2017 (SEP-NOV)	11.3 (10.9) n	226.5 (219.9) n	82 (82) e

Note: Normal values (in parentheses) and degree of abnormality defined over the period 1981-2010 with n: normal (< 6 years); a: abnormal (6-10 years); va: very abnormal (10-30 years); e: exceptional (> 30 years).

Over the last five years prior to the experiment, the following crops were grown: winter wheat (*Triticum aestivum* L.) in 2011, potato (*Solanum tuberosum* L.) in 2012, maize in 2013, flax (*Linum usitatissimum* L.) in 2014, maize in 2015, and winter wheat in 2016, which is common in the study area. The field was conventionally tilled by means of a mouldboard plough till a depth of approximately 30 cm in the previous years (more than several decades).

Table 5-2. Average of soil texture and organic carbon content in three replications.

Depth (cm)	Sand (>0.05 mm) (g kg <sup>-1</sup> )	Silt (0.05-0.002 mm) (g kg <sup>-1</sup> )	Clay (<0.002 mm) (g kg <sup>-1</sup> )	SOC (g kg <sup>-1</sup> )	Texture (USDA)
0-30	671.1	286.7	41.2	12.9	sandy loam
30-60	696.3	266.0	36.7	6.2	sandy loam

SOC: soil organic carbon content.

## 5.2.2 Experimental design

From autumn 2016 to spring 2017 (winter season), two cover crop species (see 2.3) were grown in four randomized blocks (A, B, C and D). In spring 2017, two seedbed-preparing tillage methods were introduced to each cover crop (see 5.2.4.), leading to a split plot design. Thus, four treatments in the summer maize season were created by combining the two tillage practices with the two previous cover crops (Fig. 5-1). Each plot was 6×12 m and only three blocks were selected in the summer season.

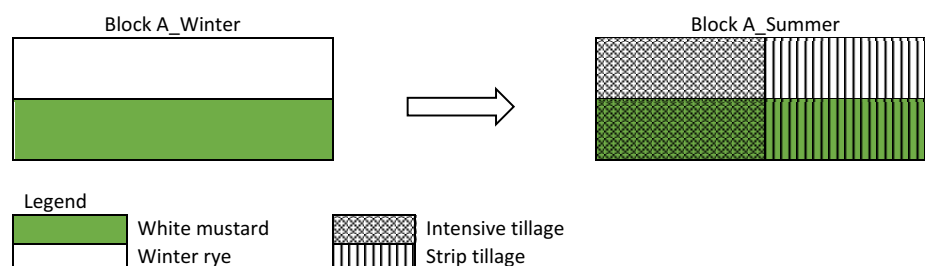


Fig. 5-1. Experimental design (shown for block A only).

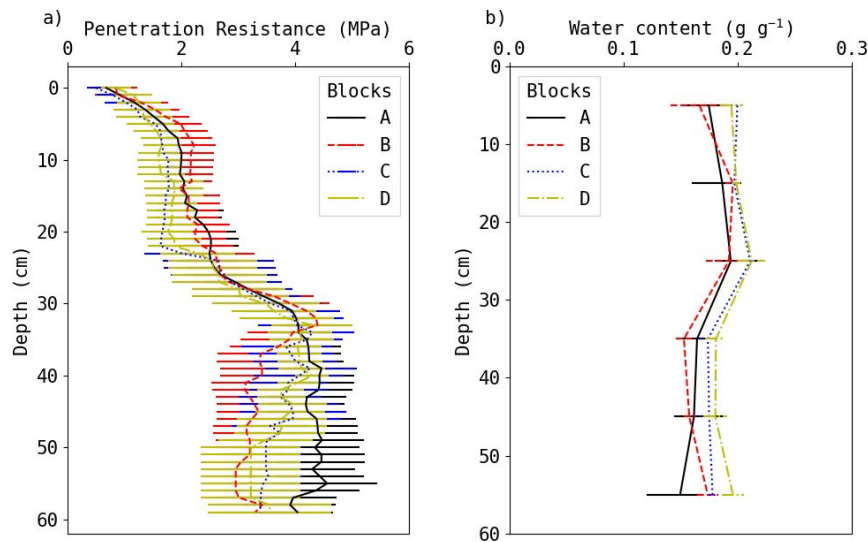


Fig. 5-2. Penetration resistance (a) and gravimetric soil water content (b, near field capacity  $0.22 \text{ g g}^{-1}$ ) in each block (A, B, C, D). Error bars indicate 95% confidence intervals ( $n=10$ ) (left) or the range, i.e. maximum and minimum ( $n=2$ ) (right).

Spatial variability in penetration resistance (PR), soil water content and growth of the previous winter wheat crop (measurement methods according to section 5.2.4) were determined prior to this experiment to select the most homogeneous study area. Figure 5-2 indicates that there was no significant difference in penetration resistance (PR) among the four blocks at most of the depths (confidence interval bars overlap), except between block A and B below 40 cm, where block B showed slightly lower penetration resistance compared to block A.

Near 30 cm depth, all plots showed PR of ~4 MPa, which results in mechanical resistance affecting root proliferation of most cash crops and is twice as high as the value of 2 MPa which is commonly considered as root-restricting (Materechera *et al.* 1991; Da Silva *et al.* 1994). Soil became much denser and thus compacted from ~27 cm depth suggesting the presence of a plough pan. It most likely resulted from previous intensive in-furrow ploughing with wheels on one side of the tractor driving inside the precedent furrow, repeated tillage operations at the same depth, and traffic with heavy machinery. Concurrent water content measurements show that soils in all blocks were near field capacity, and thus baseline PR measurements were not affected by too dry or wet conditions. The previous winter wheat crop growth (data not shown) was homogeneous across all blocks.

### **5.2.3 Winter season management, sampling and analysis**

#### **5.2.3.1 Field preparation and sowing**

Before sowing the cover crops, i.e., on August 24, 2016, pig slurry (30 kg N ha<sup>-1</sup>) was spread on the field with a line spreading boom (with GPS-Real Time Kinematic and automatic flow control) and incorporated into the soil to a depth of 10 cm by a cultivator. On August 30, 2016, white mustard was sown with a sowing machine that combined deep non-inversion tillage (till 25 cm) and standard sowing (distance between rows of 15 cm and 20 kg/ha sowing intensity). Winter rye was sown on October 7, 2016, with a sowing machine combining deep non-inversion tillage (till 25 cm), rotary harrowing (8 cm depth) and standard sowing (distance between rows of 15 cm with 150 kg/ha sowing intensity).

### **5.2.3.2 Root observation**

Root penetration was evaluated after harvesting the above-ground biomass using the core-break method (Van Noordwijk *et al.* 2001). The rooting depth and root number density of white mustard was determined before wilting/freezing on December 14, 2016, whereas for winter rye it was determined on April 06, 2017, as it can successfully survive freezing periods during winter in the study area. Root samples were taken in three locations per plot within the crop row. A root auger with an 8-cm inner diameter and 15-cm long sampling tube was used to take undisturbed soil samples (Maria do Rosário *et al.* 2000). The cylindrical soil cores were laid out horizontally and broken by hand at 2.5, 7.5, 12.5 cm along their length to make sure roots could be counted in the middle of every 5-cm interval. As one root cannot appear on both break planes, the total root number was calculated by the sum of both break surfaces. Because of the large number of winter rye roots in the top 5 cm, it was not possible to break this layer into two and root number was thus lacking in this layer. All root samples were collected up to 45 cm depth, below which no roots were found.

## **5.2.4 Summer season management, sampling and analysis**

### **5.2.4.1 Field preparation and sowing**

In spring (March 29, 2017), glyphosate was applied to kill the winter rye. One week later, a flail mower was used to cut and destroy the winter rye and the white mustard

mechanically. On April 20, cattle slurry ( $45 \text{ m}^3 \text{ ha}^{-1}$ ) was applied homogeneously in the intensive tillage plots. After that, cattle slurry was mixed with soil (10 cm depth) using a cultivator. Within the same day, a conventional mouldboard plough with four ploughshares was used to conduct intensive tillage by in-furrow ploughing (till 30 cm depth), followed by seedbed preparation with a rotary harrow (8 cm depth). For strip tillage, a strip-till machine (Carré INRO) tilled the soil till 25 cm depth in strips of 20 cm width on the same date, April 20. The same amount of cattle slurry was applied as in intensive tillage but was only placed in the tilled strip rows (pipes connected to the dents of the strip-till machine). On the same day, maize was sown (75 cm width between rows,  $1.05 \times 10^5$  seeds  $\text{ha}^{-1}$ , with 6 cm sowing depth) in all treatments. During sowing, 200 kg of mineral fertilizer, 16-6-23(-2) (-5) ( $32 \text{ kg N ha}^{-1}$ ,  $12 \text{ kg P}_2\text{O}_5 \text{ ha}^{-1}$ ,  $46 \text{ kg K}_2\text{O ha}^{-1}$ ,  $4 \text{ kg MgO ha}^{-1}$  and  $10 \text{ kg SO}_3 \text{ ha}^{-1}$ ), was added in the rows for both tillage methods.

### 5.2.4.2 Undisturbed soil sampling and measurement

To help explaining potential treatment effects on maize root growth, above-ground biomass and yield, one undisturbed soil sample was collected per plot before harvesting maize in  $100 \text{ cm}^3$  standard sharpened steel cores (5.1 cm height and 5 cm diameter) at 10, 20, 35 and 55 cm depth in the middle between two maize rows. An Edelman auger (Eijkelkamp Soil & Water, Giesbeek, the Netherlands) was used to pre-drill a small hole, followed by a Riverside auger (Eijkelkamp Soil & Water, Giesbeek, the Netherlands) to prepare a flat sampling platform at each depth, and finally a dedicated ring holder (Eijkelkamp Soil & Water, Giesbeek, the Netherlands) was used to take the samples. The

samples were used to determine the soil water retention characteristic with the sandbox method (Eijkelkamp Soil & Water) for high matric potentials and pressure plates (Soilmoisture Equipment, Santa Barbara CA, USA) for low matric potentials according to the procedure outlined in Cornelis *et al.* (2005). Selected matric potentials were -1, -3, -5, -7, -10, -33, -100 and -1500 kPa. Bulk density was determined as part of this procedure, while the water retention characteristic was used to deduce pore size distribution, i.e., micropores (equivalent diameter  $d < 0.2 \mu\text{m}$ ), mesopores ( $0.2 < d < 30 \mu\text{m}$ ) and macropores ( $d > 30 \mu\text{m}$ ) (Kay and Lal (1997)).

#### **5.2.4.3 Soil water content**

Disturbed soil samples were collected at two depths (0-30 and 30-60 cm) in each plot using a 3-cm diameter bi-partite gouge auger (Eijkelkamp Soil & Water, Giesbeek, the Netherlands) between two maize rows on June 19, July 13, August 18 and September 10, 2017. For the determination of soil moisture, three replicates were taken per treatment and each replicate was a composite from two locations within each plot. Soil samples were stored in closed plastic bags and then brought to the lab to determine wet soil mass as soon as possible. Dry soil mass was measured after oven-drying at 105 °C for 24 h. Volumetric soil water content was calculated from gravimetric soil water content and bulk density at each depth. The critical matric potential for water stress of maize was taken at -60 kPa according to Wesseling *et al.* (1991) and corresponding water contents were calculated using the Van Genuchten (1980) curve fitted to the water retention characteristics.

#### **5.2.4.4 Penetration resistance**

Penetration resistance was measured using a hand-held penetrometer (Eijkelkamp Soil & Water) to a depth of 60 cm on September 07, 2017, before harvesting maize. The cone had a 1 cm<sup>2</sup> base area, a 11.28 mm nominal diameter and a 60° top angle. Soil water content was measured concurrently. Penetration resistance was measured in a 75-cm long transect perpendicular to maize rows, i.e., from one row to the other, with two transects per plot. Row distance was 75 cm and the measurement interval was 7.5 cm. Thus, in one transect for strip tillage, there were six measured points between two strip tillage tills (out-row) and four in two strip tillage tills (in-row). Per plot, one transect was selected resulting in three transects per treatment.

#### **5.2.4.5 Root number density and above-ground biomass**

Before harvesting maize (August 9, 2017), root distribution was observed using the trench profile method (Van Noordwijk *et al.* 2001). First, a 60-cm depth trench profile was dug in between two maize rows (75 cm) of each plot. The observed profile wall was carefully prepared with a sharp knife removing soil that covered the surface to display roots. Then, a wooden frame with 2.5 × 2.5 cm cells was used to record root number by counting the number of roots in each cell.

The whole plant (corn, cob and stem) was harvested as silage (cattle feed) on September 7, 2017. Two rows in the middle of each plot were harvested over the full

length with a chopper installed at the front of the tractor and an automatic weighing unit in its rear. In every plot, a ~1 kg subsample was collected to determine the oven-dry matter content (72 h at 70°C).

### **5.2.5 Statistical analysis**

Analysis of variance (ANOVA) was performed using the SPSS statistical package (Version 25.0 for Windows, SPSS, Chicago, USA). The remaining data analyses were performed in Python. For the winter season, one-way ANOVA was used with cover crop as the only factor. For the summer season, a split-plot design with two factors (winter cover crops and tillage methods) was used. Differences between the treatments were assessed using their variance and a LSD (least significant difference) multiple comparison test at 0.05 and 0.10 probability level with the SPSS procedure UNIVARIATE. Non-parametric analyses (Mann-Whitney or Kruskal–Wallis test) were used if data failed to meet parametric assumptions.

## **5.3. Results**

### **5.3.1 Winter cover crops season: root number density**

Cover crops' root number density distribution was different from each other along the observed soil profiles (Fig. 5-3). Winter rye root number density decreased with depth, with a dramatic decrease till ~15 cm, while white mustard showed a slight increase in root number till ~22 cm depth, after which it decreased. Winter rye had significantly ( $P = 0.02$ )

more roots in the top 15 cm than white mustard while white mustard had higher root number density ( $P = 0.04$ ) between 20 and 35 cm depth. Below 45 cm depth, very few roots were observed in both treatments.

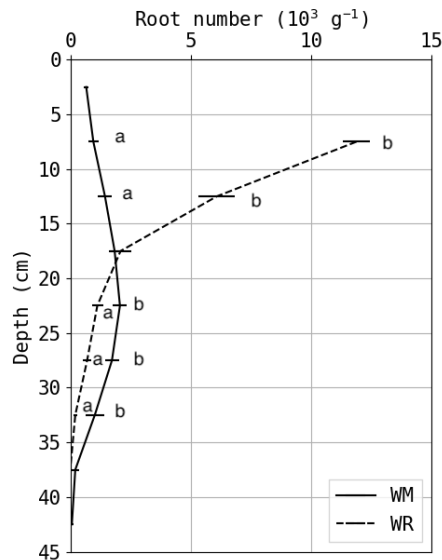


Fig. 5-3. Mean root number density distribution ( $n=24$ ) of winter cover crops (WM = white mustard, WR = winter rye). The error bars are 95% confidence interval. Letters at the same depth designate significant differences at the 5% probability level.

### 5.3.2 Summer maize season

#### 5.3.2.1 Maize root distribution

Figure 5-4 shows that maize roots were mainly distributed within the top 30 cm; few roots could penetrate the plough pan (below ~27 cm). At out-row positions, no significant difference in maize root number density was found between the cover crop treatments

above 30 cm depth. At 30-40 cm depth, the number of roots penetrating the compacted layer was significantly ( $P \leq 0.05$ ) higher following white mustard than following winter rye (Table 5-3). Intensive tillage always resulted in larger mean root number density than strip tillage in the top 40 cm at out-row positions and differences were statistically significant at 10-20 cm ( $P \leq 0.10$ ) and 20-30 cm ( $P \leq 0.05$ ). Below 40 cm depth, at out-row positions, very few roots were found in all treatments. Interaction effects were only found at 20-30 cm ( $P \leq 0.10$ , Table 5-3). At in-row positions (10 cm width at each side), no significant differences in maize root number density were found between cover crop treatment, tillage methods and their interaction except between cover crop treatments at 30-40 cm depth (Table 5-3).

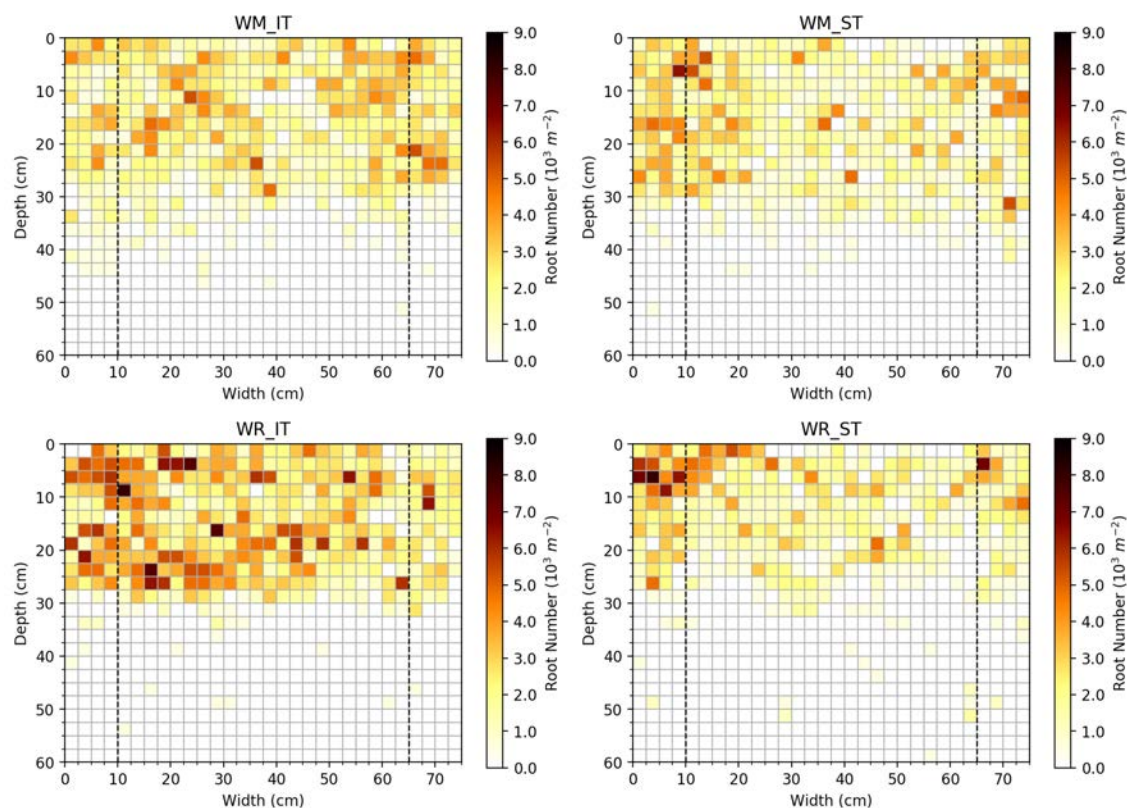


Fig. 5-4. Average ( $n=3$ ) maize root number density distribution in each treatment (WR = winter rye; WM = white mustard; IT = intensive tillage; ST = strip tillage). Dash lines indicate the border of strip tillage or the corresponding strip tillage border at intensive tillage (maize rows at  $x=0$  and  $75$  cm).

Table 5-3. Root number density distribution of maize within each 10-cm depth increment in and out of the tillage row (WR = winter rye; WM = white mustard; IT = intensive tillage; ST = strip tillage) with standard deviation in the parenthesis (n=3).  $P \leq 0.10$  is indicated in bold,  $P \leq 0.05$  is indicated in bold and underlined.

Treatment		Out-row root number density ( $10^3 \text{ m}^{-2}$ ) at various depths (cm)						In-row root number density ( $10^3 \text{ m}^{-2}$ ) at various depths (cm)					
		0-10	10-20	20-30	30-40	40-50	50-60	0-10	10-20	20-30	30-40	40-50	50-60
Crops	WM	2.03 (0.47)	1.93 (0.54)	1.62 (0.28)	<b><u>0.46 (0.22)</u></b>	0.03 (0.03)	0.00 (0.00)	2.30 (0.92)	2.42 (0.98)	2.16 (0.73)	<b><u>0.72 (0.58)</u></b>	0.11 (0.12)	0.01 (0.02)
	WR	2.41 (1.09)	2.05 (1.12)	1.71 (1.42)	<b><u>0.21 (0.12)</u></b>	0.03 (0.03)	0.02 (0.03)	3.30 (1.52)	2.40 (0.60)	1.80 (0.86)	<b><u>0.11 (0.14)</u></b>	0.06 (0.10)	0.00 (0.00)
Tillage	IT	2.62 (0.32)	<b>2.45 (0.74)</b>	<b><u>2.24 (1.01)</u></b>	0.30 (0.24)	0.03 (0.03)	0.01 (0.01)	2.63 (1.23)	2.30 (0.52)	2.19 (0.72)	0.34 (0.44)	0.10 (0.13)	0.00 (0.00)
	ST	1.82 (0.32)	<b>1.53 (0.70)</b>	<b><u>1.09 (0.52)</u></b>	0.28 (0.27)	0.03 (0.03)	0.02 (0.03)	2.96 (1.12)	2.50 (1.00)	1.77 (0.85)	0.50 (0.62)	0.08 (0.11)	0.01 (0.02)
Crops x Tillage	WM_IT	2.34 (0.49)	2.21 (0.69)	1.79 (0.12)	0.44 (0.23)	0.04 (0.04)	0.01 (0.01)	2.10 (0.80)	2.04 (0.63)	2.17 (0.49)	0.59 (0.51)	0.17 (0.15)	0.00 (0.00)
	WR_IT	2.90 (1.30)	2.70 (0.84)	2.70 (1.39)	0.15 (0.16)	0.03 (0.02)	0.01 (0.01)	3.16 (1.52)	2.57 (0.29)	2.21 (1.02)	0.10 (0.02)	0.02 (0.03)	0.00 (0.00)
	WM_ST	1.72 (0.16)	1.65 (0.12)	<b>1.45 (0.30)</b>	0.48 (0.25)	0.03 (0.03)	0.00 (0.00)	2.50 (1.16)	2.80 (1.25)	2.15 (1.04)	0.86 (0.73)	0.06 (0.06)	0.02 (0.02)
	WR_ST	1.92 (0.76)	1.41 (1.09)	<b>0.73 (0.44)</b>	0.09 (0.09)	0.03 (0.03)	0.03 (0.02)	3.43 (1.18)	2.21 (0.82)	1.39 (0.54)	0.13 (0.14)	0.10 (0.01)	0.00 (0.00)
Statistical analysis													
Crops	P value	0.42	0.78	0.83	<b><u>0.02</u></b>	0.89	0.12	0.18	0.95	0.46	<b><u>0.05</u></b>	0.42	0.37
Tillage	P value	0.12	<b>0.07</b>	<b><u>0.03</u></b>	0.92	0.89	0.31	0.64	0.69	0.40	0.58	0.78	0.37
Crops x tillage	P value	0.71	0.44	<b>0.10</b>	0.69	0.68	0.15	0.92	0.27	0.42	0.68	0.20	0.37

### 5.3.2.2 Soil physical properties

The findings described above could be further explained by the physical characteristics of the soil before maize harvesting. Figure 5-5 and 5-6 show that in the summer season before maize harvesting, penetration resistance increased with depth to more than 4 MPa with a dramatic increase from ~30 cm onward. Below 40 cm depth, penetration resistance did not substantially vary with depth. Similarly, soil bulk density increased with depth reaching the highest value at 35 cm depth (Fig. 5-7). Laterally, a larger trend value of penetration resistance was found at out-row positions compared to in-row positions in the topsoil (0-30 cm) under strip tillage, while this trend was absent under intensive tillage.

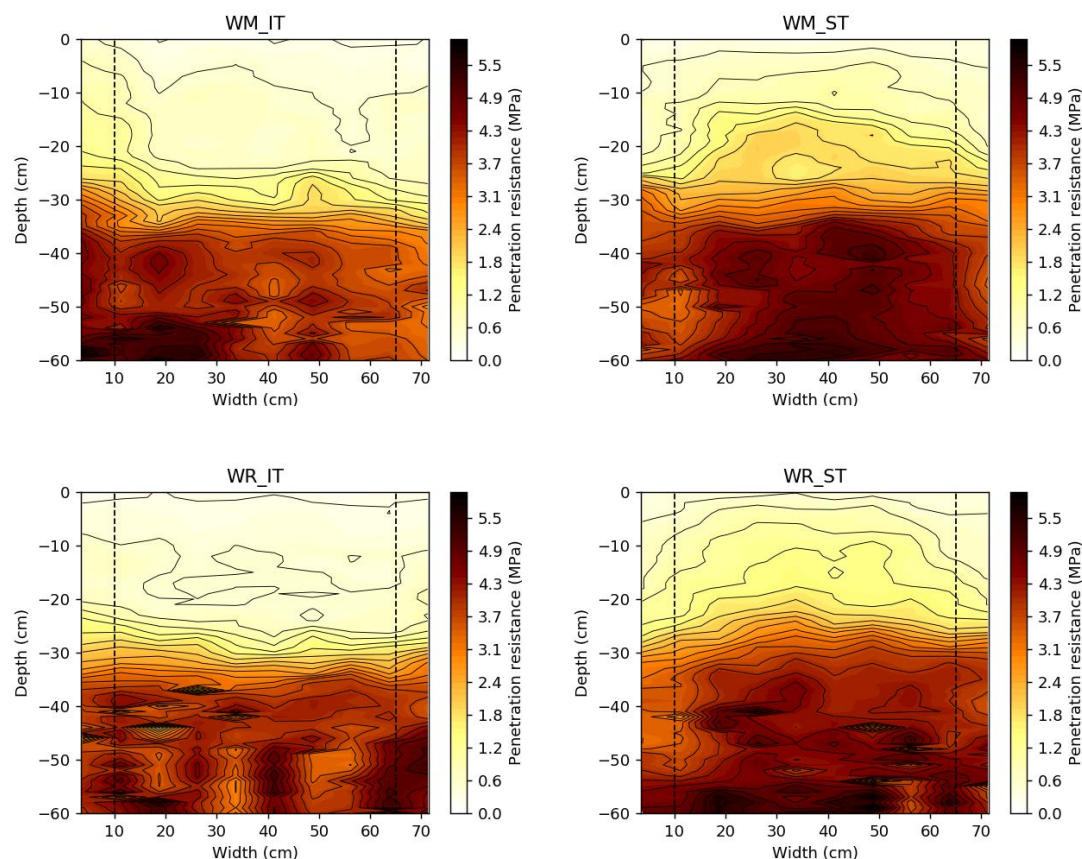


Fig. 5-5. Distribution of penetration resistance (n=6) between two maize rows (WR = winter rye; WM = white mustard; IT = intensive tillage; ST= strip tillage). Dash lines

indicate the border of strip tillage or the corresponding strip tillage border at intensive tillage before harvest (maize row at x=0 and 75 cm).

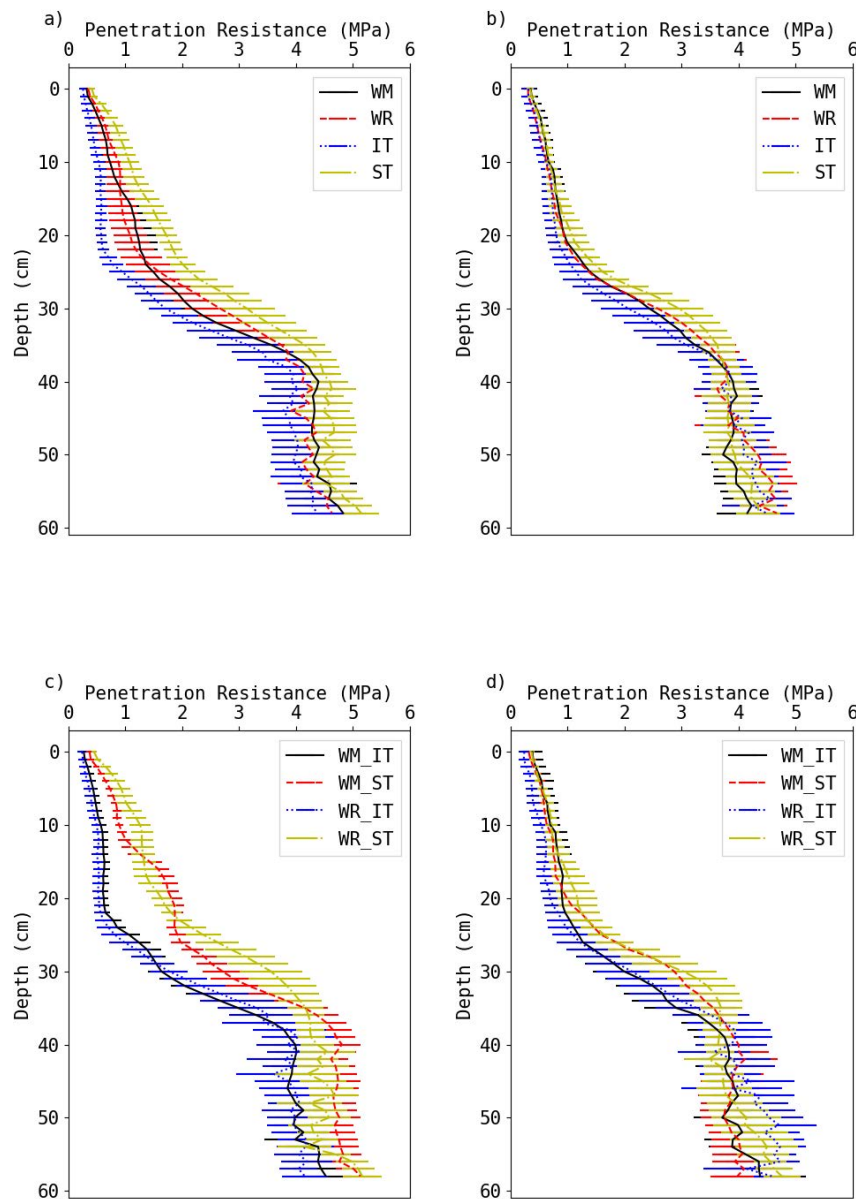


Fig. 5-6. Penetration resistance (PR) distribution among treatments (a and b) and interaction effects (c and d) before harvest (WR = winter rye; WM = white mustard; IT = intensive tillage; ST = strip tillage); a and c) out-row: between two tilled strips (PR n=18); b and d) in-row: in tilled strips (PR n=12).

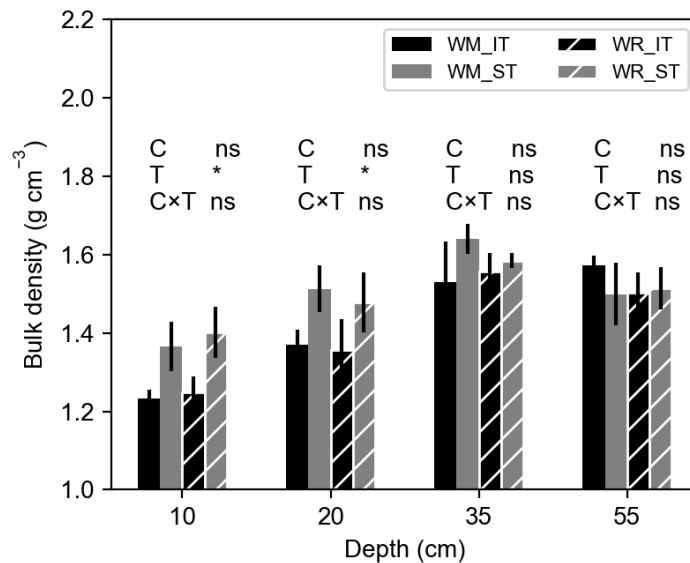


Fig. 5-7. Soil bulk density at four depths at out-row positions (WR = winter rye; WM = white mustard; IT = intensive tillage; ST = strip tillage; C = cover crop factor; T = tillage factor). The error bars indicate standard deviation (SD;  $n=3$ ). ns and \* indicates non-significant and significant at the  $P = 0.05$  probability level, respectively.

At out-row positions, there was no significant difference in penetration resistance or bulk density between the two cover crops (Fig. 5-6a and Fig. 5-7). In contrast, tillage methods greatly affected penetration resistance and bulk density. In the top 30 cm layer at out-row positions, penetration resistance and bulk density was significantly higher under strip tillage than under intensive tillage ( $P \leq 0.05$ ). However, no clear difference was found below 30 cm depth between treatments for penetration resistance or bulk density. At in-row positions, no difference was found in the top and subsoil among all treatments (Fig. 5-6b), but mean penetration resistance was slightly larger at 20-35 cm depth for strip tillage. This can be attributed to different working depths, i.e., 30 cm for intensive tillage and 25 cm for strip tillage.

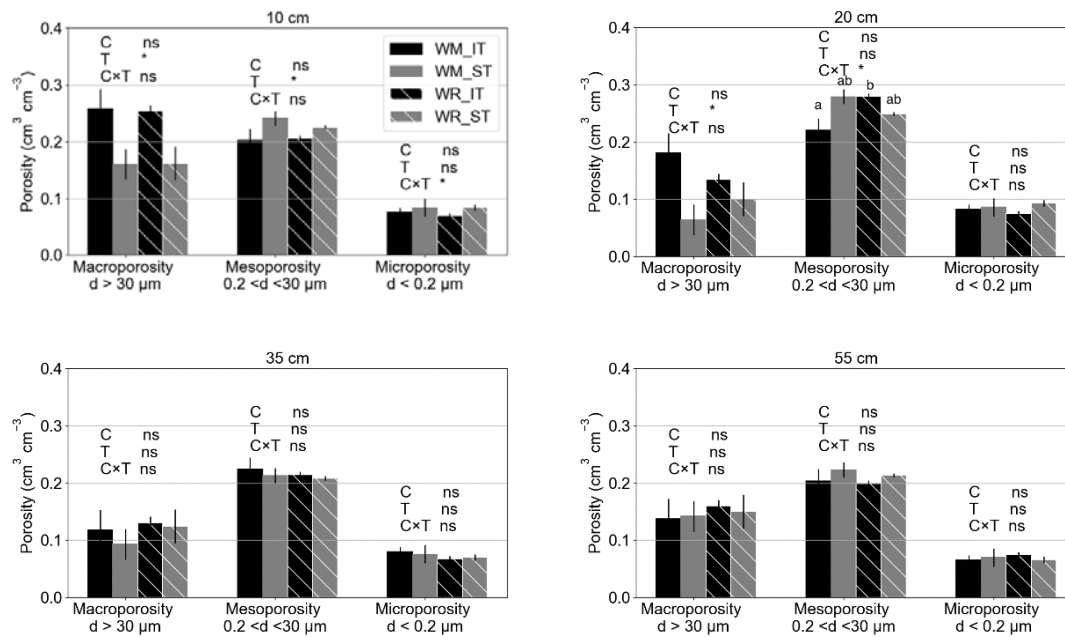


Fig. 5-8. Pore size distribution at each depth at out-row positions (WR = winter rye; WM = white mustard; IT = intensive tillage; ST = strip tillage; C = cover crop factor; T = tillage factor). The error bars are standard deviation (SD;  $n=3$ ). ns means the factor is not significant ( $P \leq 0.05$ ). \* means the factor is significantly different ( $P \leq 0.05$ ). Different letters indicate significant differences ( $P \leq 0.05$ ) for the interaction of C and T.

Pore size distribution (macro-, meso- and microporosity) was also evaluated at out-row positions (Fig. 5-8). It appears that mean macroporosity decreased with depth from  $\sim 0.25 \text{ m}^3 \text{ m}^{-3}$  at 10 cm depth to  $\sim 0.10 \text{ m}^3 \text{ m}^{-3}$  at 35 cm depth; at 55 cm depth, the mean value was slightly higher than at 35 cm. Mesoporosity was always larger than  $0.20 \text{ m}^3 \text{ m}^{-3}$  and it was largest at 20 cm. Microporosity was quite stable at all depths with values below  $0.10 \text{ m}^3 \text{ m}^{-3}$ . For completeness, complete water retention characteristics with fitted Van Genuchten (1980) curves under the different treatments are presented as supplementary information (Fig. S1). No effect of cover crops on porosity was detected, but significant effects of tillage methods at out-row positions

were found at 10 and 20 cm depth. At 10 cm depth, intensive tillage had macroporosity above  $0.20 \text{ m}^3 \text{ m}^{-3}$ , while under strip tillage values below  $0.15 \text{ m}^3 \text{ m}^{-3}$  were observed. Consequently, mesoporosity was higher under strip tillage ( $0.23 \text{ m}^3 \text{ m}^{-3}$ ) than under intensive tillage ( $0.20 \text{ m}^3 \text{ m}^{-3}$ ). A similar trend existed at 20 cm depth though less apparent and with porosity values being more variable.

### 5.3.2.3 Water content and above-ground biomass

Volumetric soil-water content decreased from June to July and then began to increase slightly at 0-30 cm depth, in response to some rainfall events (Fig. 5-9). There was a clear trend for consistently higher mean soil-water content under strip tillage compared with intensive tillage ( $P = 0.36$ ). In the subsoil layer (30-60 cm), volumetric soil-water content decreased from June to July. After that, it slightly increased under strip tillage but continued to decrease under intensive tillage. Under all treatments, soil moisture remained during the observation period above a critical (drought stress) matric potential of -60 kPa for maize growth as suggested by Wesseling *et al.* (1991).

Above-ground maize biomass did not show significant differences ( $P \leq 0.05$ ) between cover crops treatments, tillage methods and their interactions (Table 5-4). However, there was a clear trend for increasing biomass when combining strip tillage with white mustard as cover crop ( $P = 0.11$ ). The latter combinations resulted in biomass that was  $0.3 \text{ ton ha}^{-1}$  higher (or 1.3%) than when combining white mustard with intensive tillage and  $0.5 \text{ ton ha}^{-1}$  higher (or 2.2-2.4%) in comparison with the winter rye treatment, irrespective of tillage method.

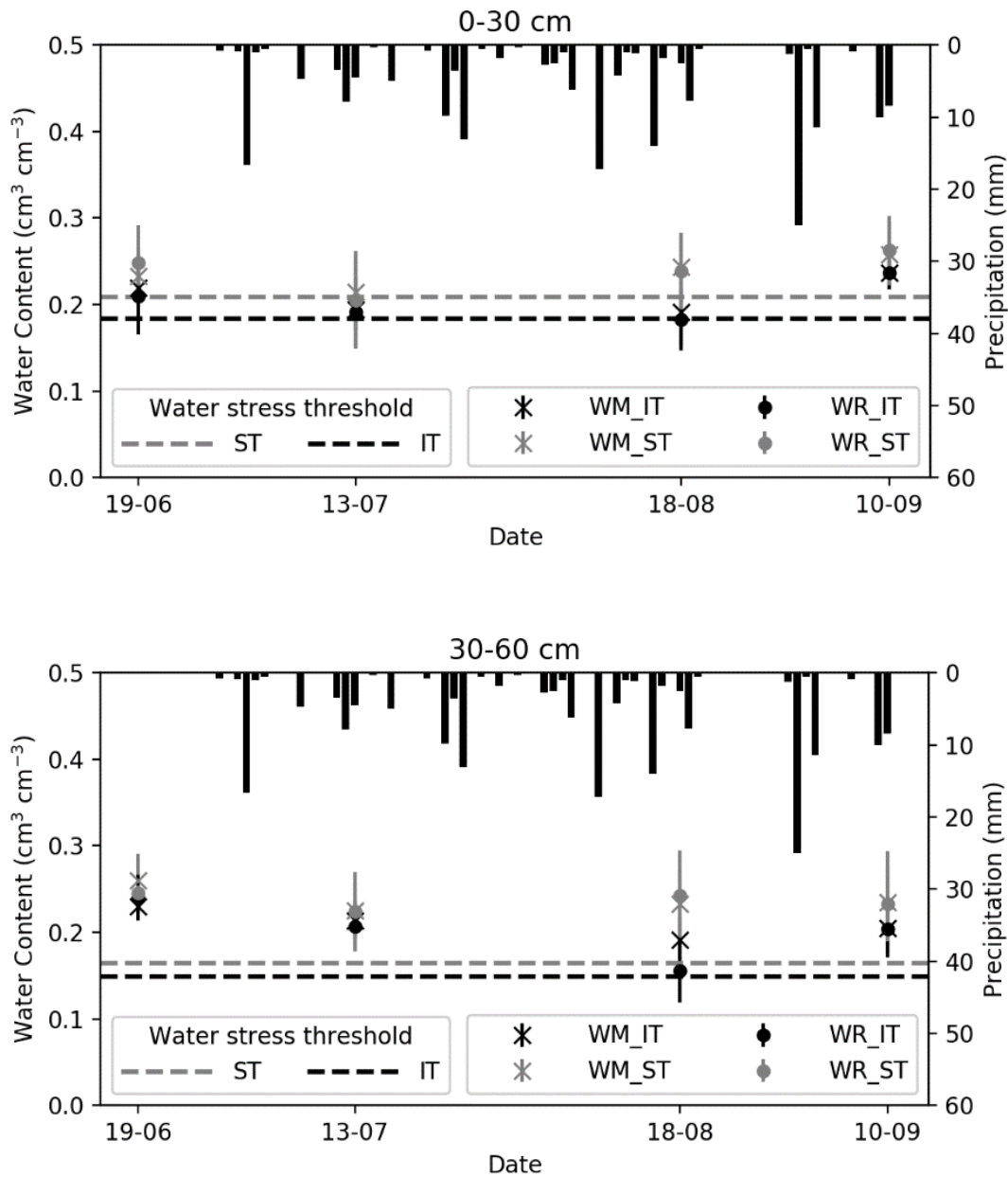


Fig. 5-9. Volumetric soil-water content variability (symbols) and precipitation (black bars) at out-row positions in the growing season (WR= winter rye; WM = white mustard; IT = intensive tillage; ST = strip tillage). The error bars are standard deviation ( $n=3$ ). The dark and gray horizontal lines represent maize water stress threshold at -60 kPa matric potential (Wesseling *et al.* 1991).

Table 5-4. Above-ground dry maize biomass (WR= winter rye; WM = white mustard; IT = intensive tillage; ST = strip tillage).

	Variance	Dry Biomass (kg/ha)	Standard deviation	Sample number
Cover Crop	WM	23,374	663	6
	WR	23,005	650	6
Tillage	IT	23,104	777	6
	ST	23,276	568	6
Cover Crop	WM_IT	23,222	780	3
×	WM_ST	23,527	647	3
Tillage	WR_IT	22,986	926	3
	WR_ST	23,025	445	3
----- Statistical analysis; P values				
Cover crop	0.17			
Tillage	0.78			
Cover crop x tillage	0.11			

#### 5.4. Discussion

With different root types, root number density distribution was significantly different within the soil profile. Fibrous-rooted cover crops (winter rye) showed higher root numbers than tap-rooted cover crops (white mustard) in loosened topsoil, whereas fibrous roots decreased severely in the compacted subsoil. Chen and Weil (2011) advocated that roots with greater diameter display better penetration of compacted soil because of higher axial root growth pressure, greater potential to relieve peak friction stress at the soil-root tip interface, less overall friction, and less tendency for lateral deflection or buckling. However, no roots were detected below 45 cm depth for

both cover crops, even though both roots can potentially reach more than 1 m in unrestricted field conditions (Clark 2008; Hodgkinson *et al.* 2017). Da Silva *et al.* (1994) suggested a limiting penetration resistance value of 2 MPa for crop growth, whereas in this study penetration resistance was larger than 4 MPa in the plough pan. The soil water content was still larger than the crop water stress limitation during winter and nutrients were sufficiently available in the top layer, which could also have contributed to restricted root deepening (Lynch 1995).

In the summer season, maize roots distribution was affected by the previous cover crops. Maize roots number density was significantly larger under the white mustard than under the winter rye treatment at 30-40 cm depth. This was consistent with the root number density distribution for the cover crops, showing that winter rye did not grow deeper than 30 cm, in contrast with white mustard that penetrated till nearly 40 cm (Fig. 5-3). Likewise, while in the winter rye treatment maize roots did not penetrate deeper than 30 cm, they reached almost 40 cm after white mustard. It might indicate that root channels left by tap-rooted cover crops grown in winter benefit summer maize root growth. Similar results were reported by Williams and Weil (2004) and (Chen and Weil 2011) on sandy loams in Maryland, USA. Recently, Colombi *et al.* (2017a) found that, using X-ray computed tomography analysis, roots of different crops preferentially grow in artificial pores because of lower resistance and higher oxygen content.

There was no significant difference in soil physical properties between the two cover crops (Fig. 5-6a, Fig. 5-7 and Fig.5-8). Similar findings were reported under different soil and weather conditions (Chan and Heenan 1996; Jokela *et al.* 2009; Chen and Weil 2011). Possible reasons could be: 1) the cover crops' root channels were too small to change the gross bulk density and the conical tip of the penetrometer was too wide in comparison with the root channel diameter, which made it impossible

to detect penetration resistance differences between cover crop treatments; 2) in field experiments soil spatial variability cannot be avoided with variances being too large to obliterate the small one year root effects. The latter is confirmed by our bulk density readings at 55 cm depth, where, though our treatments should not have affected soil properties at that depth, the white mustard-intensive tillage combination showed a higher but not significantly different bulk density than the other treatments. Additionally, Chan and Heenan (1996) and Jokela *et al.* (2009) suggested that soil physical quality indicators like the ones used in this study might only be detectable after more than four years of continuous cover crop growth.

Maize root distribution was restricted to tilled rows under strip tillage in contrast with intensive tillage which showed an even spread in roots. This is in agreement with findings of Laufer and Koch (2017) who did not find differences in fibrous root length density at in-row positions between intensive tillage and strip tillage but found higher fibrous roots under intensive tillage at out-row positions on a silt loam soil for the top 35 cm, in central Europe. This was closely related to soil physical properties because soil was denser compared with intensive tillage in out-row position at the top layer. When soil is compacted, macroporosity decreases but mesoporosity can increase (Hillel 1998). A similar soil pore size distribution trend was reported by Głąb (2014) in field experiments on a sandy loam soil under different compaction levels from 0 to 6 passes with a tractor. As a result, root growth could be limited by soil aeration under strip tillage.

Both cover crops and strip tillage did not significantly affect maize above ground biomass (Table 5-4). This could be due to water and nutrition supply being sufficient in the top layer. The applied fertilizer was sufficient for maize growth in this season, as it was based on recommended values for this area (De Haan 2013) and very close to

the legally restricted N and P fertilization recommendations in Flanders. Besides, soil-water content was also above the maize water stress threshold (Wesseling *et al.* 1991). Encouraging is that strip tillage, which is more environment-friendly than intensive mouldboard-based tillage owing to its lower energy consumption and its erosion-controlling performance, did not result in a lower biomass production. In contrast, when combining strip tillage with white mustard as cover crop, an increase of 2.4% was observed in comparison with the winter rye and traditional intensive tillage combination. Both strip tillage observations, i.e., an equal maize biomass production when combined with winter rye and a trend for increasing production with white mustard are very important in motivating farmers to consider a switch to strip tillage, at least under this study area. The message this study conveys is that strip tillage does not necessarily affect maize production negatively, as is often believed by farmers in this area. Regarding strip tillage, this is a promising result, since in the meta-regression analysis of no and reduced tillage in Europe, Van den Putte *et al.* (2010) reported a yield reduction in maize under both dry and wet conditions compared with conventional tillage, and particularly under wetter climates such as in this study area. Anyway, strip tillage did not lead to lower biomass yield and might be a relevant alternative to reduced tillage (or non-inversion tillage), particularly when sustainability is a concern.

## 5.5. Conclusions

This short-term field experiment shows that after one winter season, white mustard roots had a higher ability to penetrate compacted subsoil layers compared with winter rye. Consequently, maize root penetration was significantly deeper and its root number density at 30-40 cm depth was larger following white mustard than following winter

rye. Therefore, to alleviate soil compaction, white mustard should be a better choice than winter rye. However, one season of cover crop growth was not enough to find detectable changes in soil physical properties in the subsequent maize growth season.

Secondly, strip tillage was sufficient to temporarily loosen topsoil in crop rows: above-ground maize biomass was not significantly different between strip tillage and intensive tillage, though the out-row soil physical quality in the top 30 cm was slightly lower under strip tillage, which restricted maize root distribution. Within the maize growing season, soil moisture under strip tillage was higher than under intensive tillage, though it remained above the drought stress threshold in both tillage practices under the prevailing weather conditions. A trend was observed for an increase in maize biomass under a strip tillage with compaction-alleviating white mustard combination. Overall, the short-term results show that at least in the short term and under lower than normal precipitation in winter and spring (for the study area), strip tillage is suitable in the study area for maize production after intensive tillage in the previous year. Given the projected drier conditions in winter and spring in this Western European study area resulting from climate change, strip tillage is an alternative to intensive mouldboard-based ploughing worth the consideration.

## **Chapter 6: Impact of potential bio-subsoilers on pore network of a severely compacted subsoil**

This chapter is based on:

Mansonia Pulido-Moncada, Sheela Katuwal, Lidong Ren, Wim Cornelis, Lars Munkholm (2020). Impact of potential bio-subsoilers on pore network of a severely compacted subsoil. *Geoderma*, 363, 114154



## 6.1. Introduction

Soil compaction due to heavy vehicular traffic in wet conditions is one of the degradation problems in agricultural soils that severely affects crop growth due to its adverse effects on soil structure-related properties (Arvidsson 2001; Lipiec and Hatano 2003; Arvidsson and Håkansson 2014). Soil compaction reduces pore volume, and causes disruption of pore characteristics that affects water and gas flow, as well as increases soil density and soil penetration resistance, which together contribute to a reduction on plant root ability, among others effects (Materechera *et al.* 1991). The effects of soil compaction on soil characteristics have been found to be persistent, especially in the subsoil below tillage depth (Berisso *et al.* 2013a; Etana *et al.* 2013).

Subsoil compaction, therefore, is a severe problem because it hampers agricultural production and impacts the environment (Jones *et al.* 2003), but also because its natural recovery rate is slow (Munkholm *et al.* 2005).

Subsoil compaction mitigation can be initiated by anthropogenic mechanisms (e.g., mechanical loosening), as well as natural mechanisms that involves abiotic (e.g., wetting-drying and freezing-thawing) or biotic (e.g., plant roots and earthworm activities) processes (Keller *et al.* 2017).

A challenge for biotic mechanisms in the soil structure recovery lies on the fact that the poor soil physical conditions prevailing in compacted subsoil layers limit root development (Materechera *et al.* 1991). However, crop response depends on differences between species in the ability of roots to overcome soil compaction or physical impedance by different mechanisms, e.g. growth pressure, elongation rate, thickness or diameter, radial swelling, root anchorage (Löfkvist 2005; Lynch and Wojciechowski 2015).

Deep-rooted crops with the potential to penetrate hard layers have been assessed and proposed as bio-subsoilers (Cresswell and Kirkegaard 1995; Löfkvist 2005; Chen and Weil 2010). The term bio-subsoilers here, refers to plants with root systems that have the potential to penetrate compacted soil layers and act as biotic mechanisms for soil compaction mitigation.

The changes in soil structure brought about by bio-subsoilers, commonly used as cover crops, are linked to the creation of fissures and biopores that can improve water movement and gas flow through the dense layers (Materechera *et al.* 1992), and these biopores, burrowing organisms, existing cracks and fissures can also be reused by subsequent crop roots (Chen and Weil 2011). The reuse of biopores allows roots to explore the compacted layer for nutrients and water (Cresswell and Kirkegaard 1995).

The potential of plant species to be used for compaction mitigation has been found to differ between monocotyledons (fibrous-rooted) and dicotyledons (tap-rooted) (Clark and Barraclough 1999; Chen and Weil 2010). The pattern of root growth of monocotyledonous plants, such as grasses, consists of seminal and adventitious roots growing from the basal nodes of the shoot with approximately uniform size along their length. In contrast, the dicotyledonous root system (e.g., brassicas) is characterised by a vertical growing taproot, derived from the radicle, and lateral roots of smaller diameter, with the taproot creating continuous biopores to deep layers (Löfkvist 2005).

The most common cover crops that have been assessed as potential bio-subsoilers are fodder radish (*Raphanus sativus* L.), lucerne (alfalfa) (*Medicago sativa* L.), tall fescue (*Festuca arundinacea* L.), rapeseed (*Brassica napus*, cultivar 'Essex'), rye (*Secale cereale* L.), canola (*Brassica rapa* L.) and English ryegrass (*Lolium perenne* L.) (Raper *et al.* 2000; Williams and Weil 2004; Weil and Kremen 2007; Celette *et al.* 2008; Chen *et al.* 2014). These cover crops were found to decrease bulk density and

penetration resistance and increase porosity, hydraulic conductivity, soil moisture and water-holding capacity down to 0.60 m depth (Materechera *et al.* 1992; Löfkvist 2005; Hubbard *et al.* 2013). However, the limited profitability, high cost of establishment, diseases and weed problems are some of the concerns associated with the above-mentioned cover crops compared with other widely used cover crops (Snapp *et al.* 2005).

The benefits from the use of bio-subsoilers for root growth, water and nutrient uptake, and yield of subsequent crops are expected to be time-, site- and crop type-dependent. Consequently, the changes induced by the bio-subsoilers to the standard soil physical parameters that are used as indicators for soil structure could be negligible at initial stages of soil compaction mitigation. Therefore, the most sensible approach to evaluating the existence of soil structural changes caused by root channels and any other type of biopores is the characterisation of the pore network (Cresswell and Kirkegaard 1995) and for this there is only limited information available on the effects of root development on soil pore characteristics in heavily compacted subsoil layers.

The non-destructive imaging techniques such as X-ray Computed Tomography (CT) allows visualisation of the spatial distribution of soil pores and the quantification of changes in pore characteristics (Głąb 2007; Luo *et al.* 2010). Therefore, the 3D geometrical characterisation of the soil pore network provides a better understanding of soil pore measurements and their relation with soil hydraulic functions, solute transport, preferential flow, water-soil-root interaction, and management practices (e.g., Carminati *et al.* 2009; Naveed *et al.* 2013; Katuwal *et al.* 2015c). Previous studies have used 3D image analysis techniques to evaluate the impact of soil compaction on soil functions (e.g., Lamandé *et al.* 2013b; Naveed *et al.* 2016) and root system

architecture (e.g., Zappala *et al.* 2013; Pfeifer *et al.* 2015). However, studies evaluating the effect of different plant species on soil compaction mitigation revealed by X-ray CT of large column samples are scarce.

This study evaluated the changes caused by different bio-subsoilers in the pore network of a severely compacted subsoil located in a humid northern European agricultural area. Geometrical soil pore characteristics were assessed and quantified at three different soil depths using a medical X-ray CT scanner. It was hypothesized that the selected crops, as bio-subsoilers, would affect soil pore network positively and differently by penetrating and loosening the severely compacted soil.

## **6.2. Materials and methods**

### **6.2.1 Soil samples**

Samples were taken from a sandy loam soil located at Aarslev site in Denmark (55°18'18"N, 10°26'52"E). Previous to the sampling, a compaction experiment with farm machinery traffic had been conducted over four consecutive years (2010-2013). A detailed description of this compaction experiment can be found in Schjønning *et al.* (2016). In the present study, the soil samples were taken from the treatment that caused the most severe compaction after traffic stress, labelled M8 (78 kN) in previous publications (Schjønning *et al.* 2016; Pulido-Moncada *et al.* 2019). Briefly, the M8 compaction treatment involved multiple passes (4-5) of a tractor and slurry trailer combination applying an 8 Mg wheel load on the middle and rear trailer axles. The experiment was conducted in spring with soil being close to field capacity. The tyre inflation pressure of the tractor was 150-300 kPa, and the mean ground pressure was 56-161 kPa.

The experimental traffic under the M8 treatment resulted in a high degree of compaction (101%) at 0.30 m depth, characterized by a high bulk density ( $1.77 \text{ Mg m}^{-3}$ ) and a reduction in pore volume (air-filled porosity of  $0.08 \text{ m}^3 \text{ m}^{-3}$ ) and gas flow (air permeability of  $2.3 \mu\text{m}^2$ ) as compared to the non-trafficked control (Pulido-Moncada *et al.* 2019).

More specifically, in the M8 plot that was selected for sampling in the present study, the soil was characterized by 4% of clay ( $< 2 \mu\text{m}$ ), 26% silt ( $2\text{-}63 \mu\text{m}$ ), 70% sand ( $63\text{-}2000 \mu\text{m}$ ) and 0.23% soil organic carbon content, respectively, a bulk density of  $1.72 \text{ Mg m}^{-3}$  and a total pore volume of  $0.35 \text{ m}^3 \text{ m}^{-3}$  at 0.30 m depth (data taken from block 1 of the dataset analyzed by Pulido-Moncada *et al.* (2019)).

From the selected M8 plot, soil samples ( $\varnothing = 0.20 \text{ m}$ ,  $h = 0.50 \text{ m}$ ) were randomly extracted in spring 2017 by driving aluminum cores vertically into the soil with the hydraulic press of a tractor. The soil samples were manually excavated and transported to the Foulum site ( $56^\circ 29' 06.5''\text{N}$ ,  $9^\circ 34' 56.7''\text{E}$ ), in Denmark.

### 6.2.2 Experimental treatments

In this study, fifteen soil samples were X-ray CT-scanned immediately after sampling. Afterwards, an experimental plot (about  $24 \text{ m}^2$ ) for installing the soil cores was prepared at the Foulum site by excavating the top 0.50 m soil in an area with a homogeneous subsoil layer in terms of texture (10.6, 26.0 and  $63.4 \text{ g } 100\text{g}^{-1}$  of clay, silt and sand, respectively) and bulk density (average of  $1.90 \text{ Mg m}^{-3}$ ). All the soil cores were placed vertically in the experimental plot with the bottom in contact with the subsoil at 0.50 m depth, the top level with the soil surface and with the space between the soil columns refilled with the excavated soil (Fig.6-1).



Fig.6-1. Installation of the soil samples collected from the Aarslev site at the experimental plot at the Foulum site with the bottom of the samples in contact with the subsoil at 0.50 m depth, and the top level with the soil surface. Samples were installed vertically and surrounded by loose refilled soil.

The experiment was established with treatments consisting of spring barley (*Hordeum vulgare* L.) as the reference and four potential bio-subsoilers, i.e., chicory (*Cichorium intybus*), lucerne (*Medicago sativa* L.), radish (*Raphanus sativus* L.) and tall fescue (*Festuca arundinacea* L.). Among them, barley and tall fescue are fibrous-rooted type while chicory, radish and lucerne are tap-rooted type. Each treatment was in three replicates, using a complete randomized design. The reference used in our research counts for the root system of spring barley in interaction with bioturbation and dry/wet cycles happening in the soil under study. Bioturbation and weathering were however common factors in our control as in the plant treatments.

Seeding in the soil cores was conducted in May 2017 with a seeding rate of 150, 3, 25, 10 and 12 kg ha<sup>-1</sup> for spring barley, chicory, lucerne, radish and tall fescue, respectively, following the common agricultural practice in Denmark. Fertilization took place after germination in June 2017 and in May 2018 with 140 kg N ha<sup>-1</sup>. The above-

ground biomass of all the plants was cut on 26 July 2017. The perennial species were additionally cut successively on 9 September and 17 October 2017. Radish was reseeded in August 2017, hence two growing periods of radish per year. In April 2018, spring barley and radish were sown for the second year.

### 6.2.3 Image acquisition and processing

In summer 2018, the 15 previously CT-scanned samples were excavated from the experimental plot and went under a second scanning event. The soil samples were scanned at field moisture content close to field capacity. For both scanning events, X-ray images were acquired using a medical scanner (Siemens Biograph 64 True Point, Siemens AG, Erlangen, Germany) at the Department of Nuclear Medicine & PET-Centre of Aarhus University Hospital, Aarhus, Denmark. The soil columns were oriented horizontally for each scan. The scanning was performed using a voltage of 140 kV, an exposure time of 1000 ms (exposure of 600 mAs), and an X-ray tube current of 270 mA. The reconstruction was carried out using the manufacturer's software, resulting in a stack of 12-bit images with a slice thickness of 0.6 mm and  $512 \times 512$  pixels per slice. This led to a voxel size of  $0.43 \times 0.43 \times 0.6$  mm in the reconstructed image.

The freeware software program ImageJ version 1.52h (Abràmoff *et al.* 2004) and the associated plugins were used for image processing and analyses. The procedure of image analyses involved alignment correction, filtering, segmentation, and measurements.

For each image stack, the alignment of the slices was corrected using the 'Untilt Stack' plugin (Cooper 2011) and the center of the soil column translated to the center

of the canvas to obtain identical horizontal planes for each column at both scanning events. The aligned images of the 0.50 m of the soil column were cropped to 0.40 m height and to a region of interest (ROI) of 0.16 m diameter to avoid the uneven top soil surface and artifacts near the cylinder wall.

A 3D median filter (radius = 2.0 voxels) and contrast enhancement with saturated pixels of 0.4% were used to reduce the noise in the image and improve the contrast. Image segmentation was conducted by the auto-local threshold algorithm of Phansalkar *et al.* (2011), with a radius of 7 and default values for other parameters set in ImageJ software (i.e.  $k = 0.25$  and  $r = 0.5$ ).

In the binary images obtained from segmentation, features made up of 1 voxel were removed to avoid classification of noise in further analysis. Therefore, the pore networks quantified in this study represent macropores equal to or larger than 0.86 mm in diameter. The segmented binary images were then visually inspected for artifacts that would result in an overestimation of macroporosity. Artifacts or artificial pores close to the cylinder wall were created during sampling by the displacement of stones. These stone artifacts were manually removed from the binary image by selecting a seed voxel within the artifact and using a region-growing algorithm in the 'MorphoLibJ' plugin (Legland *et al.* 2016) to obtain all the connected voxels representing the artifact. In instances where the artifact was connected to other visible macropores, erosion and dilation operations were carried out iteratively until the two were disconnected. ImageJ's image calculator tool was used for subtracting the artifacts from the binary images.

The CT-macropores segmented include both macropores and roots. In the chicory treatment, the roots were visible inside the pores (with higher grey level value than pores) and were not segmented as pores by the local thresholding algorithm of

Phansalkar *et al.* (2011). The segmentation of roots for the chicory treatment was achieved by thresholding the roots twice. First, a threshold based on visual inspection was applied and the roots were separated from the noisy segmented image using a region-growing algorithm in the 'MorphoLibJ' plugin (Legland *et al.* 2016). Then a dilation operation was applied and the foreground voxels were represented by their original grey values. To this image another threshold, which was obtained from the minimum point in the image histogram between the peaks for pores and roots, was applied to segment the roots only. The resulting segmented roots were then added to the segmented pores to obtain the CT-total macropores.

The binary images after correction for holes and including roots in the segmented images were further used for pore quantification and analysis.

#### **6.2.3.1 Image analyses**

The analyses of the CT-macropores were performed for three layers, i.e. 'Plough', 'Transition' and 'Compacted'. These layers correspond to soil depths of 0.10-0.25, 0.25-0.35 and 0.35-0.50 m. The three soil layers were distinguished based on the compactness of the soil with soil depth, which was assessed using the average grey values of each slice in the ROI. Higher average grey values of slices are associated with more compacted soils in the ROI.

CT-derived pore characterization analysis (Table 6-1) was conducted using ImageJ (Abràmoff *et al.* 2004) and associated plugins. CT-porosity distribution with depth, was achieved by calculating the CT-macroporosity value for each slice of the binary image of each sample. The 'BoneJ' plugin (Doubé *et al.* 2010) was used for quantification of CT-derived macropore characteristics such as pore density, the

number of pore clusters per unit volume; genus density or pore connectivity, the number of loops/redundant connection per unit volume (Vogel *et al.* 2010) and mean pore diameter, the volume-weighted average thickness of pores (Katuwal *et al.* 2015a) (Table 6-1).

Table 6-1. Description of the soil pore parameters quantified using a medical X-ray Computed Tomography scanner.

Parameter	Calculation	Unit
Macropore density	$\frac{\text{total number of macropores}}{\text{volume of the ROI}}$	Number m <sup>-3</sup>
Macroporosity	$\frac{\text{total volume of macropores}}{\text{volume of the ROI}}$	m <sup>3</sup> m <sup>-3</sup>
Macropore area density	$\frac{\text{area of macropores}}{\text{volume of the ROI}}$	m <sup>2</sup> m <sup>-3</sup>
Macropore Connectivity or genus density	$\frac{\text{genus}}{\text{volume of the ROI}}$  where the genus is the total number of redundant connections or loops in the pore space network contained in a soil column	Number m <sup>-3</sup>
Mean macropore diameter	$\sum_{i=1}^n \frac{d_i V_i}{V_i}$  where $d_i$ and $V_i$ are the diameter and volume of each macropore within the ROI	m
Macropore tortuosity	$\frac{\text{total macropore length}}{\text{total Euclidean distance}}$  where the total Euclidean distance is the total shortest distance between the ends of all macropores of the ROI	

ROI is the region of interest

A skeletonised 3D image for each soil layer was obtained and analyzed using the 'Skeletonize' BoneJ-Plugin and the 'Analyse Skeleton' BoneJ-Plugin (Doubé *et al.* 2010). Analyse Skeleton was applied with and without pruning and the results combined to correct the effect of the roughness of the pore walls (Katuwal *et al.* 2015b). Macropore branch number, total branch length and average tortuosity were derived from the output of the skeletonise 3D image analysis (Table 6-1).

Additionally, CT-derived pore size and shape distribution were determined for each soil layer. The pore size distribution was determined by CT-total pore volume at five different intervals: <1; 1–10; 10–100; 100–1000 and >1000 mm<sup>3</sup>, and by pore diameter at five different ranges: <1.5; 1.5–2.0; 2.0–2.5; 2.5–3.0 and > 3.0 mm. The diameter interval used here denotes an increase per unit voxel width. The macropore diameter range considered in this study is related to air and water movement in large pores (Lal and Shukla 2004).

For the pore shape classification, the axes indices suggested by Zingg in 1935 and referenced by Bullock *et al.* (1985) were calculated using the long (L), intermediate (I) and short (S) radius of the best-fit ellipsoid (Fig.6-2) obtained from the 'Particle Analyzer' BoneJ plugin (Doubé *et al.* 2010). The axes ratio indices are described in detail in Pires *et al.* (2019). Large values of I/L and S/I ratios classify pores as spheres and small values as a-circular-planar pores (Fig.6-2). The pores were classified as either equant (spherical), oblate (disk-shaped), tri-axial (bladed), prolate (rod-like) or non-classified, the last representing pores for which the software could not determine at least one of the axes.

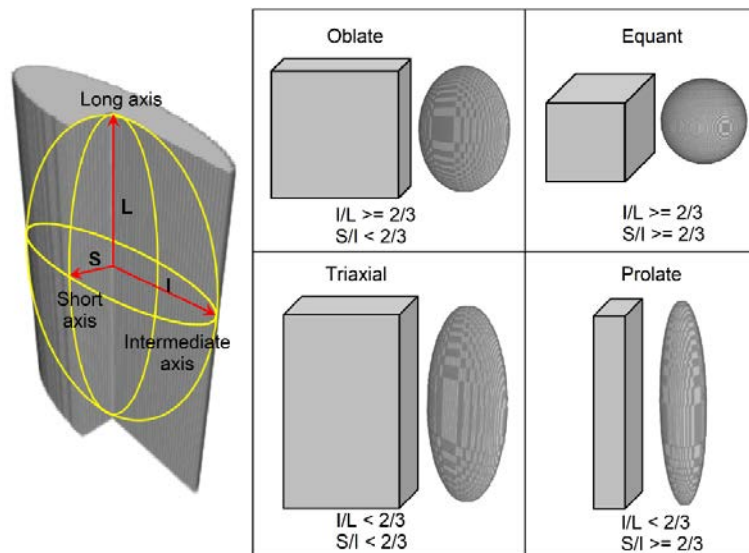


Fig.6-2. Illustration of the classification of soil pores based on shapes. The largest ellipsoid that can be fitted within a pore is measured for its diameters along the long axis (L), intermediate axis (I) and short axis (S) (left figure). The ratios between I/L and S/I are used for classifying the pores (right figures). (After Zingg diagram referenced by Bullock, 1985).

#### 6.2.4 Statistical analyses

The CT-derived pore characteristics were determined by detecting differences between barley (reference) and the potential bio-subsoilers at three different soil depths from 0.1 to 0.5 m. Because pore parameters were not normally distributed, the non-parametric Kruskal-Wallis test was used to test the effect of the plant treatments on the CT-derived pore characteristics, as well as on pore number and pore volume contribution for each size interval of the selected pore distribution. All tests were conducted at 5% significance level. The analyses were performed using the statistical package SPSS (version 24, SPSS Inc., USA).

### 6.3. Results

#### 6.3.1 Pore characteristics

The CT-derived pore characteristics are given in Table 6-2. Before the establishment of the plant treatments, there was a clear trend of decreasing macropore density with depth, e.g.: 27.4, 3.5 and 0.7 ( $\times 10^5$  number  $\text{m}^{-3}$ ) for Plough, Transition and Compacted layer, respectively. The same trend was obtained for CT-macroporosity with average values of 0.0747, 0.0179 and 0.0056  $\text{m}^3 \text{m}^{-3}$ , respectively with depth. The trend of decreasing values with depth also applied to area density, connectivity, branch number, total branch length and tortuosity, except for pore diameter which did not show apparent variation with depth.

Table 6-2. X-ray Computed Tomography (CT)-derived pore characteristics for a heavily compacted soil under potential bio-subsoilers. Median values are given for the samples before plant treatment and the absolute change one year after.

Note: Absolute change refers to the simple difference in the parameter over the two periods, i.e. Absolute change= value of the parameter one year after plant treatment – value of the parameter before plant treatment. The non-parametric test, Kruskal–Wallis, was used to test the effects of the potential bio-subsoilers on the absolute change of each CT-derived pore characteristic, considering 5% of significance level.

## Chapter 6

Soil layer	Treatment		Macropore density (x10 <sup>5</sup> ) (n <sub>o</sub> m <sup>-3</sup> )	Macro-porosity (m <sup>3</sup> m <sup>-3</sup> )	Area density (m <sup>2</sup> m <sup>-3</sup> )	Connectivity (x10 <sup>5</sup> ) (n <sub>o</sub> m <sup>-3</sup> )	Mean pore diameter (x10 <sup>-3</sup> ) (m)	Branches number	Total branch length (m)	Euclidean tortuosity
Plough (0.1-0.25 m)	Barley	Before	26.3	0.0543	77.5	2.60	2.38	7267	37.65	1.26
		Change	11.7	-0.0016 <i>ab</i>	-1.2	-0.89	-0.03 <i>ab</i>	-367	1.10	0.0004
	Chicory	Before	33.8	0.0815	101.6	6.12	2.45	9680	52.48	1.26
		Change	11.7	0.0007 <i>b</i>	-15.3	-3.47	1.51 <i>b</i>	-929	-11.29	-0.0937
	Lucerne	Before	38.7	0.1044	125.1	8.02	2.67	12499	68.50	1.26
		Change	-0.3	-0.0322 <i>a</i>	-26	-4.35	-0.20 <i>a</i>	-2338	-19.98	-0.0911
	Radish	Before	9.9	0.0378	48.7	1.69	2.29	3933	22.49	1.26
		Change	3.1	0.0001 <i>b</i>	1.8	-0.53	0.05 <i>b</i>	60	-0.14	-0.0126
	Tall fescue	Before	28.4	0.0956	121.2	5.63	2.73	11697	60.74	1.26
		Change	7.4	-0.0134 <i>ab</i>	-12.2	-2.86	-0.24 <i>a</i>	-2469	-10.78	-0.0022
p-value treatment effect for absolute change			0.261	0.045	0.086	0.115	0.015	0.116	0.086	0.087
Transition (0.25-0.35 m)	Barley	Before	1.9	0.0080	11.5	0.07	2.45	482	3.00	1.22
		Change	3.3	0.0039 <i>bc</i>	6.1	0.25	-0.06	571	3.07	0.0032
	Chicory	Before	1.7	0.0132	17.8	0.16	2.59	652	4.68	1.24
		Change	4.6	0.0054 <i>bc</i>	7.5	0.29	-0.07	1255	3.79	-0.0906
	Lucerne	Before	8.4	0.0390	50.3	1.74	2.59	2811	15.61	1.26
		Change	4.0	0.0060 <i>c</i>	11.9	0.18	-0.15	1652	4.83	-0.0784
	Radish	Before	0.6	0.0108	11.7	0.16	2.90	458	3.36	1.24
		Change	1.4	0.0033 <i>b</i>	6.1	0.27	-0.19	370	2.10	0.0166
	Tall fescue	Before	5.0	0.0186	24.2	0.38	2.67	1083	6.51	1.25
		Change	3.0	0.0007 <i>a</i>	1.1	0.02	-0.24	70	0.57	-0.0135
p-value treatment effect for absolute change			0.202	0.037	0.098	0.468	0.754	0.240	0.163	0.240
Compacted (0.35-0.50 m)	Barley	Before	0.4	0.0031	4.5	0.03	2.49	213	1.90	1.16
		Change	0.6 <i>a</i>	0.0019 <i>ab</i>	2.8 <i>ab</i>	0.10	-0.25	244 <i>a</i>	1.48 <i>ab</i>	0.0136
	Chicory	Before	0.5	0.0040	5.7	0.02	2.47	254	2.09	1.16
		Change	2.0 <i>b</i>	0.0029 <i>b</i>	4.4 <i>b</i>	0.09	-0.18	873 <i>b</i>	2.80 <i>bc</i>	-0.0378
	Lucerne	Before	0.9	0.0091	12.3	0.07	2.64	450	4.19	1.16
		Change	2.1 <i>b</i>	0.0043 <i>b</i>	7.2 <i>b</i>	0.29	-0.31	1418 <i>b</i>	4.69 <i>c</i>	-0.0120
	Radish	Before	0.6	0.0043	6.1	0.04	2.46	293	2.31	1.17
		Change	0.5 <i>a</i>	0.0006 <i>a</i>	1.8 <i>a</i>	-0.01	-0.03	100 <i>a</i>	0.76 <i>a</i>	-0.0015
	Tall fescue	Before	1.1	0.0072	10.2	0.03	2.57	354	3.76	1.16
		Change	1.0 <i>ab</i>	0.0013 <i>a</i>	1.8 <i>a</i>	0.02	-0.12	129 <i>a</i>	0.84 <i>a</i>	-0.0111
p-value treatment effect for absolute change			0.019	0.029	0.032	0.060	0.359	0.050	0.027	0.161

The absolute change in macropore density expressed as a percentage change from the first scanning varied from 50 to 225% for the Transition layer and 86 to 399% for the Compacted layer. In the Compacted layer, this change was significantly different from barley only for chicory and lucerne ( $p = 0.019$ ). While increases in macroporosity varied among the potential subsoilers ( $p < 0.05$ ), they were not significantly larger than barley in any of the studied soil layers, except for tall fescue in the Transition layer. Fig.6-3 shows the variation of CT-macroporosity with depth for the crop treatments under study. CT-macroporosity varied markedly with depth down to ~0.30 m, whereas little variation occurred between 0.30 and 0.50 m.

Absolute changes in pore area density ranged from 1.1 to 11.9 and from 1.8 to 7.2  $\text{m}^2 \text{m}^{-3}$  for the Transition and Compacted layer, respectively, whereas changes in connectivity varied from 0.07 to 1.74 and 0.02 to 0.07 ( $\times 10^5$ ) number  $\text{m}^{-3}$  (Table 6-2). In the Compacted layer, increases in area density and connectivity among the potential bio-subsoilers did not differ significantly from barley.

In the Plough layer, the mean weighted pore diameter increased for chicory and radish compared to lucerne and tall fescue ( $p = 0.015$ ) but was not significantly different from that of barley. In both the Transition and Compacted layers, reduction in pore diameter was found for all the treatments, but differences were not significant ( $p > 0.10$ ).

No significant bio-subsoiler effect was found for branch number in the Plough and Transition layer. However, in the Plough layer branch number had a negative absolute change under the plant treatments, except for radish, but a positive absolute change in the Transition layer. Similar to pore density, a significant increase was observed in the number of branches under chicory and lucerne compared to barley ( $p = 0.050$ ) in the Compacted layer.

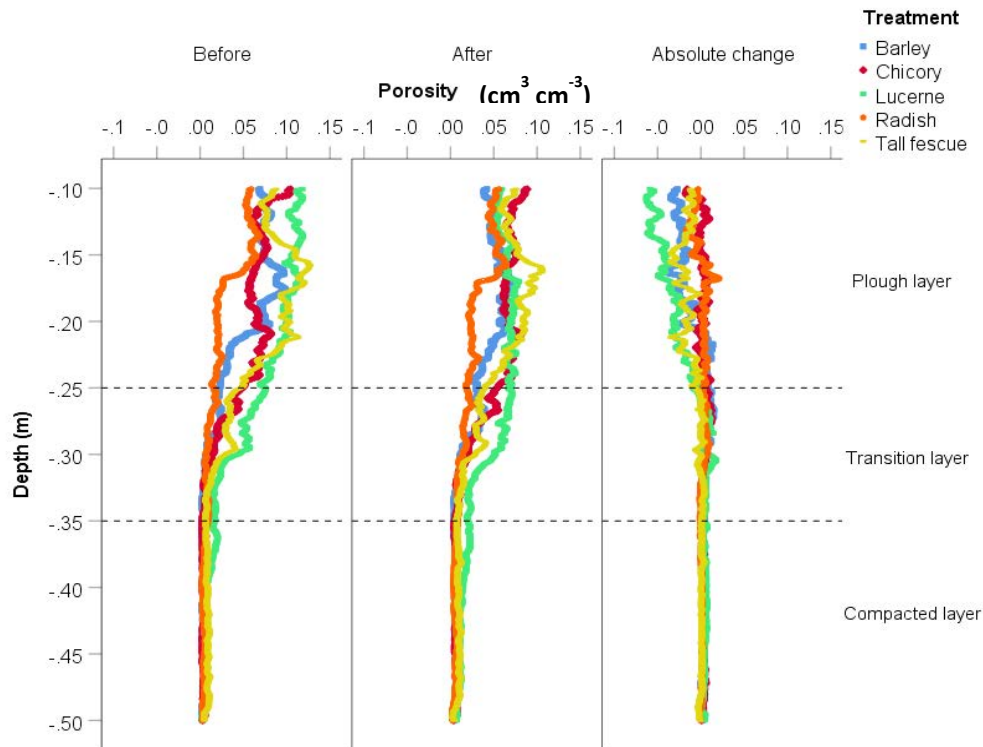


Fig.6-3. X-ray Computed Tomography-derived macroporosity distribution for heavily compacted samples Before plant treatment, one year After plant treatment, and the Absolute change in depth. Absolute change refers to the simple difference in the parameter over the two periods, i.e. Absolute change = value of the parameter one year after plant treatment – value of the parameter before plant treatment. Values shown are arithmetic means of three replicates.

The absolute change of total branch length decreased after one year in the Plough layer but increased in the Transition and Compacted layer. Increment in total branch length was significant for lucerne compared to barley, radish and tall fescue ( $p = 0.027$ ) in the Compacted layer.

The absolute change of Euclidean tortuosity was positive for barley but negative for the potential subsoilers in the three layers, although the difference to barley was not significant in any soil layer.

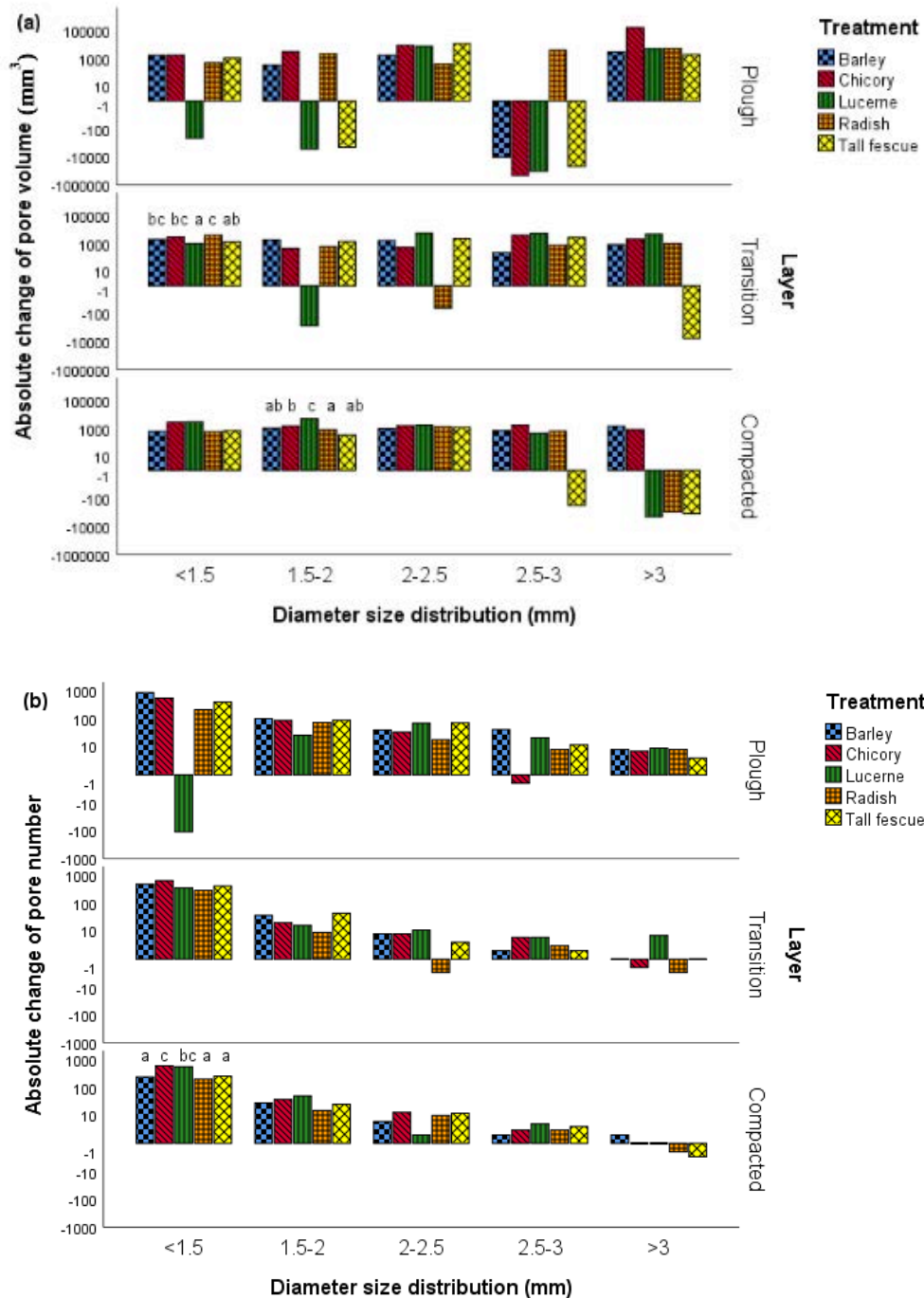
### 6.3.2 Pore size distribution

Figure 6-4a (Appendix Table A) illustrates the absolute change in pore volume as a function of pore size diameter. In the Plough layer, a trend of decreasing in the volume of pores for the size range of 2.5–3 mm for all the treatments, except for radish, was observed. There was a trend of chicory to have a larger change in pore volume for pores >3 mm in diameter compared to the other treatments in the Plough layer ( $p = 0.086$ ). In the Transition layer, lucerne had a smaller increase in pore volume for pores with a mean diameter of <1.5 mm compared to barley, chicory and radish ( $p = 0.050$ ). Lucerne reached the most substantial increase in pore volume for pores with a diameter of 1.5-2.0 mm ( $p = 0.046$ ) in the Compacted layer.

When pore number was grouped according to pore size diameter (Fig.6-4b, Appendix Table A), the biggest changes in the number of pores were observed for pores with diameter <2 mm in all layers. However, in the Plough layer the change in pore number for the different pore sizes did not significantly vary among crop treatments. In the Transition layer, chicory showed an increasing trend in the number of pores with diameter <1.5 ( $p = 0.055$ ) compared to lucerne, radish and tall fescue. There was, however, no significant difference to barley. There was also a trend that chicory or lucerne show larger change in pore number for pores <1.5 mm ( $p = 0.049$ ) and 1.5-2 mm ( $p = 0.098$ ) in diameter compared to barley in the Compacted layer.

The results in Fig.6-4c (Appendix Table B), where the absolute change in pore number is plotted as a function of pore volume intervals, indicate that differences among treatments were only significant ( $p \leq 0.05$ ) at the Transition and Compacted layers. Chicory had the largest absolute change in pore number in the Transition layer for pores 1-10 mm<sup>3</sup> and was significantly larger compared to lucerne and radish, but not significantly different from barley ( $p = 0.054$ ). For the Compacted layer, both

chicory and lucerne showed an increase in pore number (relative percentage between ~60-150%) compared to barley for volume sizes of <1 ( $p = 0.050$ ), 10-100 ( $p = 0.035$ ) and 100-1000 ( $p = 0.033$ )  $\text{mm}^3$ . In none of the soil layers did radish and tall fescue differ significantly from barley at the mentioned volume intervals.



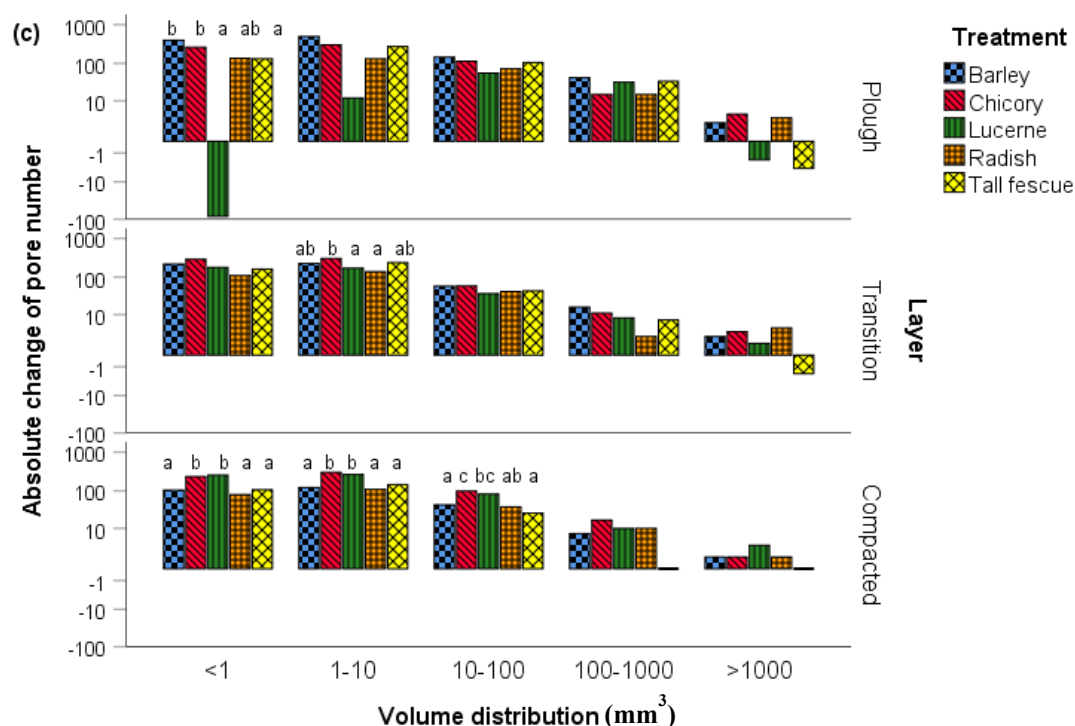
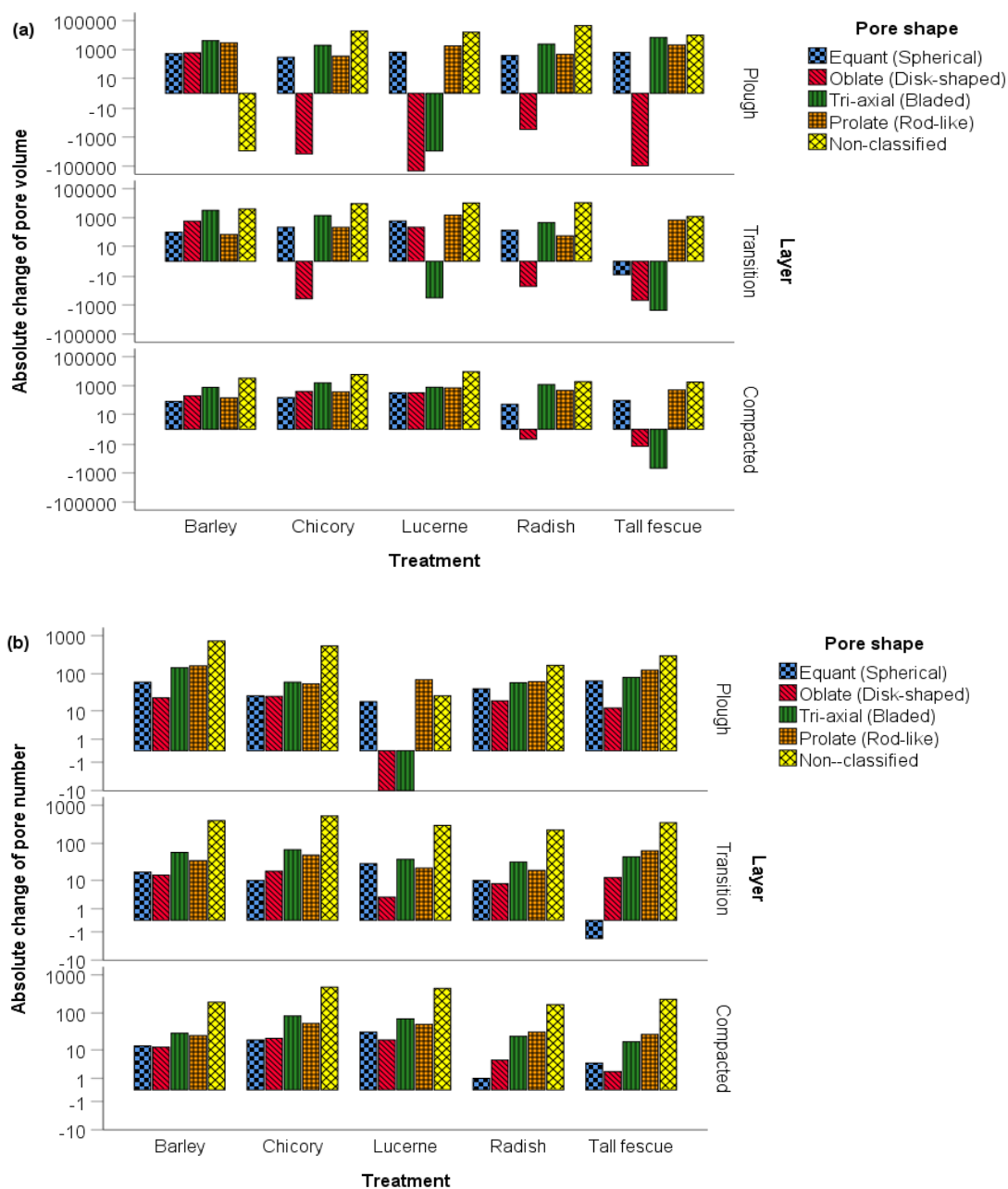


Fig.6-4. Distribution of pore volume (a) and pore number (b) as a function of diameter size intervals and the distribution of number of macropores (c) as a function of volume intervals. Pore parameters were quantified using a medical X-ray Computed Tomography scanner. Plough, Transition and Compacted layer depths are 0.10-0.25, 0.25-0.35 and 0.35-0.50 m, respectively. Absolute change refers to the simple difference in the parameter over the two periods, i.e. Absolute change= (value of the parameter one year after plant treatment – value of the parameter before plant treatment). The non-parametric test, Kruskal–Wallis, was used to test the effects of the potential biological subsoilers on the absolute change of each size interval, considering 5% of significance level.

### 6.3.3 Pore shape classification

In the Plough layer, there were evident trends in pore shape changes (Fig.6-5, Appendix Table C). After one year under crop treatment, barley showed a decrease

in the volume of non-classified pores, however, increased in number and showed no significant change in mean diameter. For chicory, radish and tall fescue, trends of increases in pore volume, number and diameter were displayed for non-classified pores. For these three crops there was a large reduction in volume with an increase in quantity for oblate pores. Whereas for lucerne, oblate and tri-axial pores decreased in volume, number and diameter.



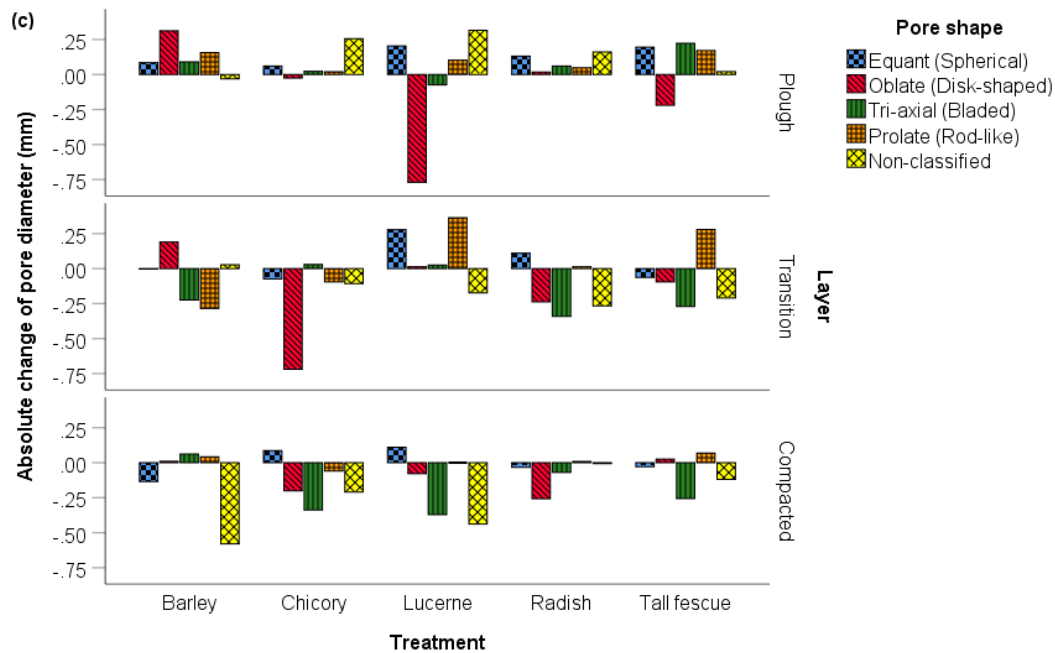


Fig.6-5. Distribution of the absolute change of macropore volume (a), number (b) and diameter (c) as a function of pore shape. Pore parameters were quantified using a medical X-ray Computed Tomography scanner. Plough, Transition and Compacted layer depths are 0.10-0.25, 0.25-0.35 and 0.35-0.50 m, respectively. Absolute change refers to the simple difference in the parameter over the two periods, i.e. Absolute change = value of the parameter one year after plant treatment – value of the parameter before plant treatment.

Non-classified pores dominated the increases in pore volume and number in the Transition layer for all the crop treatments. Oblate and tri-axial pores, however, showed general trend of a reduction in pore volume and diameter for the potential subsoilers. At the Transition layer equant and prolate pores increased in diameter for lucerne, but this was limited to prolate under tall fescue. The volume and number of prolate pores increased in all the layers in all the crop treatments.

For the Compacted layer, there was a clear trend of a larger increase in pore number of non-classified pores for the chicory and lucerne treatment, but in terms of

pore volume this did not seem to differ widely from the other plant treatments. Oblate pores for radish and tall fescue, but also tri-axial for tall fescue, showed a lower contribution to pore volume but increase in number after one year. In this dense layer, the largest reduction in pore diameter of non-classified pores was for soil under barley. Chicory and lucerne showed a decrease in diameter for all pore shapes, except equant, which increased slightly after one year of the experiment.

## **6.4. Discussion**

### **6.4.1 Effect of potential bio-subsoilers on pore network**

A decline in pore network density with depth was visualized and quantified using the CT images of the samples before the establishment of the experiment. The variation of CT-macroporosity with depth in Fig.6-3 supports the partitioning of the soil columns into three representative layers of the structural difference with depth, e.g., loose structure (0.1-0.25 m), transitioning state (0.25-0.35 m) and dense structure (0.35-0.50 m). Although the CT-macroporosity distribution with depth was very similar for all the crop treatments, the second scan event revealed changes in pore network that differed among plant treatments and attributed to root development.

In the Plough layer changes in pore network (decrease in CT-macroporosity, area density, connectivity and branch length) are related to soil consolidation by settling, wetting and drying cycles and root growth compression (Koestel and Schlüter 2019). Beneath this top layer, changes are expected to result from the roots attempting to penetrate the hard layer (Lamandé *et al.* 2013b). Our results (Fig.6-4) show evidence of several pores of small volume and diameter in the Transition layer and especially in the Compacted layer, which is an important initial state in the mitigation of

compaction. It is worth noting that the average pore diameters were reduced for all the treatments in both the Transition and Compacted layers (Table 6-2). This can be attributed to the increase in the density of small pores, i.e., pores with small diameter and volume resulting in a reduction in the mean pore diameter, which in turn may be associated with the development of fine roots for one year.

Interestingly, the vertical cross-section (Fig.6-6) displayed soil cracking and an apparent increase in macropore volume in the Transition layer (0.25-0.35 m depth) after the plant growing. Positive effects of cover crops in the transition between the top and the hard layer have been reported by previous studies (Abdollahi *et al.* 2014). In the Compacted layer (0.35-0.50 m), the pore number under chicory and lucerne was, respectively, 110 and 81% higher than the initial pore number. This represents 2.1 and 1.6 times the increase found for barley. The significant increase in CT-macropore density, branch number and total branch length produced by chicory and lucerne in the Compacted layer implies the development of a larger, more connected and complex pore network than the pre-existing one. According to Munkholm *et al.* (2012), this implies an increased likelihood of crack propagation and interaction in the soil if stressed in tension mode. In the Compacted layer, cracks, fissures or biopores are visible in the vertical cross-sections of representative samples (Fig.6-6), especially for soil columns under chicory and lucerne.

Radish and tall fescue did not show a statistically significant trend for increasing pore network density. However, a few visible cracks were formed one year after the initiation of the experiment (Fig.6-6), which can also be attributed to root pressure or to wetting and drying.

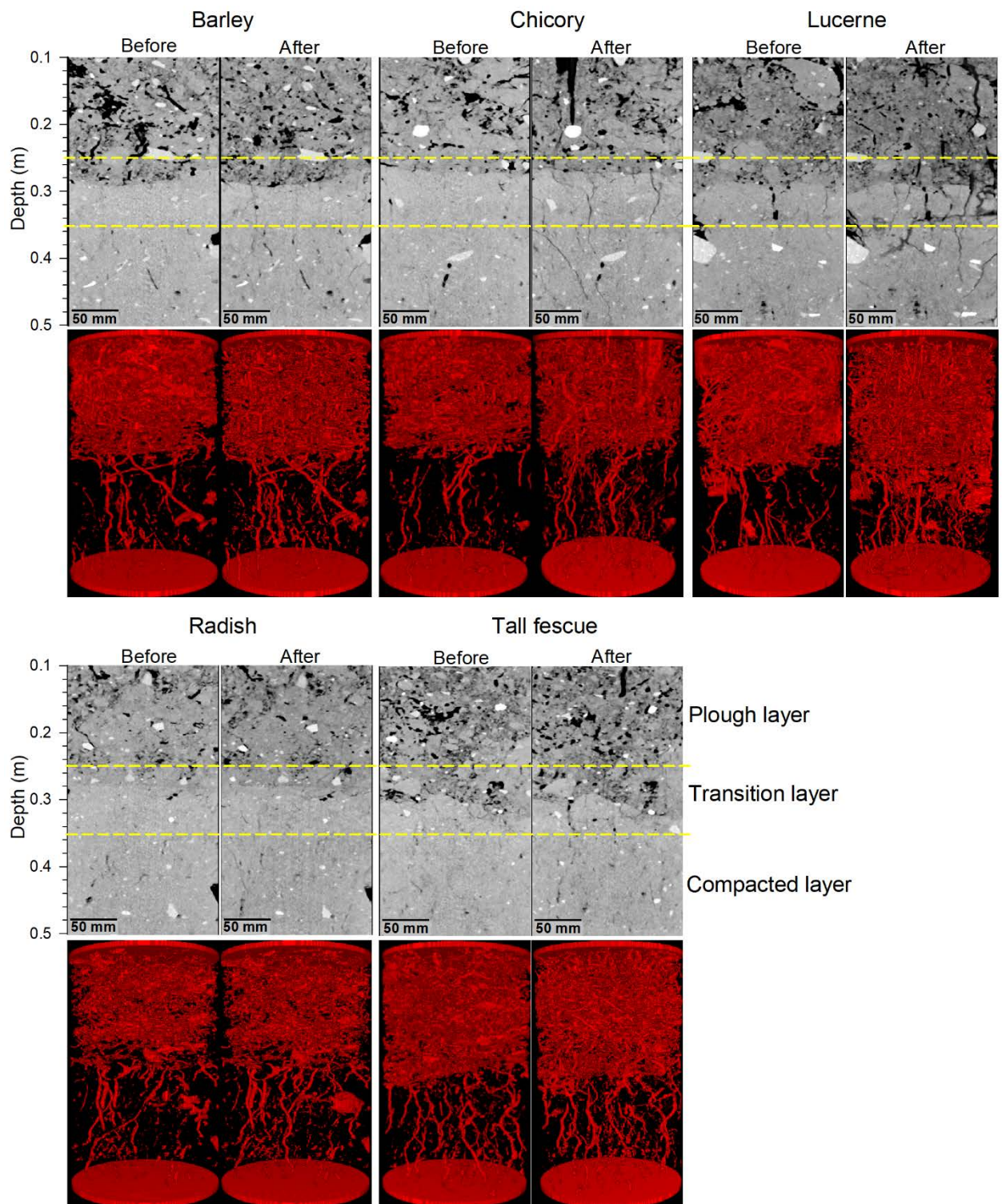


Fig.6-6. Grey images of vertical cross-sections for representative samples from each plant treatment, before and after 1 year under potential bio-subsoilers. Below each grey images are the respective 3-D renderings of the pores analyzed in this study.

Regarding connectivity, there was no significant effect of the potential bio-subsoilers. Results from Pires *et al.* (2017) suggest that high connectivity is related to the larger contribution of macropores  $>1000 \text{ mm}^3$  to CT-macroporosity. The relatively large increase in number and volume of small disconnected pores compared to the large pores in all the treatments was observed. This suggests that the effectiveness of different bio-subsoilers in altering more complex properties related to soil structure such as connectivity of macropores are not clear within a year of crop growth. Possibly, most of the effect of the bio-subsoilers are occurring for pores smaller than those resolved and quantified in this study.

In this study, changes in tortuosity with depth and among plant treatments were negligible. For the Compacted layer, this may be explained by an incipient root system after one year of growing the different crops. As illustrated by Hu *et al.* (2015), high porosity and tortuosity may be associated with well-developed root systems. However, it is worth noting that our results refer to an average value for tortuosity of large CT-pores, and which is influenced by small pores that are usually large in number but have very low tortuosity values (close to 1).

Pires *et al.* (2017) suggest that increases in tortuosity with depth and number of pores favour the formation of pores of irregular shape. In the present study, non-classified pores had the highest increase in number after one year of the experiment. This indicates an increase in complexity of the pore networks with more interconnected pores. For chicory and lucerne it is worth noting that 3D tri-axial and prolate pore shapes also contributed to the number of pores created, which tended to constitute a larger proportion than for barley and other plant treatments. According to Luo *et al.* (2010), macropores formed by roots are highly continuous, round in shape, and decrease in size with depth.

The 3D renderings of the pores analyzed from the whole soil columns shown in Fig.6-6 reveal elongated and continuous, large macropores that are visible in the Compacted layer before crop treatment. These macropores could be biopores that are not affected by traffic stress (Schäffer *et al.* 2008) and that are maintained by earthworms or persist after the decay of former large roots (Kautz 2015). They may also have been formed after compaction, as earthworm burrowing is possible in dense soils if not too dry (Whalley *et al.* 1995). As mentioned previously, one year after initiation of the experiment, the number of pores in the Compacted layer was mainly dominated by pores  $< 100 \text{ mm}^3$  (Fig.6-4c). Additionally, a few pores  $> 1000 \text{ mm}^3$  with diameter  $> 2.5 \text{ mm}$  were formed (ranging from two to four in the plant treatments), which most probably represent new earthworm burrows (Luo *et al.* 2010).

In Fig.6-6, the 3D images of the soil columns show small, randomly distributed and less continuously distributed macropores after plant growth. The formation of new biopores and the related cracks in hard layers would likely enhance pore connectivity with time, which consequently improves root exploration even in soils with dense, hard layers, especially in drier years (Galdos *et al.* 2019).

#### **6.4.2 Role of plant/root type in compaction mitigation**

The studied potential bio-subsoilers differed in their impact on the soil pore characteristics in the Compacted subsoil layer. The most common taproot cover crops assessed as potential bio-subsoilers are the brassicas (e.g., Chen and Weil 2010; Abdollahi *et al.* 2014; Gruver *et al.* 2014; Guaman *et al.* 2016). Chen and Weil (2010) showed that fodder radish had greater penetration capability and root number than rye and rapeseed on compacted, fine loamy soils. The authors attributed the root

penetration capacity of fodder radish through hard layers to its root architecture, i.e., a single, dominant, cylindrically-shaped, fleshy taproot with thick branch roots and dense fine rooting with depth. Abdollahi and Munkholm (2014) found that five consecutive years of forage radish on a sandy loam soil favoured mitigation of soil compaction (decreased penetration resistance) at 0.3-0.6 m depth.

However, in our study radish did not show a significantly different impact on the pore network compared with the reference barley for severely compacted subsoil. This is in agreement with Guamán Sarango (2015) who found no apparent mitigation effect of fodder radish in compacted soil with 3 MPa of penetration resistance at 0.3-0.6 m depth. The authors hypothesized that the full potential of the crop was not realized due to the short growing period of two years.

Our results show that for the CT-pore parameters quantified, tall fescue had a similar effect to radish and barley on the CT-porosity of the Compacted layer. Conversely, the root systems of chicory and lucerne positively affected CT- porosity at 0.3-0.5 m depth.

A root characterisation study conducted by Gentile *et al.* (2003) of, respectively, 2, 3 and 11 years of growing tall fescue, chicory and lucerne in a silty clay loam soil showed that tall fescue and chicory had a large number of root axes and root biomass at 0.2-0.3 m depth whereas lucerne had a greater number of root axes and root branching at 0.2-0.6 m depth. Tall fescue is characterised, like most grasses, by having a fibrous root system with a very small diameter that remains relatively constant with soil depth, while lucerne and chicory are taproot crops with larger root diameter that varies with depth (Gentile *et al.* 2003; Han *et al.* 2015). The root diameter was given by Perkons *et al.* (2014) as the reason for the greater number of large-sized

biopores per unit surface area up to 0.65 m depth after chicory compared to tall fescue in a Luvisol in Germany.

Even though root characterisation was not the scope of our study, the differences in terms of root density, root branching and root diameter among the cover crops under study would appear to explain the dissimilarities in how they function as bio-subsoilers. It is worth noting that crop density could also play an essential role in the results obtained. For instance, lucerne with its higher crop density resulted in a larger number of biopores than chicory in a Luvisol in Germany (Han *et al.* 2015). In our study, the ranking in decreasing order of crop density was lucerne > tall fescue > barley > chicory > radish. It is important to note that radish is an annual crop with a fine root diameter at depth and low crop density, while the perennial crops such as chicory and lucerne can develop more extensive root systems over time (Gentile *et al.* 2003), which is expected to provide a greater potential as bio-subsoiler in the subsoil.

The fact that the root system of chicory and lucerne showed a greater ability to impact soil macroporosity in the Compacted layer after only one year as a cover crop is of high importance. Although CT-derived macroporosity (> 0.86 mm in diameter) was less than  $0.05 \text{ m}^3 \text{ m}^{-3}$  in the Compacted layer, chicory and lucerne increased CT-derived macroporosity by, respectively, 94 and 52% in relation to the initial porosity at the start of the experiment. Small increases in pore volume beyond a minimum rooting density had a strong effect on soil porosity (Bodner *et al.* 2014), which in time is anticipated to be of high importance in subsoil compaction mitigation.

## 6.5. Conclusion

CT-geometrical soil pore characteristics tested in this study differed for the five bio-subsoilers after one year of the experiment. In the Compacted layer, at 0.35-0.50 m depth, chicory and lucerne had a significant positive impact on porosity ( $> 0.86$  mm in diameter). Therefore, they can be expected to perform better than radish and tall fescue when used as a bio-subsoilers for compaction mitigation. In all cases, the Compacted layer showed small changes in pore system, suggesting that it was still very compact after one year of growing the different crops. I suggest longer-term studies of plant-induced mitigation of compacted subsoils involving different soil types and climate conditions. The changes in pore network found in this study are relevant, since even small increases in macroporosity and changes in pore network can potentially boost the dynamics or mitigation processes in deep compacted subsoils that take place over time.



#### **Part IV: Detection of soil compaction spatial variability**

**Chapter 7: Detecting spatial variability of soil compaction using soil apparent  
electrical conductivity and maize canopy height**

## 7.1. Introduction

Soil compaction is a worldwide threat to sustainable agriculture with more than one quarter of the soils being compacted in Europe alone (Schjønning *et al.* 2015). Compacted soil has various adverse effects on crop growth and environment, and unlike soil erosion or salinization, soil compaction does not have a clearly visible exposure and evident marks on the surface (Håkansson 2005; Keller *et al.* 2019). Correspondingly, many adverse effects caused by soil compaction are often blamed to other causes (Hamza and Anderson 2005).

Detecting soil compaction at field level is urgently needed as the traditional sampling methods are laborious, especially for subsoils, which greatly restricts soil survey resolution. In contrast, geophysical methods, like electromagnetic induction (EMI) measurements, are regarded as a promising option for upscaling soil properties and to increase the soil survey's resolution (Jury *et al.* 2011). This is because geophysical methods normally provide a non-invasively high-resolution investigation at short time and less labour cost. According to Archie's law (Archie 1942), soil apparent electrical conductivity (ECa) is closely related to soil clay content, moisture content and salinity. When soil becomes compacted, soil bulk density (BD) increases, resulting in more clay and water (under unsaturated condition) per unit volume of soil. As a result, the contact between soil particles increases, which could increase the ECa (Romero-Ruiz *et al.* 2018). Therefore, in theory it is possible to predict soil compaction from ECa. Many researchers have reported that increasing BD causes an increase of ECa or a decrease of electrical resistivity (Brevik and Fenton 2004; Keller *et al.* 2017; Romero-Ruiz *et al.* 2018). At a soil profile scale, electrical resistivity has been found to enable detecting traffic tracks (Besson *et al.* 2004; 2013). At field level, Hoefler *et*

*al.* (2010) found a strong relationship between ECa and soil mechanical strength expressed in terms of a stress-at-rest coefficient ( $K_0$ ; see Horn *et al.* (2007)), especially in areas with high penetration resistance (PR). On a coarse sand field, Al-Gaadi (2012) found ECa to be positively correlated with man-made compaction levels and their correlation decreased with increasing soil moisture content (below field capacity). In a puddled paddy rice field, Islam *et al.* (2014) found that ECa increased with increasing soil compaction levels under saturated soil water conditions. However, those site-specific results could only be found in case the soil properties (soil clay content, moisture content and salinity) were showing limited variation. For instance, Besson *et al.* (2004) found no clear correlation between soil compaction and ECa in a newly ploughed profile scale, where variation in soil properties was substantial.

Crop growth is closely related to soil properties and its spatial variability could reflect soil heterogeneity patterns. Soil compaction can restrict plant growth by restricting root growth (Andersen *et al.* 2013; Colombi *et al.* 2018). This restriction can be expected to be more serious in dry condition as deeper water cannot be accessed. According to Ren *et al.* (2019a), maize growth indicators (yield) showed a higher response to compaction-induced soil heterogeneity than traditional lab measured soil properties. This could mean that crop indicators could provide similar information as abiotic sensors. Besides, many studies have been conducted to investigate the relationship between ECa and crop growth. However, most of them focus on crop yield and illustrate that the relationship between ECa and crop yield is not consistent. Stadler *et al.* (2015) found that crop height was better correlated with ECa than crop dry matter and leaf area index (LAI), but variable relationships were observed between fields, years and crops. The most obvious difference of maize height among locations was found at LAI maximum stage, especially in dry years. Besides this, the authors

indicated that the relationships between crop growth and soil characteristics are more complex and further investigation is needed.

Overall, it was hypothesised that ECa and maize canopy height could be suitable indicators of soil compaction patterns at field level when inherent soil properties and moisture content are not very variable. The specific objectives of this study are: 1) to evaluate the correlation between soil compaction related soil properties, and ECa of a loam soil and maize canopy height; 2) to evaluate the correlation of ECa and maize canopy height in an exceptionally dry year of 2018.

## **7.2. Materials and methods**

### **7.2.1 Study site**

The VRV field was used for this study. In 2018, a combination of tractor and slurry spreader (maximum wheel load ca. 5 Mg) was used to add manure after clipping the winter rye. The recommended pressure in the slurry spreader tires was used (100 kPa) for carrying out activities on the field. After the slurry was applied and incorporated into the soil by means of a cultivator (10-15 cm depth), a conventional mouldboard plough was used for in-furrow ploughing (till 30 cm depth), followed by seedbed preparation with a rotary harrow (8 cm depth). The next day, maize was sown (with 75 cm interrow spacing,  $10^5$  seeds  $\text{ha}^{-1}$ , and 6 cm sowing depth) in the same direction as the previous traffic tracks.

### **7.2.2 ECa measurements and analysis**

The field was scanned twice using EMI with a DUALEM-21S sensor on 04/04/2017 and on 27/03/2018 during the winter rye growing season. Where the first scanning was used for selecting sampling locations, the second one was used for further analysis. The ECa was measured at 2 m intervals between the measurement lines, with an in-line sampling resolution of ~0.2 m. Details about the DUALEM-21S sensor can be found in De Smedt (2013). In this study, ECa values abstained to 3 m depth and were inverted to vertical ECa values for 25 cm depth intervals for further analysis. Here, as the maize roots were mostly not growing deeper than 50 cm and soil properties were different between the 0-25 cm and 25-50 cm layer, only the 0-25 cm and 25-50 cm layers were used for further analysis.

Surfer® 13 (Golden Software, LLC) was used for interpolation and filtering. The nature neighbour interpolation method (Sibson 1981) was used to interpolate the inversed ECa data, with a 0.5 by 0.5 m grid. The non-linear median filter method (the output grid node value equals the fifty percentile of the neighbouring values) was applied to remove extreme values, with a filter size of 5 m<sup>2</sup>.

### **7.2.3 Soil sampling strategy**

Soil sampling was based on the first ECa scanning results of 0-25 cm and 25-50 cm layer. Ten locations (Fig.7-1) were selected according to a conditioned Latin hypercube sampling method (LHS) (Minasny and McBratney 2006), to sample the entire range of ECa variability recorded across the field, equally taking into account differences in elevation.

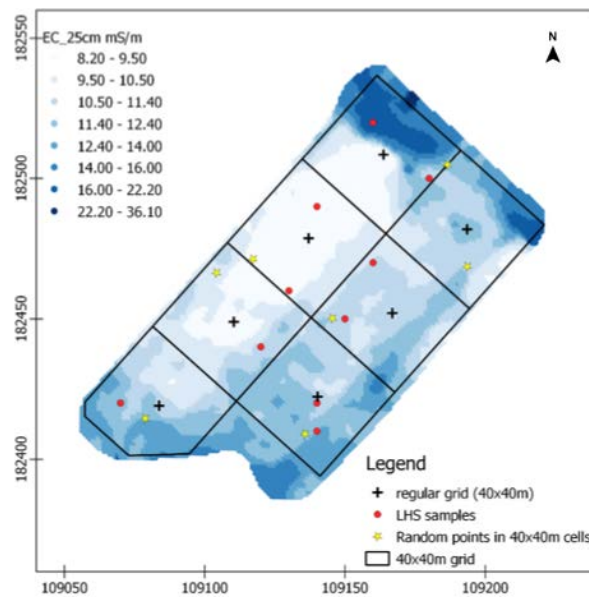


Fig. 7-1. Sampling locations according to the first ECa scanning results; 10 locations are based on LHS is (conditioned) Latin hypercube sampling, 7 on a regular grid and 7 on random positions within the regular grid.

In those 10 sampling locations, Kopecky ring samples were taken at 5, 10, 25, 35, 50 cm depth, immediately after the second EMI scanning. Soil gravimetric water content and BD were measured for all samples, while soil texture, carbon content and soil salinity were only measured for 10 and 50 cm samples (one sample lost at 10 cm depth). Soil texture and soil organic carbon were determined with the sieve-pipette method (Gee and Bauder 1986) and Walkley and Black (1934), respectively. Soil texture was classified by the USDA method and shown in Fig.7- 2a. Soil salinity (ECs) was determined by measuring the electrical conductivity (Orion™ Dura Probe™ 4-Electrode Conductivity cell 012210) of a soil solution with a soil/water ratio of 1:5.

A typical soil profile with plough plan layer at around 30-50 cm depth was present in this field (Fig.7-2b) and stones were abundant below 60 cm depth which made the deep soil layer heterogeneous.

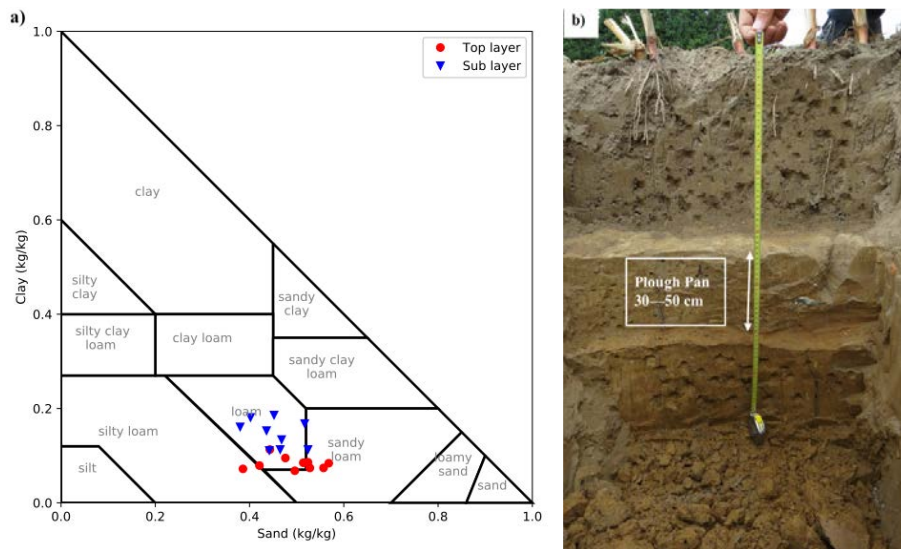


Fig.7-2. a) Soil texture distribution in the LSD based locations within two depths (top layer = 10 cm, sub layer = 50 cm); b) a typical soil profile in the studied field.

Penetration resistance was measured with a hand-held penetrometer (Eijkelkamp Soil & Water, with a cone of 1 cm<sup>2</sup> base area, 11.28 mm diameter and 60° top angle) at all locations on 27/03/2018. At each location, two 75 cm long parallel profiles were selected to measure PR at both sides of the location, with 11 replications in each side. Thus, 22 replications were measured for each location. Relative sampling positions for the above soil properties are shown in Fig.7-3.

Besides, seven sampling locations along a 40 x 40 m grid were selected by a regular grid method and the other seven sampling locations were randomly determined within the 40 x 40 m grid cells to assure spatial spreading of the random sampling (Fig.7-1). In these locations, only PR was measured with the same procedure as in the conditioned Latin hypercube sampling based locations.

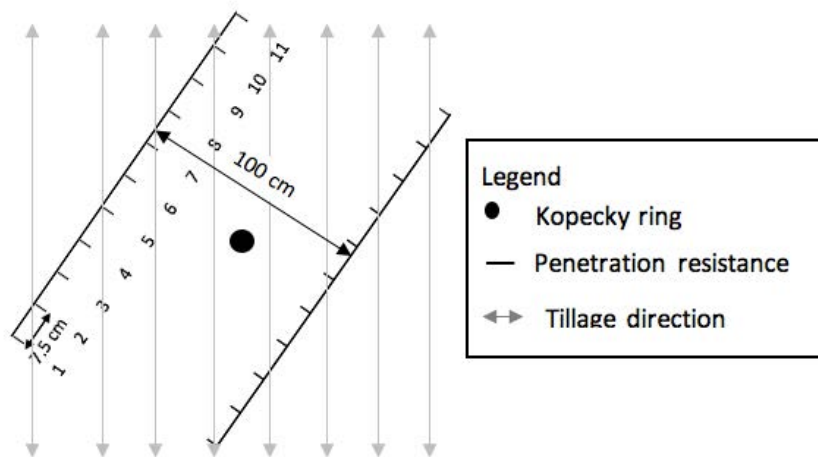


Fig.7-3. Relative positions of penetration resistance measurement, Kopecky ring sampling and tillage direction.

## 7.2.4 Maize canopy height measurements

### 7.2.4.1 Canopy height model

During the maturity stage of the 2018 maize season, an unmanned aerial vehicle (UAV, ONYXSTAR® HYDRA-12, Altigator) flight (on 14/09/2018) was performed with an RGB camera (Sony □6000, Sony Corporation) equipped with a 12 mm wide-angle lens (ZEISS Touit 2.8/12, Carl Zeiss AG). Nadir images were collected from 35 m above ground level, which had an overlap of 75 % in both directions (forward/longitudinal-lap and side-lap). The flight route was programmed with the Mikro-Tool V2.14b (HiSystems GmbH). The camera was triggered automatically based on the planned flight route and was set in manual mode to avoid different settings in successive images. Shutter time (exposure), aperture (F-stop) and sensitivity to light (ISO) were adjusted in the field at the beginning of the flight based on the present light conditions. Ground control points (GCPs) at the borders of the field were placed at the soil surface, while those in the middle were on a metal pillar

at a height of 3 meter to ensure their visibility on the images. They were placed straight with plumb rules. The GCP locations were recorded with an RTK-GPS system (Stonex S10 GNSS, Stonex SRL).

The software Agisoft Photoscan v1.2.6 Professional Edition (Agisoft LLC) was used to process the images and to build a georeferenced orthomosaic and a digital elevation model (DEM). The DEM was used to derive a canopy height model (CHM) of the field. To obtain the CHM, it is necessary to subtract the ground level from the DEM. Therefore, a digital terrain model (DTM) was build based on a previous flight carried out just after sowing (when no canopy was present and with same flight plan and camera at 2 cm spatial resolution).

#### **7.2.4.2 Remove soil background**

Before extracting the maize canopy height in the 24 locations (conditioned Latin hypercube, regular grid and random grid sampling points), CHM was refined to exclude the none cropped area (soil). A colour vegetation index, Excess Green (ExG) (Woebbecke *et al.* 1995), was calculated from the RGB bands of the orthomosaic to classify the pixels into two classes, soil or crop. After that, the pixels classified as soil were converted to a shapefile to be used as a mask to remove them from the CHM, thus their information would not be considered. All the above steps were conducted with QGIS V2.14.16-Essen (QGIS Geographic Information System; Open Source Geospatial Foundation Project).

### 7.2.5 Maize above-ground biomass

Maize above-ground biomass was harvested on 14/09/2018 at the ten conditioned Latin hypercube sampling based locations. At each location, three rows with each ~1 m long (same maize number) were harvested to determine the fresh maize above-ground biomass. After that, four plants were randomly selected to determinate dry above-ground biomass at 70 ° C for 48 hours.

### 7.2.6 Statistical

For ECa values, the statistical analysis was performed with QGIS. Firstly, by using the buffer function, a 2 m diameter circle (covering all the sampling area in Fig.7-3) was selected among all the 24 sampling locations. After that, the mean value of ECa and 90% maize canopy height in those selected circles was calculated for further analysis.

Spearman's rank correlation coefficients ( $r$ ) were calculated to evaluate the correlation among those selected properties. The mean value ( $\mu$ ), standard deviation (SD), and coefficient of variation (CV, where  $CV = SD/\mu$ ) for 0-25 cm and 25-50 cm depth were calculated. For BD at 0-25 cm and 25-50 cm depth, mean values were calculated from the data at 5, 10, 25 cm and 35, 50 cm, respectively. For PR, the mean of the maximum value per treatment at every 25 cm depth interval was used because the maximum value is the critical threshold for soil properties and crop growth.

A multiple linear regression analysis was conducted to predict the ECa from all the six selected soil properties. As the dataset with observations was relatively small for the rather high number of variables, ECa values across the two layers were pooled together with an additional factor to represent the different layers in the regression

analysis. The regression analysis was done through a manual forward stepwise linear regression analysis with the Akaike's Information Criterion (AIC) used as the indicator for selecting models (the lower the AIC, the better the model fit) (Dohoo *et al.* 2003). Significance of pair-wise interaction effects was tested by comparing the AIC's of the model with and without the interaction effects. The final model was selected as the model with the smallest AIC (difference in AIC>3) and a variable was considered to be a confounder only when the inclusion of the variable led to a change of more than 25% of the estimates of the parameters already in the model. Model assumptions were checked using QQ plot and residual versus fitted value plot. All statistical analyses were performed with Python.

To find a correlation between maize canopy height and ECa, 31,655 locations were selected according to the EMI measurement locations. Those locations were selected as a 0.2 m diameter circle (based on the resolution of EMI measurement) using the buffer function. After that, the mean values of maize canopy height and ECa were extracted from the ECa map and the removed soil ground maize canopy height map in all those locations to compare their correlation.

### **7.3. Results**

#### **7.3.1 Soil properties and maize canopy height variability**

Soil texture was distributed over silty loam, loam and sandy loam (Fig.7-2a). Within a soil layer, CV of clay content was 0.16 in the top layer and 0.20 in the sub layer, with clay content values ranging from 68 to 113 g kg<sup>-1</sup>, and 111 to 186 g kg<sup>-1</sup>, respectively. BD was variable with CV of 0.06 in both layers, and BD ranged from 1.13

to  $1.40 \text{ Mg m}^{-3}$ , and  $1.46$  to  $1.70 \text{ Mg m}^{-3}$  in the top and sub layers respectively. In contrast PR had a much higher CV,  $0.39$  and  $0.32$  for the top and sub layer, respectively (Table 7-1). Mean maximum PR values varied between  $0.53$  and  $2.04 \text{ MPa}$  in the top layer, and  $2.56$  and  $7.60 \text{ MPa}$  in the sub layer within all the 24 locations. In general, clay content,  $\theta_m$ , OC and ECs showed a higher variability in the sub layer than in the top layer. PR and ECa had a higher variability in the top layer in comparison with the sub layer. ECa had a relatively large variability ( $20\%$ ) within a relatively limited range (from  $7$  to  $24 \text{ mS m}^{-1}$ ).

The absolute variation in ECa was similar in both layers (Fig.7-4a,b). Maize canopy height ranged from  $2 \text{ m}$  to almost  $3 \text{ m}$ , with the highest values in the north-western part and lowest around the north-eastern, south-eastern and south-western field boundaries (Fig.7-4c), though its CV was rather low ( $0.08$ ).

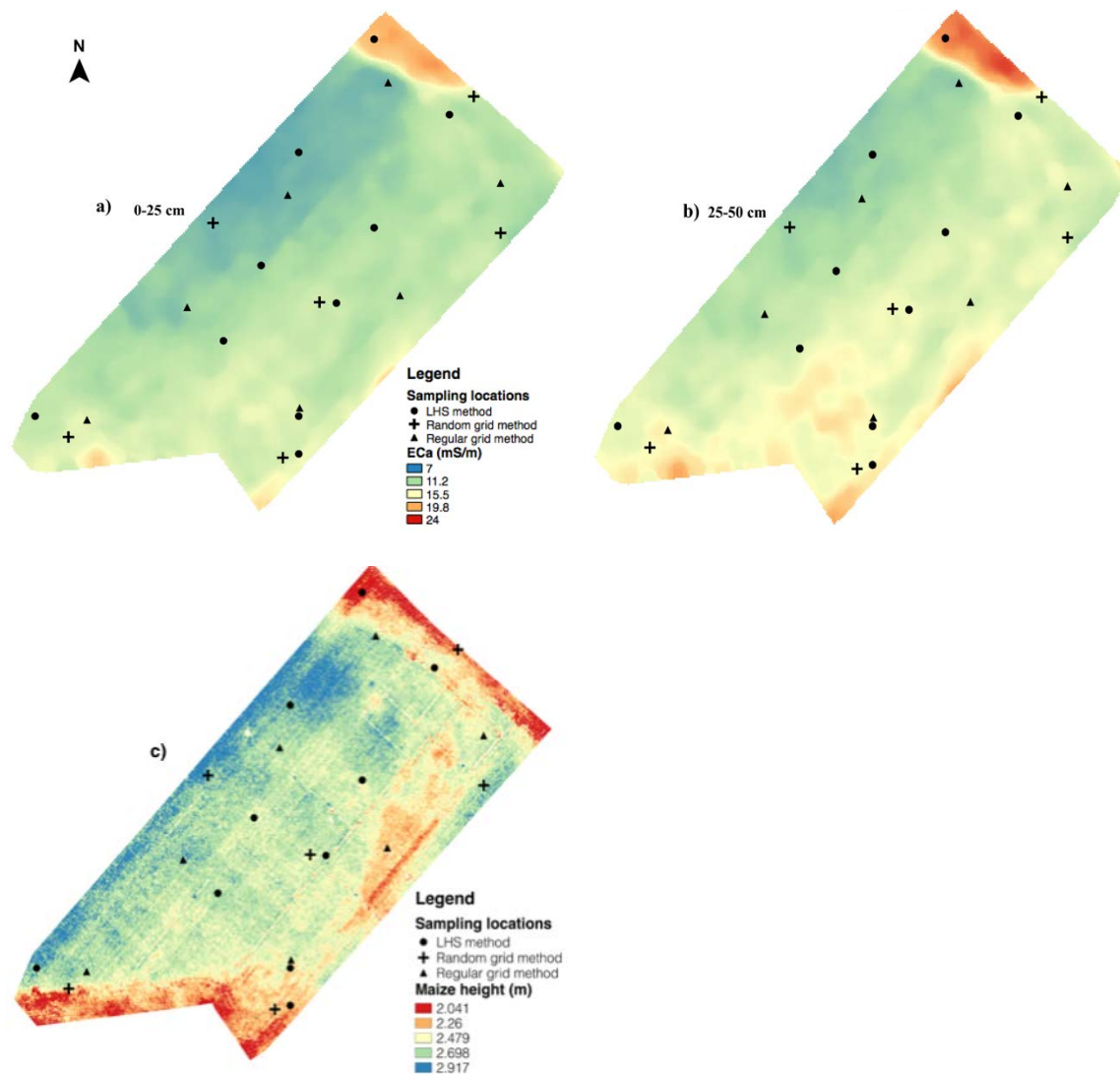


Fig.7-4. ECa distribution within different layers (a:0-25 cm, b: 25-50 cm) measured on 27/03/2018 and maize canopy height map (c) based on a drone image measured on 14/09/2018.

Table 7-1. Average values, standard deviation (SD) and coefficient of variation (CV) of the soil properties, ECa and maize canopy height.

Properties	Layer (cm)	Clay (g kg <sup>-1</sup> )	$\theta_m$ (kg kg <sup>-1</sup> )	BD (Mg m <sup>-3</sup> )	OC (g kg <sup>-1</sup> )	ECs (mS m <sup>-1</sup> )	ECa (mS m <sup>-1</sup> )	PR (MPa)	AGB_f (10 <sup>3</sup> kg ha <sup>-1</sup> )	AGB_d (10 <sup>3</sup> kg ha <sup>-1</sup> )	MCH (m)
Mean	0-25	83.0	0.28	1.23	15.1	9.00	12.83	1.01	56.13	18.81	2.62
	25-50	146.7	0.20	1.58	2.8	6.88	13.86	4.68			
SD	0-25	13.3	0.02	0.08	01.6	1.81	2.61	0.49	3.57	2.90	0.21
	25-50	29.8	0.04	0.09	0.4	1.26	1.70	1.43			
CV	0-25	0.16	0.06	0.06	0.11	0.10	0.20	0.50	0.06	0.15	0.08
	25-50	0.20	0.20	0.06	0.13	0.18	0.12	0.31			

Note: Clay is clay content,  $\theta_m$  is soil gravimetric water content, BD is bulk density, OC is organic carbon content, ECs is soil salinity, ECa is apparent soil electrical conductivity, PR is penetration resistance, AGB\_f is maize fresh above-ground biomass, AGB\_d is maize dry above-ground biomass, MCH is maize 90% canopy height. PR at 0-25 and 25-50 cm depth was calculated as the maximum value of each layer (and for every location the mean maximum of 22 measurements was calculated), respectively. All data are based on the 10 conditioned Latin hypercube sampling locations.

### 7.3.2 Relationships between soil properties and ECa

Spearman's rank correlation coefficients ( $r$ ) between ECa and soil properties in each layer are shown in Fig.7-5. In the 0-25 cm layer, ECa was not significantly correlated with soil properties; OC showed the largest correlation with ECa (Fig.7-5a). A positive relationship was found between OC and  $\theta_m$  and BD with  $r$  of 0.87 and 0.78, respectively. Clay and ECs also positively correlated to each other with  $r$  of 0.75.

In the 25-50 cm layer, ECa was not significantly correlated with any soil property; the highest correlation was now found with clay content (Fig.7-5b). In this layer, PR was strongly correlated with  $\theta_m$  and BD, with  $r$  of 0.90 and 0.92, respectively. Besides,  $\theta_m$  was negatively correlated with BD ( $r = -0.87$ ).

A multiple linear regression was conducted between ECa and all six soil properties (Table 7-2). Results show that only clay was significantly correlated with ECa ( $R^2=0.36$ ).

Table.2 Results of multiple liner regression between soil properties and ECa within two layers.

Factors	Estimate	Standard error	T values	Pr ( $> t $ )
(Intercept)	10.00	1.05	9.49	$< 0.01$
clay	0.26	0.09	3.00	0.01

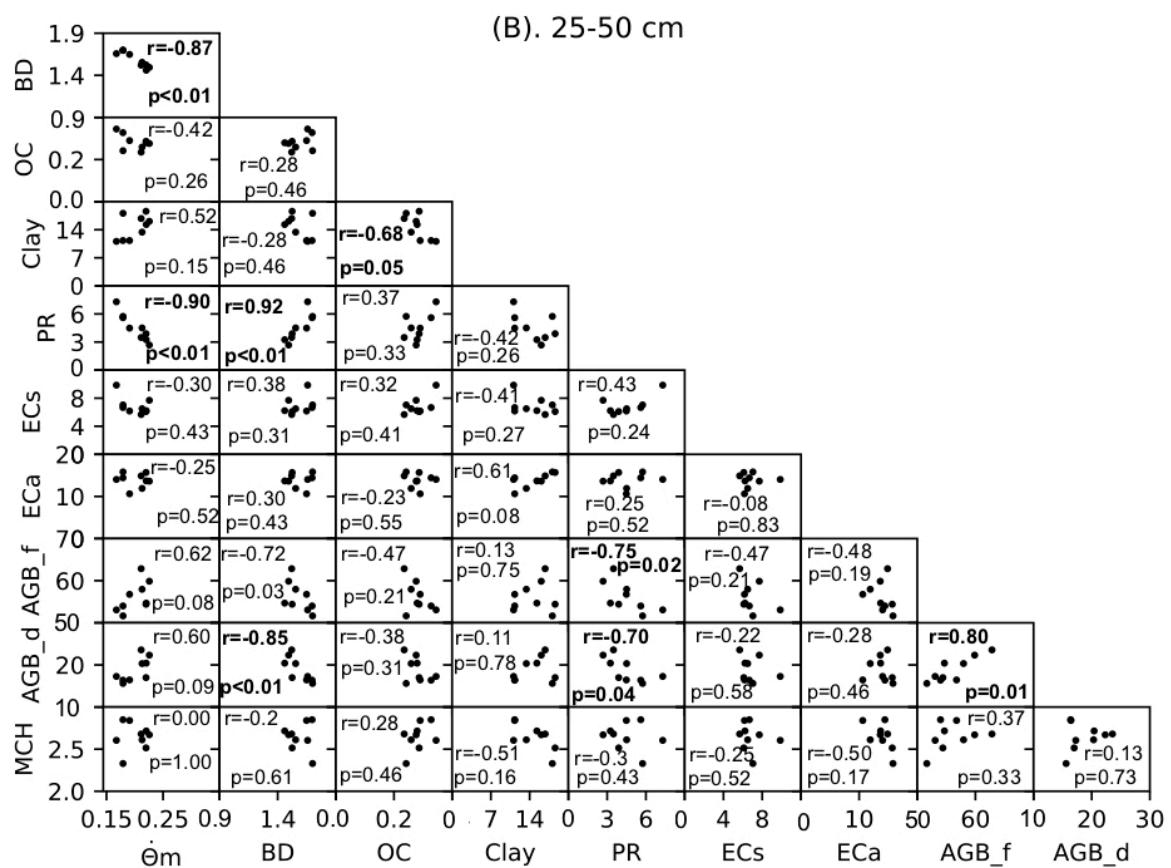
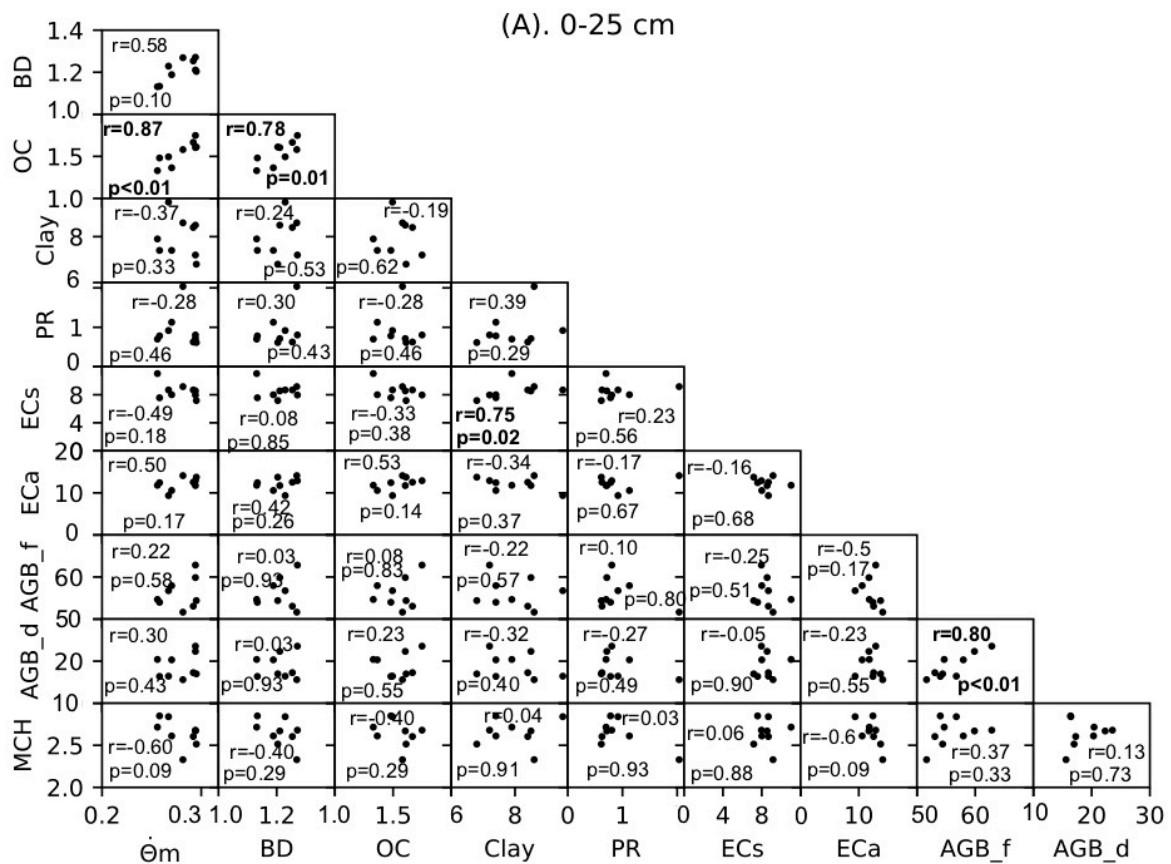


Fig.7-5. Spearman's rank correlation coefficient ( $r$ ) among soil properties and maize growth properties in 0-25 (a) and 25-50 cm (b) layer (correlation significance at 0.5% level is in bold). Clay is clay content;  $\theta_m$  is soil gravimetric water content; BD is bulk density; OC is organic carbon content; ECs is soil salinity; ECa is apparent soil electrical conductivity; PR is mean maximum penetration resistance; AGB\_f is fresh above-ground biomass; AGB\_d is dry above-ground biomass and MCH is 90% maize canopy height. All data are based on the 10 conditioned Latin hypercube sampling locations.

### 7.3.3 Relationship between maize canopy height and soil properties

Unlike the relationship between ECa and soil properties, maize canopy height measured in the dry and hot summer of 2018, was significantly negatively correlated with PR (maximum),  $\theta_m$ , and clay content at 25-50 cm layer when a multiple linear regression is conducted (Table 7-3). As PR was measured at all 24 locations, the correlation between maize canopy height and PR within all 24 locations was also evaluated (Fig.7-6). Maize canopy height had a negative correlation with PR in both layers and this correlation was stronger in the top layer than in the sub layer, with  $R^2$  being 0.27 and 0.13, respectively.

Table.3 Results of multiple liner regression between soil properties and maize canopy height.

Factors	Estimate	Standard error	T values	Pr (> t )
(Intercept)	4.17	0.50	8.25	< 0.01
PR	-0.21	0.03	-6.18	< 0.01
$\theta_m$	-9.17	2.20	-4.16	< 0.01
Clay	0.03	0.03	1.07	0.30
OC	0.60	0.29	2.10	0.06
Depth(25-50)	1.77	0.44	4.05	< 0.01
Depth (25-50)*Clay	-0.08	0.03	-2.37	0.04

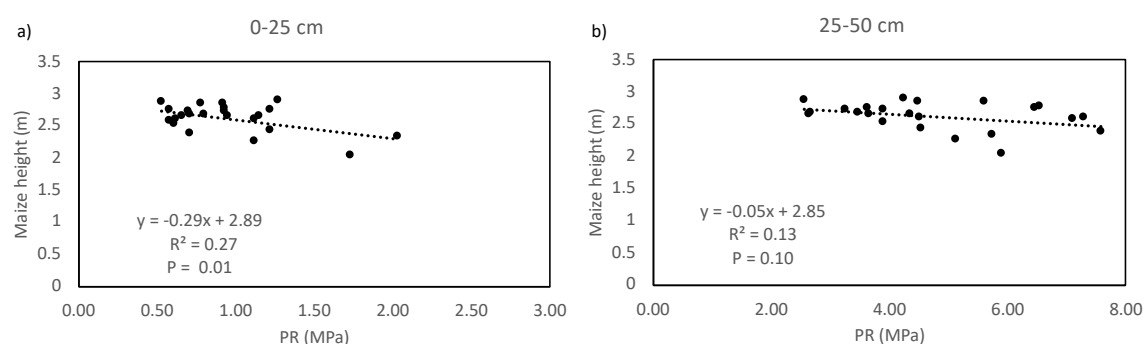


Fig.7-6. Correlation between maize canopy height and penetration resistance at 0-25 cm (a) and 25-50 cm (b) layer within 24 locations.

### 7.3.4 Relationship between maize canopy height and ECa

Maize canopy height had a relatively strong correlation with ECa (Fig.7-7). In the top layer (0-25 cm), a significant negative correlation was found ( $r = -0.67$ ) with ECa

explaining 45% of the maize canopy height variability. A similar trend but with a lower correlation was found in the sub layer (25-50 cm).

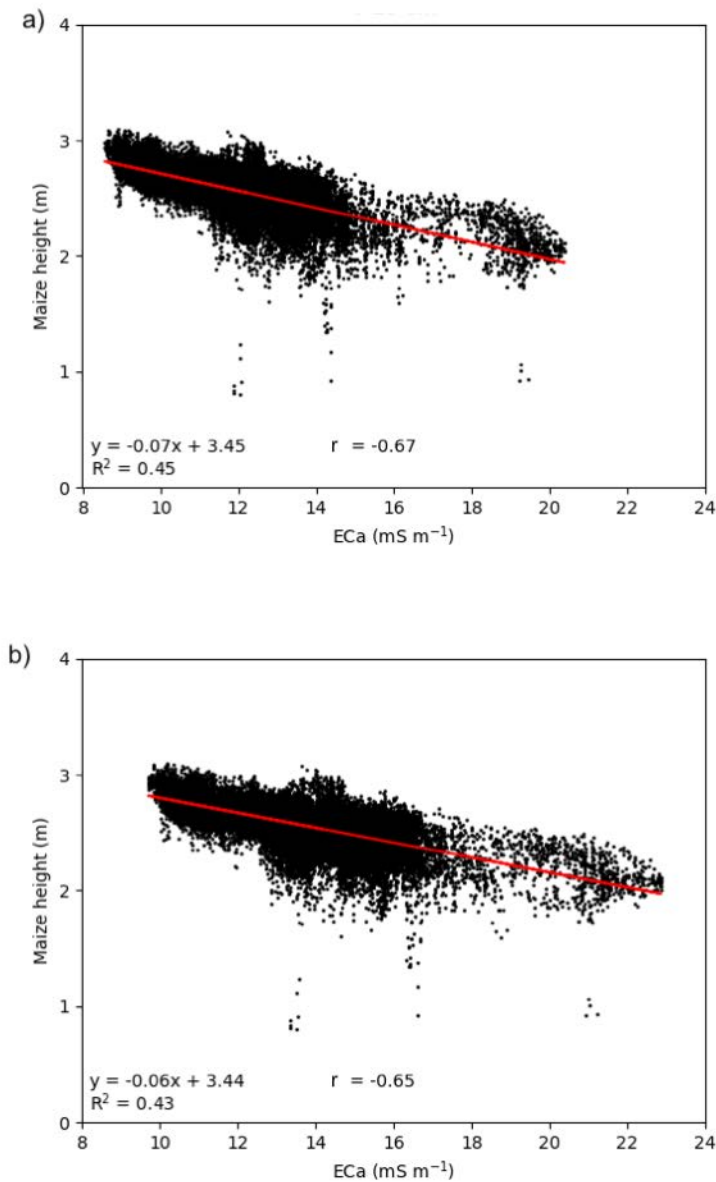


Fig.7- 7. Correlation between drone-derived maize canopy height and ECa measured with EMI within the 0-25 cm top layer (a) and the 25-50 cm sub layer (b) ('r' is spearman's rank correlation coefficient, 'R<sup>2</sup>' is coefficient of determination).

## 7.4. Discussion

### 7.4.1 Detecting soil compaction with ECa

According to Archie's law (Archie 1942), soil apparent electrical conductivity (ECa) is mainly related to soil clay content, soil moisture content and ECs. In our field, ECa was mainly related with clay content. This could be masked by the other factors with relatively small variability of moisture and ECs. For instance, OC also correlated moisture and salinity.

In contrast with what the theory suggests, detecting soil compaction with ECa was not possible in this specific field as no clear correlations were found between soil compaction related properties and ECa (Fig.7-5 and Table 7-2). There are several possible reasons that could explain why no correlation between ECa and PR or BD was detected. Firstly, the variability in clay content could have masked the relatively small contribution of soil compaction effects on ECa. For instance, clay content, OC and ECs in the 0-25 cm layer had a coefficient of variation of 16%, 11% and 10%, respectively, while that of BD was only 6%. Secondly, the ECa range from 7 to 24 mS m<sup>-1</sup> appeared too small to find a clear correlation. Similar findings were also found in a study in Germany, where even no correlation was found between clay content and ECa (Stadler *et al.* 2015). In that study ECa ranged from 8 to 24 mS m<sup>-1</sup> and soil texture ranged from silt to silt loam. Thirdly, there are some limitations to the measured soil compaction related properties. BD measurements are discontinuous within the profile and samples of only 5cm in diameter are typically used, which is much smaller than ECa based resolution (meters). On other hand, though PR is continuous and covers a transect of ~2 m long in this study, it is also relying on soil moisture content which makes PR less representative of soil compaction levels (Mouazen and Ramon

2009). Last but not least, stones were existed below 60 cm, which could have affected the ECa results (Romero-Ruiz *et al.* 2018).

#### **7.4.2 Soil compaction with maize canopy height**

Many researches show that soil compaction can restrict crop growth (Håkansson 2005; Schjønning *et al.* 2015; Colombi *et al.* 2018). However, it is not given the same results by selecting different maize growth indicators. For instance, soil compaction (PR) had a significant negative effect on maize canopy height (Table 7-3) but a negative correlation between dry above-ground biomass and penetration resistance ( $r = -0.70$ ) was only existed at 25-50 cm layer (Fig.7-5b). Overall, using crop growth indicators, like maize canopy height which can be easily accessed as ECa, could be a promising direction to detect potential soil compaction and its spatial variation.

#### **7.4.3 ECa with maize canopy height**

Though ECa could not predict soil compaction directly, it had a relatively strong negative correlation with maize canopy height (Fig.7- 7). ECa maps showed similar patterns as maize height maps and ECa explained 45% of maize canopy height variability in the 0-25 cm layer. Maize growth depends on multiple soil parameters, like soil water holding capacity, OC content, cation exchange capacity , parameters that are closely related with ECa as well. For instance, Sudduth *et al.* (2005) found ECa to be strongly correlated with clay content and CEC in 12 fields across six states of the north-central United States. Stadler *et al.* (2015) found that ECa and growth of winter

wheat and sugar beet were well related. This was most pronounced during the main growth phase. They also found that crop canopy height related better with ECa than other crop characteristics, like LAI and dry matter. However, such relationships are not uniform and vary among fields, year and crops as both ECa and crop growth indicators are affected by multiple factors. In our study, ECa was a good indicator of maize canopy height, at least during the extremely exceptionally dry and hot summer of 2018, when the drone images were taken. Besides, the  $R^2$  decreased very slightly with increasing of depth ( $R^2=0.45$  and  $0.43$  in top and sub layer, respectively).

## 7.5. Conclusions

It has evaluated correlations among soil properties, maize properties and ECa. In this site specific study, it was not possible to detect soil compaction by ECa values based on EMI scanning at this field level. Soil compaction was significantly correlated with maize canopy height, which means that maize canopy height can be used to detection soil compaction spatial distribution. Besides, a strong correlation was found between ECa and maize canopy height in the extremely exceptionally dry 2018. This indicates that though ECa cannot used to detect soil compaction distribution, it can be used to optimize soil management in precision agriculture. Overall, it confirmed that the use of crop growth indicator is a good way to detect soil compaction.



## **Chapter 8 : General conclusions and future perspectives**



There is no doubt that modernization in agriculture is the way forward towards agricultural development and mechanization is key to that. The weight of agriculture machines and soil-tyre contact stresses increased with agriculture mechanization in the past decades (Schjønning *et al.* 2015). This resulted in soil compaction which has been one of the main restrictions for sustainable modernization in agriculture. Better understanding of the effects, prevention, alleviation and detection of soil compaction is urgently needed in order to deal with this issue. In this dissertation, these aspects have been addressed and the main conclusions and recommendations are listed below.

## **8.1 Effects of soil compaction**

Once soil is compacted, there can be many adverse impacts. In this dissertation, firstly the effects of topsoil compaction induced by various machines were evaluated on sandy loam soils in the Flemish Region of Belgium. It was demonstrated that in 2017 a combination of a tractor and a rotary harrow, used during seedbed preparation, did effect the soil physical properties in the topsoil (i.e., increased penetration resistance) but there were no effects on soil water content, soil nitrogen content and maize growth (Chapter 2). However, maize grown on tracks induced by the slurry spreader showed 7% lower above-ground biomass in 2016, even after a mouldboard ploughing, in comparison with maize grown between the tracks (Chapter 4). Besides, with multiple traffic tracks, maize dry above-ground biomass was also significantly decreased (decreased 12% compared with the less traffic zone) in 2017 (Chapter 2). During the sowing of a cover crop, a seeding combination trafficking the field under both moist and dry conditions significantly ( $P < 0.05$ ) reduced winter rye's shoot

biomass and root biomass density (chapter 3). This indicates that the effects of traffic during seedbed preparation (by sowing machine) also depend on the growing season because restrictions were only detected in the wet winter season.

Secondly, in chapter 2 the long-term accumulated effects of subsoil compaction have been evaluated. Two different levels of subsoil compaction were compared, highly compacted soil in a headland zone and less compacted soil in an in-field zone. Both visual evaluation and examination methods and lab or field-based measurements indicated that soil physical and hydraulic properties, as well as root number density, were different between the headland and in-field zones. As a result, water transport and root-water uptake were restricted in the headland zone. Water percolation to the subsoil was reduced and water content in the topsoil were higher in the winter season. As a result, winter rye growth was hampered. On the contrary, in the summer season, subsoil compaction restricted maize to access water and nutrients from the subsoil, which decreased maize above-ground biomass (chapter 2). Consequently, soil mineral nitrogen leaching risk was higher in the headland zone because of reduced nutrient uptake from the subsoil (chapter 2).

### **Recommendation:**

In the study area, traffic induced topsoil compaction prior to sowing did not decrease maize growth under low intensity traffic. However, we should avoid the multiple overlapping passes as this was reflected in 12% lower summer maize yield (chapter 2). During the sowing of a cover crop, all kinds of traffics can restrict crop growth. The effect of climate conditions is still not clear and should be further

investigated because all of those effects might be different under different climate areas. Subsoil compaction not only restricted water movement and crop growth but also increased nitrogen leaching risk below the rootzone in this study (chapter 2). Therefore, subsoil compaction should be avoided by adjusting farming management. Some prevention strategies are recommended in the next section.

The groundwater table was rather deep (~5 m) in the VRV field of chapter 2 and there was no water supply from the groundwater. This is not always the case in the study area. Further studies should investigate the effect of soil compaction on capillary rise under different groundwater tables.

## 8.2 Strategies to prevent soil compaction

Prevention is the best way to deal with soil compaction as it cannot be easily alleviated and can persist for many decades, especially subsoil compaction (Schjønning *et al.* 2015). There is a risk of soil compaction when the external soil stress exceed the soil strenght, often expressed in terms of soil precompression. Therefore, soil compaction prevention strategies should consider both soil conditions (soil strenght) and traffic characteristics (soil stress). In this dissertation, both aspects were considered.

In one of the study fields, a freshly cultivated and thus relatively loose soil was selected. Both dry and moist soil conditions, and different tyre types and tyre pressures were considered while sowing a cover crop (Chapter 3). These factors did not affect several selected soil quality indicators among single trafficked treatments. Differences only existed between trafficked and control treatments. Interestingly, significant and marginal differences in penetration resistance ( $P=0.02$ ) and air capacity ( $P=0.09$ ),

respectively, were also found at 20-30 cm depth between treatments with one and two passes. Similarly, shoot biomass and root biomass density of winter rye were significantly ( $P < 0.05$ ) reduced in the trafficked parts compared to the controls under both moist and dry conditions at wheeling. No differences in winter rye growth were found among the treatments trafficked under both moisture conditions.

In another experiment, a relative compacted soil was selected (Chapter 4). The effects of soil wetness and tyre pressure on physical soil properties were evaluated by using a ~5 Mg wheel load slurry spreader mounted on a tractor. The impacts were also compared with Terranimo<sup>®</sup> model predictions and X-ray micro-computed tomography (X-ray micro-CT) parameters. In the consecutive maize growing season, soil physical properties, total mineral nitrogen content and maize above biomass were additionally evaluated between in and out track positions. Immediately after traffic, penetration resistance (PR) in the top 10 cm was significantly higher ( $P < 0.05$ ) when done under moist conditions and at in-track positions compared with a dry condition treatment and at out-track positions. Tyre pressure did not affect PR at in- or out-track positions. At 10 cm depth, bulk density and macro-porosity ( $d > 30 \mu\text{m}$ ) of soil trafficked under moist conditions was marginally different ( $P \leq 0.10$ ) from those of soil trafficked under dry conditions. Macro-porosity showed a clear response ( $P < 0.10$ ) to tyre pressure and all the trafficked treatments. Deeper in the profile, there were no significant differences in these soil physical quality indicators. X-ray micro-CT results agreed well with the soil physical quality indicators and detected slight changes in the degree of compaction more precisely. Terranimo<sup>®</sup> well predicted the contact area and mean ground pressure (RMSE=0.06  $\text{m}^2$ ). However, it indicated considerable compaction risk from the tractor's rear wheels, which seemed to contradict with the relatively minor changes in soil physical properties observed. In the maize growing

season, soil physical properties and nitrogen content showed no differences ( $P > 0.05$ ) between in- and out-track positions, while above-ground dry biomass of maize reduced with ~7% at in-track positions.

### **Recommendation:**

Trafficking soils at suitable soil wetness conditions and adjusting tyre types and pressures are generally considered as useful strategies to minimize soil compaction. Though this did not always show a significant improvement according to measured soil properties and crop response. Soil stress decreased according to simulations with Terranimo<sup>®</sup>, while soil precompression stress increased under dry conditions. Changes in soil properties typically have to be seen as an accumulation process which become effective after repeated and long-term wheeling. Therefore, long-term observations are needed to quantify those effects further and link them with the farmer's practice.

### **8.3 Alleviation of soil compaction**

Two kinds of alleviation methods were tested by using soil tillage methods and cover crops. Tillage is regarded as an efficient way to alleviate soil compaction for both top and subsoil. However, deep loosening soil in particular can sometimes do more harm than good as it can destroy existing macropores, negatively affect structure when done under too wet conditions and make the soil more vulnerable to compaction. For topsoil alleviation, the effects of two spring tillage methods were evaluated, i.e. strip tillage with a strip-till machine and intensive tillage by mouldboard ploughing (Chapter 5). Strip tillage, like intensive tillage, could sufficiently loosen soil for adequate maize

growth even though maize root distribution was restricted to tilled rows in contrast with intensive tillage. However, those tillage methods could not fully alleviate soil compaction. For instance, after mouldboard ploughing, the effects of soil compaction (induced by a slurry spreader) were still detectable and reduces maize biomass with 7% decreased at in-track positions (Chapter 4).

The effect of deep tillage to alleviate subsoil compaction was tested in Chapter 2. Unlike some of the previous studies, which show that two passes of a tractor already re-compacted the soil before the first crop was planted (Reeder *et al.* 1993), the effect of deep tillage remained for more than 1.5 years (two silage maize seasons with winter rye as cover crop) and it significantly increased maize canopy height in the exceptionally dry and hot summer of 2018.

For bio-subsoilers, both field and column-based experiments showed differences in alleviation subsoil compaction among different cover crops (Chapter 5 and 6). In the field study, white mustard showed significantly higher root penetration than winter rye at 20-45 cm depth (Chapter 5). In the following season, maize root penetration was significantly greater following white mustard than winter rye at 30-40 cm depth. In soil column-based experiment, cover crops affected the soil porosity differently among crop species (Chapter 6). Different CT-derived pore networks indicated that chicory and lucerne were likely to perform better than spring barley as reference, and radish and tall fescue when used as bio-subsoilers by creating a larger, more connected and complex pore network. Longer-term crop growth is needed to derive a marked loosening effect in the compacted layer.

### **Recommendation:**

For topsoil compaction, strip tillage had the same function with the mouldboard plough for maize growth in this study year. However, there is still debate about whether strip tillage affects crop yield or not, according to studies conducted under different conditions. As effects of strip tillage are site-specific, further studies are needed under various conditions (e.g., different soil types, weather and crop husbandry practices such as fertilization with heavy machinery). For deep tillage, long-time observations are needed to know the most beneficial time of deep tillage.

Biodrilling with cover crops has a great potential to alleviate subsoil compaction. For instance, in Chapter 6, differences in the CT-derived pore network indicate that chicory and lucerne are likely to perform better than the other crops. However, the created pores are a result of multiple factors and combination with a visual evaluation along a soil profile is recommended for future study. Cover crops need to continuously grow for a long term before a remarkable loosening effect in the compacted layer can be acquired.

#### **8.4 Detecting soil compaction**

An efficient detection method for soil compaction at a field level is urgently needed. The possibility to detect soil compaction from measurements of apparent electrical conductivity (ECa) by using electromagnetic induction (EMI) and from drone-derived maize canopy height at a ~1 ha field parcel scale (Chapter 7) was evaluated. Soil compaction related properties, like bulk density (BD) and penetration resistance (PR), as well as soil texture, salinity and soil moisture, were measured across the field based on ECa variability. Maize canopy height was derived from drone images taken at maturity stage. In this site-specific study, no correlation between soil compaction

related properties (i.e., BD and PR) and ECa was found, though soil clay content was significantly ( $P=0.01$ ) correlated with ECa. Soil compaction (i.e., PR) was significantly correlated with maize canopy height, which means that maize canopy height can be used to detect soil compaction spatial distribution. A negative correlation between ECa and maize canopy height (Spearman's rank correlation coefficients of -0.67 in the top layer) was found, under the rather dry conditions prevailing during this study. Overall, detecting soil compaction with ECa is challenging, while maize canopy height can be used to detect spatial variability of soil compaction within a field.

Besides, at the soil core scale, X-ray CT provides a valuable way to quantify soil compaction. Conventional lab methods based on undisturbed ring (cylinder) samples show limitations in both sampling and measurement compared with the X-ray micro-CT method. For instance, soil and cylinder walls do not show perfect contact because of sampling artefacts, like the presence of roots, residues or other more rigid substances. Furthermore, it is always a challenge to measure soil volume precisely, which is used to determine soil porosity and other volume-averaged composite soil properties. In contrast, X-ray micro-CT results can exclude the sample boundaries and enable to only select a specific Region of Interest which makes the results more precise. Moreover, X-ray micro-CT can provide complementary and even more information directly (Chapter 4).

### **Recommendation:**

Detecting soil compaction at a field-scale seemed not possible by EMI in this site-specific study because of the variability of other soil properties. Interestingly, crop growth characteristics were a good indicator of spatial variability of soil compaction. However, this study was restricted to one season and one field only. Further research

is encouraged to test the possibility of using EMI and crop height to map soil compaction across different soil types and climate conditions.

Detecting soil compaction at a core scale is still problematical. One of the main challenges is the downscaling from field to profile and core scale. Because of the heterogeneity of soil and the inhomogeneous distribution of soil stress from wheels, it is hard to collect the most representative small core samples. Combining lab-based core measurements with profile evaluations (e.g., visual evaluation) could provide more representative results.

### **8.5 Concluding and future perspectives**

As soil compaction has become one of the main restrictions for sustainable agriculture, fully understanding of soil compaction formation mechanisms could help to develop good prevention or alleviation strategies. In this study, they were only based on a limited number of fields and in relatively short time period. More research is needed to further understand all compaction aspects. Close cooperation between soil scientists and agricultural machinery manufacturers is strongly needed to design the most environmental-friendly machinery. Conservation tillage and bio drilling with cover crops are useful and environmental-friendly alleviation methods but further research is needed to understand their long-term effects.

## References:

- Abdollahi, L, Munkholm, LJ (2014) Tillage system and cover crop effects on soil quality: I. Chemical, mechanical, and biological properties. *Soil Science Society of America Journal* 78 (1), 262-270. doi:10.2136/sssaj2013.07.0301
- Abràmoff, MD, Magalhães, PJ, Ram, SJ (2004) Image processing with ImageJ. *Biophotonics international* 11 (7), 36-42.
- Abu-Hamdeh, NH, Reeder, RC (2003) Measuring and predicting stress distribution under tractive devices in undisturbed soils. *Biosystems Engineering* 85 (4), 493-502.
- Al-Gaadi, K (2012) Employing electromagnetic induction technique for the assessment of soil compaction. *American Journal of Agricultural and Biological Sciences* 7 (4), 425-434.
- Alameda, D, Anten, NPR, Villar, R (2012) Soil compaction effects on growth and root traits of tobacco depend on light, water regime and mechanical stress. *Soil & Tillage Research* 120 121-129. 10.1016/j.still.2011.11.013
- Alaoui, A, Lipiec, J, Gerke, HH (2011) A review of the changes in the soil pore system due to soil deformation: A hydrodynamic perspective. *Soil & Tillage Research* 115 1-15. 10.1016/j.still.2011.06.002
- Andersen, MN, Munkholm, LJ, Nielsen, AL (2013) Soil compaction limits root development, radiation-use efficiency and yield of three winter wheat (*Triticum aestivum* L.) cultivars. *Acta Agriculturae Scandinavica Section B-Soil and Plant Science* 63 (5), 409-419. 10.1080/09064710.2013.789125
- Antille, DL, Bennett, JM, Jensen, TA (2016) Soil compaction and controlled traffic considerations in Australian cotton-farming systems. *Crop and Pasture Science* 67 (1), 1-28.
- Archie, GE (1942) The electrical resistivity log as an aid in determining some reservoir characteristics. *Transactions of the AIME* 146 (01), 54-62.
- Arvidsson, J (2001) Subsoil compaction caused by heavy sugarbeet harvesters in southern Sweden - I. Soil physical properties and crop yield in six field experiments. *Soil & Tillage Research* 60 (1-2), 67-78. Doi 10.1016/S0167-1987(01)00169-6
- Arvidsson, J, Hakansson, I (2014) Response of different crops to soil compaction- Short-term effects in Swedish field experiments. *Soil & Tillage Research* 138 56-63. 10.1016/j.still.2013.12.006
- Arvidsson, J, Håkansson, I (1996) Do effects of soil compaction persist after ploughing? Results from 21 long-term field experiments in Sweden. *Soil and Tillage Research* 39 (3-4), 175-197.
- Arvidsson, J, Keller, T (2007) Soil stress as affected by wheel load and tyre inflation pressure. *Soil & Tillage Research* 96 (1-2), 284-291. 10.1016/j.still.2007.06.012

- Arvidsson, J, Trautner, A, Keller, T (2002) Influence of tyre inflation pressure on stress and displacement in the subsoil. *Sustainable Land Management - Environmental Protection* 35 331-338.
- Bakker, D, Davis, R (1995) Soil deformation observations in a Vertisol under field traffic. *Soil Research* 33 (5), 817-832.
- Ball, B, Batey, T, Munkholm, LJ (2007) Field assessment of soil structural quality—a development of the Peerlkamp test. *Soil Use and Management* 23 (4), 329-337.
- Ball, BC, Batey, T, Munkholm, LJ, Guimarães, RML, Boizard, H, McKenzie, DC, Peigné, J, Tormena, CA, Hargreaves, P (2015) The numeric visual evaluation of subsoil structure (SubVESS) under agricultural production. *Soil and Tillage Research* 148 85-96. 10.1016/j.still.2014.12.005
- Ball, BC, Smith, KA (2000) Gas movement and air-filled porosity. In 'Soil and environmental analysis'. pp. 503-542. (CRC Press:
- Batey, T (2009) Soil compaction and soil management - a review. *Soil Use and Management* 25 (4), 335-345. 10.1111/j.1475-2743.2009.00236.x
- Bengough, AG, McKenzie, B, Hallett, P, Valentine, T (2011) Root elongation, water stress, and mechanical impedance: a review of limiting stresses and beneficial root tip traits. *Journal of experimental botany* 62 (1), 59-68.
- Berisso, FE, Schjønning, P, Keller, T, Lamande, M, Etana, A, de Jonge, LW, Iversen, BV, Arvidsson, J, Forkman, J (2012) Persistent effects of subsoil compaction on pore size distribution and gas transport in a loamy soil. *Soil & Tillage Research* 122 42-51. 10.1016/j.still.2012.02.005
- Berisso, FE, Schjønning, P, Keller, T, Lamandé, M, Simojoki, A, Iversen, BV, Alakukku, L, Forkman, J (2013a) Gas transport and subsoil pore characteristics: Anisotropy and long-term effects of compaction. *Geoderma* 195 184-191.
- Berisso, FE, Schjønning, P, Lamande, M, Weisskopf, P, Stettler, M, Keller, T (2013b) Effects of the stress field induced by a running tyre on the soil pore system. *Soil & Tillage Research* 131 36-46. 10.1016/j.still.2013.03.005
- Besson, A, Cousin, I, Samouelian, A, Boizard, H, Richard, G (2004) Structural heterogeneity of the soil tilled layer as characterized by 2D electrical resistivity surveying. *Soil & Tillage Research* 79 (2), 239-249. 10.1016/j.still.2004.07.012
- Besson, A, Séger, M, Giot, G, Cousin, I (2013) Identifying the characteristic scales of soil structural recovery after compaction from three in-field methods of monitoring. *Geoderma* 204 130-139.
- Beylich, A, Oberholzer, H-R, Schrader, S, Hoepfer, H, Wilke, B-M (2010) Evaluation of soil compaction effects on soil biota and soil biological processes in soils. *Soil & Tillage Research* 109 (2), 133-143. 10.1016/j.still.2010.05.010
- Bingham, IJ, Bengough, AG, Rees, RM (2010) Soil compaction–N interactions in barley: Root growth and tissue composition. *Soil and Tillage Research* 106 (2), 241-246. 10.1016/j.still.2009.10.008
- Bluett, C, Tullberg, JN, McPhee, JE, Antille, DL (2019) Soil and Tillage Research: Why still focus on soil compaction? *Soil and Tillage Research* 194 104282.
- Bodner, G, Leitner, D, Kaul, H-P (2014) Coarse and fine root plants affect pore size distributions differently. *Plant and Soil* 380 (1-2), 133-151.

## References

- Botta, GF, Jorajuria, D, Balbuena, R, Ressia, M, Ferrero, C, Rosatto, H, Tourn, M (2006) Deep tillage and traffic effects on subsoil compaction and sunflower (*Helianthus annuus* L.) yields. *Soil & Tillage Research* 91 (1-2), 164-172. 10.1016/j.still.2005.12.011
- Boussinesq, J (1885) 'Application des potentiels à l'étude de l'équilibre et du mouvement des solides élastiques. [Application of Potentials in the Study of the Equilibrium and the Movement of Elastic Bodies.]' (Gauthier-Villars, Paris
- Brabant, L, Vlassenbroeck, J, De Witte, Y, Cnudde, V, Boone, MN, Dewanckele, J, Van Hoorebeke, L (2011) Three-dimensional analysis of high-resolution X-ray computed tomography data with Morpho+. *Microsc Microanal* 17 (2), 252-63. 10.1017/S1431927610094389
- Brevik, EC, Fenton, TE (2004) The effect of changes in bulk density on soil electrical conductivity as measured with the Geonics EM-38. *Soil Horizons* 45 (3), 96-102.
- Bullock, P, Fedoroff, N, Jongerius, A, Stoops, G, Tursina, T (1985) 'Handbook for soil thin section description.' (Waine Research:
- Cambi, M, Certini, G, Neri, F, Marchi, E (2015) The impact of heavy traffic on forest soils: A review. *Forest Ecology and Management* 338 124-138. 10.1016/j.foreco.2014.11.022
- Carminati, A, Vetterlein, D, Weller, U, Vogel, H-J, Oswald, SE (2009) When roots lose contact. *Vadose Zone Journal* 8 (3), 805-809.
- Celette, F, Gaudin, R, Gary, C (2008) Spatial and temporal changes to the water regime of a Mediterranean vineyard due to the adoption of cover cropping. *European Journal of Agronomy* 29 (4), 153-162.
- Chamen, WCT, Moxey, AP, Towers, W, Balana, B, Hallett, PD (2015) Mitigating arable soil compaction: A review and analysis of available cost and benefit data. *Soil & Tillage Research* 146 10-25. 10.1016/j.still.2014.09.011
- Chan, KY, Heenan, DP (1996) The influence of crop rotation on soil structure and soil physical properties under conventional tillage. *Soil & Tillage Research* 37 (2-3), 113-125. Doi 10.1016/0167-1987(96)01008-2
- Chaudhary, M, Gajri, P, Prihar, S, Khera, R (1985) Effect of deep tillage on soil physical properties and maize yields on coarse textured soils. *Soil and Tillage Research* 6 (1), 31-44.
- Chen, G (2009) 'Alleviation of soil compaction by Brassica cover crops.' (University of Maryland, College Park:
- Chen, G, Weil, RR (2010) Penetration of cover crop roots through compacted soils. *Plant and Soil* 331 (1-2), 31-43.
- Chen, G, Weil, RR (2011) Root growth and yield of maize as affected by soil compaction and cover crops. *Soil and Tillage Research* 117 17-27.
- Chen, G, Weil, RR, Hill, RL (2014) Effects of compaction and cover crops on soil least limiting water range and air permeability. *Soil and Tillage Research* 136 61-69.
- Clark, A (Ed. r ed (2008) 'Managing cover crops profitably.' (Diane Publishing: sustainable agriculture network)

- Clark, LJ, Barraclough, PB (1999) Do dicotyledons generate greater maximum axial root growth pressures than monocotyledons? *Journal of Experimental Botany* 50 (336), 1263-1266.
- Cnudde, V, Boone, MN (2013) High-resolution X-ray computed tomography in geosciences: A review of the current technology and applications. *Earth-Science Reviews* 123 1-17. 10.1016/j.earscirev.2013.04.003
- Colombi, T, Braun, S, Keller, T, Walter, A (2017a) Artificial macropores attract crop roots and enhance plant productivity on compacted soils. *Sci Total Environ* 574 1283-1293. 10.1016/j.scitotenv.2016.07.194
- Colombi, T, Kirchgessner, N, Walter, A, Keller, T (2017b) Root Tip Shape Governs Root Elongation Rate under Increased Soil Strength. *Plant Physiol* 174 (4), 2289-2301. 10.1104/pp.17.00357
- Colombi, T, Torres, LC, Walter, A, Keller, T (2018) Feedbacks between soil penetration resistance, root architecture and water uptake limit water accessibility and crop growth - A vicious circle. *Science of the Total Environment* 626 1026-1035. 10.1016/j.scitotenv.2018.01.129
- Colombi, T, Walter, A (2017) Genetic Diversity under Soil Compaction in Wheat: Root Number as a Promising Trait for Early Plant Vigor. *Front Plant Sci* 8 420. 10.3389/fpls.2017.00420
- Cooper, J, 2011. The untilt stack plugin for ImageJ.
- Cornelis, W (2014) Subsoil Compaction: The Invisible Enemy. *ESSC NEWSLETTER* 1/2014 1-10.
- Cornelis, WM, Khlosi, M, Hartmann, R, Van Meirvenne, M, De Vos, B (2005) Comparison of unimodal analytical expressions for the soil-water retention curve. *Soil Science Society of America Journal* 69 (6), 1902-1911. 10.2136/sssaj2004.0238
- Correa, J, Postma, JA, Watt, M, Wojciechowski, T (2019) Soil compaction and the architectural plasticity of root systems. *Journal of experimental botany* 70 (21), 6019-6034.
- Cresswell, H, Kirkegaard, J (1995) Subsoil amelioration by plant-roots-the process and the evidence. *Soil Research* 33 (2), 221-239.
- D'Haene, K (2008) The potential of reduced tillage agriculture in Flanders. Doctoraal proefschrift, Faculteit Bio-ingenieurswetenschappen, Universiteit Gent
- Da Silva, A, Kay, B, Perfect, E (1994) Characterization of the least limiting water range of soils. *Soil Science Society of America Journal* 58 (6), 1775-1781.
- Day, SD, Bassuk, NL (1994) A review of the effects of soil compaction and amelioration treatments on landscape trees. *Journal of Arboriculture* 20 (1), 9-17.
- De Haan, WvG, 2013. Adviesbasis Voor De Bemesting Van Akkerbouwgewassen – Samenstelling En Werking Van Organische Meststoffen. [online]. <http://www.kennisakker.nl/kenniscentrum/handleidingen/adviesbasis-voor-de-bemesting-van-akkerbouwgewassen-samenstelling-en-wer>.

## References

- De Pue, J, Di Emidio, G, Flores, RDV, Bezuijen, A, Cornelis, WM (2019a) Calibration of DEM material parameters to simulate stress-strain behaviour of unsaturated soils during uniaxial compression. *Soil and Tillage Research* 194 104303.
- De Pue, J, Rezaei, M, Van Meirvenne, M, Cornelis, WM (2019b) The relevance of measuring saturated hydraulic conductivity: Sensitivity analysis and functional evaluation. *Journal of Hydrology* 576 628-638.
- De Smedt, P (2013) Reconstructing human-landscape interactions through multi-receiver electromagnetic induction survey. Ghent University.
- Dexter, AR (2004) Soil physical quality - Part I. Theory, effects of soil texture, density, and organic matter, and effects on root growth. *Geoderma* 120 (3-4), 201-214. 10.1016/j.geodermaa.2003.09.005
- Dohoo, IR, Martin, W, Stryhn, H (2003) 'Veterinary epidemiologic research.' (AVC Incorporated Charlottetown, Canada:
- Dondeyne, S, Vanierschot, L, Langohr, R, Van Ranst, E, Deckers, S (2014) The soil map of the Flemish region converted to the 3rd edition of the World Reference Base for soil resources.
- Doube, M, Kłosowski, MM, Arganda-Carreras, I, Cordelières, FP, Dougherty, RP, Jackson, JS, Schmid, B, Hutchinson, JR, Shefelbine, SJ (2010) BoneJ: free and extensible bone image analysis in ImageJ. *Bone* 47 (6), 1076-1079.
- Duiker, SW, 2005a. Avoiding Soil Compaction. Penn State Extension. Penn State Extension,
- Duiker, SW, 2005b. Effects of soil compaction. Penn State Extension. Penn State Extension,
- Dyck, J, 2017. Soil Compaction: Stay Off the Field Until the Soil is Ready.
- Etana, A, Larsbo, M, Keller, T, Arvidsson, J, Schjønning, P, Forkman, J, Jarvis, N (2013) Persistent subsoil compaction and its effects on preferential flow patterns in a loamy till soil. *Geoderma* 192 430-436.
- Fröhlich, OK (1934) 'Druckverteilung im Baugrunde.' (Springer Verlag, Wien
- Fukuma, Y (2007) On the sectional invariants of polarized manifolds. *Journal of Pure and Applied Algebra* 209 (1), 99-117. 10.1016/j.jpaa.2006.05.023
- Gajri, P, Arora, V, Chaudhary, M (1994) Maize growth responses to deep tillage, straw mulching and farmyard manure in coarse textured soils of NW India. *Soil Use and Management* 10 (1), 15-19.
- Galdos, M, Pires, L, Cooper, H, Calonego, J, Rosolem, C, Mooney, S (2019) Assessing the long-term effects of zero-tillage on the macroporosity of Brazilian soils using X-ray Computed Tomography. *Geoderma* 337 1126-1135.
- Gasso, V, Sorensen, CAG, Oudshoorn, FW, Green, O (2013) Controlled traffic farming: A review of the environmental impacts. *European Journal of Agronomy* 48 66-73. 10.1016/j.eja.2013.02.002
- Gee, GW, Bauder, JW (1986) Particle-size analysis1. *Methods of soil analysis: Part 1—Physical and mineralogical methods (methodsofsoilan1)*, 383-411.
- Gentile, R, Martino, D, Entz, M (2003) Root characterization of three forage species grown in southwestern Uruguay. *Canadian journal of plant science* 83 (4), 785-788.

- Glaž, T (2007) Application of image analysis for soil macropore characterization according to pore diameter. *Int. Agrophysics* 21 61-66.
- Glaž, T (2014) Effect of soil compaction and N fertilization on soil pore characteristics and physical quality of sandy loam soil under red clover/grass sward. *Soil and Tillage Research* 144 8-19. 10.1016/j.still.2014.05.010
- Gomez, KA, Gomez, KA, Gomez, AA (1984) 'Statistical procedures for agricultural research.' (John Wiley & Sons:
- Goutal, N, Parent, F, Bonnaud, P, Demaison, J, Nourrisson, G, Epron, D, Ranger, J (2012) Soil CO<sub>2</sub> concentration and efflux as affected by heavy traffic in forest in northeast France. *European Journal of Soil Science* 63 (2), 261-271. 10.1111/j.1365-2389.2011.01423.x
- Grover, BL (1955) Simplified Air Permeameters for Soil in Place 1. *Soil Science Society of America Journal* 19 (4), 414-418.
- Gruver, J, Weil, R, White, C, Lawley, Y (2014) Radishes: a new cover crop for organic farming systems. Michigan State University. Retrieved 10-01.
- Guamán Sarango, V (2015) Biological and mechanical subsoiling in potato production—a participatory research approach. Doctoral Thesis 'thesis', Swedish University of Agricultural Sciences.
- Guaman, V, Båth, B, Hagman, J, Gunnarsson, A, Persson, P (2016) Short time effects of biological and inter-row subsoiling on yield of potatoes grown on a loamy sand, and on soil penetration resistance, root growth and nitrogen uptake. *European Journal of Agronomy* 80 55-65.
- Guimarães, RML, Ball, BC, Tormena, CA (2011) Improvements in the visual evaluation of soil structure. *Soil Use and Management* no-no. 10.1111/j.1475-2743.2011.00354.x
- Håkansson, I (2005) Machinery-induced compaction of arable soils: incidence - consequences - counter-measures. Institutionen för markvetenskap, Avdelningen för jordbearbetning Number 0348-0976, Uppsala, Sweden. Available at <http://urn.kb.se/resolve?urn=urn:nbn:se:slu:epsilon-8-901>
- Håkansson, I, Reeder, RC (1994) Subsoil compaction by vehicles with high axle load—extent, persistence and crop response. *Soil and Tillage Research* 29 (2-3), 277-304.
- Hamza, MA, Anderson, WK (2005) Soil compaction in cropping systems - A review of the nature, causes and possible solutions. *Soil & Tillage Research* 82 (2), 121-145. 10.1016/j.still.2004.08.009
- Han, E, Kautz, T, Perkons, U, Lüsebrink, M, Pude, R, Köpke, U (2015) Quantification of soil biopore density after perennial fodder cropping. *Plant and Soil* 394 (1-2), 73-85.
- Hillel, D (1998) 'Environmental soil physics: Fundamentals, applications, and environmental considerations.' (Elsevier:
- Hodgkinson, L, Dodd, IC, Binley, A, Ashton, RW, White, RP, Watts, CW, Whalley, WR (2017) Root growth in field-grown winter wheat: Some effects of soil conditions, season and genotype. *European Journal of Agronomy* 91 74-83. 10.1016/j.eja.2017.09.014

## References

- Hoefler, G, Bachmann, J, Hartge, K (2010) Can the EM38 probe detect spatial patterns of subsoil compaction? In 'Proximal Soil Sensing'. pp. 265-273. (Springer:
- Horn, R, Domzal, H, Slowinskajurkiewicz, A, Vanouwerkerk, C (1995) Soil Compaction Processes and Their Effects on the Structure of Arable Soils and the Environment. *Soil & Tillage Research* 35 (1-2), 23-36. Doi 10.1016/0167-1987(95)00479-C
- Horn, R, Hartge, K, Bachmann, J, Kirkham, M (2007) Mechanical stresses in soils assessed from bulk-density and penetration-resistance data sets. *Soil Science Society of America Journal* 71 (5), 1455-1459.
- Horn, R, Van den Akker, J, Arvidsson, J (2000) 'Subsoil compaction: distribution, processes and consequences.' (Catena Verlag:
- Hu, X, Li, Z-C, Li, X-Y, Liu, Y (2015) Influence of shrub encroachment on CT-measured soil macropore characteristics in the Inner Mongolia grassland of northern China. *Soil and Tillage Research* 150 1-9.
- Hubbard, RK, Strickland, TC, Phatak, S (2013) Effects of cover crop systems on soil physical properties and carbon/nitrogen relationships in the coastal plain of southeastern USA. *Soil and Tillage Research* 126 276-283.
- Huber, S, Prokop, G, Arrouays, D, Banko, G, Bispo, A, Jones, R, Kibblewhite, M, Lexer, W, Möller, A, Rickson, R (2008) Environmental assessment of soil for monitoring: volume I, indicators & criteria. Office for the Official Publications of the European Communities, Luxembourg
- Iden, SC, Durner, W (2014) Comment on "Simple consistent models for water retention and hydraulic conductivity in the complete moisture range" by A. Peters. *Water Resources Research* 50 (9), 7530-7534.
- Islam, MM, Meerschman, E, Saey, T, De Smedt, P, De Vijver, EV, Delefortrie, S, Van Meirvenne, M (2014) Characterizing Compaction Variability with an Electromagnetic Induction Sensor in a Puddled Paddy Rice Field. *Soil Science Society of America Journal* 78 (2), 579-588. 10.2136/sssaj2013.07.0289
- Johannes, A, Weisskopf, P, Schulin, R, Boivin, P (2017) To what extent do physical measurements match with visual evaluation of soil structure? *Soil and Tillage Research* 173 24-32.
- Jokela, WE, Grabber, JH, Karlen, DL, Balser, TC, Palmquist, DE (2009) Cover Crop and Liquid Manure Effects on Soil Quality Indicators in a Corn Silage System. *Agronomy Journal* 101 (4), 727-737. 10.2134/agronj2008.0191
- Jones, RJ, Spoor, G, Thomasson, A (2003) Vulnerability of subsoils in Europe to compaction: a preliminary analysis. *Soil and Tillage Research* 73 (1-2), 131-143.
- Jury, WA, Or, D, Pachepsky, Y, Vereecken, H, Hopmans, JW, Ahuja, L, Clothier, B, Bristow, K, Kluitenberg, G, Moldrup, P (2011) Kirkham's legacy and contemporary challenges in soil physics research. *Soil Science Society of America Journal* 75 (5), 1589-1601.
- Karafiath, LL, Nowatzki, EA (1978) 'Soil mechanics for off-road vehicle engineering.' (Trans Tech Pubn:

- Katuwal, S, Arthur, E, Tuller, M, Moldrup, P, de Jonge, LW (2015a) Quantification of soil pore network complexity with X-ray computed tomography and gas transport measurements. *Soil Science Society of America Journal* 79 (6), 1577-1589.
- Katuwal, S, Moldrup, P, Lamandé, M, Tuller, M, De Jonge, LW (2015b) Effects of CT number derived matrix density on preferential flow and transport in a macroporous agricultural soil. *Vadose Zone Journal* 14 (7),
- Katuwal, S, Norgaard, T, Moldrup, P, Lamande, M, Wildenschild, D, de Jonge, LW (2015c) Linking air and water transport in intact soils to macropore characteristics inferred from X-ray computed tomography. *Geoderma* 237 9-20. 10.1016/j.geoderma.2014.08.006
- Kautz, T (2015) Research on subsoil biopores and their functions in organically managed soils: A review. *Renewable Agriculture and Food Systems* 30 (4), 318-327.
- Kay, B, Lal, R (1997) Soil structure and organic carbon: a review. *Soil processes and the carbon cycle* 198 169-197.
- Keller, T (2005) A model for the prediction of the contact area and the distribution of vertical stress below agricultural tyres from readily available tyre parameters. *Biosystems Engineering* 92 (1), 85-96. 10.1016/j.biosystemseng.2005.05.012
- Keller, T, Arvidsson, J, Schjønning, P, Lamande, M, Stettler, M, Weisskopf, P (2012) In Situ Subsoil Stress-Strain Behavior in Relation to Soil Precompression Stress. *Soil Science* 177 (8), 490-497. 10.1097/SS.0b013e318262554e
- Keller, T, Colombi, T, Ruiz, S, Manalili, MP, Rek, J, Stadelmann, V, Wunderli, H, Breitenstein, D, Reiser, R, Oberholzer, H (2017) Long-term soil structure observatory for monitoring post-compaction evolution of soil structure. *Vadose Zone Journal* 16 (4), 1-16.
- Keller, T, Defosse, P, Weisskopf, P, Arvidsson, J, Richard, G (2007) SoilFlex: A model for prediction of soil stresses and soil compaction due to agricultural field traffic including a synthesis of analytical approaches. *Soil & Tillage Research* 93 (2), 391-411. 10.1016/j.still.2006.05.012
- Keller, T, Lamand, M, Peth, S, Berli, M, Delenne, JY, Baumgarten, W, Rabbel, W, Radja, F, Rajchenbach, J, Selvadurai, APS, Or, D (2013) An interdisciplinary approach towards improved understanding of soil deformation during compaction. *Soil and Tillage Research* 128 61-80. 10.1016/j.still.2012.10.004
- Keller, T, Lamande, M (2010) Challenges in the development of analytical soil compaction models. *Soil & Tillage Research* 111 (1), 54-64. 10.1016/j.still.2010.08.004
- Keller, T, Ruiz, S, Stettler, M, Berli, M (2016) Determining Soil Stress beneath a Tire: Measurements and Simulations. *Soil Science Society of America Journal* 80 (3), 541-553. 10.2136/sssaj2015.07.0252
- Keller, T, Sandin, M, Colombi, T, Horn, R, Or, D (2019) Historical increase in agricultural machinery weights enhanced soil stress levels and adversely affected soil functioning. *Soil and Tillage Research* 194 104293.

## References

- Kirby, J (1999) Soil stress measurement. Part 2: transducer beneath a circular loaded area. *Journal of agricultural engineering research* 73 (2), 141-149.
- Koestel, J, Schlüter, S (2019) Quantification of the structure evolution in a garden soil over the course of two years. *Geoderma* 338 597-609.
- Kottek, M, Grieser, J, Beck, C, Rudolf, B, Rubel, F (2006) World map of the Koppen-Geiger climate classification updated. *Meteorologische Zeitschrift* 15 (3), 259-263. 10.1127/0941-2948/2006/0130
- Krebstien, K, von Janowsky, K, Kuht, J, Reintam, E (2014) The effect of tractor wheeling on the soil properties root growth of smooth brome. *Plant Soil and Environment* 60 (2), 74-79. 10.17221/804/2013-Pse
- Kuncoro, PH, Koga, K, Satta, N, Muto, Y (2014) A study on the effect of compaction on transport properties of soil gas and water. II: Soil pore structure indices. *Soil and Tillage Research* 143 180-187. 10.1016/j.still.2014.01.008
- Kussow, WR 'Six-year nitrogen leaching and runoff study on residential turf, Proceedings of the 70th Annual Michigan Turfgrass Conference, East Lansing, MI.'. 2000. Available
- Lal, R, Shukla, MK (2004) 'Principles of soil physics.' (CRC Press:
- Lamandé, M, Schjønning, P (2011a) Transmission of vertical stress in a real soil profile. Part I: Site description, evaluation of the Söhne model, and the effect of topsoil tillage. *Soil and Tillage Research* 114 (2), 57-70. 10.1016/j.still.2011.05.004
- Lamandé, M, Schjønning, P (2011b) Transmission of vertical stress in a real soil profile. Part II: Effect of tyre size, inflation pressure and wheel load. *Soil and Tillage Research* 114 (2), 71-77. 10.1016/j.still.2010.08.011
- Lamandé, M, Schjønning, P (2011c) Transmission of vertical stress in a real soil profile. Part III: Effect of soil water content. *Soil and Tillage Research* 114 (2), 78-85. 10.1016/j.still.2010.10.001
- Lamandé, M, Schjønning, P, Tøgersen, FA (2007) Mechanical behaviour of an undisturbed soil subjected to loadings: Effects of load and contact area. *Soil and Tillage Research* 97 (1), 91-106. 10.1016/j.still.2007.09.002
- Lamandé, M, Wildenschild, D, Berisso, FE, Garbout, A, Marsh, M, Moldrup, P, Keller, T, Hansen, SB, de Jonge, LW, Schjønning, P (2013a) X-ray CT and Laboratory Measurements on Glacial Till Subsoil Cores. *Soil Science* 178 (7), 359-368. 10.1097/SS.0b013e3182a79e1a
- Lamandé, M, Wildenschild, D, Berisso, FE, Garbout, A, Marsh, M, Moldrup, P, Keller, T, Hansen, SB, de Jonge, LW, Schjønning, P (2013b) X-ray CT and laboratory measurements on glacial till subsoil cores: Assessment of inherent and compaction-affected soil structure characteristics. *Soil Science* 178 (7), 359-368.
- Lapen, DR, Topp, GC, Edwards, ME, Gregorich, EG, Curnoe, WE (2004) Combination cone penetration resistance/water content instrumentation to evaluate cone penetration-water content relationships in tillage research. *Soil & Tillage Research* 79 (1), 51-62. 10.1016/j.still.2004.03.023
- Lassen, P, Lamandé, M, Stettler, M, Keller, T, Jørgensen, MS, Lilja, H, Alakukku, L, Pedersen, J, Schjønning, P 'Terranimo®-A soil compaction model with

- internationally compatible input options, EFITA/WCCA/CIGR 2013'. 2013. Available
- Laufer, D, Koch, HJ (2017) Growth and yield formation of sugar beet (*Beta vulgaris* L.) under strip tillage compared to full width tillage on silt loam soil in Central Europe. *European Journal of Agronomy* 82 182-189. 10.1016/j.eja.2016.10.017
- Lebert, M, Horn, R (1991) A method to predict the mechanical strength of agricultural soils. *Soil and Tillage Research* 19 (2-3), 275-286.
- Legland, D, Arganda-Carreras, I, Andrey, P (2016) MorphoLibJ: integrated library and plugins for mathematical morphology with ImageJ. *Bioinformatics* 32 (22), 3532-3534.
- Licht, MA, Al-Kaisi, M (2005) Corn response, nitrogen uptake, and water use in strip-tillage compared with no-tillage and chisel plow. *Agronomy Journal* 97 (3), 705-710. 10.2134/agronj2004.0102
- Linh, T (2016) Soil-improving cropping systems for sustainable rice production in the Vietnamese Mekong Delta. Ghent University.
- Lipiec, J, Arvidsson, J, Murer, E (2003) Review of modelling crop growth, movement of water and chemicals in relation to topsoil and subsoil compaction. *Soil & Tillage Research* 73 (1-2), 15-29. 10.1016/S0167-1987(03)00096-5
- Lipiec, J, Hatano, R (2003) Quantification of compaction effects on soil physical properties and crop growth. *Geoderma* 116 (1-2), 107-136. 10.1016/S0016-7061(03)00097-1
- Löfkvist, J (2005) Modifying soil structure using plant roots. Doctoral thesis 'thesis', Swedish University of Agricultural Sciences.
- Luo, L, Lin, H, Li, S (2010) Quantification of 3-D soil macropore networks in different soil types and land uses using computed tomography. *Journal of Hydrology* 393 (1-2), 53-64.
- Lynch, J (1995) Root Architecture and Plant Productivity. *Plant Physiol* 109 (1), 7-13.
- Lynch, JP, Wojciechowski, T (2015) Opportunities and challenges in the subsoil: pathways to deeper rooted crops. *Journal of Experimental Botany* 66 (8), 2199-2210.
- Maria do Rosário, GO, Van Noordwijk, M, Gaze, S, Brouwer, G, Bona, S, Mosca, G, Hairiah, K (2000) Auger sampling, ingrowth cores and pinboard methods. In 'Root methods'. pp. 175-210. (Springer:
- Materechera, S, Alston, A, Kirby, J, Dexter, A (1992) Influence of root diameter on the penetration of seminal roots into a compacted subsoil. *Plant and Soil* 144 (2), 297-303.
- Materechera, S, Dexter, A, Alston, AM (1991) Penetration of very strong soils by seedling roots of different plant species. *Plant and Soil* 135 (1), 31-41.
- Minasny, B, McBratney, AB (2006) A conditioned Latin hypercube method for sampling in the presence of ancillary information. *Computers & Geosciences* 32 (9), 1378-1388.

## References

- Mouazen, AM, Ramon, H (2009) Expanding implementation of an on-line measurement system of topsoil compaction in loamy sand, loam, silt loam and silt soils. *Soil and Tillage Research* 103 (1), 98-104.
- Munkholm, LJ, Heck, RJ, Deen, B (2012) Soil pore characteristics assessed from X-ray micro-CT derived images and correlations to soil friability. *Geoderma* 181 22-29.
- Munkholm, LJ, Schjønning, P, Jørgensen, MH, Thorup-Kristensen, K (2005) Mitigation of subsoil recompaction by light traffic and on-land ploughing: II. Root and yield response. *Soil and Tillage Research* 80 (1-2), 159-170.
- Naderi-Boldaji, M, Keller, T (2016) Degree of soil compactness is highly correlated with the soil physical quality index S. *Soil & Tillage Research* 159 41-46. 10.1016/j.still.2016.01.010
- Naveed, M, Moldrup, P, Arthur, E, Wildenschild, D, Eden, M, Lamandé, M, Vogel, H-J, De Jonge, LW (2013) Revealing soil structure and functional macroporosity along a clay gradient using X-ray computed tomography. *Soil Science Society of America Journal* 77 (2), 403-411.
- Naveed, M, Schjønning, P, Keller, T, de Jonge, LW, Moldrup, P, Lamandé, M (2016) Quantifying vertical stress transmission and compaction-induced soil structure using sensor mat and X-ray computed tomography. *Soil and Tillage Research* 158 110-122.
- Nawaz, MF, Bourrie, G, Trolard, F (2013) Soil compaction impact and modelling. A review. *Agronomy for Sustainable Development* 33 (2), 291-309. 10.1007/s13593-011-0071-8
- Nelissen, V, Ruyschaert, G, Manka'Abusi, D, D'Hose, T, De Beuf, K, Al-Barri, B, Cornelis, W, Boeckx, P (2015) Impact of a woody biochar on properties of a sandy loam soil and spring barley during a two-year field experiment. *European Journal of Agronomy* 62 65-78.
- Nevens, F, Reheul, D (2003) The consequences of wheel-induced soil compaction and subsoiling for silage maize on a sandy loam soil in Belgium. *Soil & Tillage Research* 70 (2), 175-184. Pii S0167-1987(02)00140-X
- Olesen, JE, Munkholm, LJ (2007) Subsoil loosening in a crop rotation for organic farming eliminated plough pan with mixed effects on crop yield. *Soil and Tillage Research* 94 (2), 376-385.
- Perkons, U, Kautz, T, Uteau, D, Peth, S, Geier, V, Thomas, K, Holz, KL, Athmann, M, Pude, R, Köpke, U (2014) Root-length densities of various annual crops following crops with contrasting root systems. *Soil and Tillage Research* 137 50-57.
- Peters, A (2013) Simple consistent models for water retention and hydraulic conductivity in the complete moisture range. *Water Resources Research* 49 (10), 6765-6780.

- Peters, A (2014) Reply to comment by S. Iden and W. Durner on “Simple consistent models for water retention and hydraulic conductivity in the complete moisture range”. *Water Resources Research* 50 (9), 7535-7539.
- Pfeifer, J, Kirchgessner, N, Colombi, T, Walter, A (2015) Rapid phenotyping of crop root systems in undisturbed field soils using X-ray computed tomography. *Plant methods* 11 (1), 41.
- Phansalkar, N, More, S, Sabale, A, Joshi, M 'Adaptive local thresholding for detection of nuclei in diversity stained cytology images, *Communications and Signal Processing (ICCSP), 2011 International Conference on*'. 2011. (IEEE. Available
- Pires, L, Roque, W, Rosa, J, Mooney, S (2019) 3D analysis of the soil porous architecture under long term contrasting management systems by X-ray computed tomography. *Soil and Tillage Research* 191 197-206.
- Pires, LF, Borges, JA, Rosa, JA, Cooper, M, Heck, RJ, Passoni, S, Roque, WL (2017) Soil structure changes induced by tillage systems. *Soil and Tillage Research* 165 66-79.
- Pöhlitz, J, Rücknagel, J, Koblenz, B, Schlüter, S, Vogel, H-J, Christen, O (2018) Computed tomography and soil physical measurements of compaction behaviour under strip tillage, mulch tillage and no tillage. *Soil and Tillage Research* 175 205-216.
- Poodt, M, Koolen, A, Van der Linden, J (2003) FEM analysis of subsoil reaction on heavy wheel loads with emphasis on soil preconsolidation stress and cohesion. *Soil and Tillage Research* 73 (1-2), 67-76.
- Popova, L, van Dusschoten, D, Nagel, KA, Fiorani, F, Mazzolai, B (2016) Plant root tortuosity: an indicator of root path formation in soil with different composition and density. *Annals of botany* 118 (4), 685-698.
- Pulido Moncada, M, Helwig Penning, L, Timm, LC, Gabriels, D, Cornelis, WM (2017) Visual examination of changes in soil structural quality due to land use. *Soil and Tillage Research* 173 83-91. 10.1016/j.still.2016.08.011
- Pulido-Moncada, M, Munkholm, LJ, Schjønning, P (2019) Wheel load, repeated wheeling, and traction effects on subsoil compaction in northern Europe. *Soil and Tillage Research* 186 300-309.
- Radford, BJ, Yule, DF, McGarry, D, Playford, C (2001) Crop responses to applied soil compaction and to compaction repair treatments. *Soil & Tillage Research* 61 (3-4), 157-166. Doi 10.1016/S0167-1987(01)00194-5
- Raper, R, Reeves, D, Burmester, C, Schwab, E (2000) Tillage depth, tillage timing, and cover crop effects on cotton yield, soil strength, and tillage energy requirements. *Applied Engineering in Agriculture* 16 (4), 379-386.
- Rasse, DP, Smucker, AJM (1998) Root recolonization of previous root channels in corn and alfalfa rotations. *Plant and soil* 204 (2), 203-212. Doi 10.1023/A:1004343122448
- Reeder, R, Wood, R, Finck, C (1993) Five subsoiler designs and their effects on soil properties and crop yields. *Transactions of the Asae* 36 (6), 1525-1531.
- Ren, L, D'Hose, T, Ruyschaert, G, De Pue, J, Meftah, R, Cnudde, V, Cornelis, WM (2019a) Effects of soil wetness and tyre pressure on soil physical quality and

## References

- maize growth by a slurry spreader system. *Soil and Tillage Research* 195 104344.
- Ren, L, Nest, TV, Ruyschaert, G, D'Hose, T, Cornelis, WM (2019b) Short-term effects of cover crops and tillage methods on soil physical properties and maize growth in a sandy loam soil. *Soil and Tillage Research* 192 76-86.
- Reynolds, W, Elrick, D (2002) 3.4. 3.3 Constant head well permeameter (vadose zone). *Methods of Soil Analysis: Part 4 Physical Methods (methodsofsoilan4)*, 844-858.
- Reynolds, WD, Drury, CF, Tan, CS, Fox, CA, Yang, XM (2009) Use of indicators and pore volume-function characteristics to quantify soil physical quality. *Geoderma* 152 (3-4), 252-263. 10.1016/j.geoderma.2009.06.009
- Roger-Estrade, J, Richard, G, Caneill, J, Boizard, H, Coquet, Y, Defosse, P, Manichon, H (2004) Morphological characterisation of soil structure in tilled fields: from a diagnosis method to the modelling of structural changes over time. *Soil & Tillage Research* 79 (1), 33-49. 10.1016/j.still.2004.03.009
- Romero-Ruiz, A, Linde, N, Keller, T, Or, D (2018) A review of geophysical methods for soil structure characterization. *Reviews of Geophysics* 56 (4), 672-697.
- Rücknagel, J, Hofmann, B, Deumelandt, P, Reinicke, F, Bauhardt, J, Hülsbergen, K-J, Christen, O (2015) Indicator based assessment of the soil compaction risk at arable sites using the model REPRO. *Ecological indicators* 52 341-352.
- Ryken, N, Nest, TV, Al-Barri, B, Blake, W, Taylor, A, Bode, S, Ruyschaert, G, Boeckx, P, Verdoodt, A (2018) Soil erosion rates under different tillage practices in central Belgium: New perspectives from a combined approach of rainfall simulations and Be-7 measurements. *Soil & Tillage Research* 179 29-37. 10.1016/j.still.2018.01.010
- Schäfer-Landefeld, L, Brandhuber, R, Fenner, S, Koch, H-J, Stockfisch, N (2004) Effects of agricultural machinery with high axle load on soil properties of normally managed fields. *Soil and Tillage Research* 75 (1), 75-86.
- Schäffer, B, Mueller, TL, Stauber, M, Müller, R, Keller, M, Schulin, R (2008) Soil and macro-pores under uniaxial compression. II. Morphometric analysis of macro-pore stability in undisturbed and repacked soil. *Geoderma* 146 (1), 175-182. <https://doi.org/10.1016/j.geoderma.2008.05.020>
- Schjønning, P, Lamandé, M (2010) A note on the vertical stresses near the soil-tyre interface. *Soil and Tillage Research* 108 (1-2), 77-82.
- Schjønning, P, Lamandé, M, Berisso, FE, Simojoki, A, Alakukku, L, Andreasen, RR (2013) Gas Diffusion, Non-Darcy Air Permeability, and Computed Tomography Images of a Clay Subsoil Affected by Compaction. *Soil Science Society of America Journal* 77 (6), 1977. 10.2136/sssaj2013.06.0224
- Schjønning, P, Lamandé, M, Créten, V, Nielsen, JA (2017) Upper subsoil pore characteristics and functions as affected by field traffic and freeze-thaw and dry-wet treatments. *Soil Research* 55 (3), 234-244.
- Schjønning, P, Lamandé, M, Keller, T, Pedersen, J, Stettler, M (2012) Rules of thumb for minimizing subsoil compaction. *Soil Use and Management* 28 (3), 378-393.

- Schjønning, P, Lamandé, M, Munkholm, LJ, Lyngvig, HS, Nielsen, JA (2016) Soil precompression stress, penetration resistance and crop yields in relation to differently-trafficked, temperate-region sandy loam soils. *Soil and Tillage Research* 163 298-308. 10.1016/j.still.2016.07.003
- Schjønning, P, Lamande, M, Tøgersen, FA, Arvidsson, J, Keller, T (2006) Distribution of vertical stress at the soil-tyre interface: Effects of tyre inflation pressure and the impact on stress propagation in the soil profile. *Soil Management for Sustainability* 38 38-+.
- Schjønning, P, Lamandé, M, Tøgersen, FA, Arvidsson, J, Keller, T (2008) Modelling effects of tyre inflation pressure on the stress distribution near the soil-tyre interface. *Biosystems Engineering* 99 (1), 119-133.
- Schjønning, P, Lamandé, M., Lassen, P. (2019) An introduction to Terranimo® ([www.terranimodk.dk](http://www.terranimodk.dk)). Unpublished note, Aarhus University, Dept. Agroecology
- Schjønning, P, Lamandé, Mathieu, M.H Thorsøe, A. Freluh-Larsen (2018) subsoil compaction – a threat to sustainable food production and soil ecosystem services  
. Available
- Schjønning, P, van den Akker, JJH, Keller, T, Greve, MH, Lamandé, M, Simojoki, A, Stettler, M, Arvidsson, J, Breuning-Madsen, H (2015) Driver-Pressure-State-Impact-Response (DPSIR) Analysis and Risk Assessment for Soil Compaction—A European Perspective. 133 183-237. 10.1016/bs.agron.2015.06.001
- Schneider, F, Don, A, Hennings, I, Schmittmann, O, Seidel, SJ (2017) The effect of deep tillage on crop yield – What do we really know? *Soil and Tillage Research* 174 193-204. 10.1016/j.still.2017.07.005
- Sibson, R (1981) 'A brief description of natural neighbour interpolation.'
- Smith, R, Ellies, A, Horn, R (2000) Modified Boussinesq's equations for nonuniform tire loading. *Journal of Terramechanics* 37 (4), 207-222. Doi 10.1016/S0022 4898(00)00007-0
- Snapp, S, Swinton, S, Labarta, R, Mutch, D, Black, J, Leep, R, Nyiraneza, J, O'neil, K (2005) Evaluating cover crops for benefits, costs and performance within cropping system niches. *Agronomy Journal* 97 (1), 322-332.
- Soane, B, Van Ouwerkerk, C (1994) Soil compaction problems in world agriculture. In 'Developments in agricultural engineering'. Vol. 11, pp. 1-21. (Elsevier:
- Soane, BD, Blackwell, PS, Dickson, JW, Painter, DJ (1980a) Compaction by agricultural vehicles: A review I. Soil and wheel characteristics. *Soil and Tillage Research* 1 207-237. 10.1016/0167-1987(80)90026-4
- Soane, BD, Blackwell, PS, Dickson, JW, Painter, DJ (1980b) Compaction by agricultural vehicles: A review II. Compaction under tyres and other running gear. *Soil and Tillage Research* 1 373-400. 10.1016/0167-1987(80)90039-2
- Soane, BD, Dickson, JW, Campbell, DJ (1982) Compaction by agricultural vehicles: A review III. Incidence and control of compaction in crop production. *Soil and Tillage Research* 2 (1), 3-36. 10.1016/0167-1987(82)90030-7

## References

- Söhne, W (1953) Druckverteilung im Boden und Bodenformung unter Schleppereiffen (Pressure distribution in the soil and soil deformation under tractor tyres). *Grundlagen der Landtechnik* 5 49-63.
- Soil Science Society of America, S (1997) Glossary of Soil Science Terms. SSSA Madison, Wisconsin (WI).
- Stadler, A, Rudolph, S, Kupisch, M, Langensiepen, M, van der Kruk, J, Ewert, F (2015) Quantifying the effects of soil variability on crop growth using apparent soil electrical conductivity measurements. *European Journal of Agronomy* 64 8-20.
- Stettler, M, Keller, T, Weisskopf, P, Lamandé, M, Lassen, P, Schjønning, P (2014) Terranimo®—a web-based tool for evaluating soil compaction. *landtechnik* 69 (3), 132-138.
- Stott, P (2016) How climate change affects extreme weather events. *Science* 352 (6293), 1517-1518.
- Sudduth, K, Kitchen, N, Wiebold, W, Batchelor, W, Bollero, GA, Bullock, D, Clay, D, Palm, H, Pierce, F, Schuler, R (2005) Relating apparent electrical conductivity to soil properties across the north-central USA. *Computers and Electronics in Agriculture* 46 (1-3), 263-283.
- Temesgen, M, Savenije, HHG, Rockstrom, J, Hoogmoed, WB (2012) Assessment of strip tillage systems for maize production in semi-arid Ethiopia: Effects on grain yield, water balance and water productivity. *Physics and Chemistry of the Earth* 47-48 156-165. 10.1016/j.pce.2011.07.046
- Torbert, H, Reeves, D (1995) Interactions of traffic and tillage applied to cotton on N movement below the root zone of a subsequent wheat crop. *Soil and Tillage Research* 33 (1), 3-16.
- Tracy, SR, Black, CR, Roberts, JA, Mooney, SJ (2011) Soil compaction: a review of past and present techniques for investigating effects on root growth. *J Sci Food Agric* 91 (9), 1528-37. 10.1002/jsfa.4424
- Tracy, SR, Black, CR, Roberts, JA, Sturrock, C, Mairhofer, S, Craigon, J, Mooney, SJ (2012) Quantifying the impact of soil compaction on root system architecture in tomato (*Solanum lycopersicum*) by X-ray micro-computed tomography. *Annals of botany* 110 (2), 511-519.
- Unger, PW, Kaspar, TC (1994) Soil compaction and root growth: a review. *Agronomy Journal* 86 (5), 759-766.
- van Asselen, S, Stouthamer, E, van Asch, TWJ (2009) Effects of peat compaction on delta evolution: A review on processes, responses, measuring and modeling. *Earth-Science Reviews* 92 (1-2), 35-51. 10.1016/j.earscirev.2008.11.001
- Van den Akker, J (2004) SOCOMO: a soil compaction model to calculate soil stresses and the subsoil carrying capacity. *Soil and Tillage Research* 79 (1), 113-127.
- Van den Putte, A, Govers, G, Diels, J, Gillijns, K, Demuzere, M (2010) Assessing the effect of soil tillage on crop growth: A meta-regression analysis on European crop yields under conservation agriculture. *European Journal of Agronomy* 33 (3), 231-241. 10.1016/j.eja.2010.05.008

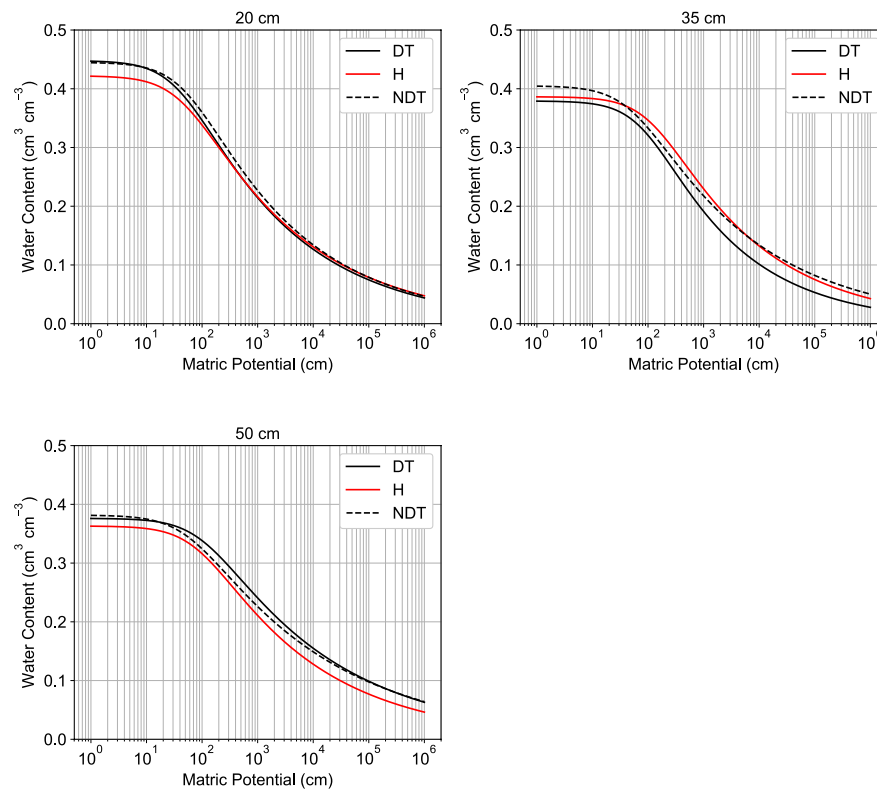
- Van Genuchten, MT (1980) A closed-form equation for predicting the hydraulic conductivity of unsaturated soils 1. *Soil Science Society of America Journal* 44 (5), 892-898.
- Van Noordwijk, M, Brouwer, G, Meijboom, F, Oliveira, MdRG, Bengough, A (2001) Trench profile techniques and core break methods. In 'Root methods'. pp. 211-233. (Springer:
- Vermang, J (2012) Erosion processes and physical quality of loamy soils as affected by reduced tillage (Doctoral dissertation, Ghent University).
- Vetsch, JA, Randall, GW, Lamb, JA (2007) Corn and Soybean Production as Affected by Tillage Systems. *Agronomy Journal* 99 (4), 952. 10.2134/agronj2006.0149
- Vlassenbroeck, J, Dierick, M, Masschaele, B, Cnudde, V, Van Hoorebeke, L, Jacobs, P (2007) Software tools for quantification of X-ray microtomography at the UGCT. *Nuclear Instruments and Methods in Physics Research Section A: Accelerators, Spectrometers, Detectors and Associated Equipment* 580 (1), 442-445.
- Vogel, H-J, Weller, U, Schlüter, S (2010) Quantification of soil structure based on Minkowski functions. *Computers & Geosciences* 36 (10), 1236-1245.
- Vyn, TJ, Raimbault, BA (1992) Evaluation of Strip Tillage Systems for Corn Production in Ontario. *Soil & Tillage Research* 23 (1-2), 163-176. Doi 10.1016/0167-1987(92)90012-Z
- Walkley, A, Black, IA (1934) An examination of the Degtjareff method for determining soil organic matter, and a proposed modification of the chromic acid titration method. *Soil Science* 37 (1), 29-38.
- Wang, Y, Zhang, JH, Zhang, ZH (2015) Influences of intensive tillage on water-stable aggregate distribution on a steep hillslope. *Soil & Tillage Research* 151 82-92. 10.1016/j.still.2015.03.003
- Weil, R, Kremen, A (2007) Thinking across and beyond disciplines to make cover crops pay. *Journal of the Science of Food and Agriculture* 87 (4), 551-557.
- Wesseling, J, Elbers, J, Kabat, P, Van den Broek, B (1991) SWATRE: Instructions for input. Internal Note, Winand Staring Centre, Wageningen, the Netherlands
- Whalley, W, Dumitru, E, Dexter, A (1995) Biological effects of soil compaction. *Soil and Tillage Research* 35 (1-2), 53-68.
- Williams, SM, Weil, RR (2004) Crop cover root channels may alleviate soil compaction effects on soybean crop. *Soil Science Society of America Journal* 68 (4), 1403-1409. DOI 10.2136/sssaj2004.1403
- Woebbecke, DM, Meyer, GE, Von Bargen, K, Mortensen, D (1995) Color indices for weed identification under various soil, residue, and lighting conditions. *Transactions of the Asae* 38 (1), 259-269.
- Zappala, S, Mairhofer, S, Tracy, S, Sturrock, CJ, Bennett, M, Pridmore, T, Mooney, SJ (2013) Quantifying the effect of soil moisture content on segmenting root system architecture in X-ray computed tomography images. *Plant and Soil* 370 (1-2), 35-45.
- Zhang, CX, Miller, GL, Rufty, TW, Bowman, DC (2013) Nitrate Leaching from Two Kentucky Bluegrass Cultivars as Affected by Nitrate Uptake Capacity and

## References

- Subsurface Soil Compaction. Crop Science 53 (4), 1722-1733.  
10.2135/cropsci2012.10.0600
- Zhou, H, Mooney, SJ, Peng, XH (2017) Bimodal Soil Pore Structure Investigated by a Combined Soil Water Retention Curve and X-Ray Computed Tomography Approach. Soil Science Society of America Journal 81 (6), 1270-1278.  
10.2136/sssaj2016.10.0338

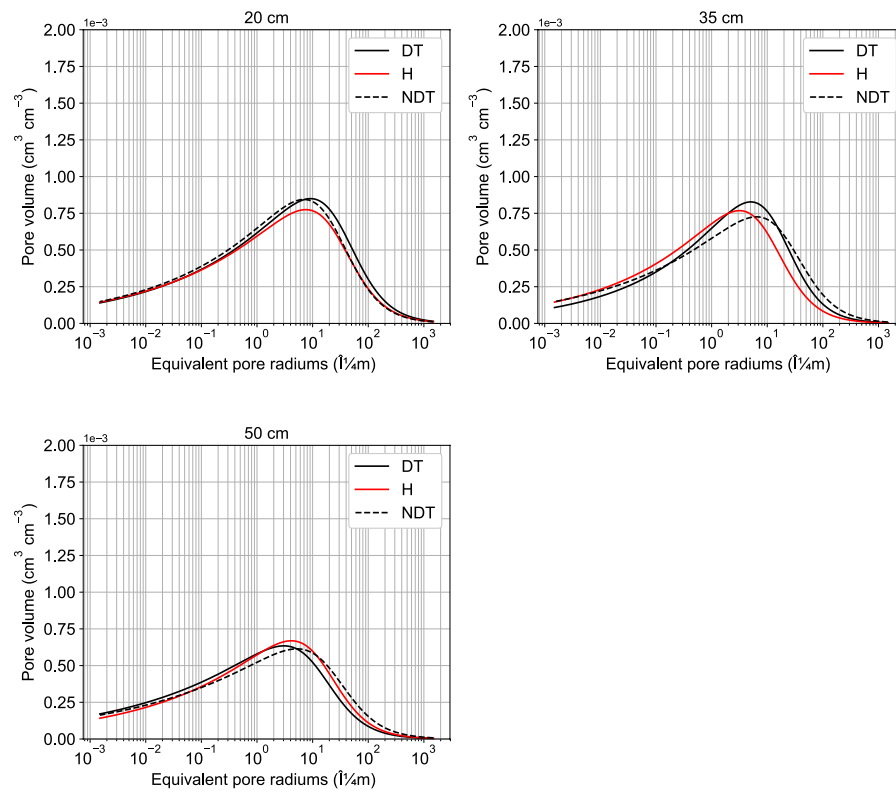
## Appendices:

### Appendices in chapter 2:

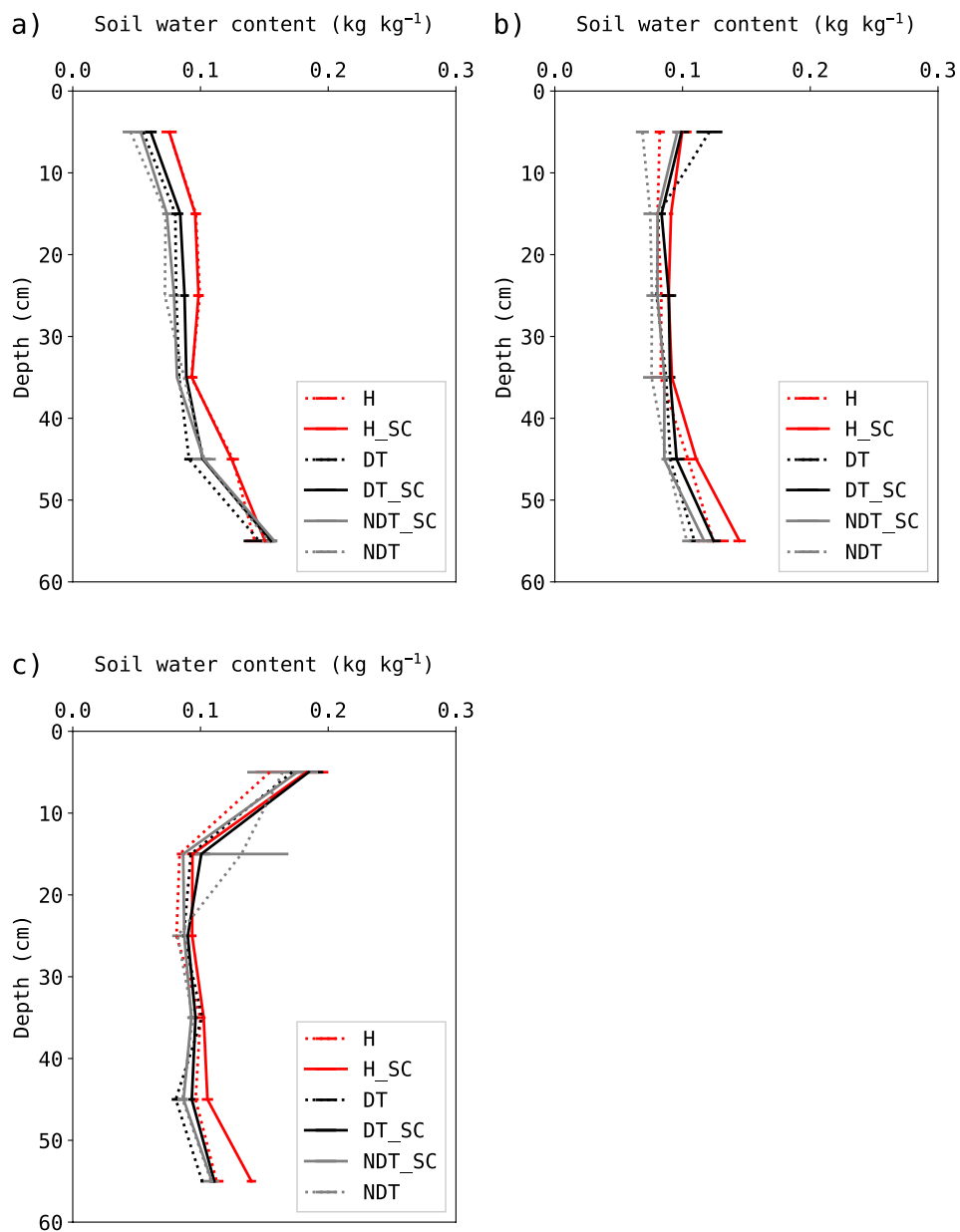


S1. Soil water retention curves (SWRC) for each treatment (H=highly compacted; DT= deep tillage; NDT= no deep tillage).

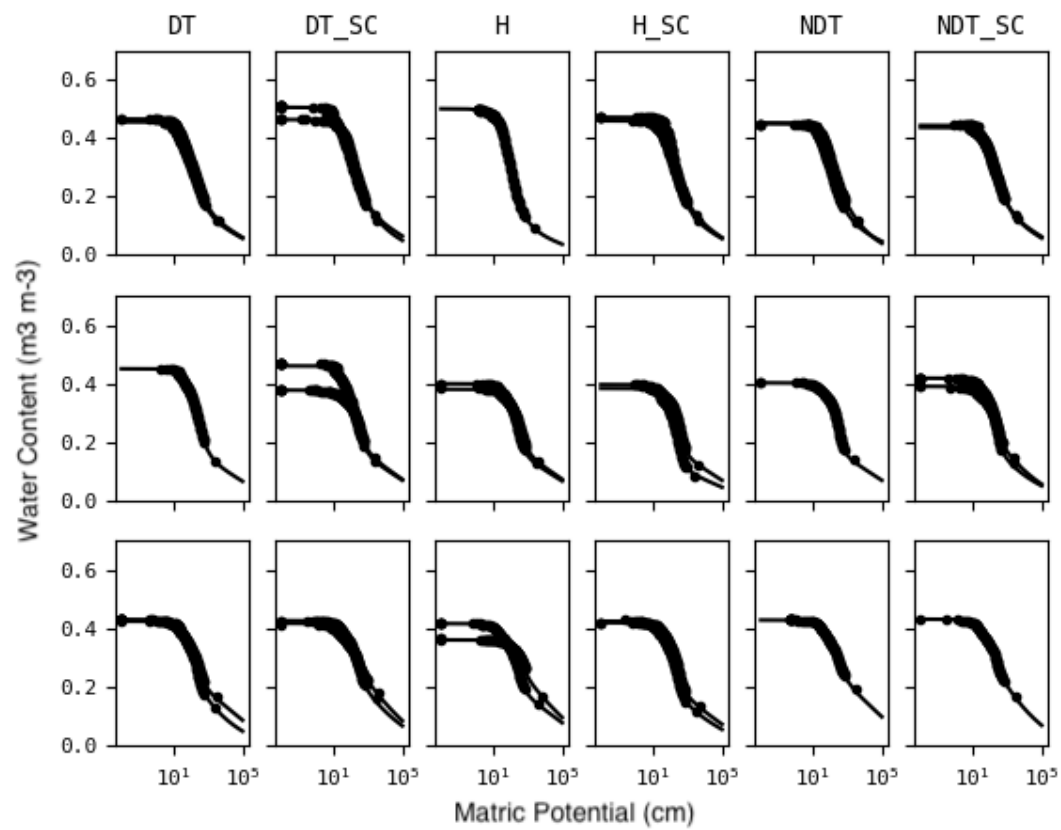
## Appendices



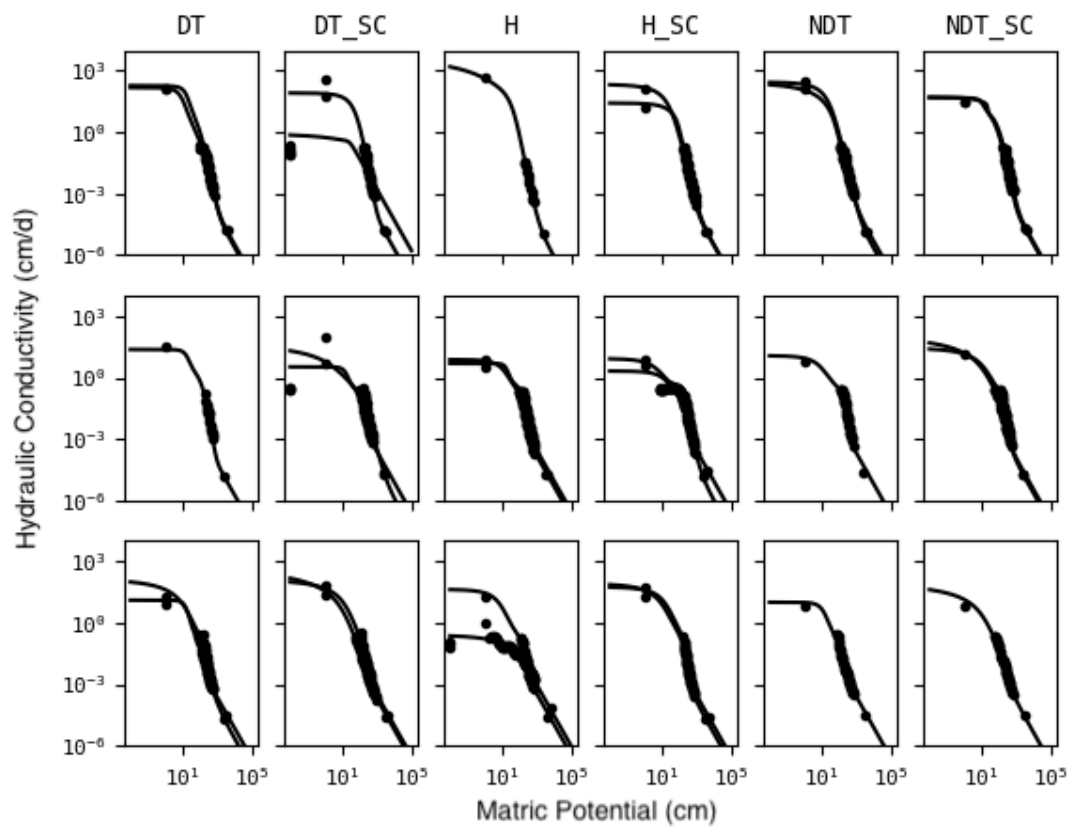
S2. Pore size distribution (H=highly compacted; DT= deep tillage; NDT= no deep tillage).



S3. Manually measured soil water content on 30/06 (a), 27/07 (b) and 18/08 (c). (H = high subsoil compaction; DT = deep tillage; NDT = no deep tillage). Error bars are standard deviation with  $n = 3$ .



S4. Measured and fitted soil water retention curves (fitted with PDI biomodal) in each treatments with all replicatons among three depth (first row = 15 cm; second row = 35 cm; third row = 50 cm).



S5. Measured and fitted hydraulic conductivity curves (fitted with PDI model using  $K_s$  and  $K_u$ ) in each treatment with two replicates among three depth (first row = 15 cm; second row = 35 cm; third row = 50 cm).

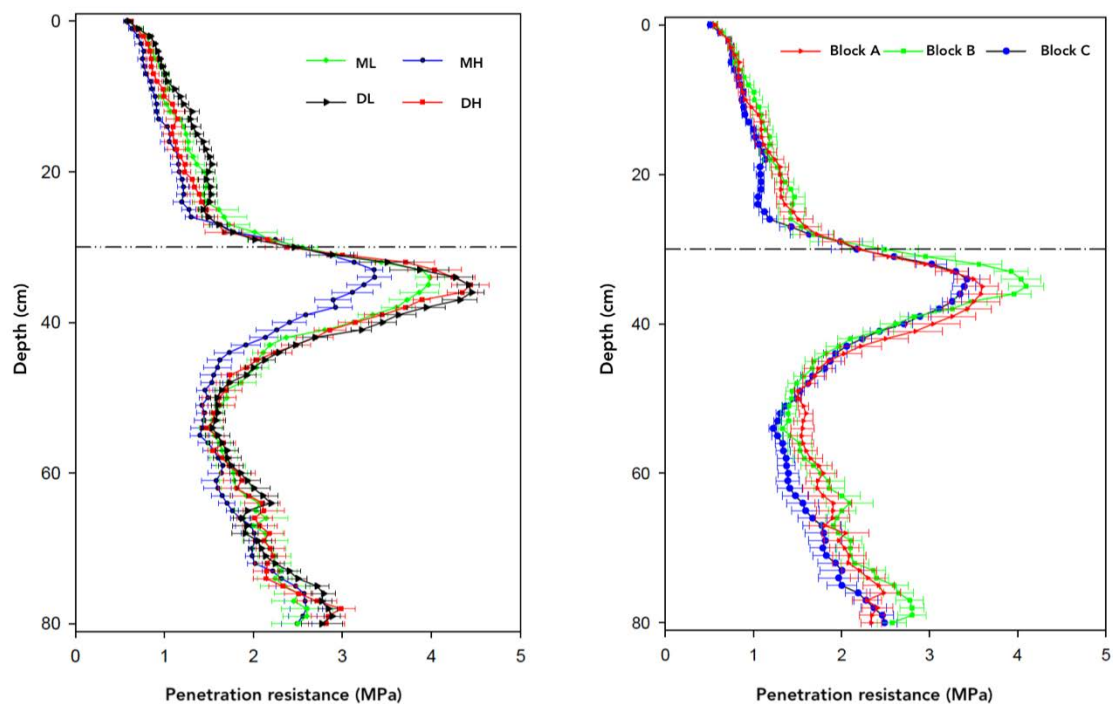


S6. Soil core at 50 cm in the in-field zone (left) and headland zone (right).



S7. Maize growth conditions at highly subsoil compaction area (headland zone) (left) and normal subsoil compaction area (in-field zone) (right) on 09/09/2017.

#### Appendices in chapter 4:



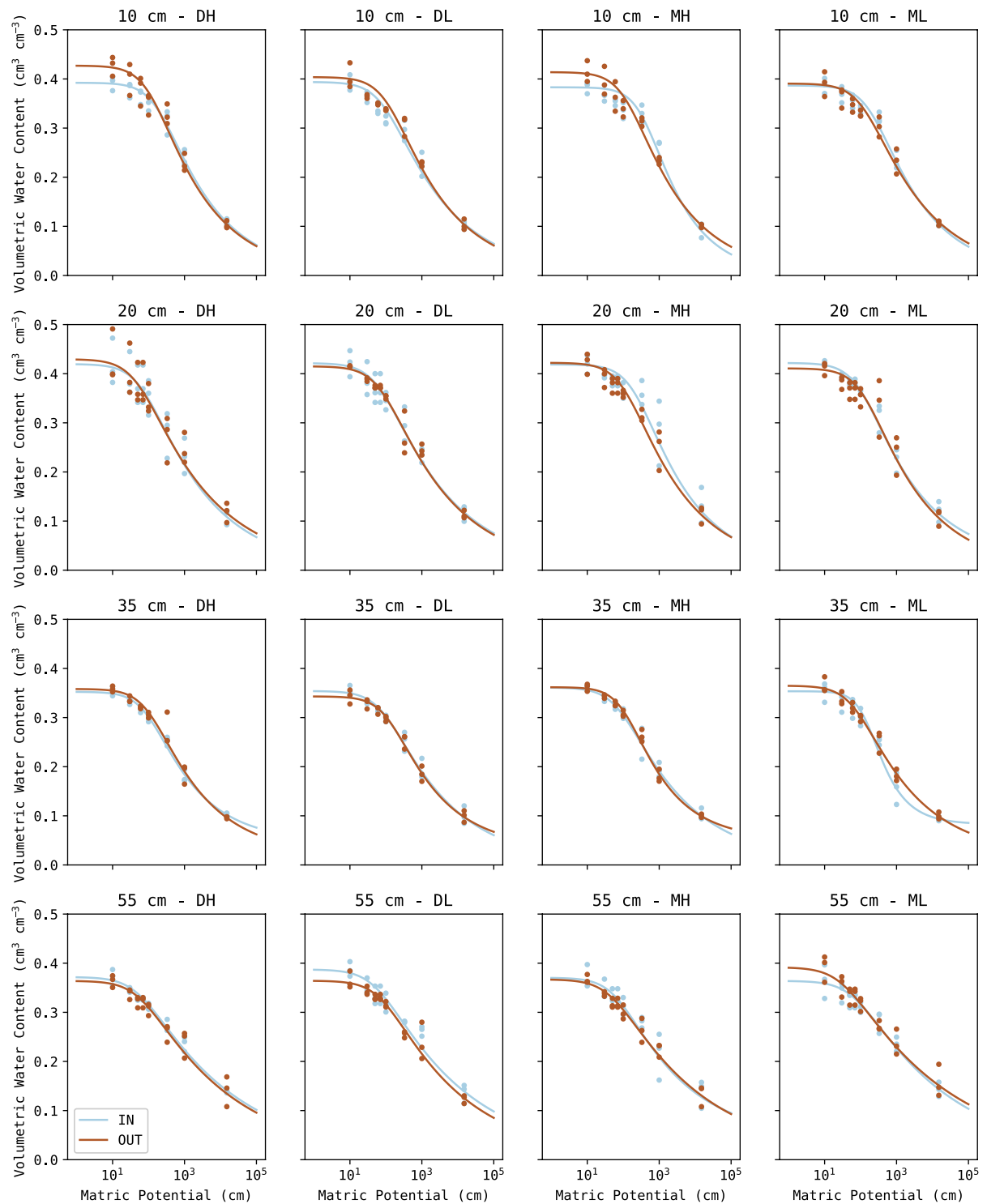
S1. Penetration resistance (average  $\pm$  standard deviation) for treatments (left;  $n = 30$ ) and blocks (right;  $n = 40$ ) before traffic conduction (the dotted line indicates the plough depth: 30 cm). DH=dry-high pressure; DL=dry-low pressure; MH=moist-high pressure; ML=moist-low pressure.

S2. Soil chemical properties in each treatment before the test (average  $\pm$  standard deviation, n = 3).

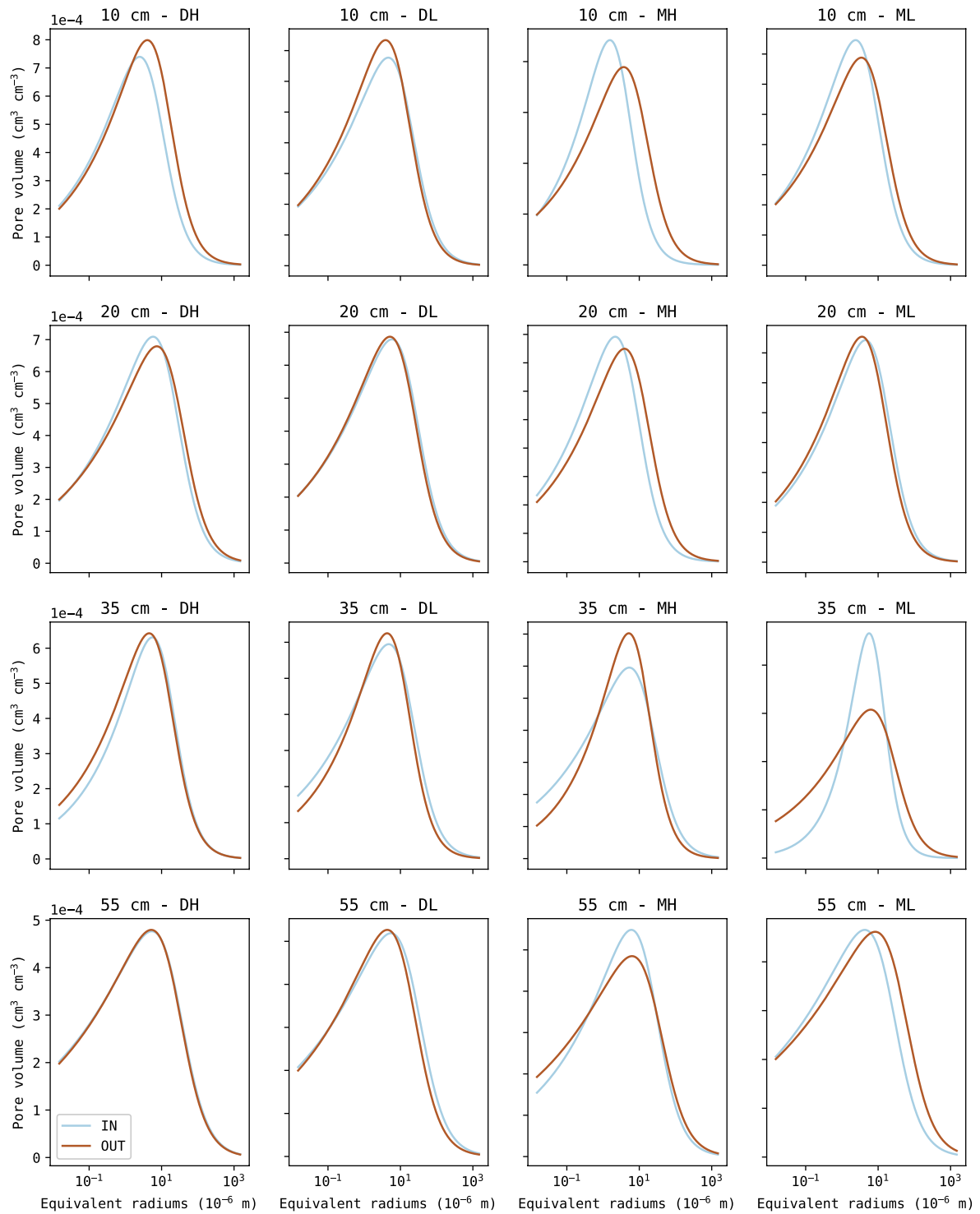
Treatments	0-30 cm		0-90 cm		
			NO <sub>3</sub> -N	NH <sub>4</sub> -N	total-N
	SOC (%)	Total-N (kg ha <sup>-1</sup> )	(kg ha <sup>-1</sup> )	(kg ha <sup>-1</sup> )	(kg ha <sup>-1</sup> )
DL	1.60 $\pm$ 0.09	0.14 $\pm$ 0.01	8.7 $\pm$ 0.1	16.9 $\pm$ 0.7	25.6 $\pm$ 0.7
DH	1.57 $\pm$ 0.03	0.14 $\pm$ 0.01	9.3 $\pm$ 1.0	17.6 $\pm$ 0.5	26.9 $\pm$ 0.9
ML	1.63 $\pm$ 0.08	0.15 $\pm$ 0.01	11.2 $\pm$ 3.0	17.1 $\pm$ 1.4	28.3 $\pm$ 2.6
MH	1.57 $\pm$ 0.11	0.14 $\pm$ 0.01	8.9 $\pm$ 0.3	17.7 $\pm$ 1.1	26.6 $\pm$ 0.8

No significant effects ( $p > 0.05$ ) of treatment on soil chemical properties were found; SOC = soil organic carbon content; DH=dry-high pressure; DL=dry-low pressure; MH=moist-high pressure; ML=moist-low pressure.

## Appendices



S3. Soil water retention curves at each depth for in and out track position (DH=dry-high pressure; DL=dry-low pressure; MH=moist-high pressure; ML=moist-low pressure), with dots are measured values (n=3) and line are fitted by Van Genuchten (1980) model.



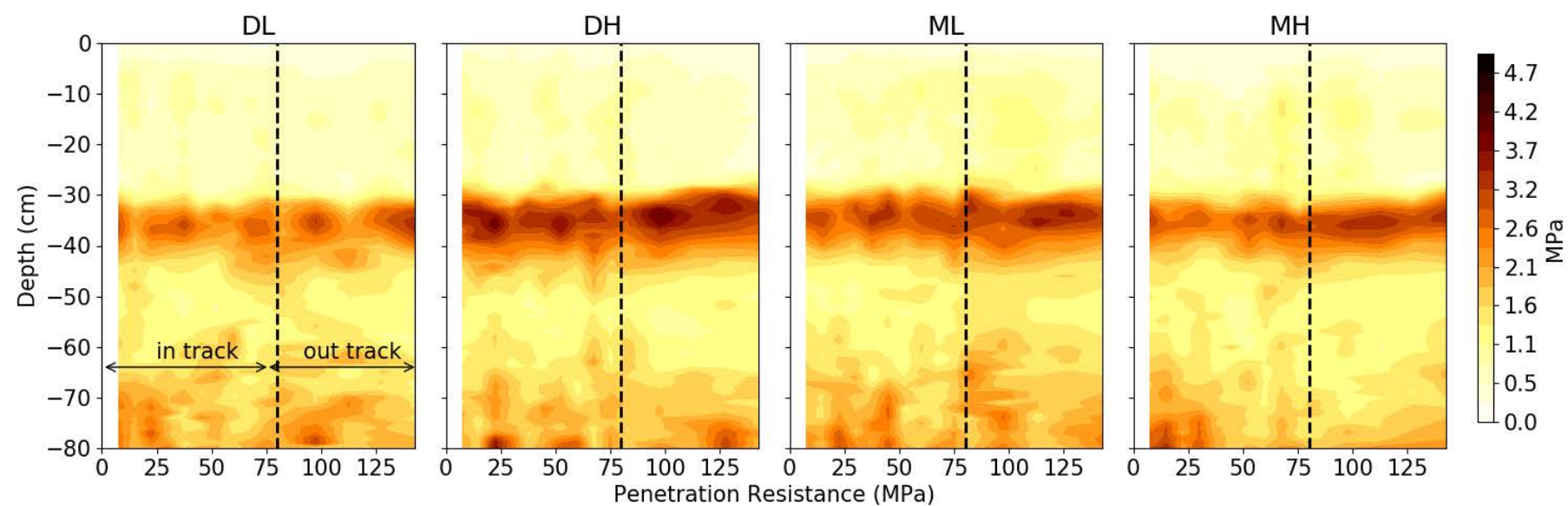
S4. Soil pore size distribution curves at each depth for in and out track position (DH=dry-high pressure; DL=dry-low pressure; MH=moist-high pressure; ML=moist-low pressure).

## Appendices

S5. Bulk density, porosity and soil moisture content at different pF value at 35 (left) and 55 cm (right) depth (average  $\pm$  standard deviation).

Factor	Bulk density	Total porosity	Ka	Pore size distribution (m³ m⁻³)			Bulk density	Total porosity	Ka	Pore size distribution (m³ m⁻³)			
	Mg m⁻³	m³ m⁻³		µm²	d > 30 µm	30 µm > d > 0.2 µm				d < 0.2 µm	Mg m⁻³	m³ m⁻³	µm²
Moisture conditions													
Moist	1.62 ± 0.03	0.39 ± 0.01	4.21 ± 3.21	0.08 ± 0.01	0.21 ± 0.02	0.10 ± 0.01	1.58 ± 0.06	0.40 ± 0.03	5.30 ± 5.73	0.09 ± 0.02	0.17 ± 0.02	0.14 ± 0.02	
Dry	1.63 ± 0.06	0.38 ± 0.02	2.92 ± 3.42	0.09 ± 0.02	0.20 ± 0.01	0.10 ± 0.01	1.50 ± 0.06	0.43 ± 0.02	9.09 ± 4.02	0.12 ± 0.03	0.18 ± 0.01	0.14 ± 0.01	
Tire pressure													
low	1.64 ± 0.05	0.38 ± 0.02	3.64 ± 3.31	0.08 ± 0.02	0.20 ± 0.02	0.10 ± 0.01	1.52 ± 0.06	0.43 ± 0.02	9.60 ± 5.78	0.11 ± 0.03	0.17 ± 0.02	0.14 ± 0.02	
High	1.61 ± 0.04	0.39 ± 0.02	3.48 ± 3.46	0.09 ± 0.02	0.20 ± 0.01	0.10 ± 0.01	1.56 ± 0.09	0.41 ± 0.03	4.79 ± 3.17	0.10 ± 0.03	0.17 ± 0.01	0.14 ± 0.02	
Treatments													
DL	1.66 ± 0.06	0.37 ± 0.02	2.77 ± 3.41	1.66 ± 0.06	0.20 ± 0.01	0.10 ± 0.01	1.56 ± 0.08	0.41 ± 0.03	7.08 ± 5.12	0.10 ± 0.04	0.19 ± 0.01	0.13 ± 0.01	
DH	1.61 ± 0.05	0.39 ± 0.02	5.47 ± 5.53	1.61 ± 0.05	0.20 ± 0.01	0.10 ± 0.00	1.51 ± 0.08	0.43 ± 0.03	9.53 ± 10.38	0.12 ± 0.03	0.17 ± 0.01	0.14 ± 0.02	
ML	1.63 ± 0.06	0.38 ± 0.02	5.28 ± 4.62	1.63 ± 0.06	0.20 ± 0.02	0.10 ± 0.01	1.52 ± 0.04	0.43 ± 0.02	12.09 ± 8.33	0.11 ± 0.02	0.16 ± 0.03	0.15 ± 0.02	
MH	1.65 ± 0.05	0.38 ± 0.02	4.32 ± 2.85	1.65 ± 0.05	0.21 ± 0.01	0.10 ± 0.01	1.59 ± 0.06	0.40 ± 0.02	6.16 ± 4.46	0.10 ± 0.03	0.17 ± 0.02	0.14 ± 0.02	
Track													
in	1.63 ± 0.05	0.39 ± 0.02	3.56 ± 3.31	1.63 ± 0.05	0.20 ± 0.01	0.10 ± 0.01	1.54 ± 0.07	0.42 ± 0.03	7.19 ± 5.07	0.11 ± 0.03	0.17 ± 0.01	0.14 ± 0.02	
out	1.65 ± 0.06	0.38 ± 0.02	5.50 ± 4.90	1.65 ± 0.06	0.20 ± 0.01	0.10 ± 0.01	1.54 ± 0.07	0.42 ± 0.03	9.63 ± 8.47	0.11 ± 0.03	0.17 ± 0.02	0.14 ± 0.03	
Statistical analysis													
Moisture <sup>1</sup>	0.84	1.00	0.32	0.71	0.28	0.61	0.08	0.08	0.40	0.20	0.47	0.79	
Tire pressure <sup>1</sup>	0.32	0.26	0.90	0.40	0.86	0.52	0.33	0.33	0.24	0.49	0.98	0.84	
Moisture x Treatments <sup>2</sup>	0.84	1.00	0.03	0.95	0.89	0.76	0.30	0.30	0.96	0.30	0.39	0.73	
Track <sup>2</sup>	0.22	0.49	0.05	0.32	0.56	0.76	0.94	0.94	0.44	0.83	0.66	1.00	
Treatment x track <sup>2</sup>	0.19	0.20	0.00	0.26	0.62	0.79	0.20	0.20	0.33	0.24	0.81	0.76	

<sup>1</sup> p-values are displayed using two-way ANOVA; p < 0.10 is indicated in bold; p < 0.05 is indicated in bold and underlined. <sup>2</sup> p-value are displayed using Split-Plot Design with two factors (treatment and track). DH=dry-high pressure; DL=dry-low pressure; MH=moist-high pressure; ML=moist-low pressure.



S6. Soil PR (n=6) after ploughing in maize growing season for each treatment within 80 cm depth (D: dry condition; M: moist condition; L: low pressure; H: high pressure).

## Appendices

### S7. Sub soil physical properties in the summer maize season (average $\pm$ standard deviation).

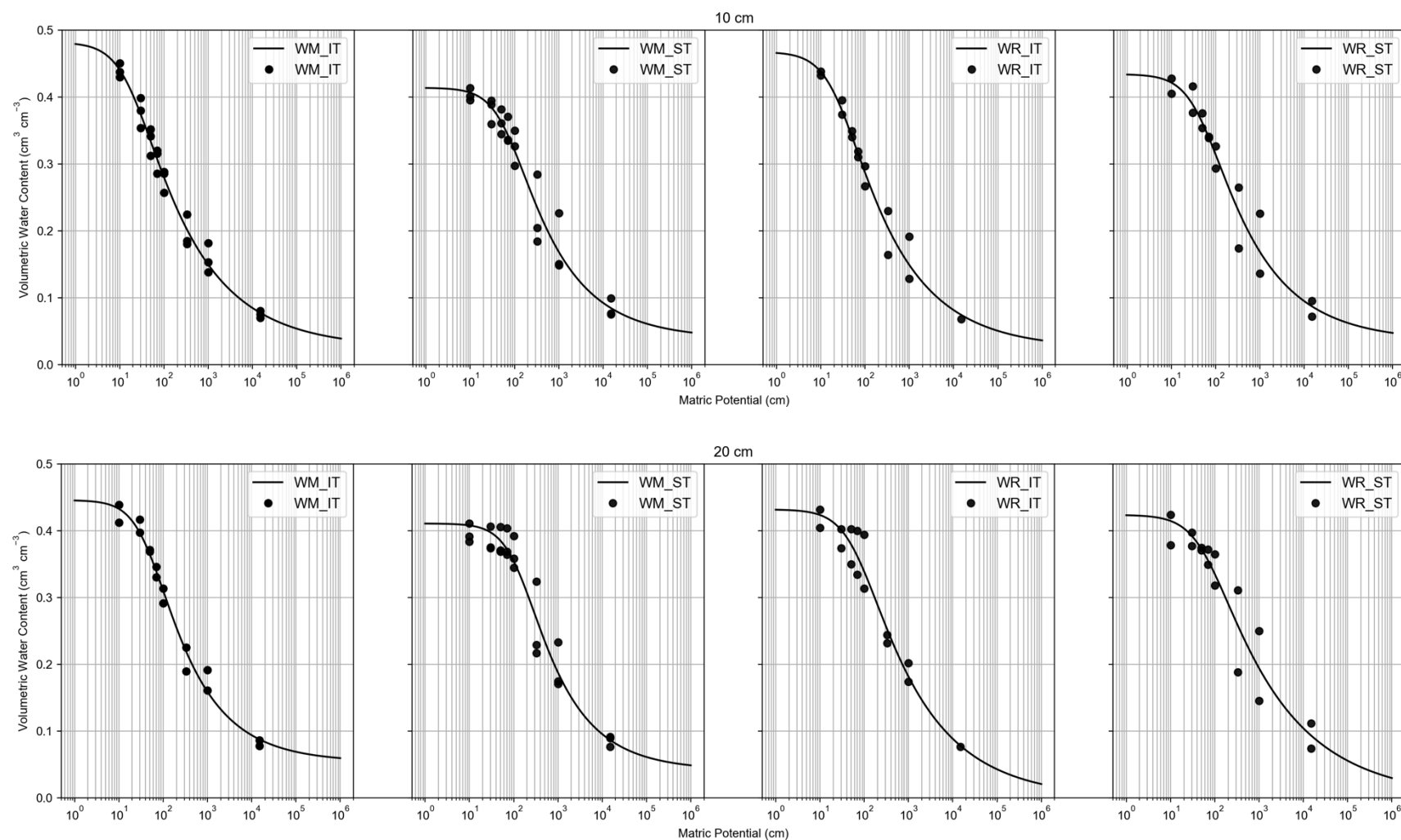
Factor	Bulk density ( $\text{g cm}^{-3}$ )		Macro-pores ( $\text{m}^3 \text{m}^{-3}$ )		Penetration resistance (MPa)
	35 cm	55 cm	35 cm	55 cm	30-80 cm
Moisture conditions					
Moist	x	x	x	x	$1.61 \pm 0.30$
Dry	x	x	x	x	$1.63 \pm 0.35$
Tire pressure					
Low	$1.65 \pm 0.07$	$1.64 \pm 0.12$	$0.07 \pm 0.02$	$0.05 \pm 0.05$	$1.58 \pm 0.26$
High	$1.67 \pm 0.05$	$1.49 \pm 0.12$	$0.06 \pm 0.03$	$0.12 \pm 0.05$	$1.66 \pm 0.38$
Treatments					
DL	x	x	x	x	$1.56 \pm 0.24\text{a}$
DH	x	x	x	x	$1.70 \pm 0.45\text{b}$
ML	$1.64 \pm 0.05$	$1.60 \pm 0.11$	$0.06 \pm 0.03$	$0.08 \pm 0.05$	$1.64 \pm 0.33\text{ab}$
MH	$1.64 \pm 0.05$	$1.51 \pm 0.08$	$0.06 \pm 0.04$	$0.12 \pm 0.03$	$1.60 \pm 0.30\text{a}$
Track					
In	$1.66 \pm 0.06$	$1.57 \pm 0.14$	$0.07 \pm 0.02$	$0.09 \pm 0.06$	$1.62 \pm 0.33$
Out	$1.63 \pm 0.03$	$1.54 \pm 0.08$	$0.06 \pm 0.04$	$0.11 \pm 0.03$	$1.65 \pm 0.37$
Moisture conditions <sup>1</sup>	x	x	x	x	0.70
Tire pressure <sup>1</sup>	0.77	0.20	0.76	0.13	0.06
Moisture x Pressure <sup>1</sup>	x	x	x	x	0.15
Treatments <sup>2</sup>	0.90	0.17	0.80	0.10	<b><u>0.03</u></b>
Track <sup>2</sup>	0.34	0.63	0.60	0.37	0.48
Treatment x track <sup>2</sup>	0.68	0.34	0.54	0.22	0.38

<sup>1</sup> p-values are displayed using two-way ANOVA (only in-track data used);  $p < 0.10$  is indicated in bold;  $p < 0.05$  is indicated in bold and

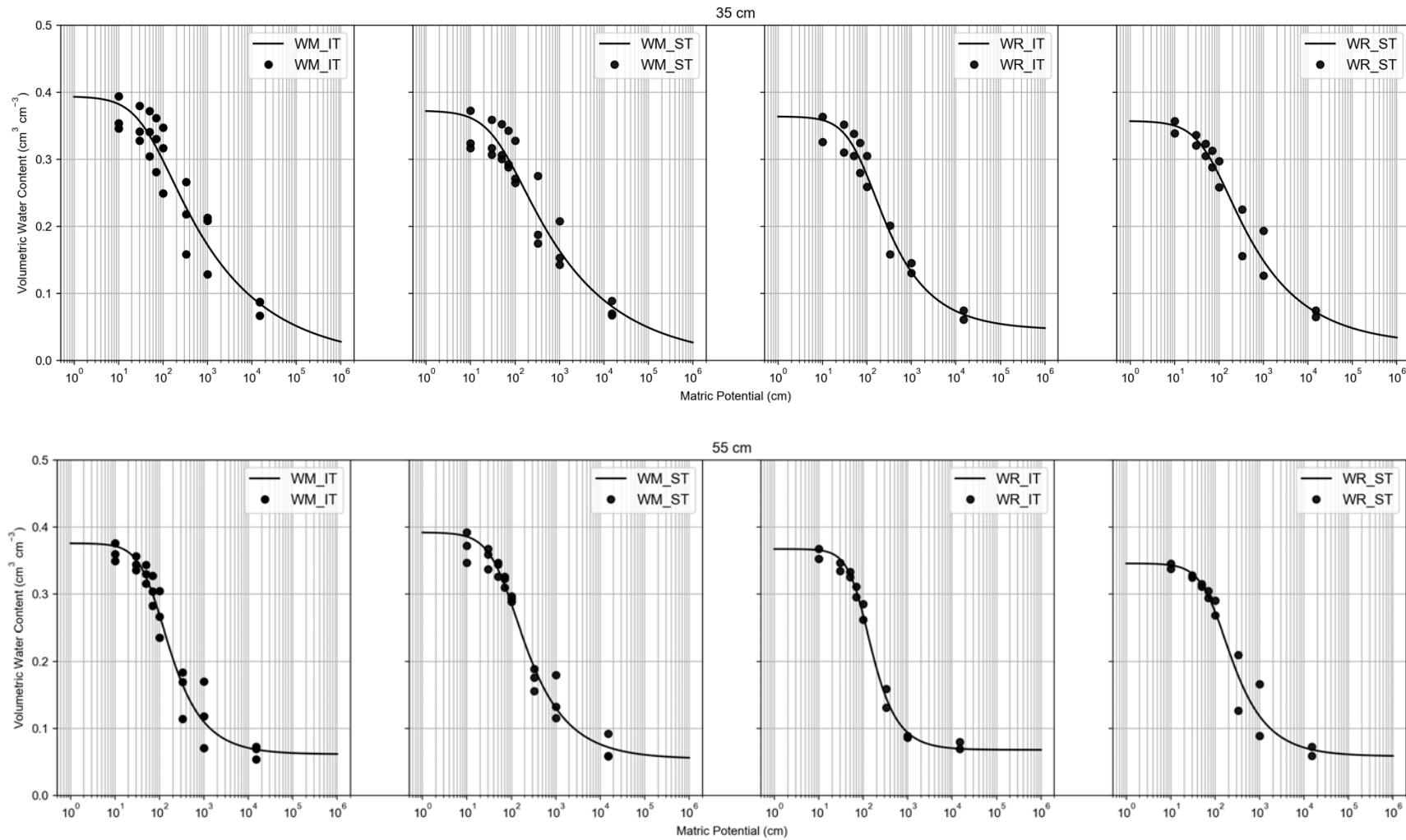
underlined. <sup>2</sup> p-value are displayed using Split-Plot Design with two factors (treatment and track). D: dry condition; M: moist condition ;

L: low pressure; H high pressure.

# Appendices in chapter 5:



## Appendices



S1. Soil water retention curves at each depth in out-row positions (WR = winter rye; WM = white mustard; IT = intensive tillage; ST = strip tillage), with dots are measured values and line are fitted with Van Genuchten (1980) model.

**Appendices in chapter 6:**

Table A. Distribution of pore volume and pore number as a function of diameter size intervals. Pore parameters were quantified using a medical X-ray Computed Tomography scanner. Plough, Transition and Compacted layer depths are 0.10-0.25, 0.25-0.35 and 0.35-0.50 m, respectively.

Treatment	Soil layer	Scan	Pore volume (mm <sup>3</sup> )					Pore number				
			Diameter size distribution (mm)					Diameter size distribution (mm)				
			<1.5	1.5-2	2-2.5	2.5-3	>3	<1.5	1.5-2	2-2.5	2.5-3	>3
Barley	Plough	Before	9472	18619.6	17718.3	79165.5	1545.9	3112	661	158	24	4
		After	11113	18972.6	31847.4	68684	4429.9	3905	846	188	54	11
	Transition	Before	1856	3449.9	3178	6612.6	2134.9	688	140	38	15	5
		After	3888	5321.9	4793.6	7744.3	2952.9	1220	176	42	18	5
	Compacted	Before	1066	1641.1	2295	2213.4	2051.4	348	80	34	11	3
		After	1676	2657.4	3035.9	3565.6	1972.8	612	116	40	13	4
Chicory	Plough	Before	10319	21400.3	14009.3	211357.9	1647.4	3580	700	156	28	7
		After	12137	19778	21235.3	6780.1	174715.2	3859	672	170	20	13
	Transition	Before	1753	5520.1	8364.2	5460.4	7857.8	590	156	55	18	12
		After	4774	5221.2	8611.6	14800.7	7918.8	1314	175	55	23	11
	Compacted	Before	1071	2057.1	3278.7	2077.9	3102.3	387	91	43	13	3
		After	3779	3702.2	4867.5	3822.3	3177.3	1061	136	52	15	4
Lucerne	Plough	Before	11722	21366.4	18862.2	260768.6	1183.9	3943	733	135	20	2
		After	11270	18600.6	26165.8	141029.4	7041.5	3840	724	242	40	10
	Transition	Before	4288	10073.3	9751.8	50630.7	7873.4	1453	313	78	20	10
		After	5304	9316.2	15993.9	32600.6	12721.2	1830	323	80	31	16
	Compacted	Before	1758	2476.6	4405.7	4168.4	7481.7	587	94	40	12	5
		After	5033	7302.4	6818.1	8368.5	4036	1137	156	41	16	5
Radish	Plough	Before	6184	10478.5	12054.5	49824.8	274.2	1940	381	110	18	1
		After	7559	14944.7	15016	67482	5603.9	2640	508	127	33	8
	Transition	Before	1298	4377.3	2034.1	4208.5	9253.9	395	70	29	14	9
		After	5091	4955.1	2238.7	4991.6	8982.8	894	107	23	16	6
	Compacted	Before	1441	2066.5	3274.8	2743.8	3542.4	465	88	38	13	5
		After	2164	2880.5	4647.2	3517.9	2618.3	663	120	46	13	6

## Appendices

Tall fescue	Plough	Before	10257	20210.8	17278.7	210956.8	1823	3330	611	160	23	5
		After	11405	18146.5	19664.4	160776.8	2919.9	3726	700	181	34	7
	Transition	Before	3205	6129.2	8268.6	7475.1	13161.5	1122	201	67	18	13
		After	8152	3588.8	7484.7	10571.7	10630.1	1355	241	60	25	12
	Compacted	Before	1690	3194.6	4167	7387.1	6247.4	585	134	59	32	9
		After	2696	4385	4890.8	7086.5	8504.6	880	180	70	26	11

Table B. Distribution of number of macropores as a function of volume intervals. Pore parameters were quantified using a medical X-ray Computed Tomography scanner. Plough, Transition and Compacted layer depths are 0.10-0.25, 0.25-0.35 and 0.35-0.50 m, respectively.

Treatment	Soil layer	Scan	Volume distribution (mm <sup>3</sup> )				
			<1	1-10	10-100	100-1000	>1000
Barley	Plough	Before	1185	1950	754	87	6
		After	1541	2387	941	121	12
	Transition	Before	271	433	155	26	2
		After	493	713	213	36	4
	Compacted	Before	148	225	97	15	0
		After	252	362	152	23	1
Chicory	Plough	Before	1413	2167	819	92	4
		After	1564	2278	833	83	8
	Transition	Before	231	365	192	37	6
		After	563	699	251	49	6
	Compacted	Before	165	234	111	21	2
		After	468	577	213	31	2
Lucerne	Plough	Before	1550	2380	819	75	9
		After	1466	2392	851	107	6
	Transition	Before	563	884	342	55	5
		After	745	1077	383	66	5
	Compacted	Before	226	359	125	26	2
		After	481	625	205	36	5
Radish	Plough	Before	769	1176	449	57	2
		After	1054	1613	563	85	7
	Transition	Before	151	240	88	24	3
		After	393	459	149	26	7
	Compacted	Before	182	286	122	17	1
		After	262	395	160	28	1
Tall fescue	Plough	Before	1297	2016	731	84	9
		After	1429	2289	836	88	5
	Transition	Before	451	675	241	44	9
		After	551	799	283	48	6
	Compacted	Before	225	373	173	39	3
		After	356	537	221	39	1

Table C. Median values of pore parameters quantified using an X-ray Computed Tomography scanner, before and one year after establishing potential bio-subsoilers on a heavily compacted soil. Plough, Transition and Compacted layer depths are 0.10-0.25, 0.25-0.35 and 0.35-0.50 m, respectively.

## Appendices

Treatment	Pore shape	Scan	Pore number			Pore volume (mm <sup>3</sup> )			Pore diameter (mm)		
			Plough	Transition	Compacted	Plough	Transition	Compacted	Plough	Transition	Compacted
Barley	Equant	Before	297	68	37	2346.4	654.2	408.0	1.8	1.8	2.1
		After	357	85	50	2770.1	556.8	449.4	1.9	1.8	1.9
	Non Classified	Before	2421	559	296	132578.7	8959.1	3951.8	2.5	2.5	2.6
		After	3060	979	492	123950.0	15664.7	7346.7	2.5	2.4	2.5
	Oblate	Before	174	27	11	2947.9	481.0	126.0	1.8	1.7	1.8
		After	234	55	23	5062.5	1057.1	322.5	2.2	1.9	1.9
	Prolate	Before	551	126	96	6922.9	1760.8	1295.0	1.7	2.1	1.8
		After	643	150	118	7276.8	1602.4	1522.3	2.0	1.7	1.9
Chicory	Triaxial	Before	520	107	57	11813.0	4288.5	2155.8	2.0	2.4	2.2
		After	697	189	80	19877.9	5547.4	5350.8	2.1	2.6	2.5
	Equant	Before	292	68	41	2228.3	750.6	404.0	1.8	2.0	1.9
		After	292	76	60	2328.0	817.2	470.9	1.9	2.4	1.9
	Non Classified	Before	2871	501	310	27899.7	14876.5	4955.6	2.2	2.6	2.5
		After	3054	1080	906	41899.6	26983.0	11486.0	2.4	2.6	2.5
	Oblate	Before	203	35	11	208935.6	1473.5	230.5	2.6	2.9	2.0
		After	176	50	36	2847.4	1360.7	748.9	1.8	2.2	1.9
Lucerne	Prolate	Before	576	126	110	6583.9	2784.2	2118.3	1.8	2.1	2.1
		After	608	207	175	6981.2	3473.3	2743.6	1.8	2.0	2.0
	Triaxial	Before	567	102	68	15615.4	5917.7	2279.6	2.0	2.2	2.1
		After	615	169	153	17620.4	6336.3	4929.8	1.9	2.5	2.0
	Equant	Before	324	126	48	2399.2	1026.7	486.4	1.7	1.8	2.0
		After	334	162	76	3095.7	1615.9	718.5	2.0	2.0	2.0
	Non Classified	Before	3011	1199	483	33201.3	60974.5	15919.4	2.0	2.6	2.8
		After	3037	1496	924	44928.1	50186.8	21064.2	2.2	2.7	2.1
Radish	Oblate	Before	203	83	19	216867.2	1634.8	298.1	2.8	2.0	2.0
		After	182	86	29	3504.0	1856.9	626.3	2.0	2.0	1.9
	Prolate	Before	632	257	115	6380.6	3296.2	1686.5	1.7	2.0	2.0
		After	664	279	165	8088.2	4396.5	4248.9	1.9	2.3	2.1
	Triaxial	Before	606	239	79	24319.1	10333.6	7299.9	2.3	2.4	2.7
		After	591	277	149	115317.5	9384.7	7405.3	2.5	2.2	2.3
	Equant	Before	211	43	46	1800.6	566.5	593.9	1.8	1.9	2.2
		After	268	53	58	2404.0	564.0	588.7	2.0	1.8	2.1
Tall fescue	Non Classified	Before	1479	286	364	62374.4	9515.8	6804.6	2.3	2.5	2.4
		After	2103	717	539	94597.1	21760.9	7464.7	2.4	2.4	2.4
	Oblate	Before	106	21	11	3774.7	1239.9	305.5	1.9	2.2	2.2
		After	121	29	17	3644.6	326.2	348.5	1.9	1.9	1.9
	Prolate	Before	353	85	116	4198.0	1306.3	1866.7	1.8	2.4	2.1
		After	433	104	147	5344.4	1361.8	2938.3	1.8	2.4	2.1
	Triaxial	Before	299	67	72	7766.0	4770.4	4878.5	2.0	3.1	2.7
		After	405	125	99	10206.1	4806.8	4422.0	2.0	2.5	2.7
Tall fescue	Equant	Before	271	96	58	2134.6	1111.1	671.7	1.8	2.0	2.0
		After	285	94	71	2567.6	891.8	799.6	2.2	2.0	2.0
	Non Classified	Before	2629	907	463	46561.5	24633.9	12954.9	1.9	2.6	2.8
		After	2925	1100	722	33572.2	21494.4	17364.4	2.1	2.5	2.6
	Oblate	Before	161	52	23	210751.2	2254.1	317.9	2.8	2.6	2.1
		After	176	67	35	92947.4	1871.9	501.6	2.6	2.2	2.0
	Prolate	Before	537	187	164	5787.0	2679.1	2569.7	1.8	1.9	2.1
		After	645	220	198	7805.0	3080.8	3252.1	2.0	2.2	2.2
Tall fescue	Triaxial	Before	540	177	101	19858.0	11205.2	5353.1	2.0	2.7	2.5
		After	620	221	134	15715.2	10772.6	5311.7	2.2	2.4	2.2

---

## Curriculum Vitae

### Personal information

---

**Full name:** Lidong Ren

**Date of birth:** 01/10/1987, Shaanxi, China

**Nationality:** Chinese

**Affiliation:** Department of Environment,  
Faculty of Bioscience Engineering, Ghent  
University, 9000 Ghent, Belgium.

**Contact details:** phone: +32486446398, Fax: +3292646247  
E-mail: [Lidong.ren@ugent.be](mailto:Lidong.ren@ugent.be); [renld315@163.com](mailto:renld315@163.com)



### Education and training

---

**2015 – Now** Doctor of Bioscience Engineering: Natural Resources, Ghent  
University, Belgium.

**2018 AUG-NOV** Guest researcher in Aarhus University, Denmark.

**2011 – 2015** Master in Soil sciences, Northwest Agriculture & Forest University,  
Yanglin, China.

**2007 – 2011** Bachelor in Agriculture resources and environment, Inner Mongolia  
Agricultural University, Hohhot, China.

### Regular courses followed

<b>Title</b>	<b>Coordinator/ Teacher</b>	<b>Organizers / Institute</b>	<b>Date/period</b>
-Data Analysis with Python	Koen Plevoets	KU Leuven	2017-2018
- Introduction to Python	Prof. Goetghebeur	Ghent University	2015-2016
- Method in data collection	Assist. Prof. Jarl Kampen	Ghent University	2015-2016
- Method in research design	Assist. Prof. Jarl Kampen	Ghent University	2015-2016
- Presentation Skills in English	-	Ghent University	2015-2016
- Advanced Academic English: Writing Skills	-	Ghent University	2015-2016

### Seminars and summer school

<b>Title</b>	<b>Coordinator/ Teacher</b>	<b>Organizers / Institute</b>	<b>Date/period</b>
- Merging measurements and modeling in soil physics	Dep. Agroecology	Aarhus University	2017-2018
- International Short Course on Advanced High-resolution 3D Imaging	UGCT	Ghent University	2017-2018
- Imaging and modelling of (reactive) fluid transport in geomaterials: from pore to continuum scale	UGCT	Ghent University	2017-2018

## Publications

---

### International/national peer reviewed

- Mansonia Pulido-Moncada, Sheela Katuwal, **Lidong Ren**, Wim Cornelis, Lars Munkholm (2020). Impact of potential bio-subsoilers on pore characteristics of a severely compacted subsoil. *Geoderma*, 363, 114154.
- **Lidong Ren**, Tommy D'Hose, Greet Ruyschaert, Jan De Pue, Redouane Meftah, Veerle Cnudde, Wim M. Cornelis (2019). Effects of soil wetness and tyre pressure on soil physical quality and maize growth by a slurry spreader system. *Soil and tillage research* 195: 104344.
- **Lidong Ren**, Thijs Vanden Nest, Greet Ruyschaert, Tommy D'Hose, Wim M. Cornelis (2019). Short-term Effects of Cover Crops and Tillage Methods on Soil Physical Properties and Maize Growth in a Sandy Loam Soil. *Soil and Tillage Research* 192: 76-86.
- **Lidong Ren** & Mingbin Huang (2016). Fine root distributions and water consumption of alfalfa grown in layered soils with different layer thicknesses. *Soil Research*, 54(6), 730-738.
- **Lidong Ren**, Mingbin Huang, Jun Fan (2013). Study on water retention capacity for drained soils with different textural layering. *Transactions of the Chinese Society of Agricultural Engineering*, 29(19): 105-111. (in Chinese).
- **Lidong Ren** & Mingbin Huang (2014). Experiment and numerical simulation of soil evaporation from layered sandy soil columns. *Acta Pedologica Sinica*, 51 (6): 104-110. (in Chinese).

- Qingli Xiao, Mingbin Huang, Ming'an Shao, **Lidong Ren** (2013). Infiltration and drainage processes of different textural soil moisture in middle reaches of Heihe River Basin. Transactions of the Chinese Society of Agricultural Engineering, 30(2): 124—131. (in Chinese)

### Conference Papers/reports:

---

- **Lidong Ren**, Tommy D'Hose, Irene Borra-Serrano, Peter Lootens, Wim M. Cornelis, Greet Ruyschaert (2020). Oral presentation: Detecting spatial variability of soil compaction using soil apparent electrical conductivity and maize canopy height. Seminar of "Geophysics and Agriculture: the perfect match?". January 31st, 2020 at Gembloux, Belgium.
- **Lidong Ren**, Greet Ruyschaert, Tommy D'Hose, Wim M. Cornelis (2019). Oral presentation: "Strategies to prevent, detect and alleviate soil compaction in a field scale". 9th PEDOFRACT Conference: Advances in soil scaling: theories, techniques and applications, 8-12 July, Barco de Ávila, Spain.
- **Lidong Ren**, Thijs Vanden Nest, Greet Ruyschaert, Tommy D'Hose, Wim M. Cornelis (2019). Poster presentation: "Effects of cover crops and tillage methods on maize growth – a soil compaction perspective". Soil works 2019, 29 January, Brussels, Belgium.
- **Lidong Ren**, Thijs Vanden Nest, Greet Ruyschaert, Tommy D'Hose, Wim M. Cornelis (2018). Oral presentation: "Effects of cover crops and tillage methods on maize

growth and soil physical properties in a sandy loam soil – From a Soil Compaction Perspective”. 21<sup>th</sup> ISTRO International Conference, 24-27 September, Paris, France.

- **Lidong Ren**, Mingbin Huang (2014). Oral presentation: “Water movement and its effect on plant growth in layered soils”. The academic seminar on soil physics progress and ecological security by the Soil Science Society of China, 8-10 August, Guilin, China.
- Amélia Baibay, **Lidong Ren**, Greet Ruyschaert, Tommy D’Hose, Wim M. Cornelis (2017). Poster presentation: “Effects of traffic-induced soil compaction on crop growth and soil properties”. EGU2017, 23 -28 April, Vienna, Austria.
- Chiheb Khemis , Khaoula Abrougui, **Lidong Ren**, Eunice Ann Mutuku, Sayed Chehaibi, and Wim Cornelis (2017). Poster presentation: “Effects of tractor loads and tyre pressures on soil compaction in Tunisia under different moisture condition”. EGU2017, 23 -28 April, Vienna, Austria.

### Research interest

---

**Soil compaction, Land and water management, X-ray computed tomography, Python with soil physics, Geophysics methods with agriculture, Root growth.**

### More information

---

Google scholar: <https://scholar.google.be/citations?user=JJ6mV5UAAAAJ&hl=en>

ResearchGate: [https://www.researchgate.net/profile/Lidong\\_Ren](https://www.researchgate.net/profile/Lidong_Ren)